JOHANNES GUTENBERG UNIVERSITÄT MAINZ

JG|U

Discovery and Biosynthesis of Bioactive Fungal Natural Products

Dissertation

Zur Erlangung des Grades

Doktor der Naturwissenschaften (Dr. rer. nat.)

Am Fachbereich Biologie

Der Johannes Gutenberg-Universität Mainz

Carsten Wieder

geb. am 03.11.1995 in Worms, Deutschland

Mainz, September 2025

Discovery and Biosynthesis of Bioactive Fungal Natural Products

Dekan:	Prof. Dr. Eckhard Thines
1. Berichterstatter:	Prof. Dr. Eckhard Thines
2. Berichterstatter:	Prof. Dr. Till Opatz
Tag der mündlichen Prüfung:	18.11.2025

“The joy of discovery is certainly the liveliest that the mind of man can ever feel.”

– Claude Bernard

– for my Mum –

Eidesstattliche Erklärung

Hiermit versichere ich, die vorgelegte Dissertation selbstständig und ohne Nutzung anderer als der angegebenen Quellen und Hilfsmittel angefertigt zu haben. Weiterhin erkläre ich, dass ich zur Anfertigung der Dissertation keine entgeltliche Hilfe Dritter in Anspruch genommen habe. Die vorgelegte Dissertation wurde zuvor nicht zur Erlangung eines anderen akademischen Grades eingereicht.

Mainz, den

Carsten Wieder

Table of Contents

List of Abbreviations

A, adenylation

ACP, acyl carrier protein

AT, acyltransferase

BGC, biosynthetic gene cluster

C, condensation

CMeT, *C*-methyltransferase

C_T, terminal condensation

CYP450, cytochrome P450 monooxygenase

DH, dehydratase

DMAPP, dimethylallyl pyrophosphate

E, epimerization

ER, enoyl reductase

FMO, flavin-dependent monooxygenase

hr, highly reducing

ICS, isocyanide synthase

IPP, isopentenyl pyrophosphate

KR, keto reductase

KS, ketosynthase

M, module

MA, myristic acid

(m)FAS, (metazoan) fatty acid synthase

MFS, major facilitator superfamily transporter

MβL, metallo-β-lactamase-like TE

NMeT, *N*-methyltransferase

nr, non-reducing

NRPS, non-ribosomal peptide synthetase

PCP, peptidyl carrier protein

PKS, polyketide synthase

PMA, phomenoic acid

PPT, phosphopantetheinyl

PT, product template

R, reductase

RCDPS, arginine-containing cyclodipeptides synthase

RiPP, ribosomally synthesized and post-translationally modified peptides

SAT, starter acyltransferase

SM, secondary/specialized metabolite

SRE, self-resistance enzyme

T, thiolation

TC, terpene cyclase

TE, thioesterase

t-ER, trans-acting enoyl reductase

TF, transcription factor

tr, truncated

αKGD, α-ketoglutarate-dependent dioxygenase

Abstract

The current rise of antimicrobial resistant pathogens threatens human health and global food security, underscoring the urgent need for new antimicrobial drugs. Bioactive natural products have been a continuous source of inspiration for the development of new pharmaceuticals and agrochemicals for decades. Fungi are enormously rich in biodiversity, prolific producers of natural products, and pose a treasure trove of untapped chemical diversity. Many species encode numerous natural product biosynthetic gene clusters (BGCs), most of which remain uncharacterized and are merely waiting to be unlocked. Therefore, fungi hold great promise as a source for the discovery of new bioactive molecules.

To this end, the present thesis aimed to discover bioactive natural products from fungi and uncover how they are biosynthesized. Therefore, various fungi were analyzed for the production of antimicrobial or otherwise bioactive natural products, resulting in the isolation of four target compounds that were investigated. These were acrophialocinol produced by *Acrophialophora levis*, allantofuranone produced by *Allantophomopsis lycopodina*, pleosporacin produced by *Pleosporales* sp., and saintopin produced by *Paecilomyces marquandii*. Allantofuranone and saintopin had previously been described, whereas acrophialocinol and pleosporacin are newly reported natural products. While acrophialocinol exhibits broad antifungal activity against a variety of fungal pathogens, pleosporacin selectively inhibits the phytopathogen *Botrytis cinerea* at a concentration as low as 3.2 µM. Saintopin and allantofuranone had previously been reported to exhibit topoisomerase I/II inhibitory and mild antifungal activity, respectively. BGCs presumably involved in the biosynthesis of these natural products (namely: *acr*, *alf*, *ple*, and *stp*) were identified from the genomes of the producing organisms by genome mining. Heterologous reconstitution of the biosynthetic genes in *Aspergillus oryzae* successfully allowed for the elucidation of all their biosynthetic pathways. Furthermore, it was shown that the RTA1-like protein encoded in the *acr* BGC mediated self-resistance towards the produced compounds, representing a new type of self-resistance enzyme. Additionally, combinatorial biosynthesis was applied to the allantofuranone biosynthetic pathway, successfully yielding hydroxylated derivatives, including some new natural products.

These findings provide a basis for the further investigation of the reported natural products as potential drug leads and fundamentally contribute to our understanding of how natural products are biosynthesized. The discovery of a new type of self-resistance enzyme might be useful in identifying a new mode of action for antifungal drugs, while simultaneously enabling the targeted discovery of bioactive natural products exerting this effect. Moreover, the findings display how combinatorial biosynthesis can be applied to expand the natural chemical diversity and derive new (non-)natural products.

Zusammenfassung

Der aktuelle Anstieg Antibiotika-resistenter Pathogene gefährdet sowohl die menschliche Gesundheit sowie die globale Nahrungssicherung und unterstreicht den dringenden Bedarf an neuen Wirkstoffen. Bioaktive Naturstoffe sind schon seit Jahrzehnten eine stetige Quelle der Inspiration zur Entwicklung neuer Pharmazeutika und Agrochemikalien. Pilze zeichnen sich durch eine außerordentliche Biodiversität aus und sind effiziente Produzenten verschiedenster Naturstoffe. Viele Pilzarten verfügen über eine Vielzahl von Biosynthesegenclustern (BGCs) für Naturstoffe, von denen die meisten bislang uncharakterisiert sind und darauf warten, erforscht und zugänglich gemacht zu werden. Ihre genetische und biochemische Vielfalt macht sie zu einer Schatzkammer bislang unerschlossener chemischer Diversität und bietet ein enormes Potenzial für die Entdeckung neuer bioaktiver Substanzen.

Vor diesem Hintergrund verfolgte die vorgelegte Thesis das Ziel, neue bioaktive Naturstoffe aus Pilzen zu entdecken sowie deren Biosynthese aufzuklären. Hierzu wurden verschiedene Pilze auf deren Produktion antimikrobieller oder anderweitig bioaktiver Naturstoffe analysiert. Daraus resultierte die Isolation von vier Zielmolekülen, welche weiter untersucht wurden. Es handelt sich dabei um Acrophialocinol aus *Acrophialophora levis*, Allantofuranon aus *Allantophomopsis lycopodina*, Pleosporacin aus *Pleosporales* sp., sowie Saintopin aus *Paecilomyces marquandii*. Allantofuranon und Saintopin wurden bereits zuvor beschrieben, wohingegen Acrophialocinol und Pleosporacin neue Naturstoffe darstellen. Während Acrophialocinol eine breite antifungische Aktivität gegen verschiedene pathogene Pilze aufweist, inhibiert Pleosporacin selektiv den phytopathogenen Pilz *Botrytis cinerea* ab einer Konzentration von bereits 3,2 µM. Über Saintopin und Allantofuranon wurde bereits zuvor berichtet, dass sie eine Topoisomerase I/II-inhibitorische Wirkung bzw. leicht antifungische Aktivität besitzen. Mit Hilfe von *genome mining* konnten BGCs (namentlich: *acr*, *alf*, *ple* und *stp*) identifiziert werden, welche vermutlich an der Biosynthese dieser Naturstoffe beteiligt sind. Die heterologe Rekonstitution der jeweiligen Biosynthesegene in *Aspergillus oryzae* erlaubte die erfolgreiche Aufklärung aller Biosynthesewege. Darüber hinaus konnte gezeigt werden, dass ein RTA1-ähnliches Protein, welches im *acr* BGC kodiert ist, Selbstresistenz gegenüber den produzierten Naturstoffen vermittelt. Weiterhin konnten durch die gezielte Manipulation der Allantofuranon Biosynthese-maschinerie neue hydroxylierte Derivate gewonnen werden, wovon einige neue Naturstoffe darstellen.

Die gewonnenen Erkenntnisse legen den Grundstein zur weiteren Erforschung der berichteten Naturstoffe als potenzielle Wirkstoffkandidaten und tragen fundamental zu unserem Verständnis von Naturstoffbiosynthesen bei. Die Entdeckung eines neuen Selbstresistenz-vermittelnden Enzyms könnte künftig nützlich zur Identifizierung eines neuen Wirkungsmechanismus sein und ermöglicht gleichzeitig die gezielte Entdeckung bioaktiver Stoffe mit dieser Wirkweise. Außerdem demonstrieren die Ergebnisse, wie kombinatorische Biosynthese genutzt werden kann, um die natürliche chemische Diversität zu erweitern und neue Naturstoffe zu produzieren.

Introduction

Bioactive Fungal Natural Products as a Source for Drug Leads

The kingdom of Fungi represents a branch in the domain of the Eukarya that is enormously rich in biodiversity, currently being estimated to encompass 2.2–3.8 million species, merely ~3–8 % of which have been described to date[1]. Due to their vast metabolic capacity, fungi excel at the utilization of complex substrates[2], and can conquer even harsh ecological niches[3]. They do not only greatly contribute to the decomposition of dead organic matter[4], but also engage in a plethora of symbiotic and pathogenic interactions[5–13]. Fungi harbor significant economic value[14], and are industrially exploited for the production of foods, beverages, organic acids, proteins, enzymes, vitamins, pharmaceuticals, and more[14–16].

The ecological and metabolic diversity of fungi is also mirrored by their remarkable ability to produce structurally and functionally diverse natural products, also known as specialized or secondary metabolites (SMs)[17,18]. While they are mostly dispensable for growth and reproduction, they are closely intertwined with development and crucial for the interaction with the environment and other organisms[17,18]. One of the most famous examples of a fungal SM is penicillin, an antibiotic first isolated by Alexander Fleming in 1928[19], which revolutionized the treatment of bacterial infections. Indeed, many fungi produce SMs with antimicrobial activity to outcompete other microbes for nutrients in their ecological niche[20,21]. The function of fungal natural products is, however, not limited to inflicting harm, but they are also used for defense[22,23], communication[24,25], nutrient acquisition[26,27] and protection against environmental stressors[28], amongst others.

The concurrent rise of antimicrobial resistant bacterial and fungal pathogens worldwide poses a major threat to human health and global food security that urgently demands solutions[29–33]. Indeed, natural products have long provided antimicrobial agents and been a source for drug leads for decades due to their structural and functional diversity[34]. While some natural products are employed natively (e.g., penicillin), others are semi-synthetically modified (e.g., anidulafungin based on echinocandin B[35]) or inspire the design of fully synthetic analogues (e.g., kresoxim-methyl based on strobilurin A[36]). One recent example is the siderophore-type fungal natural product ASP2397, first isolated in 2017[37]. This compound exhibits potent antifungal activity and has already advanced into clinical trials for treatment of invasive Aspergillosis[37,38]. Simultaneously, natural products also hold promise to treat other, non-infectious diseases such as coronary heart disease[39], cancer[40] and Alzheimer's disease[41]. Finding cures for these maladies is of great interest to the general public, and therefore, the discovery of new bioactive natural products is of significant importance.

Basic Logic of Fungal Natural Product Biosynthesis

Natural products can be categorized into distinct classes based on their chemical structure and biosynthetic origin, such as polyketides, non-ribosomal peptides, and terpenes. They are mostly derived from common central metabolites such as amino acids and acyl-CoAs. The main scaffold of a natural product is usually synthesized by a dedicated core enzyme. The initial intermediate is then modified by auxiliary tailoring enzymes that catalyze various transformations[42] ranging from simple redox reactions[43] to complex molecular rearrangements[44]. Genes encoding enzymes involved in the biosynthesis of a given natural product are most frequently colocalized in fungal genomes in so-called biosynthetic gene clusters (BGCs)[45]. Aside from biosynthetic enzymes, such BGCs can also encode transporters for substrates or products, enzymes conferring self-resistance towards toxic products, and cluster-specific regulators. The number of BGCs encoded in fungal genomes varies substantially between different genera, ranging from very few to more than 100 per genome, with an average of ~30 BGCs[46,47]. Great progress has been made in the last decades linking BGCs to their respective natural products, nonetheless, there is still a big discrepancy between the amount of BGCs encoded in fungal genomes and the natural products isolated from fungi. For instance, even in the model ascomycete *Aspergillus nidulans*, over half of the BGCs encoded are still uncharacterized and their products

unknown[48]. Therefore, it can be assumed that fungi still hold great potential for the discovery of new natural products and are a source not yet exhausted.

– *Polyketides* –

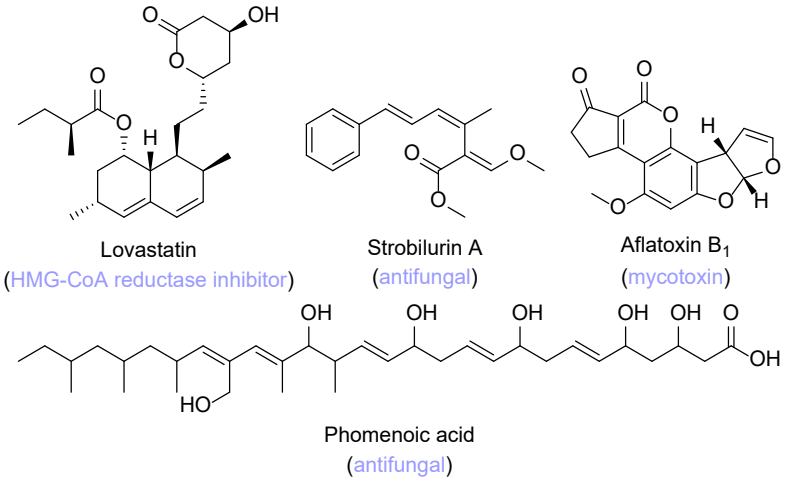

Figure 1: Chemical structures of exemplary fungal polyketides.

Polyketides are a diverse and abundant class of natural products, including many bioactive compounds such as lovastatin[49], strobilurin A[50], aflatoxin B_1[51] and phomenoic acid[52] (Figure 1). They are synthesized by dedicated polyketide synthases (PKSs) that catalyze the repeated decarboxylative Claisen condensation of activated acyl-units to facilitate the assembly of the carbon backbone. Fungal genomes predominantly encode iterative type I PKSs (henceforth referred to as PKS), monomodular, multidomain enzymes that catalyze multiple rounds of chain elongation. They are structurally and functionally related to metazoan fatty acid synthases (mFAS) and share a common domain architecture[53]. In contrast to mFAS, however, PKS do not necessarily produce fully saturated products. Instead, they produce a wide variety of compounds whose structural diversity arises from incomplete reduction of the nascent intermediate during elongation cycles. This is caused by the absence or dysfunction of certain reductive domains, as well as by programmed domain skipping[53–56]. PKSs are composed of a minimal set of a ketosynthase (KS) domain, acyl-carrier protein (ACP) domain, and acyltransferase (AT) domain, which collectively orchestrate the elongation of the polyketide backbone (Figure 2)[54,55]. First, a starter unit, most commonly acetyl-CoA, is loaded onto the KS domain. Next, the AT domain catalyzes transfer of an extender unit, most commonly malonyl-CoA, onto the ACP domain.

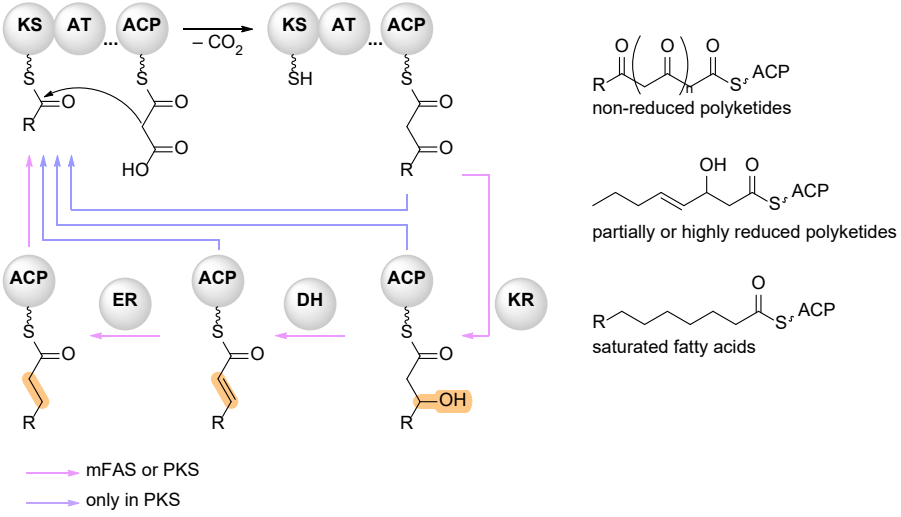

Figure 2: Polyketide chain elongation. Adapted from Hertweck, 2009[54].

Subsequently, the KS domain facilitates the decarboxylative Claisen condensation of the KS- and ACP-bound acyl-units, thereby extending the carbon backbone by a C_2 unit. After any tailoring by additional domains, the bound intermediate is re-transferred to the KS domain for a subsequent catalytic cycle[54,55]. This is repeated until the nascent polyketide is off-loaded from the assembly line by an intrinsic off-loading domain or trans-acting releasing enzyme. Product release can occur through a variety of different mechanisms, commonly by hydrolysis or (macro-)cyclization[57]. Based on the presence of optional reductive domains, PKSs are distinguished into non-reducing (nr), partially reducing, and highly reducing (hr) types. hrPKS contain a full set of reductive domains, namely a ketoreductase (KR) domain, a dehydratase (DH) domain, and an enoyl reductase (ER) domain, that facilitate the sequential reduction of the β-ketone to saturation. All PKS types can optionally harbor a *C*-methyltransferase (CMeT) domain that can methylate the C_α prior to the action of the KR domain and encompass an intrinsic off-loading domain such as a thioesterase (TE) domain, reductase (R) domain, or carnitine acyltransferase (cAT)[58] domain. Recently, a stereochemical rule has been proposed for the CMeT, KR, and ER domains of PKSs that allows the prediction of the absolute configuration of polyketides, although exceptions do exist[52]. nrPKS produce aromatic compounds that derive from the cyclization of the nascent, non-reduced poly-β-ketone. They lack all reductive domains but additionally encompass a starter acyl transferase (SAT) domain[59] and a product template (PT) domain[60]. The SAT domain selects and loads the starter unit in nrPKS and allows for higher substrate flexibility, although it is not necessarily required in all nrPKS[61]. nrPKS more often than hrPKS load unusual starter units such as, e.g., hexanoic acid in the biosynthesis of the aflatoxin precursor norsolorinic acid[62] or even other polyketides, as in the biosynthesis of resorcylic acid lactones[63]. These substrates are often directly transferred from the FAS or PKS synthesizing them. The PT domain prefolds the nascent polyketide and facilitates the cyclization thereof via aldol cycloaddition. The chain length of polyketides is predominantly determined by the KS domain in nrPKS systems[64,65], but polyketide homologation is majorly affected by tailoring domains and collaborating enzymes in both nrPKS and hrPKS systems[66–69]. The programming of hrPKS is not yet fully understood, but believed to be determined by the substrate selectivity of a given domain and the competition of different domains for the ACP-bound substrate[55,67].

– *Non-Ribosomal Peptides* –

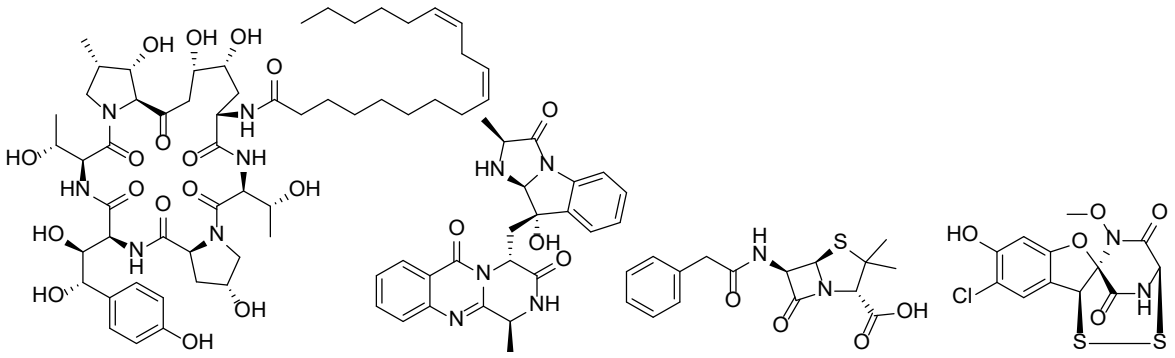

Figure 3: Chemical structures of exemplary fungal NRPs.

Non-ribosomal peptides (NRPs) are another major class of natural products, including diverse bioactive compounds such as penicillin G[70], echinocandin B[71], fumiquinazoline A[72], and aspirochlorine[73] (Figure 3). They are synthesized by dedicated non-ribosomal peptide synthetases (NRPSs), multimodular enzymes that facilitate the condensation of proteinogenic and non-proteinogenic amino acids as well as some hydroxy acids[74]. Canonical NRPS modules (M) are composed of an adenylation (A) domain, a thiolation (T; also: peptidyl carrier protein, PCP) domain, and a condensation (C) domain. The A domain loads the substrate onto the prosthetic phosphopantetheinyl (PPT) moiety of the T domain. The C domain then facilitates condensation of two adjacent T-bound substrates to form either a peptide or ester bond (Figure 4). Modules can additionally contain optional domains: Epimerization (E) domains catalyze L- to D- stereoinversion of the bound substrate prior to condensation,

whereas *N*-methyltransferase (NMeT) domains methylate the amine of the bound substrate. NRPSs can also include an additional terminal domain for product-offloading, such as an R domain, a TE domain, or a terminal C_T domain. Release frequently occurs via either hydrolysis, lactonization, lactamization, or Dieckmann cyclization[57,75].

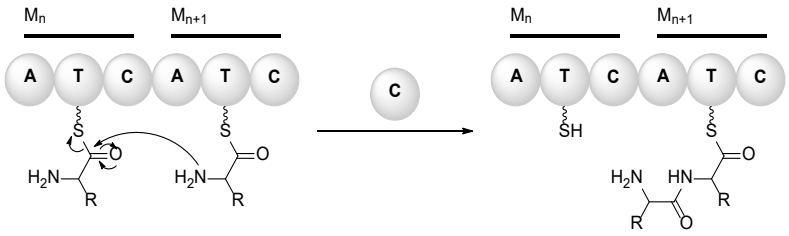

Figure 4: Scheme of non-ribosomal peptide formation.

In contrast to canonical NRPS, NRPS-like enzymes harbor only a single module and lack a C domain. They can be subdivided into reducing and non-reducing types. Reducing NRPS-like enzymes harbor a terminal R domain (A-T-R) and catalyze the reduction of the activated substrate. They frequently act as reductive tailoring enzymes[76], but can also facilitate the formation of dihydropyrazine or pyrazinone natural products via the spontaneous dimerization of reduction-derived amino aldehydes[77–79]. Non-reducing NRPS-like enzymes harbor a terminal TE domain (A-T-TE) and catalyze the condensation of two aromatic α-keto acids, resulting in the formation of various cyclic products, including benzoquinones[80–82], furanones[83–85], and dioxolanones[86] (Figure 5).

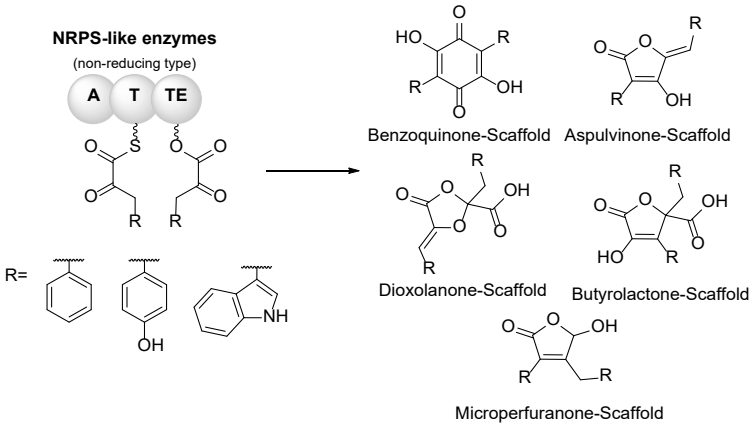

Figure 5: Substrate and product scope of non-reducing NRPS-like enzymes. Taken from Wieder *et al.*, 2025[87].

– *Terpenes and Miscellaneous Natural Product Classes* –

Besides polyketides and NRPs, terpenes are another major class of natural products with very vast structural diversity, including bioactive compounds such as pleuromutilin[88], deoxynivalenol[89], aspterric acid[90] and clavaric acid[91] (Figure 6). Terpenes are derived from the isoprenoid blocks dimethylallyl pyrophosphate (DMAPP) and isopentenyl pyrophosphate (IPP), which are synthesized in fungi via the mevalonate pathway from acetyl-CoA[92]. Multiple isoprenoid units are first fused by prenyltransferases to produce precursors of different chain lengths, which are then cyclized by terpene cyclases (TCs) via a cationic cascade kickstarted by either dephosphorylation (class I TCs) or protonation (class II TCs) of the substrate and finally terminated by deprotonation or hydration[92]. Whereas class II TCs mostly produce head-to-tail cyclized products, including various sterols, class I TCs can produce a plethora of complex carbon scaffolds facilitated through complex cyclizations and molecular rearrangements.

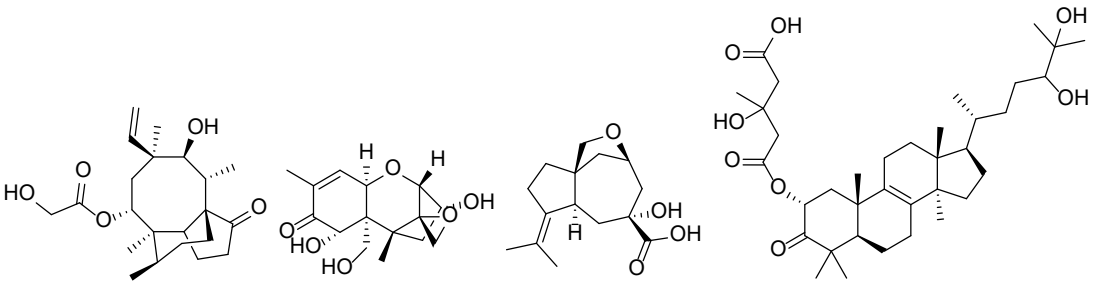

Figure 6: Chemical structures of exemplary fungal terpenes.

Moreover, hybrid natural products composed of different chemical classes frequently occur. These include polyketide-NRP hybrids such as tenellin[93] and aspcandine[94], polyketide-terpene hybrids such as ascochlorin[76] or NRP-terpene hybrids such as aculene A[95] (Figure 7). They are either synthesized by collaborating enzymes/pathways or by chimeric enzymes that harbor both PKS and NRPS domains. The latter can be subdivided into PKS-NRPS hybrids and NRPS-PKS hybrids based on the order of the domains, the latter of which are encountered more rarely in fungal genomes.

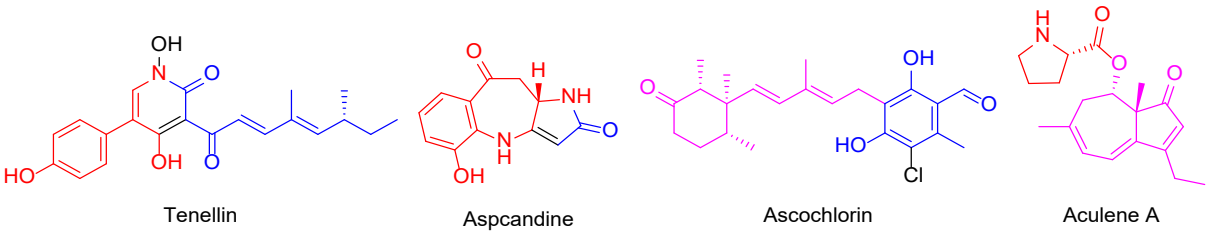

Figure 7: Chemical structures of exemplary fungal hybrid natural products. Polyketide (blue), NRP (red) and terpene (magenta) moieties are highlighted in different colors.

Furthermore, peptide natural products can also be synthesized by enzymes other than NRPS. Ribosomally synthesized and post-translationally modified peptides (RiPPs) are derived from precursor peptides encoded in the genome via proteolytic cleavage, with modifications occurring before or after release of the core peptide[96]. Arginine-containing cyclodipeptides (RCDPs) are a recently discovered class of peptide natural products that are synthesized by RCDP synthases (RCDPS), a previously unknown enzyme class that utilizes aminoacyl-tRNAs as substrates[97]. Furthermore, only recently ATP-grasp enzymes and amide bond synthases have been described to be involved in the biosynthesis of fungal peptide natural products[98,99]. Beyond these, there are, however, many further natural product classes, e.g., various indole-containing compounds such as tryptamines (e.g. psilocybin)[100] or ergot alkaloids (e.g. lysergic acid)[101] that are synthesized from tryptophan, and isocyanides (e.g. xanthocillin)[102] synthesized from amino acids by dedicated isocyanide synthases (ICS). Even now, new natural product classes and biosynthetic routes are still discovered, as many non-canonical enzymes and BGCs have previously been overlooked by genome mining algorithms[97,98,102–105]. Unraveling these hidden treasures holds great promise to further expand the diversity of natural products and the biosynthetically accessible chemical space.

Strategies for Discovering Fungal Natural Products and Uncovering their Biosynthesis

Natural products can be extracted from fungal cultures using organic solvents, isolated using chromatographic techniques, and their structures elucidated using analytical chemistry. Simple variation of fermentation parameters can yield various natural products even from a single species, a technique commonly referred to as the OSMAC (one strain, many compounds) approach[106]. In that manner, many natural products have been isolated from many fungal species to date. Coupling this fermentation-based approach with bioactivity assays can help prioritize natural products possessing desired activities. Based

on the choice of assay, one may screen for antimicrobial compounds or even compounds that bind to a specific target protein. Bioactivity-guided isolation has, for instance, been successfully employed to identify penicillic acid as a probe against Alzheimer's disease associated tau aggregation[41].

Unfortunately, the likelihood of discovering new chemistry using a simple fermentation-based approach is slowly declining as more natural products are being reported. This is not because the biosynthetic capacity of fungi is exhausted, but instead because only few natural products are produced under laboratory conditions[107,108]. As the production of SMs is highly energy-intensive and their function is often very specific, it is not feasible or beneficial for a fungus to produce its entire repertoire of SMs at all times. Instead, SM production is tightly regulated through the action of both global and specific regulators in response to environmental stimuli[17,18], and the respective stimuli might not be given under laboratory conditions. BGCs whose natural products are not observed are referred to as silent. The seemingly limited number of natural products produced under laboratory conditions has brought upon the increasing issue of rediscovering previously identified compounds instead of new ones when investigating the composition of fungal extracts. It should, however, also be noted that fermentation and bioactivity-guided approaches are slightly biased towards compounds produced in larger quantities, as trace compounds might elude the detection by common analytical tools, i.e. HPLC-MS or bioassays and are difficult to purify in sufficient amounts for structure elucidation. Molecular networking has emerged as a powerful tool for analyzing tandem mass spectrometry (MS^2) data to dereplicate natural products, making use of spectral libraries such as the GNPS[109]. This enables fast identification of known, deposited natural products in a complex extract without the need for isolation and structure elucidation, which in turn helps to target unknown metabolites. Moreover, microcrystal electron diffraction (microED) has recently been successfully employed to solve natural product crystal structures from crude extracts, enabling elucidation of new metabolites from nanogram quantities[110,111].

The discovery of new natural products is increasingly reliant on targeted genetic manipulation, with a focus on accessing cryptic BGCs whose products remain unknown[108,112]. To this end, both genetic manipulation of native organisms and transfer of genetic material into heterologous hosts have been employed successfully many times. Genome mining efforts are usually prefaced by the prediction of all BGCs in an annotated genome using elaborate bioinformatic tools such as antiSMASH[113] or FunBGCeX[104]. One can then search these predicted BGCs for a target BGC involved in the biosynthesis of a previously identified natural product based on chemical cues and biosynthetic logic (top-down forward genetic approach) or pick candidate BGCs for activation or heterologous reconstitution based on desired features (bottom-up reverse genetic approach). The activation of silent BGCs can be achieved by overexpression, deletion or refactoring of global or cluster-specific regulators and biosynthetic genes[114–120]. CRISPR-mediated transcriptional activation (CRISPRa) has also been successfully used in this context[121]. Furthermore, employing engineered hybrid transcription factors (composed of a native DNA-binding domain fused to a strong transcriptional activator) has proven helpful in cases where overexpression of a native transcription factor did not lead to sufficient transcriptional activation[122,123]. The successful activation of a silent BGC results in the production of one or more new metabolites, which become apparent by comparison with the parental strain and can subsequently be isolated and characterized. A limitation in working with native organisms is their amenability to genetic manipulation. As many fungi are not at all or only poorly amenable to genetic manipulation, heterologous expression poses a convenient and powerful alternative. Various filamentous fungi have successfully been established as chassis hosts for heterologous reconstitution of natural product biosynthetic pathways. *Aspergillus* species such as *A. nidulans*[124], *A. oryzae*[80,125] and *A. niger*[126] are amongst the most widely used model hosts, but various other genera such as *Trichoderma*[127], *Penicillium*[128], and *Fusarium*[129,130] are also being used. Similar to the activation in a native host, reconstitution of BGCs in a heterologous host usually requires refactoring of either all biosynthetic genes or a contained cluster specific transcription factor that regulates expression of the other BGC genes. In order to elucidate the biosynthetic pathway of a natural product, the individual transformations and order of reactions catalyzed by the implied enzymes have to be characterized. This can be achieved by either deleting single genes from a BGC or reconstituting a BGC one enzyme at a time, resulting in the accumulation of biosynthetic intermediates, based on which the biosynthetic route

can be proposed. This is frequently complemented by probing single enzymatic transformations *in vitro*, especially for more intricate reactions. Besides genome mining, combinatorial biosynthesis strategies can also be employed to access new chemical diversity[131]. In this regard, every new biosynthetic enzyme and pathway characterized broadens the possibilities for the rational (re-)design of new (non-)natural products.

While genome mining is an efficient strategy to uncover new natural products, it is more laborious than classic screening approaches, and the obtained natural products might not exhibit bioactive properties at all. However, self-resistance enzyme (SRE)-guided genome mining has recently emerged as a very powerful approach to identify BGCs that encode bioactive natural products[132]. Logically, organisms that produce bioactive substances they would themselves be susceptible to, e.g., fungi producing antifungal compounds, must employ some type of self-resistance to prevent autotoxicity. For instance, toxic molecules are frequently modified enzymatically to render them inactive. Moreover, BGCs do occasionally encode a duplicate of an essential housekeeping gene that is resistant to the bioactive product encoded by that BGC. This can be used to selectively search for BGCs that potentially encode natural products targeting a specific protein and has already been successfully employed to identify various bioactive natural products[90,133–139]. The recently introduced application FunARTS[140] facilitates SRE-guided genome mining efforts by searching genomes for duplications of essential genes and known resistance-conferring enzymes in the vicinity of predicted BGCs.

Studying biosynthetic pathways, however, comes with a few challenges. Firstly, heterologous expression of solely a core biosynthetic gene, such as a PKS or NRPS, is frequently not sufficient for metabolite production, as additional enzymes might be required for formation of the initial product. Such enzymes might facilitate substrate loading[62,71,141], introduce on-line modifications[142], catalyze product release[143–145], or produce a non-physiological precursor for the core biosynthetic enzyme[71,94]. This complicates the process of sequentially reconstituting a BGC, as all required enzymes need to be identified first, which might only be achieved by trial-and-error probing. Furthermore, the boundaries of a BGC are not readily apparent, and the bioinformatic predictions might not always be correct. Even then, not all genes located within a BGC do necessarily act in the biosynthetic pathway. Conversely, genes that are only annotated as hypothetical proteins or lack any conclusive sequence homologies might still be catalytically relevant to the biosynthesis[97]. Although encountered only infrequently, BGCs can also be split across the genome[146]. Functional reconstitution of a BGC might moreover require the coexpression of transporter[147,148], or resistance genes. Lastly, but very importantly, although this is only very rarely addressed publicly, not all BGCs are necessarily (fully) functional even when successfully activated or reconstituted[17]. This can be due to one or more enzymes being dysfunctional, thereby terminating a biosynthetic pathway early or entirely preventing the formation of any product. In a recent study, complete heterologous reconstitution of the octacyclin A BGC initially only resulted in production of the first biosynthetic intermediate, as the second enzyme was dysfunctional[79]. Only upon replacement of the dysfunctional enzyme with a functional homolog of a similar biosynthetic pathway did the heterologous expression result in the production of the final product octacyclin A.

Research Objective and Scope

The present thesis aimed to discover new fungal natural products with a focus on antifungal or otherwise bioactive compounds and elucidate their biosynthetic pathways. Fungi pose a treasure trove of new chemistry, and their repertoire has not yet been exhausted, as is evidenced by the discrepancy between the abundance of genomically encoded BGCs and the comparably few metabolites produced. We are only starting to look past long-standing paradigms, and therefore, these are exciting times for the fungal natural product community. The identification of new bioactive molecules is crucial for the development of new drugs, especially for combating emergent antimicrobial resistant pathogens. Natural products have been a major inspiration for drug development in the past and will continue to be in the future. Furthermore, elucidation of biosynthetic pathways and characterization of implicated enzymes catalyzing new reactions deepens our understanding of how nature orchestrates the assembly of these small yet meticulous molecules. This not only expands the biologically tractable chemical space but enables us to transfer this knowledge to other biosynthetic pathways, exploit it for synthetic biology,

biotechnology, and biocatalysis applications, and even manipulate pathways to create new-to-nature “designer compounds”.

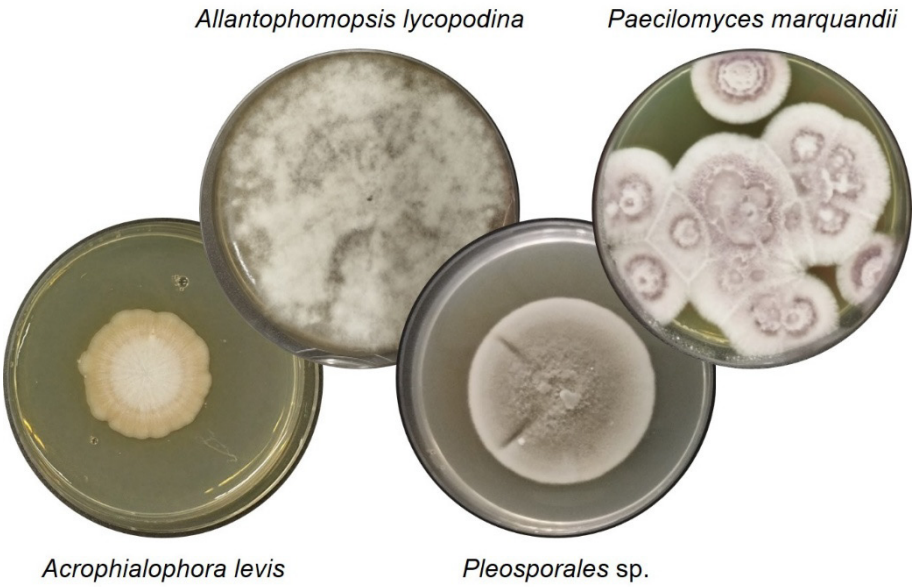

Figure 8: Fungal species investigated in the present thesis. Morphology on agar plates.

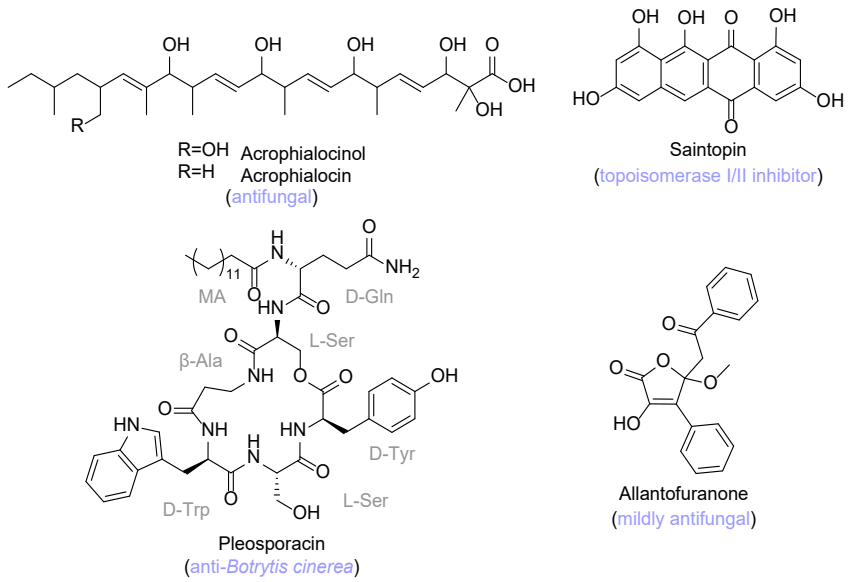

Figure 9: Bioactive fungal natural products investigated in the present thesis.

To this end, bioactive compounds of four different fungi of the phylum Ascomycota were studied (Figures 8 and 9). Acrophialocin(-ol) and pleosporacin were identified from *Acrophialophora levis* and *Pleosporales* sp., respectively, based on their potent antifungal activity. Whereas acrophialocin and acrophialocinol are broadly active with promising anti-*Candida* activity (MIC 2.5 µg/mL), pleosporacin, in contrast selectively inhibits the plant pathogen *B. cinerea*. While their exact mechanisms of action remain unclear, these compounds make interesting candidates for further investigation as potential drug leads. Saintopin was rediscovered as the purple colorant of *Paecilomyces marquandii* conidia and was previously reported to exhibit potent topoisomerase I/II inhibitory activity. Although it was overlooked for some time, this study provides a foundation for its scalable production and further research on saintopin as a potential anticancer lead. Lastly, the mildly antifungal agent allantofuranone produced by *Allantophomopsis lycopodina* was investigated for its uniquely substituted furanone scaffold, the biosynthesis of which has hitherto been elusive.

Candidate BGCs for all the aforementioned compounds were identified by genome mining based on structural cues, and the biosynthetic pathways were elucidated by reconstitution of the respective biosynthetic genes in the heterologous host *Aspergillus oryzae*. This enabled characterization of the biosynthetic intermediates and offered insight into how these compounds are synthesized. Intriguingly, the study of the acrophialocinol BGC additionally revealed a new type of self-resistance enzyme, an RTA1-like protein, which confers resistance to the toxic products of the BGC. Beyond that, the allantofuranone biosynthetic machinery was successfully manipulated (combinatorial biosynthesis) to synthesize some new-to-nature hydroxylated derivatives.

References

[1] D. L. Hawksworth, R. Lücking, "Fungal Diversity Revisited: 2.2 to 3.8 Million Species" *Microbiol. Spectr.* **2017**, *5*, 10.1128/microbiolspec.funk-0052–2016.

[2] D. Floudas, M. Binder, R. Riley, K. Barry, R. A. Blanchette, B. Henrissat, A. T. Martínez, R. Otillar, J. W. Spatafora, J. S. Yadav, A. Aerts, I. Benoit, A. Boyd, A. Carlson, A. Copeland, P. M. Coutinho, R. P. de Vries, P. Ferreira, K. Findley, B. Foster, J. Gaskell, D. Glotzer, P. Górecki, J. Heitman, C. Hesse, C. Hori, K. Igarashi, J. A. Jurgens, N. Kallen, P. Kersten, A. Kohler, U. Kües, T. K. A. Kumar, A. Kuo, K. LaButti, L. F. Larrondo, E. Lindquist, A. Ling, V. Lombard, S. Lucas, T. Lundell, R. Martin, D. J. McLaughlin, I. Morgenstern, E. Morin, C. Murat, L. G. Nagy, M. Nolan, R. A. Ohm, A. Patyshakuliyeva, A. Rokas, F. J. Ruiz-Dueñas, G. Sabat, A. Salamov, M. Samejima, J. Schmutz, J. C. Slot, F. St. John, J. Stenlid, H. Sun, S. Sun, K. Syed, A. Tsang, A. Wiebenga, D. Young, A. Pisabarro, D. C. Eastwood, F. Martin, D. Cullen, I. V. Grigoriev, D. S. Hibbett, "The Paleozoic Origin of Enzymatic Lignin Decomposition Reconstructed from 31 Fungal Genomes" *Science* **2012**, *336*, 1715–1719.

[3] C. Coleine, J. E. Stajich, L. Selbmann, "Fungi are key players in extreme ecosystems" *Trends Ecol. Evol.* **2022**, *37*, 517–528.

[4] J. M. Talbot, S. D. Allison, K. K. Treseder, "Decomposers in disguise: mycorrhizal fungi as regulators of soil C dynamics in ecosystems under global change" *Funct. Ecol.* **2008**, *22*, 955–963.

[5] A. Genre, L. Lanfranco, S. Perotto, P. Bonfante, "Unique and common traits in mycorrhizal symbioses" *Nat. Rev. Microbiol.* **2020**, *18*, 649–660.

[6] T. Spribille, P. Resl, D. E. Stanton, G. Tagirdzhanova, "Evolutionary biology of lichen symbioses" *New Phytol.* **2022**, *234*, 1566–1582.

[7] H. Li, S. E. Young, M. Poulsen, C. R. Currie, "Symbiont-Mediated Digestion of Plant Biomass in Fungus-Farming Insects" *Annu. Rev. Entomol.* **2021**, *66*, 297–316.

[8] G. Doehlemann, B. Ökmen, W. Zhu, A. Sharon in *Fungal Kingd.*, John Wiley & Sons, Ltd, **2017**, pp. 701–726.

[9] A. Rokas, "Evolution of the human pathogenic lifestyle in fungi" *Nat. Microbiol.* **2022**, *7*, 607–619.

[10] B. Lovett, R. J. St. Leger in *Fungal Kingd.*, John Wiley & Sons, Ltd, **2017**, pp. 923–943.

[11] B. C. Scheele, F. Pasmans, L. F. Skerratt, L. Berger, A. Martel, W. Beukema, A. A. Acevedo, P. A. Burrowes, T. Carvalho, A. Catenazzi, I. De la Riva, M. C. Fisher, S. V. Flechas, C. N. Foster, P. Frías-Álvarez, T. W. J. Garner, B. Gratwicke, J. M. Guayasamin, M. Hirschfeld, J. E. Kolby, T. A. Kosch, E. La Marca, D. B. Lindenmayer, K. R. Lips, A. V. Longo, R. Maneyro, C. A. McDonald, J. Mendelson, P. Palacios-Rodriguez, G. Parra-Olea, C. L. Richards-Zawacki, M.-O. Rödel, S. M. Rovito, C. Soto-Azat, L. F. Toledo, J. Voyles, C. Weldon, S. M. Whitfield, M. Wilkinson, K. R. Zamudio, S. Canessa, "Amphibian fungal panzootic causes catastrophic and ongoing loss of biodiversity" *Science* **2019**, *363*, 1459–1463.

[12] J. R. Hoyt, A. M. Kilpatrick, K. E. Langwig, "Ecology and impacts of white-nose syndrome on bats" *Nat. Rev. Microbiol.* **2021**, *19*, 196–210.

[13] T. L. R. Coker, J. Rozsypálek, A. Edwards, T. P. Harwood, L. Butfoy, R. J. A. Buggs, "Estimating mortality rates of European ash (*Fraxinus excelsior*) under the ash dieback (*Hymenoscyphus fraxineus*) epidemic" *PLANTS PEOPLE PLANET* **2019**, *1*, 48–58.

[14] A. G. T. Niego, C. Lambert, P. Mortimer, N. Thongklang, S. Rapior, M. Grosse, H. Schrey, E. Charria-Girón, A. Walker, K. D. Hyde, M. Stadler, "The contribution of fungi to the global economy" *Fungal Divers.* **2023**, *121*, 95–137.

[15] V. Meyer, E. Y. Basenko, J. P. Benz, G. H. Braus, M. X. Caddick, M. Csukai, R. P. de Vries, D. Endy, J. C. Frisvad, N. Gunde-Cimerman, T. Haarmann, Y. Hadar, K. Hansen, R. I. Johnson, N. P. Keller, N. Kraševec, U. H. Mortensen, R. Perez, A. F. J. Ram, E. Record, P. Ross, V. Shapaval, C. Steiniger, H. van den Brink, J. van Munster, O. Yarden, H. A. B. Wösten, "Growing a circular economy with fungal biotechnology: a white paper" *Fungal Biol. Biotechnol.* **2020**, *7*, 5.

[16] K. D. Hyde, J. Xu, S. Rapior, R. Jeewon, S. Lumyong, A. G. T. Niego, P. D. Abeywickrama, J. V. S. Aluthmuhandiram, R. S. Brahamanage, S. Brooks, A. Chaiyasen, K. W. T. Chethana, P. Chomnunti, C. Chepkirui, B. Chuankid, N. I. de Silva, M. Doilom, C. Faulds, E. Gentekaki, V. Gopalan, P. Kakumyan, D. Harishchandra, H. Hemachandran, S. Hongsanan, A. Karunarathna, S. C. Karunarathna, S. Khan, J. Kumla, R. S. Jayawardena, J.-K. Liu, N. Liu, T. Luangharn, A. P. G. Macabeo, D. S. Marasinghe, D. Meeks, P. E. Mortimer, P. Mueller, S. Nadir, K. N. Nataraja, S. Nontachaiyapoom, M. O'Brien, W. Penkhrue, C. Phukhamsakda, U. S. Ramanan, A. R. Rathnayaka, R. B. Sadaba, B. Sandargo, B. C. Samarakoon, D. S.

Tennakoon, R. Siva, W. Sriprom, T. S. Suryanarayanan, K. Sujarit, N. Suwannarach, T. Suwunwong, B. Thongbai, N. Thongklang, D. Wei, S. N. Wijesinghe, J. Winiski, J. Yan, E. Yasanthika, M. Stadler, "The amazing potential of fungi: 50 ways we can exploit fungi industrially" *Fungal Divers.* **2019**, *97*, 1–136.

[17] N. P. Keller, "Fungal secondary metabolism: regulation, function and drug discovery" *Nat. Rev. Microbiol.* **2019**, *17*, 167–180.

[18] J. Macheleidt, D. J. Mattern, J. Fischer, T. Netzker, J. Weber, V. Schroeckh, V. Valiante, A. A. Brakhage, "Regulation and Role of Fungal Secondary Metabolites" *Annu. Rev. Genet.* **2016**, *50*, 371–392.

[19] A. Fleming, "On the antibacterial action of cultures of a *penicillium*, with special reference to their use in the isolation of B. influenzae" *Br. J. Exp. Pathol.* **1929**, *10*, 226.

[20] Y. Fan, X. Liu, N. O. Keyhani, G. Tang, Y. Pei, W. Zhang, S. Tong, "Regulatory cascade and biological activity of *Beauveria bassiana* oosporein that limits bacterial growth after host death" *Proc. Natl. Acad. Sci.* **2017**, *114*, E1578–E1586.

[21] J. E. Spraker, P. Wiemann, J. A. Baccile, N. Venkatesh, J. Schumacher, F. C. Schroeder, L. M. Sanchez, N. P. Keller, "Conserved Responses in a War of Small Molecules between a Plant-Pathogenic Bacterium and Fungi" *mBio* **2018**, *9*, 10.1128/mbio.00820-18.

[22] H. Büttner, J. Rassbach, C. Schultz, J. Popp, M. Gressler, C. Hertweck, "Beneficial Soil Fungus Kills Predatory Nematodes with Dehydropeptides Translocating into the Animal Gut" *J. Am. Chem. Soc.* **2024**, DOI 10.1021/jacs.4c12989.

[23] Y. Xu, M. Vinas, A. Alsarrag, L. Su, K. Pfohl, M. Rohlfs, W. Schäfer, W. Chen, P. Karlovsky, "Bis-naphthopyrone pigments protect filamentous ascomycetes from a wide range of predators" *Nat. Commun.* **2019**, *10*, 3579.

[24] T. Netzker, J. Fischer, J. Weber, D. J. Mattern, C. C. König, V. Valiante, V. Schroeckh, A. A. Brakhage, "Microbial communication leading to the activation of silent fungal secondary metabolite gene clusters" *Front. Microbiol.* **2015**, *6*, DOI 10.3389/fmicb.2015.00299.

[25] K. Scherlach, C. Hertweck, "Mediators of mutualistic microbe–microbe interactions" *Nat. Prod. Rep.* **2018**, *35*, 303–308.

[26] F. Shah, D. Schwenk, C. Nicolás, P. Persson, D. Hoffmeister, A. Tunlid, "Involutin is an Fe3+ reductant secreted by the ectomycorrhizal fungus *Paxillus involutus* during Fenton-based decomposition of organic matter" *Appl. Environ. Microbiol.* **2015**, *81*, 8427–8433.

[27] H. Haas, "Fungal siderophore metabolism with a focus on Aspergillus fumigatus" *Nat. Prod. Rep.* **2014**, *31*, 1266–1276.

[28] R. J. Cordero, A. Casadevall, "Functions of fungal melanin beyond virulence" *Fungal Biol. Rev.* **2017**, *31*, 99–112.

[29] *WHO Bacterial Priority Pathogens List 2024: Bacterial Pathogens of Public Health Importance, to Guide Research, Development, and Strategies to Prevent and Control Antimicrobial Resistance*, World Health Organization, Geneva, **2024**.

[30] *WHO Fungal Priority Pathogens List to Guide Research, Development and Public Health Action*, World Health Organization, Geneva, **2022**.

[31] M. Hahn, "The rising threat of fungicide resistance in plant pathogenic fungi: *Botrytis* as a case study" *J. Chem. Biol.* **2014**, *7*, 133–141.

[32] M. C. Fisher, N. J. Hawkins, D. Sanglard, S. J. Gurr, "Worldwide emergence of resistance to antifungal drugs challenges human health and food security" *Science* **2018**, *360*, 739–742.

[33] F. Prestinaci, P. Pezzotti, A. Pantosti, "Antimicrobial resistance: a global multifaceted phenomenon" *Pathog. Glob. Health* **2015**, *109*, 309–318.

[34] D. J. Newman, G. M. Cragg, "Natural Products as Sources of New Drugs over the Nearly Four Decades from 01/1981 to 09/2019" *J. Nat. Prod.* **2020**, *83*, 770–803.

[35] D. W. Denning, "Echinocandin antifungal drugs" *The Lancet* **2003**, *362*, 1142–1151.

[36] H. Sauter, W. Steglich, T. Anke, "Strobilurins: Evolution of a New Class of Active Substances" *Angew. Chem. Int. Ed.* **1999**, *38*, 1328–1349.

[37] I. Nakamura, S. Yoshimura, T. Masaki, S. Takase, K. Ohsumi, M. Hashimoto, S. Furukawa, A. Fujie, "ASP2397: a novel antifungal agent produced by *Acremonium persicinum* MF-347833" *J. Antibiot. (Tokyo)* **2017**, *70*, 45–51.

[38] K. J. Shaw, "GR-2397: Review of the Novel Siderophore-like Antifungal Agent for the Treatment of Invasive Aspergillosis" *J. Fungi* **2022**, *8*, 909.

[39] J. A. Tobert, "Lovastatin and beyond: the history of the HMG-CoA reductase inhibitors" *Nat. Rev. Drug Discov.* **2003**, *2*, 517–526.

[40] Q. Nie, F. Zhao, X. Yu, M. C. Madhusudhanan, C. Chang, S. Li, S. R. Chowdhury, B. Kille, A. Xu, R. Sharkey, C. Sun, H. Zeng, S. Liu, D. Zhou, X. Yu, K. Yang, S. A. C. Figueiredo, M. Zotova, Z. Hu, A. Y. Du, D. Guan, R. Tang, T. Treangen, J. Wang, P. N. Leão, Y. Gao, J. Chen, P. Liu, H. Renata, X. Gao, "A class of benzofuranoindoline-bearing heptacyclic fungal RiPPs with anticancer activities" *Nat. Chem. Biol.* **2025**, 1–10.

[41] J. Shyong, J. Wang, Q.-D. Tran Huynh, M. Fayzullina, B. Yuan, C.-K. Lee, T. Minehan, P. M. Seidler, C. C. C. Wang, "Discovery of penicillic acid as a chemical probe against tau aggregation in Alzheimer's disease" *Chem. Sci.* **2024**, *15*, 20467–20477.

[42] C. T. Walsh, "Tailoring enzyme strategies and functional groups in biosynthetic pathways" *Nat. Prod. Rep.* **2023**, *40*, 326–386.

[43] Y. Sun, J. Gerke, K. Becker, E. Kuhnert, B. Verwaaijen, D. Wibberg, J. Kalinowski, M. Stadler, R. J. Cox, "Rapid discovery of terpene tailoring enzymes for total biosynthesis" *Chem. Sci.* **2023**, *14*, 13463–13467.

[44] Y. Nakashima, T. Mitsuhashi, Y. Matsuda, M. Senda, H. Sato, M. Yamazaki, M. Uchiyama, T. Senda, I. Abe, "Structural and Computational Bases for Dramatic Skeletal Rearrangement in Anditomin Biosynthesis" *J. Am. Chem. Soc.* **2018**, *140*, 9743–9750.
[45] A. Rokas, M. E. Mead, J. L. Steenwyk, H. A. Raja, N. H. Oberlies, "Biosynthetic gene clusters and the evolution of fungal chemodiversity" *Nat. Prod. Rep.* **2020**, *37*, 868–878.
[46] M. T. Robey, L. K. Caesar, M. T. Drott, N. P. Keller, N. L. Kelleher, "An interpreted atlas of biosynthetic gene clusters from 1,000 fungal genomes" *Proc. Natl. Acad. Sci.* **2021**, *118*, e2020230118.
[47] B. Wei, T.-T. Ying, H.-W. Lv, Z.-Y. Zhou, H. Cai, G.-A. Hu, H.-M. Liang, W.-C. Yu, Y.-L. Yu, A.-L. Fan, K. Hong, X.-N. Li, H. Wang, "Global analysis of fungal biosynthetic gene clusters reveals the diversification of diketopiperazine biosynthesis" *Bioresour. Technol.* **2025**, *422*, 132218.
[48] L. K. Caesar, N. L. Kelleher, N. P. Keller, "In the fungus where it happens: History and future propelling *Aspergillus nidulans* as the archetype of natural products research" *Fungal Genet. Biol. FG B* **2020**, *144*, 103477.
[49] L. Hendrickson, C. Ray Davis, C. Roach, D. Kim Nguyen, T. Aldrich, P. C. McAda, C. D. Reeves, "Lovastatin biosynthesis in *Aspergillus terreus*: Characterization of blocked mutants, enzyme activities and a multifunctional polyketide synthase gene" *Chem. Biol.* **1999**, *6*, 429–439.
[50] R. Nofiani, K. de Mattos-Shipley, K. E. Lebe, L.-C. Han, Z. Iqbal, A. M. Bailey, C. L. Willis, T. J. Simpson, R. J. Cox, "Strobilurin biosynthesis in Basidiomycete fungi" *Nat. Commun.* **2018**, *9*, 3940.
[51] J. Yu, P.-K. Chang, K. C. Ehrlich, J. W. Cary, D. Bhatnagar, T. E. Cleveland, G. A. Payne, J. E. Linz, C. P. Woloshuk, J. W. Bennett, "Clustered Pathway Genes in Aflatoxin Biosynthesis" *Appl. Environ. Microbiol.* **2004**, *70*, 1253–1262.
[52] J. Takino, A. Kotani, T. Ozaki, W. Peng, J. Yu, Y. Guo, S. Mochizuki, K. Akimitsu, M. Hashimoto, T. Ye, A. Minami, H. Oikawa, "Biochemistry-Guided Prediction of the Absolute Configuration of Fungal Reduced Polyketides" *Angew. Chem. Int. Ed Engl.* **2021**, *60*, 23403–23411.
[53] D. A. Herbst, C. A. Townsend, T. Maier, "The architectures of iterative type I PKS and FAS" *Nat. Prod. Rep.* **2018**, *35*, 1046–1069.
[54] C. Hertweck, "The biosynthetic logic of polyketide diversity" *Angew. Chem. Int. Ed Engl.* **2009**, *48*, 4688–4716.
[55] R. J. Cox, "Curiouser and curiouser: progress in understanding the programming of iterative highly-reducing polyketide synthases" *Nat. Prod. Rep.* **2023**, *40*, 9–27.
[56] Y.-H. Chooi, Y. Tang, "Navigating the fungal polyketide chemical space: from genes to molecules" *J. Org. Chem.* **2012**, *77*, 9933–9953.
[57] R. F. Little, C. Hertweck, "Chain release mechanisms in polyketide and non-ribosomal peptide biosynthesis" *Nat. Prod. Rep.* **2022**, *39*, 163–205.
[58] A. A. Arishi, Z. Shang, E. Lacey, A. Crombie, D. Vuong, H. Li, J. Bracegirdle, P. Turner, W. Lewis, G. R. Flematti, A. M. Piggott, Y.-H. Chooi, "Discovery and heterologous biosynthesis of glycosylated polyketide luteodienoside A reveals unprecedented glucinol-mediated product offloading by a fungal carnitine O-acyltransferase domain" *Chem. Sci.* **2024**, *15*, 3349–3356.
[59] J. M. Crawford, B. C. R. Dancy, E. A. Hill, D. W. Udwary, C. A. Townsend, "Identification of a starter unit acyl-carrier protein transacylase domain in an iterative type I polyketide synthase" *Proc. Natl. Acad. Sci. U. S. A.* **2006**, *103*, 16728–16733.
[60] J. M. Crawford, P. M. Thomas, J. R. Scheerer, A. L. Vagstad, N. L. Kelleher, C. A. Townsend, "Deconstruction of iterative multidomain polyketide synthase function" *Science* **2008**, *320*, 243–246.
[61] N. A. Löhr, M. Rakhmanov, J. M. Wurlitzer, G. Lackner, M. Gressler, D. Hoffmeister, "Basidiomycete non-reducing polyketide synthases function independently of SAT domains" *Fungal Biol. Biotechnol.* **2023**, *10*, 17.
[62] C. M. H. Watanabe, C. A. Townsend, "Initial characterization of a type I fatty acid synthase and polyketide synthase multienzyme complex NorS in the biosynthesis of aflatoxin B(1)" *Chem. Biol.* **2002**, *9*, 981–988.
[63] H. Zhou, K. Qiao, Z. Gao, M. J. Meehan, J. W.-H. Li, X. Zhao, P. C. Dorrestein, J. C. Vederas, Y. Tang, "Enzymatic Synthesis of Resorcylic Acid Lactones by Cooperation of Fungal Iterative Polyketide Synthases Involved in Hypothemycin Biosynthesis" *J. Am. Chem. Soc.* **2010**, *132*, 4530–4531.
[64] A. L. Vagstad, A. G. Newman, P. A. Storm, K. Belecki, J. M. Crawford, C. A. Townsend, "Combinatorial domain swaps provide insights into the rules of fungal polyketide synthase programming and the rational synthesis of non-native aromatic products" *Angew. Chem. Int. Ed Engl.* **2013**, *52*, 1718–1721.
[65] A. G. Newman, A. L. Vagstad, P. A. Storm, C. A. Townsend, "Systematic Domain Swaps of Iterative, Nonreducing Polyketide Synthases Provide a Mechanistic Understanding and Rationale For Catalytic Reprogramming" *J. Am. Chem. Soc.* **2014**, *136*, 7348–7362.
[66] A. O. Zabala, Y.-H. Chooi, M. S. Choi, H.-C. Lin, Y. Tang, "Fungal Polyketide Synthase Product Chain-Length Control by Partnering Thiohydrolase" *ACS Chem. Biol.* **2014**, *9*, 1576–1586.
[67] X.-L. Yang, S. Friedrich, S. Yin, O. Piech, K. Williams, T. J. Simpson, R. J. Cox, "Molecular basis of methylation and chain-length programming in a fungal iterative highly reducing polyketide synthase" *Chem. Sci.* **2019**, *10*, 8478–8489.
[68] P. A. Storm, P. Pal, C. R. Huitt-Roehl, C. A. Townsend, "Exploring Fungal Polyketide C-Methylation through Combinatorial Domain Swaps" *ACS Chem. Biol.* **2018**, *13*, 3043–3048.
[69] R. A. Cacho, J. Thuss, W. Xu, R. Sanichar, Z. Gao, A. Nguyen, J. C. Vederas, Y. Tang, "Understanding Programming of Fungal Iterative Polyketide Synthases: The Biochemical Basis for Regioselectivity by the Methyltransferase Domain in the Lovastatin Megasynthase" *J. Am. Chem. Soc.* **2015**, *137*, 15688–15691.
[70] B. Díez, S. Gutiérrez, J. L. Barredo, P. van Solingen, L. H. van der Voort, J. F. Martín, "The cluster of penicillin biosynthetic genes. Identification and characterization of the pcbAB gene encoding the alpha-aminoadipyl-

cysteinyl-valine synthetase and linkage to the pcbC and penDE genes." *J. Biol. Chem.* **1990**, *265*, 16358–16365.
[71] R. A. Cacho, W. Jiang, Y.-H. Chooi, C. T. Walsh, Y. Tang, "Identification and characterization of the echinocandin B biosynthetic gene cluster from Emericella rugulosa NRRL 11440" *J. Am. Chem. Soc.* **2012**, *134*, 16781–16790.
[72] B. D. Ames, X. Liu, C. T. Walsh, "Enzymatic Processing of Fumiquinazoline F: A Tandem Oxidative-Acylation Strategy for the Generation of Multicyclic Scaffolds in Fungal Indole Alkaloid Biosynthesis" *Biochemistry* **2010**, *49*, 8564–8576.
[73] P. Chankhamjon, D. Boettger-Schmidt, K. Scherlach, B. Urbansky, G. Lackner, D. Kalb, H.-M. Dahse, D. Hoffmeister, C. Hertweck, "Biosynthesis of the Halogenated Mycotoxin Aspirochlorine in Koji Mold Involves a Cryptic Amino Acid Conversion" *Angew. Chem.* **2014**, *126*, 13627–13631.
[74] L. Zhang, C. Wang, K. Chen, W. Zhong, Y. Xu, I. Molnár, "Engineering the biosynthesis of fungal nonribosomal peptides" *Nat. Prod. Rep.* **2023**, *40*, 62–88.
[75] X. Gao, S. W. Haynes, B. D. Ames, P. Wang, L. P. Vien, C. T. Walsh, Y. Tang, "Cyclization of fungal nonribosomal peptides by a terminal condensation-like domain" *Nat. Chem. Biol.* **2012**, *8*, 823–830.
[76] Y. Araki, T. Awakawa, M. Matsuzaki, R. Cho, Y. Matsuda, S. Hoshino, Y. Shinohara, M. Yamamoto, Y. Kido, D. K. Inaoka, K. Nagamune, K. Ito, I. Abe, K. Kita, "Complete biosynthetic pathways of ascofuranone and ascochlorin in *Acremonium egyptiacum*" *Proc. Natl. Acad. Sci. U. S. A.* **2019**, *116*, 8269–8274.
[77] H. Li, P. M. Mirzayans, M. S. Butler, A. E. Lacey, D. Vuong, R. Chen, J. A. Kalaitzis, S. A. Moggach, E. Lacey, A. M. Piggott, Y.-H. Chooi, "Discovery of brevijanazines from *Aspergillus brevijanus* reveals the molecular basis for p-nitrobenzoic acid in fungi" *Chem. Commun.* **2022**, *58*, 6296–6299.
[78] B. Yuan, M. F. Grau, R. M. Murata, T. Torok, K. Venkateswaran, J. E. Stajich, C. C. C. Wang, "Identification of the Neoaspergillic Acid Biosynthesis Gene Cluster by Establishing an In Vitro CRISPR-Ribonucleoprotein Genetic System in *Aspergillus melleus*" *ACS Omega* **2023**, *8*, 16713–16721.
[79] Y. Zhang, L. Wu, T. A. Kerr, N. K. Garg, Y. Tang, "Fragment-Guided Genome Mining of Octacyclic Cyclophane Alkaloids from Fungi" *J. Am. Chem. Soc.* **2024**, *146*, 23933–23942.
[80] E. Geib, F. Baldeweg, M. Doerfer, M. Nett, M. Brock, "Cross-Chemistry Leads to Product Diversity from Atromentin Synthetases in Aspergilli from Section Nigri" *Cell Chem. Biol.* **2019**, *26*, 223-234.e6.
[81] C. Wieder, R. Da Peres Silva, J. Witts, C. M. Jäger, E. Geib, M. Brock, "Characterisation of ascocorynin biosynthesis in the purple jellydisc fungus *Ascocoryne sarcoides*" *Fungal Biol. Biotechnol.* **2022**, *9*, 8.
[82] C. J. Balibar, A. R. Howard-Jones, C. T. Walsh, "Terrequinone A biosynthesis through L-tryptophan oxidation, dimerization and bisprenylation" *Nat. Chem. Biol.* **2007**, *3*, 584–592.
[83] C.-J. Guo, B. P. Knox, J. F. Sanchez, Y.-M. Chiang, K. S. Bruno, C. C. C. Wang, "Application of an efficient gene targeting system linking secondary metabolites to their biosynthetic genes in *Aspergillus terreus*" *Org. Lett.* **2013**, *15*, 3562–3565.
[84] E. Geib, M. Gressler, I. Viediernikova, F. Hillmann, I. D. Jacobsen, S. Nietzsche, C. Hertweck, M. Brock, "A Non-canonical Melanin Biosynthesis Pathway Protects *Aspergillus terreus* Conidia from Environmental Stress" *Cell Chem. Biol.* **2016**, *23*, 587–597.
[85] H.-H. Yeh, Y.-M. Chiang, R. Entwistle, M. Ahuja, K.-H. Lee, K. S. Bruno, T.-K. Wu, B. R. Oakley, C. C. C. Wang, "Molecular genetic analysis reveals that a nonribosomal peptide synthetase-like (NRPS-like) gene in *Aspergillus nidulans* is responsible for microperfuranone biosynthesis" *Appl. Microbiol. Biotechnol.* **2012**, *96*, 739–748.
[86] W.-W. Sun, C.-J. Guo, C. C. C. Wang, "Characterization of the product of a nonribosomal peptide synthetase-like (NRPS-like) gene using the doxycycline dependent Tet-on system in *Aspergillus terreus*" *Fungal Genet. Biol. FG B* **2016**, *89*, 84–88.
[87] C. Wieder, C. Simon-Sánchez, J. C. Liermann, R. Wiechert, K. Andresen, E. Thines, T. Opatz, A. Schüffler, "Allantofuranone Biosynthesis and Precursor-Directed Mutasynthesis of Hydroxylated Analogues" *J. Nat. Prod.* **2025**, DOI 10.1021/acs.jnatprod.5c00197.
[88] F. Alberti, K. Khairudin, E. R. Venegas, J. A. Davies, P. M. Hayes, C. L. Willis, A. M. Bailey, G. D. Foster, "Heterologous expression reveals the biosynthesis of the antibiotic pleuromutilin and generates bioactive semi-synthetic derivatives" *Nat. Commun.* **2017**, *8*, 1831.
[89] M. Kimura, T. Tokai, N. Takahashi-Ando, S. Ohsato, M. Fujimura, "Molecular and Genetic Studies of *Fusarium* Trichothecene Biosynthesis: Pathways, Genes, and Evolution" *Biosci. Biotechnol. Biochem.* **2007**, *71*, 2105–2123.
[90] Y. Yan, Q. Liu, X. Zang, S. Yuan, U. Bat-Erdene, C. Nguyen, J. Gan, J. Zhou, S. E. Jacobsen, Y. Tang, "Resistance-gene-directed discovery of a natural-product herbicide with a new mode of action" *Nature* **2018**, *559*, 415–418.
[91] R. P. Godio, J. F. Martín, "Modified oxidosqualene cyclases in the formation of bioactive secondary metabolites: Biosynthesis of the antitumor clavaric acid" *Fungal Genet. Biol.* **2009**, *46*, 232–242.
[92] M. B. Quin, C. M. Flynn, C. Schmidt-Dannert, "Traversing the fungal terpenome" *Nat. Prod. Rep.* **2014**, *31*, 1449–1473.
[93] K. L. Eley, L. M. Halo, Z. Song, H. Powles, R. J. Cox, A. M. Bailey, C. M. Lazarus, T. J. Simpson, "Biosynthesis of the 2-Pyridone Tenellin in the Insect Pathogenic Fungus *Beauveria bassiana*" *ChemBioChem* **2007**, *8*, 289–297.
[94] L. Chen, J.-W. Tang, Y. Y. Liu, Y. Matsuda, "Aspcandine: A Pyrrolobenzazepine Alkaloid Synthesized by a Fungal Nonribosomal Peptide Synthetase-Polyketide Synthase Hybrid" *Org. Lett.* **2022**, *24*, 4816–4819.
[95] C.-F. Lee, L.-X. Chen, C.-Y. Chiang, C.-Y. Lai, H.-C. Lin, "The Biosynthesis of Norsesquiterpene Aculenes Requires Three Cytochrome P450 Enzymes to Catalyze a Stepwise Demethylation Process" *Angew. Chem. Int. Ed.* **2019**, *58*, 18414–18418.

[96] S. C. Kessler, Y.-H. Chooi, “Out for a RiPP: challenges and advances in genome mining of ribosomal peptides from fungi” *Nat. Prod. Rep.* **2022**, *39*, 222–230.
[97] D. A. Yee, K. Niwa, B. Perlatti, M. Chen, Y. Li, Y. Tang, “Genome mining for unknown–unknown natural products” *Nat. Chem. Biol.* **2023**, *19*, 633–640.
[98] M. Liu, X. Zang, N. W. Vlahakis, J. A. Rodriguez, M. Ohashi, Y. Tang, “Enzymatic combinatorial synthesis of E-64 and related cysteine protease inhibitors” *Nat. Chem. Biol.* **2025**, 1–11.
[99] Y. Zhang, L. Wu, Z. Wang, W. Han, T. A. Kerr, Y. Tang, “Genome Mining of Isoindolinone-Containing Peptide Natural Products” *J. Am. Chem. Soc.* **2025**, DOI 10.1021/jacs.5c03321.
[100] J. Fricke, F. Blei, D. Hoffmeister, “Enzymatic Synthesis of Psilocybin” *Angew. Chem. Int. Ed.* **2017**, *56*, 12352–12355.
[101] G. Wong, L. R. Lim, Y. Q. Tan, M. K. Go, D. J. Bell, P. S. Freemont, W. S. Yew, “Reconstituting the complete biosynthesis of D-lysergic acid in yeast” *Nat. Commun.* **2022**, *13*, 712.
[102] F. Y. Lim, T. H. Won, N. Raffa, J. A. Baccile, J. Wisecaver, A. Rokas, F. C. Schroeder, N. P. Keller, “Fungal Isocyanide Synthases and Xanthocillin Biosynthesis in *Aspergillus fumigatus*” *mBio* **2018**, *9*, DOI 10.1128/mbio.00785-18.
[103] C. W. Johnson, M. Ohashi, Y. Tang, “How Fungi Biosynthesize 3-Nitropropanoic Acid: The Simplest yet Lethal Mycotoxin” *Org. Lett.* **2024**, *26*, 3158–3163.
[104] J. Tang, Y. Matsuda, “Discovery of fungal onoceroid triterpenoids through domainless enzyme-targeted global genome mining” *Nat. Commun.* **2024**, *15*, 4312.
[105] D.-S. Tian, E. Kuhnert, J. Ouazzani, D. Wibberg, J. Kalinowski, R. J. Cox, “The sporothriolides. A new biosynthetic family of fungal secondary metabolites” *Chem. Sci.* **2020**, *11*, 12477–12484.
[106] H. B. Bode, B. Bethe, R. Höfs, A. Zeeck, “Big Effects from Small Changes: Possible Ways to Explore Nature’s Chemical Diversity” *ChemBioChem* **2002**, *3*, 619.
[107] C. Hertweck, “Hidden biosynthetic treasures brought to light” *Nat. Chem. Biol.* **2009**, *5*, 450–452.
[108] A. A. Brakhage, V. Schroeckh, “Fungal secondary metabolites - strategies to activate silent gene clusters” *Fungal Genet. Biol. FG B* **2011**, *48*, 15–22.
[109] M. Wang, J. J. Carver, V. V. Phelan, L. M. Sanchez, N. Garg, Y. Peng, D. D. Nguyen, J. Watrous, C. A. Kapono, T. Luzzatto-Knaan, C. Porto, A. Bouslimani, A. V. Melnik, M. J. Meehan, W.-T. Liu, M. Crüsemann, P. D. Boudreau, E. Esquenazi, M. Sandoval-Calderón, R. D. Kersten, L. A. Pace, R. A. Quinn, K. R. Duncan, C.-C. Hsu, D. J. Floros, R. G. Gavilan, K. Kleigrewe, T. Northen, R. J. Dutton, D. Parrot, E. E. Carlson, B. Aigle, C. F. Michelsen, L. Jelsbak, C. Sohlenkamp, P. Pevzner, A. Edlund, J. McLean, J. Piel, B. T. Murphy, L. Gerwick, C.-C. Liaw, Y.-L. Yang, H.-U. Humpf, M. Maansson, R. A. Keyzers, A. C. Sims, A. R. Johnson, A. M. Sidebottom, B. E. Sedio, A. Klitgaard, C. B. Larson, C. A. Boya P, D. Torres-Mendoza, D. J. Gonzalez, D. B. Silva, L. M. Marques, D. P. Demarque, E. Pociute, E. C. O’Neill, E. Briand, E. J. N. Helfrich, E. A. Granatosky, E. Glukhov, F. Ryffel, H. Houson, H. Mohimani, J. J. Kharbush, Y. Zeng, J. A. Vorholt, K. L. Kurita, P. Charusanti, K. L. McPhail, K. F. Nielsen, L. Vuong, M. Elfeki, M. F. Traxler, N. Engene, N. Koyama, O. B. Vining, R. Baric, R. R. Silva, S. J. Mascuch, S. Tomasi, S. Jenkins, V. Macherla, T. Hoffman, V. Agarwal, P. G. Williams, J. Dai, R. Neupane, J. Gurr, A. M. C. Rodríguez, A. Lamsa, C. Zhang, K. Dorrestein, B. M. Duggan, J. Almaliti, P.-M. Allard, P. Phapale, L.-F. Nothias, T. Alexandrov, M. Litaudon, J.-L. Wolfender, J. E. Kyle, T. O. Metz, T. Peryea, D.-T. Nguyen, D. VanLeer, P. Shinn, A. Jadhav, R. Müller, K. M. Waters, W. Shi, X. Liu, L. Zhang, R. Knight, P. R. Jensen, B. Ø. Palsson, K. Pogliano, R. G. Linington, M. Gutiérrez, N. P. Lopes, W. H. Gerwick, B. S. Moore, P. C. Dorrestein, N. Bandeira, “Sharing and community curation of mass spectrometry data with Global Natural Products Social Molecular Networking” *Nat. Biotechnol.* **2016**, *34*, 828–837.
[110] D. A. Delgadillo, J. E. Burch, L. J. Kim, L. S. de Moraes, K. Niwa, J. Williams, M. J. Tang, V. G. Lavallo, B. Khatri Chhetri, C. G. Jones, I. H. Rodriguez, J. A. Signore, L. Marquez, R. Bhanushali, S. Woo, J. Kubanek, C. Quave, Y. Tang, H. M. Nelson, “High-Throughput Identification of Crystalline Natural Products from Crude Extracts Enabled by Microarray Technology and microED” *ACS Cent. Sci.* **2024**, *10*, 176–183.
[111] D. A. Delgadillo, L. Wu, C. Wang, Y. Zhang, K. K. Jha, J. E. Burch, L. S. de Moraes, I. H. Rodriguez, M. J. Tang, G. F. Bills, B. P. Tu, Y. Tang, H. M. Nelson, “Microcrystal Electron Diffraction-Guided Discovery of Fungal Metabolites” *J. Am. Chem. Soc.* **2025**, *147*, 26158–26164.
[112] K. Seshadri, A. N. D. Abad, K. K. Nagasawa, K. M. Yost, C. W. Johnson, M. J. Dror, Y. Tang, “Synthetic Biology in Natural Product Biosynthesis” *Chem. Rev.* **2025**, *125*, 3814–3931.
[113] K. Blin, S. Shaw, L. Vader, J. Szenei, Z. L. Reitz, H. E. Augustijn, J. D. D. Cediel-Becerra, V. de Crécy-Lagard, R. A. Koetsier, S. E. Williams, P. Cruz-Morales, S. Wongwas, A. E. Segurado Luchsinger, F. Biermann, A. Korenskaia, M. M. Zdouc, D. Meijer, B. R. Terlouw, J. J. J. van der Hooft, N. Ziemert, E. J. N. Helfrich, J. Masschelein, C. Corre, M. G. Chevrette, G. P. van Wezel, M. H. Medema, T. Weber, “antiSMASH 8.0: extended gene cluster detection capabilities and analyses of chemistry, enzymology, and regulation” *Nucleic Acids Res.* **2025**, gkaf334.
[114] B. Yuan, N. P. Keller, B. R. Oakley, J. E. Stajich, C. C. C. Wang, “Manipulation of the Global Regulator mcrA Upregulates Secondary Metabolite Production in *Aspergillus wentii* Using CRISPR-Cas9 with In Vitro Assembled Ribonucleoproteins” *ACS Chem. Biol.* **2022**, *17*, 2828–2835.
[115] Y.-M. Chiang, E. Szewczyk, A. D. Davidson, N. Keller, B. R. Oakley, C. C. C. Wang, “A Gene Cluster Containing Two Fungal Polyketide Synthases Encodes the Biosynthetic Pathway for a Polyketide, Asperfuranone, in Aspergillus nidulans” *J. Am. Chem. Soc.* **2009**, *131*, 2965–2970.
[116] H. Li, S. Shu, J. A. Kalaitzis, Z. Shang, D. Vuong, A. Crombie, E. Lacey, A. M. Piggott, Y.-H. Chooi, “Genome Mining of *Aspergillus hancockii* Unearths Cryptic Polyketide Hancockinone A Featuring a Prenylated 6/6/6/5 Carbocyclic Skeleton” *Org. Lett.* **2021**, *23*, 8789–8793.

[117] J. A. Baccile, J. E. Spraker, H. H. Le, E. Brandenburger, C. Gomez, J. W. Bok, J. Macheleidt, A. A. Brakhage, D. Hoffmeister, N. P. Keller, F. C. Schroeder, "Plant-like biosynthesis of isoquinoline alkaloids in *Aspergillus fumigatus*" *Nat. Chem. Biol.* **2016**, *12*, 419–424.
[118] J. W. Bok, N. P. Keller, "LaeA, a Regulator of Secondary Metabolism in *Aspergillus* spp" *Eukaryot. Cell* **2004**, *3*, 527–535.
[119] C. E. Oakley, M. Ahuja, W.-W. Sun, R. Entwistle, T. Akashi, J. Yaegashi, C.-J. Guo, G. C. Cerqueira, J. Russo Wortman, C. C. C. Wang, Y.-M. Chiang, B. R. Oakley, "Discovery of McrA, a master regulator of *Aspergillus* secondary metabolism" *Mol. Microbiol.* **2017**, *103*, 347–365.
[120] R. Darma, Z. Shang, J. Bracegirdle, S. Moggach, M. C. McDonald, A. M. Piggott, P. S. Solomon, Y.-H. Chooi, "Transcriptomics-Driven Discovery of New Meroterpenoid Rhynchospenes Involved in the Virulence of the Barley Pathogen *Rhynchosporium commune*" *ACS Chem. Biol.* **2025**, *20*, 421–431.
[121] I. Roux, C. Woodcraft, J. Hu, R. Wolters, C. L. M. Gilchrist, Y.-H. Chooi, "CRISPR-Mediated Activation of Biosynthetic Gene Clusters for Bioactive Molecule Discovery in Filamentous Fungi" *ACS Synth. Biol.* **2020**, *9*, 1843–1854.
[122] M. F. Grau, R. Entwistle, Y.-M. Chiang, M. Ahuja, C. E. Oakley, T. Akashi, C. C. C. Wang, R. B. Todd, B. R. Oakley, "Hybrid Transcription Factor Engineering Activates the Silent Secondary Metabolite Gene Cluster for (+)-Asperlin in *Aspergillus nidulans*" *ACS Chem. Biol.* **2018**, *13*, 3193–3205.
[123] C. Rabot, M. F. Grau, R. Entwistle, Y.-M. Chiang, Y. Zamora de Roberts, M. Ahuja, C. E. Oakley, C. C. C. Wang, R. B. Todd, B. R. Oakley, "Transcription Factor Engineering in Aspergillus nidulans Leads to the Discovery of an Orsellinaldehyde Derivative Produced via an Unlinked Polyketide Synthase Gene" *J. Nat. Prod.* **2024**, *87*, 2384–2392.
[124] Y.-M. Chiang, M. Ahuja, C. E. Oakley, R. Entwistle, A. Asokan, C. Zutz, C. C. C. Wang, B. R. Oakley, "Development of Genetic Dereplication Strains in *Aspergillus nidulans* Results in the Discovery of Aspercryptin" *Angew. Chem. Int. Ed Engl.* **2016**, *55*, 1662–1665.
[125] F. J. Jin, J.-I. Maruyama, P. R. Juvvadi, M. Arioka, K. Kitamoto, "Development of a novel quadruple auxotrophic host transformation system by argB gene disruption using adeA gene and exploiting adenine auxotrophy in *Aspergillus oryzae*" *FEMS Microbiol. Lett.* **2004**, *239*, 79–85.
[126] E. Geib, M. Brock, "ATNT: an enhanced system for expression of polycistronic secondary metabolite gene clusters in *Aspergillus niger*" *Fungal Biol. Biotechnol.* **2017**, *4*, 13.
[127] I. Tomico-Cuenca, R. L. Mach, A. R. Mach-Aigner, C. Derntl, "An overview on current molecular tools for heterologous gene expression in *Trichoderma*" *Fungal Biol. Biotechnol.* **2021**, *8*, 11.
[128] J. Zhou, X. Chen, S.-M. Li, "Construction of an expression platform for fungal secondary metabolite biosynthesis in *Penicillium crustosum*" *Appl. Microbiol. Biotechnol.* **2024**, *108*, 427.
[129] J. C. Royer, D. L. Moyer, S. G. Reiwitch, M. S. Madden, E. B. Jensen, S. H. Brown, C. C. Yonker, J. A. Johnstone, E. J. Golightly, W. T. Yoder, J. R. Shuster, "*Fusarium graminearum* A 3/5 as a Novel Host for Heterologous Protein Production" *Bio/Technology* **1995**, *13*, 1479–1483.
[130] M. R. Nielsen, R. D. Wollenberg, K. R. Westphal, T. E. Sondergaard, R. Wimmer, D. M. Gardiner, J. L. Sørensen, "Heterologous expression of intact biosynthetic gene clusters in *Fusarium graminearum*" *Fungal Genet. Biol.* **2019**, *132*, 103248.
[131] E. Skellam, S. Rajendran, L. Li, "Combinatorial biosynthesis for the engineering of novel fungal natural products" *Commun. Chem.* **2024**, *7*, 89.
[132] Y. Yan, N. Liu, Y. Tang, "Recent developments in self-resistance gene directed natural product discovery" *Nat. Prod. Rep.* **2020**, *37*, 879–892.
[133] Z. Shang, A. A. Arishi, C. Wu, F. Lao, C. L. M. Gilchrist, S. A. Moggach, E. Lacey, A. M. Piggott, Y.-H. Chooi, "Self-Resistance Gene-Guided Discovery of the Molecular Basis for Biosynthesis of the Fatty Acid Synthase Inhibitor Cerulenin" *Angew. Chem. Int. Ed.* **2025**, *64*, e202414941.
[134] L. Xie, X. Zang, W. Cheng, Z. Zhang, J. Zhou, M. Chen, Y. Tang, "Harzianic Acid from *Trichoderma afroharzianum* Is a Natural Product Inhibitor of Acetohydroxyacid Synthase" *J. Am. Chem. Soc.* **2021**, *143*, 9575–9584.
[135] H.-H. Yeh, M. Ahuja, Y.-M. Chiang, C. E. Oakley, S. Moore, O. Yoon, H. Hajovsky, J.-W. Bok, N. P. Keller, C. C. C. Wang, B. R. Oakley, "Resistance Gene-Guided Genome Mining: Serial Promoter Exchanges in *Aspergillus nidulans* Reveal the Biosynthetic Pathway for Fellutamide B, a Proteasome Inhibitor" *ACS Chem. Biol.* **2016**, *11*, 2275–2284.
[136] N. Liu, E. D. Abramyan, W. Cheng, B. Perlatti, C. J. B. Harvey, G. F. Bills, Y. Tang, "Targeted Genome Mining Reveals the Biosynthetic Gene Clusters of Natural Product CYP51 Inhibitors" *J. Am. Chem. Soc.* **2021**, *143*, 6043–6047.
[137] K. L. Dunbar, B. Perlatti, N. Liu, A. Cornelius, D. Mummau, Y.-M. Chiang, L. Hon, M. Nimavat, J. Pallas, S. Kordes, H. L. Ng, C. J. B. Harvey, "Resistance gene–guided genome mining reveals the roseopurpurins as inhibitors of cyclin-dependent kinases" *Proc. Natl. Acad. Sci.* **2023**, *120*, e2310522120.
[138] W. Zhang, X. Zhang, D. Feng, Y. Liang, Z. Wu, S. Du, Y. Zhou, C. Geng, P. Men, C. Fu, X. Huang, X. Lu, "Discovery of a Unique Flavonoid Biosynthesis Mechanism in Fungi by Genome Mining" *Angew. Chem. Int. Ed.* **2023**, *62*, e202215529.
[139] Y. Yan, X. Zang, C. S. Jamieson, H.-C. Lin, K. N. Houk, J. Zhou, Y. Tang, "Biosynthesis of the fungal glyceraldehyde-3-phosphate dehydrogenase inhibitor heptelidic acid and mechanism of self-resistance" *Chem. Sci.* **2020**, *11*, 9554–9562.
[140] T. M. Yılmaz, M. D. Mungan, A. Berasategui, N. Ziemert, "FunARTS, the Fungal bioActive compound Resistant Target Seeker, an exploration engine for target-directed genome mining in fungi" *Nucleic Acids Res.* **2023**, *51*, W191–W197.

[141] L. Chen, Q. Yue, X. Zhang, M. Xiang, C. Wang, S. Li, Y. Che, F. J. Ortiz-López, G. F. Bills, X. Liu, Z. An, "Genomics-driven discovery of the pneumocandin biosynthetic gene cluster in the fungus *Glarea lozoyensis*" *BMC Genomics* **2013**, *14*, 339.
[142] H. Tao, T. Mori, X. Wei, Y. Matsuda, I. Abe, "One Polyketide Synthase, Two Distinct Products: Trans-Acting Enzyme-Controlled Product Divergence in Calbistrin Biosynthesis" *Angew. Chem. Int. Ed Engl.* **2021**, *60*, 8851–8858.
[143] T. Awakawa, K. Yokota, N. Funa, F. Doi, N. Mori, H. Watanabe, S. Horinouchi, "Physically discrete beta-lactamase-type thioesterase catalyzes product release in atrochrysone synthesis by iterative type I polyketide synthase" *Chem. Biol.* **2009**, *16*, 613–623.
[144] D.-W. Gao, C. S. Jamieson, G. Wang, Y. Yan, J. Zhou, K. N. Houk, Y. Tang, "A Polyketide Cyclase That Forms Medium-Ring Lactones" *J. Am. Chem. Soc.* **2021**, *143*, 80–84.
[145] D. Kong, Q. He, D.-M. Lin, H. Zhang, L. Chen, Y. Fan, M.-C. Tang, Y. Zou, "Serine Hydrolase-Catalyzed Polyol Lipids are Necessary for Rodlet Layer Formation on the Cell Wall of Entomopathogenic Fungi" *J. Am. Chem. Soc.* **2025**, *147*, 4701–4706.
[146] H.-C. Lo, R. Entwistle, C.-J. Guo, M. Ahuja, E. Szewczyk, J.-H. Hung, Y.-M. Chiang, B. R. Oakley, C. C. C. Wang, "Two separate gene clusters encode the biosynthetic pathway for the meroterpenoids austinol and dehydroaustinol in *Aspergillus nidulans*" *J. Am. Chem. Soc.* **2012**, *134*, 4709–4720.
[147] C. Duan, S. Wang, Y. Yao, Y. Pan, G. Liu, "MFS Transporter as the Molecular Switch Unlocking the Production of Cage-Like Acresorbicillinol C" *J. Agric. Food Chem.* **2024**, *72*, 19061–19070.
[148] S. Kishimoto, R. Takahashi, A. Nagasawa, K. Watanabe, "Discovery, Biological Activity, and Biosynthesis of Pinocicolin A, an Antibiotic Isocyanide Metabolite Produced by *Penicillium pinophilum*" *J. Nat. Prod.* **2025**, *88*, 1068–1074.

Publications

The present cumulative thesis comprises the following four original publications:

C. Wieder, M. Künzer, R. Wiechert, K. Seipp, K. Andresen, P. Stark, A. Schüffler, T. Opatz, E. Thines. Biosynthesis of the Antifungal Polyhydroxy-Polyketide Acrophialocinol. *Org. Lett.* **2025**, *27*, 1036–1041.

C. Wieder, C. Simon-Sánchez, J. C. Liermann, R. Wiechert, K. Andresen, E. Thines, T. Opatz, A. Schüffler. Allantofuranone Biosynthesis and Precursor-Directed Mutasynthesis of Hydroxylated Analogues. *J. Nat. Prod.* **2025**, *88*, 1191–1200.

C. Wieder, R. Wiechert, A. Yemelin, L. P. Sandjo, E. Thines, T. Opatz, A. Schüffler. Biosynthesis of the Fungal Cyclic Lipodepsipeptide Pleosporacin, a New Selective Inhibitor of the Phytopathogen *Botrytis cinerea*. *ChemBioChem* **2025**, *26*, e202500315.

C. Wieder, S. Galwas, R. Wiechert, K. Seipp, A. Yemelin, E. Thines, T. Opatz, A. Schüffler. Biosynthesis of the *Paecilomyces marquandii* conidial pigment saintopin. *Fungal Biol. Biotechnol.* **2025**, *12*, 11.

Summary of Included Publications

The publications included in the present thesis address the identification, characterization, and biosynthesis of bioactive natural products isolated from fungi of the phylum Ascomycota. Each publication separately addresses one or more compounds of a different species.

The first publication reports the bioactivity-guided discovery of the new polyhydroxy-polyketides acrophialocin and acrophialocinol produced by *Acrophialophora levis* that exhibit potent antifungal activity against various plant and human pathogens. Heterologous reconstitution of the biosynthetic genes *acrA–F* enabled the elucidation of their biosynthetic pathway. The polyketide backbone is synthesized by the PKS AcrA, the truncated didomain NRPS AcrC and the trans-acting enoyl-reductase AcrB, resulting in production of the intermediate pre-acrophialocin. Subsequently, the biosynthetic pathway branches with either the CYP450 AcrE catalyzing hydroxylation of the ρ-methyl-group or the α-ketoglutarate-dependent dioxygenase AcrF catalyzing hydroxylation of the α-carbon of pre-acrophialocin, resulting in the production of either malaysic acid or acrophialocin. Finally, the biosynthetic pathway reconverges by the action of AcrF or AcrE to yield acrophialocinol. Intriguingly, the tertiary alcohol moiety introduced by AcrF seems to be crucial for antifungal activity, as the non-containing compounds exhibit reduced antifungal activity. The RTA1-like protein AcrD encoded in the *acr* BGC was shown to confer resistance to these toxic compounds, posing a new type of self-resistance that can potentially be harnessed for self-resistance enzyme-guided genome mining in the future.

The second publication reports the biosynthesis of the previously identified natural product allantofuranone, which exhibits mild to moderate antifungal activity towards some species. It was previously postulated that allantofuranone derives from the benzoquinone polyporic acid. Genome-mining of the producer *Allantophomopsis lycopodina* led to the identification of a candidate NRPS-like enzyme BGC. Heterologous expression of the NRPS-like coding gene *alfA* indeed resulted in production of polyporic acid. Subsequent reconstitution of the other biosynthetic genes allowed for full elucidation of the allantofuranone biosynthetic pathway. In brief, polyporic acid is reductively dehydrated by the bifunctional enzyme AlfC, methylated by AlfD and finally oxidatively cleaved and rearranged by the dioxygenase AlfB to produce allantofuranone. In an effort to expand the biologically tractable chemical space and potentially improve the bioactivity of allantofuranone and its biosynthetic intermediates, a combinatorial biosynthesis approach was applied to the biosynthetic pathway. To this end, polyporic acid was substituted for either ascocorynin or atromentin, mono- and dihydroxylated congeners of polyporic acid, by coexpression of the monooxygenase-coding gene AsMO6277 or replacement of AlfA with the atromentin synthase AtrA, respectively. This successfully enabled production of almost all of the respective mono- and dihydroxylated derivatives, some of which have not been reported previously.

The third publication reports the bioactivity-guided discovery of the cyclic lipodepsipeptide pleosporacin from an isolated fungal strain *Pleosporales* sp. Pleosporacin was shown to exhibit potent and selective antifungal activity against the plant pathogen *Botrytis cinerea*. Pleosporacin causes swelling of *B. cinerea* conidia upon treatment and also exhibits biosurfactant properties. Based on these observations, pleosporacin is discussed to potentially interfere with cell wall biogenesis or membrane integrity. Pleosporacin is structurally very closely related to previously reported cyclic lipodepsipeptides, however, none of their biosynthetic pathways have been characterized. Therefore, the genome of the fungal isolate *Pleosporales* sp. was mined to identify a candidate BGC responsible for pleosporacin biosynthesis. Reconstitution of the biosynthetic genes in *A. oryzae* indeed enabled heterologous production of pleosporacin, validating the identity of the *ple* BGC and allowing the proposal of a biosynthetic route. In brief, the acyl-AMP-ligase PleB activates myristic acid, which is subsequently transferred to the T_0-domain of the NRPS PleA. PleA then facilitates the condensation of L-Ser, β-Ala, D-Trp, L-Ser and D-Tyr, followed by C_T-domain-catalyzed macrolactonization. The aspartate decarboxylase PleC is proposed to provide β-Ala for the assembly line, although it is not required for heterologous production of pleosporacin.

The fourth publication reports the identification of the purple *Paecilomyces marquandii* conidial pigment as the previously reported topoisomerase I/II inhibitor saintopin. As saintopin structurally differs from other fungal naphthacenediones, its biosynthesis was investigated. A candidate nrPKS StpA was

identified by a heterologous expression of *P. marquandii* nrPKSs and subsequently validated by gene deletion in the native producer. Accessory genes required for saintopin biosynthesis were not collocated with *stpA* but encoded elsewhere in the genome. By probing candidate biosynthetic enzymes in the heterologous host *A. oryzae*, it was possible to elucidate saintopin biosynthesis. Interestingly, only two enzymes, the nrPKS StpA and a flavin-dependent monooxygenase (FMO) StpC, sufficed for heterologous saintopin production. By coexpressing *stpC* alongside either the nona- or decaketide synthase coding genes *aptA* or *adaA*, it was shown that saintopin biosynthesis proceeds via a decaketide intermediate. The mechanism by which StpC facilitates cyclization and polyketide shortening to produce saintopin from a decaketide intermediate remains elusive as of yet.

In conclusion, these publications address the biosynthesis of four bioactive fungal natural products, not only contributing to drug discovery but also expanding the biologically tractable chemical space, highlighting fungi and fungal biotechnology as a treasure trove for natural product research. The reported findings might aid in the scalable biotechnological production of the reported molecules, the identification of further bioactive molecules, the characterization of further biosynthetic pathways, or spark the interest of the medicinal chemistry and biocatalysis communities in the future.

Zusammenfassung der beinhalteten Publikationen

Die Publikationen dieser vorgelegten kumulativen Dissertation befassen sich mit der Identifikation, Charakterisierung und Biosynthese bioaktiver Naturstoffe, die aus Pilzen des Phylums Ascomycota isoliert wurden. Dabei behandelt jede Publikation separat einen oder mehrere Naturstoffe, die aus je einer Spezies isoliert wurden.

Die erste Publikation berichtet von der Bioaktivitäts-gerichteten Isolation der neuen Polyhydroxy-Polyketide Acrophialocin und Acrophialocinol aus *Acrophialophora levis*, welche vielversprechende antifungische Aktivität gegenüber einigen pflanzen- und humanpathogenen Pilzen aufweisen. Die heterologe Rekonstitution der Biosynthesegene *acrA–F* ermöglichte die Aufklärung der Biosynthese dieser Stoffe. Das Polyketid-Grundgerüst wird von der PKS AcrA, der verkürzten NRPS AcrC und der trans-agierenden Enoyl-Reduktase AcrB synthetisiert, was in der Produktion des Intermediates Pre-Acrophialocin resultiert. Anschließend zweigt der Biosyntheseweg: Entweder katalysiert die CYP450 AcrE die Hydroxylierung der ρ-Methyl-Gruppe oder die α-Ketoglutarat-abhängige Dioxygenase AcrF katalysiert die Hydroxylierung des α-Kohlenstoffs, was in der Produktion von entweder Malaysic Acid oder Acrophialocin resultiert. Letztlich konvergiert der Biosyntheseweg erneut durch die katalytische Aktivität des jeweils anderen Enzymes AcrF oder AcrE, was in der Produktion des finalen Metaboliten Acrophialocinol resultiert. Interessanterweise scheint der tertiäre Alkohol, der durch AcrF in die Verbindung eingeführt wird, eine wichtige Rolle für die antifungische Aktivität zu spielen, da die Verbindungen, die diese funktionelle Gruppe nicht besitzen, eine deutlich verringerte Wirkung aufweisen. Weiterhin wurde gezeigt, dass das RTA1-ähnliche Protein AcrD, das im *acr* BGC kodiert ist, Resistenz gegenüber diesen toxischen Verbindungen vermittelt. Dies stellt einen neuen Typ von Selbstresistenz-Mechanismus dar, welcher eventuell künftig für das Selbstresistenz-gerichtete *genome mining* genutzt werden kann.

Die zweite Publikation berichtet von der Biosynthese des zuvor bekannten Naturstoffes Allantofuranon, welcher leichte antifungische Aktivität gegenüber einzelner Spezies aufweist. Es wurde bereits zuvor postuliert, dass Allantofuranon vermutlich über das Benzochinon Polyporsäure synthetisiert wird. *Genome mining* des Produzenten *Allantophomopsis lycopodina* führte zur Identifikation eines geeigneten Kandidaten-BGC, welches ein NRPS-like Enzym kodiert. Die heterologe Expression des NRPS-like-kodierenden Gens *alfA* führte tatsächlich zur Produktion von Polyporsäure. Die anschließende Rekonstitution der anderen Biosynthesegene erlaubte die Aufklärung der vollständigen Allantofuranon Biosynthese. Kurz gesagt wird Polyporsäure zunächst vom bifunktionalen Enzym AlfC reduktiv dehydriert, von AlfD methyliert und letztlich von der Dioxygenase AlfB oxidativ gespalten und zum Furanon kontrahiert. Mit dem Ziel, die biologisch erreichbare chemische Vielfalt zu erweitern und gegebenenfalls die Bioaktivität von Allantofuranon und dessen Biosynthese-Intermediate zu verbessern, wurde kombinatorische Biosynthese betrieben. Hierzu wurde Polyporsäure im Biosyntheseweg entweder durch Ascocorynin oder Atromentin, mono- und dihydroxylierte Derivate der Polyporsäure, ersetzt. Dies gelang durch die Koexpression des Monooxygenase-kodierenden Gens AsMO6277 beziehungsweise den Austausch von AlfA durch die Atromentin-Synthase AtrA. Dieser Ansatz ermöglichte die erfolgreiche Produktion fast aller mono- und dihydroxylierten Derivate der Biosynthese-Intermediate. Einige dieser waren zuvor noch nicht bekannt.

Die dritte Publikation berichtet von der Bioaktivitäts-gerichteten Entdeckung des zyklischen Lipodepsipeptids Pleosporacin aus einem Pilz-Isolat der Ordnung *Pleosporales*. Pleosporacin weist starke und selektive antifungische Aktivität gegenüber dem Pflanzenpathogen *Botrytis cinerea* auf. Es verursacht das Anschwellen von *B. cinerea* Konidien und weist biotenside Eigenschaften auf. Basierend auf diesen Beobachtungen wird diskutiert, dass Pleosporacin möglicherweise mit der Biogenese der Zellwand oder der Membranintegrität interferiert. Pleosporacin ist mit bereits bekannten zyklischen Lipodepsipeptiden verwandt, jedoch wurde deren Biosynthese bislang noch nicht charakterisiert. Durch *genome mining* im Genom von *Pleosporales* sp. wurde deshalb ein Kandidaten-BGC identifiziert, welches mutmaßlich an der Biosynthese von Pleosporacin beteiligt sein könnte. Rekonstitution der Biosynthesegene in *A. oryzae* ermöglichte tatsächlich die heterologe Produktion von Pleosporacin. Dies bestätigte die Identität des *ple* BGCs und ermöglichte das Postulieren des Biosynthesewegs. Kurz

gesagt aktiviert die Acyl-AMP-Ligase PleB Myristinsäure, welche anschließend auf die T_0-Domäne der NRPS PleA geladen wird. PleA katalysiert anschließend die Kondensation von L-Ser, β-Ala, D-Trp, L-Ser und D-Tyr, gefolgt von Macrolactonisation durch die C_T-Domäne. Die Aspartat-Decarboxylase PleC ist vermutlich für die Bereitstellung von β-Ala für die Biosynthese verantwortlich, wobei das Enzym nicht notwendig für die heterologe Produktion von Pleosporacin ist.

Die vierte Publikation berichtet von der Identifikation des violetten *Paecilomyces marquandii* Konidien-Pigments als den zuvor bekannten Topoisomerase I/II Inhibitor Saintopin. Da Saintopin sich strukturell von anderen pilzlichen Naphthacenedionen unterscheidet, wurde dessen Biosynthese untersucht. Eine Kandidaten-nrPKS, StpA, wurde durch heterologe Expression aller nrPKS aus *P. marquandii* identifiziert und anschließend durch Gendeletion im natürlichen Produzenten bestätigt. Akzessorische Gene, die zur Biosynthese von Saintopin benötigt werden, sind nicht in der Nähe von *stpA,* sondern an einer anderen Stelle im Genom kodiert. Durch die Koexpression möglicher beteiligter Biosynthese-Enzyme im heterologen Wirtsorganismus *A. oryzae* war es möglich, die Biosynthese von Saintopin aufzuklären. Interessanterweise reichen zwei Enzyme, die nrPKS StpA und die Flavin-abhängige Monooxygenase (FMO) StpC, für die heterologe Produktion von Saintopin aus. Durch Koexpression von stpC mit den Nona- bzw. Decaketid-Synthase-kodierenden Genen *aptA* und *adaA* konnte gezeigt werden, dass die Biosynthese von Saintopin über ein Decaketid-Intermediat verläuft. Der Mechanismus, durch welchen StpC die Zyklisierung und Polyketid-Verkürzung bewirkt, um aus dem Decaketid-Intermediat Saintopin zu produzieren, ist bislang nicht aufgeklärt.

Die angeführten Publikationen adressieren zusammengefasst die Isolation und Biosynthese bioaktiver pilzlicher Naturstoffe und tragen dadurch zur Entdeckung neuer Leitstrukturen und der Ausweitung der biologisch erreichbaren chemische Vielfalt bei. Somit werden Pilze als Schatzkammer der Naturstoff-Forschung beleuchtet. Die gewonnenen Erkenntnisse können künftig zur skalierten Produktion der beschriebenen Naturstoffe genutzt werden, zur Identifikation weiterer bioaktiver Naturstoffe und Charakterisierung anderer Biosynthesewege beitragen oder das Interesse Forschender im Bereich der medizinischen Chemie und Biokatalyse wecken.

First Publication

Biosynthesis of the Antifungal Polyhydroxy-Polyketide Acrophialocinol

Carsten Wieder[1,2], Moritz Künzer[1], Rainer Wiechert[3], Kevin Seipp[3], Karsten Andresen[1], Petra Stark[2], Anja Schüffler[2], Till Opatz[3], Eckhard Thines[1,2]

[1] Institute of Molecular Physiology, Johannes Gutenberg-University, Hanns-Dieter-Huesch Weg 17, D-55128 Mainz, Germany

[2] Institut für Biotechnologie und Wirkstoff-Forschung gGmbH, Mainz, Hanns-Dieter-Huesch Weg 17, D-55128 Mainz, Germany

[3] Department of Chemistry, Johannes Gutenberg-University, Duesbergweg 10–14, D-55128 Mainz, Germany

Type of authorship:	First author
Type of article:	Research article
Share of work:	65 %
Contribution:	Conceived project and designed experiments; fermentation; natural product purification; genome mining; cloning of plasmids; generation of mutant strains; HPLC analysis; bioactivity assays; analysis and interpretation of data; writing and editing of the manuscript
Journal:	Organic Letters
Date of publication:	22.01.2025
DOI:	10.1021/acs.orglett.4c04656

OL Organic Letters

pubs.acs.org/OrgLett

Letter

Biosynthesis of the Antifungal Polyhydroxy-Polyketide Acrophialocinol

Carsten Wieder,* Moritz Künzer, Rainer Wiechert, Kevin Seipp, Karsten Andresen, Petra Stark, Anja Schüffler, Till Opatz, and Eckhard Thines*

Cite This: *Org. Lett.* 2025, 27, 1036−1041

Read Online

ACCESS | Metrics & More | Article Recommendations | Supporting Information

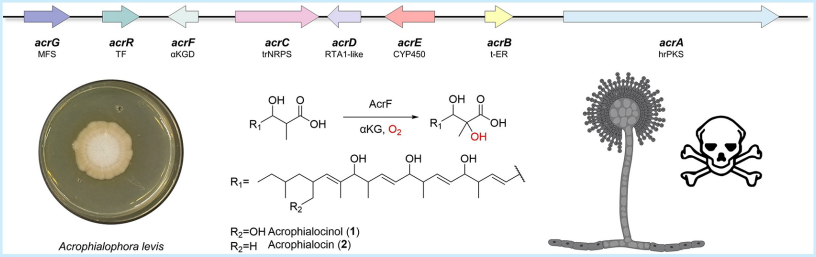

ABSTRACT: Bioactivity-guided isolation identified the main antifungal compounds produced by *Acrophialophora levis* as the new polyhydroxy-polyketides acrophialocinol (**1**) and acrophialocin (**2**). Their biosynthesis was elucidated by heterologous reconstitution in *Aspergillus oryzae* and involves an α-ketoglutarate-dependent dioxygenase-catalyzed α-hydroxylation, resulting in the formation of a tertiary alcohol that is indispensable for antifungal activity. Furthermore, self-resistance toward the polyhydroxy-polyketides is mediated by a conserved RTA1-like protein encoded in the *acr* biosynthetic gene cluster.

In recent decades, fungi have received increasing attention in the research community, particularly as a rich source for new bioactive natural products and lead structures for the development of agrochemicals and pharmaceuticals.[1,2] Employing tailor-made bioassays in combination with bioactivity-guided isolation can yield natural products with desired bioactivities. The current rise of fungal pathogens, which is contrasted by the very limited repertoire of antifungal drugs for both human and agricultural application, demands the discovery and development of novel drugs.[3−5] The biosyntheses of numerous secondary metabolites are encoded in biosynthetic gene clusters (BGCs).[6,7] While their exact biological function for the producing organism in the environment is often exceptionally difficult to determine, they can still be exploited as lead structures for therapeutic agents in medicine and agriculture.[8] Recent advances in bioinformatics[9−13] enable rapid screening of fungal genomes and prediction of BGCs, while the simultaneous establishment of robust methodologies for genetic manipulation of fungi[14−17] allows for subsequent characterization of predicted BGCs and oftentimes the discovery of new products. Linking secondary metabolites to genomic loci and understanding their biosynthesis can help to improve yields, enable manipulation for accessing novel chemical diversity, and increase knowledge on enzymatic functionalities. Fungal iterative type I highly reducing polyketide synthases (hrPKS) are multidomain enzymes that produce an enormously vast range of different polyketide scaffolds through decarboxylative Claisen condensation of acyl-CoA units complemented by optional reduction of the β-ketone and α-methylation during elongation cycles.[18−20] While not yet fully understood, the programming of hrPKS is proposed to be mediated by competition of the domains for the nascent polyketide.[21−24] Off-loading of the finished polyketide chain is often catalyzed by trans-acting enzymes in hrPKS as they frequently lack intrinsic off-loading domains.[19,25] Postsynthesis, most natural products are modified by tailoring enzymes, catalyzing a vast variety of reactions[26] ranging from simple oxidations[27] to coupling reactions[28] and molecular rearrangements,[29] thus increasing structural complexity. Intriguingly, even small structural changes, such as methylations can drastically shape and change the bioactivity of a given compound.[30] Here we report the discovery and biosynthesis of highly reduced fungal polyketides that exhibit potent antifungal activity against

Received: December 12, 2024
Revised: December 24, 2024
Accepted: December 27, 2024
Published: January 22, 2025

https://doi.org/10.1021/acs.orglett.4c04656
Org. Lett. 2025, 27, 1036−1041

Scheme 1. Structures of Acrophialocinol (1) and Acrophialocin (2)

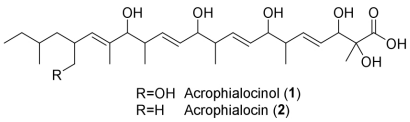

pathogenic fungal species such as *C. albicans* once a tertiary alcohol moiety is introduced into the scaffold by a tailoring enzyme.

In ongoing efforts to isolate and characterize novel bioactive natural products, we isolated and elucidated the structure of two antifungal compounds with 525 Da [M−H$^+$] (**1**) and 509 Da [M−H$^+$] (**2**) from cultivation of the fungal strain *Acrophialophora levis* IBWF 127-08 (Scheme 1). While **2** has not been reported in the literature, **1** has previously been isolated from *Chaetomium venezuelense* and patented for its antifungal activity in 1998 under the name BE-54573.[31] Based on the producing organism, we propose the common names acrophialocin (**2**) and acrophialocinol (**1**). Structurally, **1** and **2** are polyhydroxy-polyketides, more precisely belonging to the phomenoic acid (PMA)-clade of highly reduced polyketides, established by Takino et al.[32,33] PMA-clade polyketides are reminiscent of fatty acids and generally share an acyclic scaffold decorated by multiple methyl and hydroxyl moieties, although intramolecular condensation is also observed in some cases.[32,34] Multiple PMA-clade polyketides have been associated with diverse bioactivities, such as the antifungal activity of phomenoic acid[33] and sporminarins,[35] potentiation of the antifungal capacity of amphotericin B up to 32-fold (phialotide F),[36] anti-DGAT (diacylglycerol acyltransferase) activity of roselipins[37] and cytotoxicity of cladionol A.[38]

Genome mining based on the phomenoic acid BGC of *Leptosphaeria maculans* assisted by clinker[11] analysis identified a target BGC (*acr* cluster) likely involved in the biosynthesis of **1** in *A. levis IBWF 127-08* (Figure 1, Figure S3; GenBank accession number: PQ181459). The *acr* cluster encodes a major facilitator superfamily (MFS) transporter *acrG*, a transcription factor (TF) *acrR*, an α-ketoglutarate-dependent dioxygenase (αKGD) *acrF*, a truncated nonribosomal peptide synthetase (trNRPS) *acrC* only harboring a C- and an A-domain, an RTA1-like protein *acrD*, a cytochrome P450 monooxygenase (CYP450) *acrE*, a trans-acting enoyl-reductase (t-ER) *acrB* and a hrPKS *acrA* with the domain structure KS-AT-DH-CMeT-ER-KR-ACP (Figure 1, Table S5). The biosynthetic genes were heterologously reconstituted in the expression host *Aspergillus oryzae* OP12 (Figure 2).[17,27] The expression of solely hrPKS *acrA* did not lead to the production of any compounds absent in the control strain, as it lacks an intrinsic domain for product off-loading. This function is frequently fulfilled by a collaborating enzyme, and indeed, the coexpression of *acrA* alongside the trNRPS *acrC* resulted in the production of **3** with 489 Da [M−H$^+$]. Therefore, *acrC* is

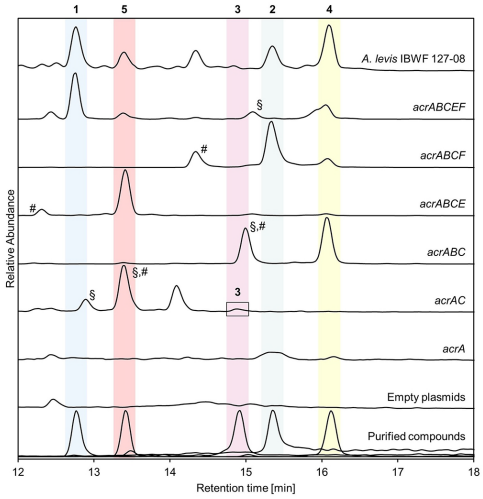

Figure 2. Heterologous reconstitution of acrophialocinol (**1**) biosynthesis in *A. oryzae* OP12. Total Ion chromatograms of mycelia extracts from *A. levis* IBWF 127-08, *A. oryzae* OP12 mutant strains expressing *acr* genes, and purified compounds. The peak highlighted by the black box corresponds to **3**. Peaks labeled with § do not correspond to the boxes in which they are (partially) in. Peaks labeled with # correspond to hypothesized degradation products.

proposed to catalyze the hydrolytic release of the nascent polyketide, which is in accord with previous findings.[32] Despite efforts in purifying **3**, we did not manage to obtain sufficient amounts for structure elucidation, as yields were too low in both the native and heterologous producer. We hypothesized that the terminal saturation in **1** and **2** was dependent on the action of the t-ER AcrB, as hrPKS-intrinsic ER domains are frequently dysfunctional.[19,32,34,39−41] Additional coexpression of tER AcrB led to the production of **4** with 493 Da [M−H$^+$], which was then purified from *A. levis* for structure elucidation. **4** appears to be the first actual intermediate in the biosynthesis of **1**, and therefore, we propose the name pre-acrophialocin. Given the structure of **4** and the MW difference between **3** and **4**, **3** is likely the terminally unsaturated congener of **4** we propose to name didehydro-pre-acrophialocin. **3** is likely a biosynthetic shunt product that is not being converted any further. Introduction of CYP450 *acrE* into OP12_*acrABC* resulted in the production of **5** with 509 Da [M−H$^+$]. Purification and structure elucidation confirmed its identity with the previously reported compound malaysic acid,[42] harboring the ρ-methyl hydroxylation also found in **1**. While it was not possible to assign any stereochemistry to compounds **1**, **2**, **4** and **5**, a putative stereochemistry for the polyketide scaffold can be proposed based on the stereo-

Figure 1. Scheme of *acr* biosynthetic gene cluster encoding acrophialocinol (**1**) biosynthesis in *Acrophialophora levis* IBWF 127-08: ACP, acyl carrier protein domain; AT, acyl transferase domain; C, condensation domain; A, adenylation domain; CMeT, C-methyl transferase domain; DH, dehydratase domain; ER, enoyl reductase domain; KR, ketoreductase domain; KS, ketosynthase domain

https://doi.org/10.1021/acs.orglett.4c04656
Org. Lett. 2025, 27, 1036−1041

Scheme 2. Proposed Acrophialocinol (1) Biosynthetic Pathway (*Structure Proposed)

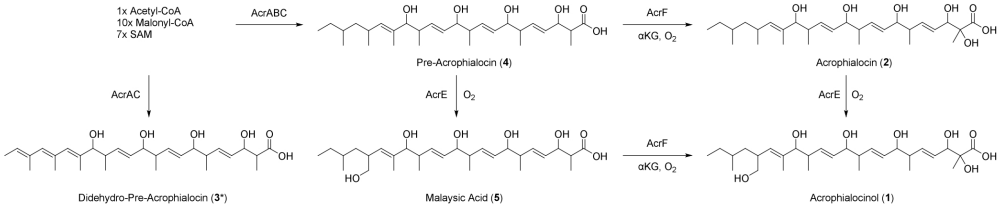

chemical rule introduced by Takino et al.,[32] who assigned canonical stereospecificities to the reductive domains of hrPKS (Figure S4). However, the configuration of the α-hydroxyl group exclusive to compounds **1** and **2** remains elusive. The αKGD encoded by *acrF* is absent in other reported PMA-clade BGCs and was therefore hypothesized to catalyze the α-hydroxylation of **4** and **5** to produce **2** and **1**. αKGDs are abundantly found in natural product biosynthesis, catalyzing a vast range of different, mostly oxygenating reactions.[43] Indeed, when *acrF* was introduced into OP12_*acrABC* and OP12_*acrABCE*, **2** and **1** were the major products produced, respectively. As both **2** and **5** are produced by the native producer, biosynthesis can progress via both routes. Interestingly, both the *acr*-gene-expressing mutants and *A. levis* additionally produced compounds with mass shifts of −40 Da (not visible in the *acrABCEF* trace, Figure S5) compared to the biosynthetic intermediates, which likely are degradation products derived from spontaneous oxidation similar to the findings of Kotani et al.[34] This concluded heterologous reconstitution of the biosynthetic pathway, highlighting (1) a diverging/converging biosynthetic route and (2) a new functionality in polyhydroxy-polyketide biosynthesis, namely, an α-hydroxylation introduced by the αKGD *acrF* (Scheme 2). In chemical synthesis, hydroxylation of C(sp^3)−H bonds and particularly asymmetric synthesis of chiral tertiary alcohols is rather challenging.[44−48] Therefore, biochemists have already explored the potential of enzymes such as α-KGDs to overcome these challenges and access these functionalities more efficiently.[49−51] Next, we examined the conidia germination inhibitory, antifungal, and antibacterial activity (Table 1) of the isolated compounds. None of the substances exhibited any antibacterial activity. **1** and **2** exhibited broad conidia germination inhibitory and antifungal activity, with **2** exhibiting the highest activity against all species, with a peak antifungal capacity of as low as 2.5 μg/mL against *Candida albicans*. For comparison, while dependent on the particular test setup, the MIC of archetype antifungal drug Amphotericin B, which is frequently used for treating systemic mycoses such as candidiasis or aspergillosis, against AmB-susceptible *C. albicans* strain ATC90028 is reported multiple times to be ≤0.5 μg/mL.[52,53] In comparison, **4** and **5** barely exhibited any activity in the assays. The observed discrepancy in bioactivity between **1**, **2** and **4**, **5**, indicates a potential role of the tertiary alcohol moiety in potentiating the biological activity of the scaffold. Although their contribution to bioactivity has not been described in itself, tertiary alcohol moieties can be found in a variety of different pharmaceuticals, such as the anticancer drugs camptothecin and doxorubicin, the antifungal drugs fluconazole and nystatin A1, the antituberculosis agent bedaquiline, and the angiogenesis inhibitor (−)-ovalicin (Scheme S1). In the case of **1** and **2**, the improved antifungal activity might arise from enhancing the inherently amphiphilic character of these scaffolds, which might contribute to solubility, permeability or sequestration. Besides the catalytically active enzymes, the *acr* cluster encodes an RTA1-like protein AcrD (24.12% identity, e-value: 3e-08 when compared to ScRTA1) that is conserved in PMA-clade BGCs.[32,54] RTA1-like proteins are a class of transmembrane lipid-translocating exporters, with the eponymous protein RTA1 having first been reported in *Saccharomyces cerevisiae* to mediate resistance to 7-aminocholesterol.[55] While 7-aminocholesterol inhibits ergosterol biosynthesis, the presence or absence of RTA1 does not affect sterol composition; therefore, RTA1-mediated resistance is likely not due to efflux of the toxin.[55,56] Other fungal RTA1-like proteins have been associated with sphingoid base translocation,[57] transport of heme,[57] secretion of virulence factors[58] and azole resistance.[59,60] The high antifungal capacity of **1** and **2** likely requires a self-resistance mechanism in *A. levis*. To investigate the function and involvement of *acrD* in polyhydroxy-polyketide self-resistance, we introduced *acrD* into *A. oryzae* RIB40 and performed a germination inhibition assay in the presence of **2.** While wild-type RIB40 was already inhibited at a concentration of 5 μg/mL, OE:*acrD* was still able to germinate and grow in the presence of 100 μg/mL **2** (Figure S6). While the exact mechanism remains elusive, *acrD* is likely involved in the self-resistance of *A. levis* IBWF 127-08 toward the produced polyhydroxy-polyketides. The coexpression of *acrD* did, however, not seem to substantially increase the production of polyhydroxy-polyketides when introduced into the *acr*-gene-expressing OP12 strains (data not shown). To the best of our knowledge, this is the first time an RTA1-like

Table 1. Bioactivity of Compounds 1, 2, 4 and 5

	MIC [μg/mL]			
	1	**2**	**4**	**5**
Ascomycetes				
M. oryzae (CM)[a]	25	10	>100[d]	>100[d]
M. oryzae (H_2O)[a]	25	10	>100[d]	10
B. cinerea[a]	25	5[c]	>100[d]	>100[d]
F. graminearum[a]	100[c]	25[c]	/	/
C. albicans[b]	25	2.5	>100[d]	100
A. oryzae[a]	25	5	>100[d]	>100[d]
Oomycetes				
P. infestans[b]	10	5	>100[d]	>100[d]
Bacteria				
A. migulanus[b]	>100[d]	>100[d]	>100[d]	>100[d]
E. dissolvens[b]	>100[d]	>100[d]	>100[d]	>100[d]

[a]Germination inhibition. [b]Growth inhibition. [c]Only 90% inhibition. [d]Only partially inhibited at maximum tested concentration.

https://doi.org/10.1021/acs.orglett.4c04656
Org. Lett. 2025, 27, 1036−1041

protein has been associated with self-resistance toward an endogenously produced toxin. Therefore, RTA1-like proteins might potentially be used as a query for self-resistance guided genome mining.[13,61,62] In summary, we report the isolation and biosynthesis of three new and one previously described polyhydroxy-polyketides **1**, **2**, **4** and **5** in *A. levis* IBWF 127-08. Evaluation of bioactivity revealed potent antifungal activity of **1** and **2** against multiple different species, including plant and human pathogens, which seems to be dependent on the tertiary alcohol moiety introduced by AcrF. Furthermore, we report the involvement of an RTA1-like protein AcrD in self-resistance against these bioactive polyhydroxy-polyketides.

■ ASSOCIATED CONTENT

Data Availability Statement

The data underlying this study are available in the published article and its Supporting Information.

Supporting Information

The Supporting Information is available free of charge at https://pubs.acs.org/doi/10.1021/acs.orglett.4c04656.

Experimental procedures; supplementary figures; supplementary tables; analytical data and NMR spectra (PDF)

■ AUTHOR INFORMATION

Corresponding Authors

Carsten Wieder − *Institute of Molecular Physiology, Johannes Gutenberg-University, D-55128 Mainz, Germany; Institut für Biotechnologie und Wirkstoff-Forschung gGmbH, D-55128 Mainz, Germany;* orcid.org/0009-0008-7991-5524; Email: cawieder@uni-mainz.de

Eckhard Thines − *Institute of Molecular Physiology, Johannes Gutenberg-University, D-55128 Mainz, Germany; Institut für Biotechnologie und Wirkstoff-Forschung gGmbH, D-55128 Mainz, Germany*; Email: thines@uni-mainz.de

Authors

Moritz Künzer − *Institute of Molecular Physiology, Johannes Gutenberg-University, D-55128 Mainz, Germany;* orcid.org/0009-0000-2518-8618

Rainer Wiechert − *Department of Chemistry, Johannes Gutenberg-University, D-55128 Mainz, Germany;* orcid.org/0009-0009-1385-4738

Kevin Seipp − *Department of Chemistry, Johannes Gutenberg-University, D-55128 Mainz, Germany*

Karsten Andresen − *Institute of Molecular Physiology, Johannes Gutenberg-University, D-55128 Mainz, Germany;* orcid.org/0000-0003-1790-325X

Petra Stark − *Institut für Biotechnologie und Wirkstoff-Forschung gGmbH, D-55128 Mainz, Germany*

Anja Schüffler − *Institut für Biotechnologie und Wirkstoff-Forschung gGmbH, D-55128 Mainz, Germany*

Till Opatz − *Department of Chemistry, Johannes Gutenberg-University, D-55128 Mainz, Germany;* orcid.org/0000-0002-3266-4050

Complete contact information is available at: https://pubs.acs.org/10.1021/acs.orglett.4c04656

Author Contributions

C.W. conceived the study. C.W. designed the experiments. C.W. and M.K. conducted the biological experiments. K.A. performed bioinformatic analysis. C.W., P.S., and M.K. performed metabolite purification. K.S. and R.W. performed structure elucidation of purified metabolites. E.T., A.S., and T.O. supervised the experiments. All authors reviewed and interpreted the obtained data and results. C.W. wrote the manuscript. All authors contributed to editing and revising of the manuscript. All authors read and approved the final version of the manuscript.

Notes

The authors declare no competing financial interest.

■ ACKNOWLEDGMENTS

Aspergillus oryzae strain OP12 *pyrG*$^-$ and plasmids SM-Xpress_URA and SM-Xpress_pabA were kindly provided by Matthias Brock (University of Nottingham, UK). We thank Andreas Schneider (ibwf, Mainz) for insightful discussions on the manuscript. This work was supported by the Rhineland-Palatinate Center for Natural Products Research. Parts of the abstract graphic were created with BioRender.com.

■ REFERENCES

(1) Newman, D. J.; Cragg, G. M. Natural Products as Sources of New Drugs over the Nearly Four Decades from 01/1981 to 09/2019. *J. Nat. Prod.* **2020**, *83* (3), 770−803.

(2) Schueffler, A.; Anke, T. Fungal natural products in research and development. *Natural product reports* **2014**, *31* (10), 1425−1448.

(3) Organization, W. H. *WHO fungal priority pathogens list to guide research, development and public health action*; World Health Organization, 2022.

(4) Chowdhary, A.; Sharma, C.; Meis, J. F. Candida auris: A rapidly emerging cause of hospital-acquired multidrug-resistant fungal infections globally. *PLoS pathogens* **2017**, *13* (5), e1006290.

(5) Lockhart, S. R.; Chowdhary, A.; Gold, J. A. W. The rapid emergence of antifungal-resistant human-pathogenic fungi. *Nature Reviews Microbiology* **2023**, *21* (12), 818−832.

(6) Fischbach, M. A.; Walsh, C. T.; Clardy, J. The evolution of gene collectives: How natural selection drives chemical innovation. *Proc. Natl. Acad. Sci. U.S.A.* **2008**, *105* (12), 4601−4608.

(7) Rokas, A.; Mead, M. E.; Steenwyk, J. L.; Raja, H. A.; Oberlies, N. H. Biosynthetic gene clusters and the evolution of fungal chemodiversity. *Natural product reports* **2020**, *37* (7), 868−878.

(8) Cragg, G. M.; Newman, D. J. Natural products: a continuing source of novel drug leads. *Biochimica et biophysica acta* **2013**, *1830* (6), 3670−3695.

(9) Blin, K.; Shaw, S.; Augustijn, H. E.; Reitz, Z. L.; Biermann, F.; Alanjary, M.; Fetter, A.; Terlouw, B. R.; Metcalf, W. W.; Helfrich, E. J. N.; van Wezel, G. P.; Medema, M. H.; Weber, T. antiSMASH 7.0: new and improved predictions for detection, regulation, chemical structures and visualisation. *Nucleic acids research* **2023**, *51* (W1), W46−W50.

(10) Zdouc, M.; Blin, K.; Louwen, N. L. L.; Navarro-Muñoz, J. C.; Loureiro, C.; van der Hooft, J.; Linington, R.; Weber, T.; Medema, M. MIBiG 4.0: Advancing Biosynthetic Gene Cluster Curation through Global Collaboration. *Nucl. Acids Res.* **2024**, gkae1115.

(11) Gilchrist, C. L. M.; Chooi, Y.-H. clinker & clustermap.js: automatic generation of gene cluster comparison figures. *Bioinformatics (Oxford, England)* **2021**, *37* (16), 2473−2475.

(12) Tang, J.; Matsuda, Y. Discovery of fungal onoceroid triterpenoids through domainless enzyme-targeted global genome mining. *Nat. Commun.* **2024**, *15* (1), 4312.

(13) Yılmaz, T. M.; Mungan, M. D.; Berasategui, A.; Ziemert, N. FunARTS, the Fungal bioActive compound Resistant Target Seeker, an exploration engine for target-directed genome mining in fungi. *Nucleic acids research* **2023**, *51* (W1), W191−W197.

(14) Jin, F. J.; Maruyama, J.-I.; Juvvadi, P. R.; Arioka, M.; Kitamoto, K. Development of a novel quadruple auxotrophic host transformation system by argB gene disruption using adeA gene and

exploiting adenine auxotrophy in Aspergillus oryzae. *FEMS microbiology letters* **2004**, *239* (1), 79−85.
(15) Chiang, Y.-M.; Ahuja, M.; Oakley, C. E.; Entwistle, R.; Asokan, A.; Zutz, C.; Wang, C. C. C.; Oakley, B. R. Development of Genetic Dereplication Strains in Aspergillus nidulans Results in the Discovery of Aspercryptin. *Angewandte Chemie (International ed. in English)* **2016**, *55* (5), 1662−1665.
(16) Geib, E.; Brock, M. ATNT: an enhanced system for expression of polycistronic secondary metabolite gene clusters in Aspergillus niger. *Fungal biology and biotechnology* **2017**, *4*, 13.
(17) Geib, E.; Baldeweg, F.; Doerfer, M.; Nett, M.; Brock, M. Cross-Chemistry Leads to Product Diversity from Atromentin Synthetases in Aspergilli from Section Nigri. *Cell chemical biology* **2019**, *26* (2), 223−234.e6.
(18) Hertweck, C. The biosynthetic logic of polyketide diversity. *Angewandte Chemie (International ed. in English)* **2009**, *48* (26), 4688−4716.
(19) Cox, R. J. Curiouser and curiouser: progress in understanding the programming of iterative highly-reducing polyketide synthases. *Natural product reports* **2023**, *40* (1), 9−27.
(20) Chooi, Y.-H.; Tang, Y. Navigating the fungal polyketide chemical space: from genes to molecules. *Journal of organic chemistry* **2012**, *77* (22), 9933−9953.
(21) Cacho, R. A.; Thuss, J.; Xu, W.; Sanichar, R.; Gao, Z.; Nguyen, A.; Vederas, J. C.; Tang, Y. Understanding Programming of Fungal Iterative Polyketide Synthases: The Biochemical Basis for Regioselectivity by the Methyltransferase Domain in the Lovastatin Megasynthase. *J. Am. Chem. Soc.* **2015**, *137* (50), 15688−15691.
(22) Storm, P. A.; Pal, P.; Huitt-Roehl, C. R.; Townsend, C. A. Exploring Fungal Polyketide C-Methylation through Combinatorial Domain Swaps. *ACS Chem. Biol.* **2018**, *13* (11), 3043−3048.
(23) Yang, X.-L.; Friedrich, S.; Yin, S.; Piech, O.; Williams, K.; Simpson, T. J.; Cox, R. J. Molecular basis of methylation and chain-length programming in a fungal iterative highly reducing polyketide synthase. *Chem. Sci.* **2019**, *10* (36), 8478−8489.
(24) Ma, S. M.; Li, J. W.-H.; Choi, J. W.; Zhou, H.; Lee, K. K. M.; Moorthie, V. A.; Xie, X.; Kealey, J. T.; Da Silva, N. A.; Vederas, J. C.; Tang, Y. Complete reconstitution of a highly reducing iterative polyketide synthase. *Science (New York, N.Y.)* **2009**, *326* (5952), 589−592.
(25) Little, R. F.; Hertweck, C. Chain release mechanisms in polyketide and non-ribosomal peptide biosynthesis. *Natural product reports* **2022**, *39* (1), 163−205.
(26) Walsh, C. T. Tailoring enzyme strategies and functional groups in biosynthetic pathways. *Natural product reports* **2023**, *40* (2), 326−386.
(27) Wieder, C.; Da Peres Silva, R.; Witts, J.; Jäger, C. M.; Geib, E.; Brock, M. Characterisation of ascocorynin biosynthesis in the purple jellydisc fungus Ascocoryne sarcoides. *Fungal biology and biotechnology* **2022**, *9* (1), 8.
(28) Platz, L.; Löhr, N. A.; Girkens, M. P.; Eisen, F.; Braun, K.; Fessner, N.; Bär, C.; Hüttel, W.; Hoffmeister, D.; Müller, M. Regioselective Oxidative Phenol Coupling by a Mushroom Unspecific Peroxygenase. *Angewandte Chemie (International ed. in English)* **2024**, *63* (42), e202407425.
(29) Matsuda, Y.; Wakimoto, T.; Mori, T.; Awakawa, T.; Abe, I. Complete biosynthetic pathway of anditomin: nature's sophisticated synthetic route to a complex fungal meroterpenoid. *J. Am. Chem. Soc.* **2014**, *136* (43), 15326−15336.
(30) Barreiro, E. J.; Kümmerle, A. E.; Fraga, C. A. M. The methylation effect in medicinal chemistry. *Chem. Rev.* **2011**, *111* (9), 5215−5246.
(31) Tsukamoto, M.; Kushida, H.; Nakajima, S.; Uchiyama, S.; Nukaga, Y.; Kondo, H.; Suda, H.; Ojiri, K.; Nagashima, M. Antifungal Substance BE-54753 and Its Production. JPH11269124A.
(32) Takino, J.; Kotani, A.; Ozaki, T.; Peng, W.; Yu, J.; Guo, Y.; Mochizuki, S.; Akimitsu, K.; Hashimoto, M.; Ye, T.; Minami, A.; Oikawa, H. Biochemistry-Guided Prediction of the Absolute Configuration of Fungal Reduced Polyketides. *Angewandte Chemie (International ed. in English)* **2021**, *60* (43), 23403−23411.
(33) Devys, M.; Férézou, J.-P.; Topgi, R. S.; Barbier, M.; Bousquet, J.-F.; Kollmann, A. Structure and biosynthesis of phomenoic acid, an antifungal compound isolated from Phoma lingam Tode. *J. Chem. Soc., Perkin Trans. 1* **1984**, No. 0, 2133−2137.
(34) Kotani, A.; Ozaki, T.; Takino, J.; Mochizuki, S.; Akimitsu, K.; Minami, A.; Oikawa, H. Heterologous expression of a polyketide synthase ACRTS2 in Aspergillus oryzae produces host-selective ACR toxins: coproduction of minor metabolites. *Bioscience, biotechnology, and biochemistry* **2022**, *86* (3), 287−293.
(35) Mudur, S. V.; Gloer, J. B.; Wicklow, D. T. Sporminarins A and B: antifungal metabolites from a fungicolous isolate of Sporormiella minimoides. *Journal of antibiotics* **2006**, *59* (8), 500−506.
(36) Yagi, A.; Uchida, R.; Kobayashi, K.; Tomoda, H. Polyketide glycosides phialotides A to H, new potentiators of amphotericin B activity, produced by Pseudophialophora sp. BF-0158. *Journal of antibiotics* **2020**, *73* (4), 211−223.
(37) Tomoda, H.; Ohyama, Y.; Abe, T.; Tabata, N.; Namikoshi, M.; Yamaguchi, Y.; Masuma, R.; Omura, S. Roselipins, inhibitors of diacylglycerol acyltransferase, produced by Gliocladium roseum KF-1040. *Journal of antibiotics* **1999**, *52* (8), 689−694.
(38) Kasai, Y.; Komatsu, K.; Shigemori, H.; Tsuda, M.; Mikami, Y.; Kobayashi, J. Cladionol A, a polyketide glycoside from marine-derived fungus Gliocladium species. *J. Nat. Prod.* **2005**, *68* (5), 777−779.
(39) Halo, L. M.; Marshall, J. W.; Yakasai, A. A.; Song, Z.; Butts, C. P.; Crump, M. P.; Heneghan, M.; Bailey, A. M.; Simpson, T. J.; Lazarus, C. M.; Cox, R. J. Authentic heterologous expression of the tenellin iterative polyketide synthase nonribosomal peptide synthetase requires coexpression with an enoyl reductase. *Chembiochem: a European journal of chemical biology* **2008**, *9* (4), 585−594.
(40) Ugai, T.; Minami, A.; Fujii, R.; Tanaka, M.; Oguri, H.; Gomi, K.; Oikawa, H. Heterologous expression of highly reducing polyketide synthase involved in betaenone biosynthesis. *Chemical communications (Cambridge, England)* **2015**, *51* (10), 1878−1881.
(41) Tao, H.; Mori, T.; Wei, X.; Matsuda, Y.; Abe, I. One Polyketide Synthase, Two Distinct Products: Trans-Acting Enzyme-Controlled Product Divergence in Calbistrin Biosynthesis. *Angewandte Chemie (International ed. in English)* **2021**, *60* (16), 8851−8858.
(42) ADEBOYA, M. O. Metabolites of the higher fungi. Part 27. Berteric acid, cameronic acid and malaysic acid, three new polysubstituted fatty acids related to cubensic acid from species of the fungus genus Xylaria. *J. Chem. Res. Syn.* **1995**, *9*, 356−357.
(43) Gao, S.-S.; Naowarojna, N.; Cheng, R.; Liu, X.; Liu, P. Recent examples of α-ketoglutarate-dependent mononuclear non-haem iron enzymes in natural product biosyntheses. *Natural product reports* **2018**, *35* (8), 792−837.
(44) Palone, A.; Casadevall, G.; Ruiz-Barragan, S.; Call, A.; Osuna, S.; Bietti, M.; Costas, M. C-H Bonds as Functional Groups: Simultaneous Generation of Multiple Stereocenters by Enantioselective Hydroxylation at Unactivated Tertiary C-H Bonds. *J. Am. Chem. Soc.* **2023**, *145* (29), 15742−15753.
(45) Hahn, P. L.; Lowe, J. M.; Xu, Y.; Burns, K. L.; Hilinski, M. K. Amine Organocatalysis of Remote, Chemoselective C(sp3)-H Hydroxylation. *ACS Catal.* **2022**, *12* (8), 4302−4309.
(46) Dantignana, V.; Milan, M.; Cussó, O.; Company, A.; Bietti, M.; Costas, M. Chemoselective Aliphatic C-H Bond Oxidation Enabled by Polarity Reversal. *ACS central science* **2017**, *3* (12), 1350−1358.
(47) McNeill, E.; Du Bois, J. Ruthenium-catalyzed hydroxylation of unactivated tertiary C-H bonds. *J. Am. Chem. Soc.* **2010**, *132* (29), 10202−10204.
(48) White, M. C.; Zhao, J. Aliphatic C-H Oxidations for Late-Stage Functionalization. *J. Am. Chem. Soc.* **2018**, *140* (43), 13988−14009.
(49) Münch, J.; Püllmann, P.; Zhang, W.; Weissenborn, M. J. Enzymatic Hydroxylations of sp 3 -Carbons. *ACS Catal.* **2021**, *11* (15), 9168−9203.
(50) Zwick, C. R.; Renata, H. Remote C-H Hydroxylation by an α-Ketoglutarate-Dependent Dioxygenase Enables Efficient Chemo-

https://doi.org/10.1021/acs.orglett.4c04656
Org. Lett. 2025, 27, 1036−1041

enzymatic Synthesis of Manzacidin C and Proline Analogs. *J. Am. Chem. Soc.* **2018**, *140* (3), 1165−1169.
(51) Renata, H. Exploration of Iron- and a-Ketoglutarate-Dependent Dioxygenases as Practical Biocatalysts in Natural Product Synthesis. *Synlett: accounts and rapid communications in synthetic organic chemistry* **2021**, *32* (8), 775−784.
(52) Liao, R. S.; Rennie, R. P.; Talbot, J. A. Assessment of the effect of amphotericin B on the vitality of Candida albicans. *Antimicrob. Agents Chemother.* **1999**, *43* (5), 1034−1041.
(53) Cantón, E.; Pemán, J.; Gobernado, M.; Viudes, A.; Espinel-Ingroff, A. Patterns of amphotericin B killing kinetics against seven Candida species. *Antimicrob. Agents Chemother.* **2004**, *48* (7), 2477−2482.
(54) Elliott, C. E.; Callahan, D. L.; Schwenk, D.; Nett, M.; Hoffmeister, D.; Howlett, B. J. A gene cluster responsible for biosynthesis of phomenoic acid in the plant pathogenic fungus, Leptosphaeria maculans. *Fungal genetics and biology: FG & B* **2013**, *53*, 50−58.
(55) Soustre, I.; Letourneux, Y.; Karst, F. Characterization of the Saccharomyces cerevisiae RTA1 gene involved in 7-aminocholesterol resistance. *Current genetics* **1996**, *30* (2), 121−125.
(56) Elkihel, L.; Soustre, I.; Karst, F.; Letourneux, Y. Amino- and aminomethylcholesterol derivatives with fungicidal activity. *FEMS microbiology letters* **1994**, *120* (1−2), 163−167.
(57) Manente, M.; Ghislain, M. The lipid-translocating exporter family and membrane phospholipid homeostasis in yeast. *FEMS yeast research* **2009**, *9* (5), 673−687.
(58) Smith-Peavler, E. S.; Patel, R.; Onumajuru, A. M.; Bowring, B. G.; Miller, J. L.; Brunel, J. M.; Djordjevic, J. T.; Prabu, M. M.; McClelland, E. E. RTA1 Is Involved in Resistance to 7-Amino-cholesterol and Secretion of Fungal Proteins in Cryptococcus neoformans. *Pathogens (Basel, Switzerland)* **2022**, *11* (11), 1239.
(59) Jia, X. M.; Wang, Y.; Jia, Y.; Gao, P. H.; Xu, Y. G.; Wang, L.; Cao, Y. Y.; Cao, Y. B.; Zhang, L. X.; Jiang, Y. Y. RTA2 is involved in calcineurin-mediated azole resistance and sphingoid long-chain base release in Candida albicans. *Cellular and molecular life sciences: CMLS* **2009**, *66* (1), 122−134.
(60) Srivastava, A.; Sircaik, S.; Husain, F.; Thomas, E.; Ror, S.; Rastogi, S.; Alim, D.; Bapat, P.; Andes, D. R.; Nobile, C. J.; Panwar, S. L. Distinct roles of the 7-transmembrane receptor protein Rta3 in regulating the asymmetric distribution of phosphatidylcholine across the plasma membrane and biofilm formation in Candida albicans. *Cellular microbiology* **2017**, *19* (12), e12767.
(61) Yan, Y.; Liu, N.; Tang, Y. Recent developments in self-resistance gene directed natural product discovery. *Natural product reports* **2020**, *37* (7), 879−892.
(62) Liu, N.; Abramyan, E. D.; Cheng, W.; Perlatti, B.; Harvey, C. J. B.; Bills, G. F.; Tang, Y. Targeted Genome Mining Reveals the Biosynthetic Gene Clusters of Natural Product CYP51 Inhibitors. *J. Am. Chem. Soc.* **2021**, *143* (16), 6043−6047.

https://doi.org/10.1021/acs.orglett.4c04656
Org. Lett. 2025, 27, 1036−1041

Supporting Information

Biosynthesis of the antifungal polyhydroxy-polyketide acrophialocinol

Carsten Wieder[1,2,], Moritz Künzer[1], Rainer Wiechert[3], Kevin Seipp[3], Karsten Andresen[1], Petra Stark[2], Anja Schüffler[2], Till Opatz[3], Eckhard Thines[1,2,*]*

[1] Institute of Molecular Physiology, Johannes Gutenberg-University, Hanns-Dieter-Huesch Weg 17, D-55128 Mainz, Germany

[2] Institute for Biotechnology and Drug Research (ibwf), Mainz, Hanns-Dieter-Hüsch Weg 17, D-55128 Mainz, Germany

[3] Department of Chemistry, Johannes Gutenberg-University, Duesbergweg 10–14, D-55128 Mainz, Germany

Correspondence: cawieder@uni-mainz.de (C. Wieder); thines@uni-mainz.de (E. Thines)

Table of Contents

I. Experimental Section

Organisms

Acrophialophora levis IBWF 127-08 was isolated from a soil sample (Göttingen, Germany) in 2008 and is deposited at the Institute for Biotechnology and Drug Research (ibwf), Mainz, Germany. *A. levis* IBWF 127-08 and CBS 484.70 (type strain, Westerdijk Institute, Utrecht, Netherlands) were routinely maintained on YMG agar at RT (although capable of growing at 37°C).

Aspergillus oryzae strains (RIB40 and OP12 3Δ [*pyrG*$^{-}$, *ΔpabA*, *ΔargB*]) were routinely cultivated on GG10 agar at 30 °C. For cultivation of the triple auxotroph OP12 3Δ, supplementing 10 mM uridine, 0.0001 % paba and 0,05 % arginine was required, other auxotrophic mutants were supplemented accordingly as necessary. For induction of expression OP12 mutant strains were cultivated in 2 % starch media. All mutant strains created and/or used in this study are listed in Table S. 1.

Escherichia coli DH5α was used for routine cloning work.

Table S. 1: Mutant strains used in this study

Strain	Parental Strain	Genotype	Produces	Source
OP12 *pyrG*$^{-}$	/	PamyB:terR_ptrA; *pyrG*$^{-}$	/	Geib et al. 2019
OP12 *ΔpabA*	OP12 *pyrG*$^{-}$	PamyB:terR_ptrA; ΔpabA::Ura	/	Wieder et al. 2020; This study
OP12 2Δ	OP12 *ΔpabA*	PamyB:terR_ptrA; *pyrG*$^{-}$, ΔpabA	/	Wieder et al. 2020; This study
OP12 *ΔpabA ΔargB*	OP12 2Δ	PamyB:terR_ptrA; ΔpabA; ΔargB::Ura	/	This study
OP12 3Δ	OP12 *ΔpabA ΔargB*	PamyB:terR_ptrA; *pyrG*$^{-}$, ΔpabA, ΔargB	/	This study
OP12 empty plasmid control	OP12 3Δ	PamyB:terR_ptrA	/	This study
OP12_*acrA*	OP12 3Δ	PamyB:terR_ptrA; ΔpabA, ΔargB, PterA:acrA_URA	/	This study
OP12_*acrAC*	OP12 3Δ	PamyB:terR_ptrA; ΔpabA, PterA:acrA_URA, PterA:acrC_argB	**3**	This study
OP12_*acrABC*	OP12 3Δ	PamyB:terR_ptrA, PterA:acrA_URA, PterA:acrB_paba, PterA:acrC_argB	**4**	This study

OP12_*acrABC pyrG*$^-$	OP12_*acrABC*	PamyB:terR_ptrA, PterA:acrA_URA, PterA:acrB_paba, PterA:acrC_argB, *pyrG*$^-$	**4**	This study
OP12_*acrABCE*	OP12_*acrABC pyrG*$^-$	PamyB:terR_ptrA, PterA:acrA_URA, PterA:acrB_paba, PterA:acrC_argB, PterA:acrE_URA	**5**	This study
OP12_*acrABCE pyrG*$^-$	OP12_*acrABCE*	PamyB:terR_ptrA, PterA:acrA_URA, PterA:acrB_paba, PterA:acrC_argB, PterA:acrE_URA, *pyrG*$^-$	**5**	This study
OP12_*acrABCF*	OP12_*acrABC pyrG*$^-$	PamyB:terR_ptrA, PterA:acrA_URA, PterA:acrB_paba, PterA:acrC_argB, PterA:acrF_URA	**2**	This study
OP12_*acrABCF pyrG*$^-$	OP12_*acrABCF*	PamyB:terR_ptrA, PterA:acrA_URA, PterA:acrB_paba, PterA:acrC_argB, PterA:acrF_URA, *pyrG*$^-$	**2**	This study
OP12_*acrABCEF*	OP12_*acrABCE pyrG*$^-$	PamyB:terR_ptrA, PterA:acrA_URA, PterA:acrB_paba, PterA:acrC_argB, PterA:acrE_URA, PterA:acrF_URA	**1**	This study
OP12_*acrABCEF pyrG*$^-$	OP12_*acrABCEF*	PamyB:terR_ptrA, PterA:acrA_URA, PterA:acrB_paba, PterA:acrC_argB, PterA:acrE_URA, PterA:acrF_URA, *pyrG*$^-$	**1**	This study
OP12_*acrACD*	OP12_*acrAC*	PamyB:terR_ptrA; ΔpabA, PterA:acrA_URA, PterA:acrC_argB, PterA:acrD_paba	**3**	This study
OP12_*acrABCD*	OP12_*acrABC pyrG*$^-$	PamyB:terR_ptrA, PterA:acrA_URA, PterA:acrB_paba, PterA:acrC_argB, PterA:acrD_URA	**4**	This study
OP12_*acrABCDE*	OP12_*acrABCE pyrG*$^-$	PamyB:terR_ptrA, PterA:acrA_URA, PterA:acrB_paba, PterA:acrC_argB, PterA:acrE_URA, PterA:acrD_URA	**5**	This study
OP12_*acrABCDF*	OP12_*acrABCF pyrG*$^-$	PamyB:terR_ptrA, PterA:acrA_URA, PterA:acrB_paba, PterA:acrC_argB,	**2**	This study

		PterA:acrF_URA, PterA:acrD_URA		
OP12_*acrABCDEF*	OP12_*acrABCEF* *pyrG*⁻	PamyB:terR_ptrA, PterA:acrA_URA, PterA:acrB_paba, PterA:acrC_argB, PterA:acrE_URA, PterA:acrF_URA, PterA:acrD_URA	**1**	This study
RIB40_OE:*acrD*	*A. oryzae RIB40*	PgpdA:acrD_ptrA	/	This study

Identification of fungal strain IBWF 127-08

Genomic DNA of IBWF 127-08 was purified from lyophilized mycelium using the GeneJET Plant Genomic DNA Purification Kit (Thermo Fisher). ITS and β-tubulin barcode regions were amplified from gDNA of IBWF 127-08 using the primer sets ITS1F & ITS4 and Bt2a & Bt2b with Phire Green Hot Start II PCR Mastermix (Thermo Fisher), the amplicons were purified using the Monarch PCR & DNA Cleanup Kit (NEB) and analyzed by Sanger sequencing. The consensuses of forward and reverse sequencing (found below) were used for BLAST searching the NCBI ITS and standard reference database, respectively.

```
>ITS IBWF 127-08 consensus
AGAGGAAGTAAAAGTCGTAACAAGGTCTCCGTTGGTGAACCAGCGGAGGGATCATTACAGAGTTGCAAAACTCCC
CAAACCATTGTGAACCTTACCTTCAACCGTTGCTTCGGCGGGCGGGCCACAGCGCCCCCCGGGCCCCCCCAGCGG
GGCGCCCGCCGGAGGATACCCAAACTCTTGATACTTTATGGCCTCTCTGAGTCTTCTGTACTGAATAAGTCAAAA
CTTTCAACAACGGATCTCTTGGTTCTGGCATCGATGAAGAACGCAGCGAAATGCGATAAGTAATGTGAATTGCAG
AATTCAGTGAATCATCGAATCTTTGAACGCACATTGCGCCCGCCAGTATTCTGGCGGGCATGCCTGTTCGAGCGT
CATTTCAACCATCAAGCCCCCGGGCTTGTGTTGGGGACCTGCGGCTGCCCGCAGGCCCTGAAAACCAGTGGCGGG
CTCGCTGTCACACCGAGCGTAGTAGCATCATCTCGCTCAGGGCGTGCTGCGGGTTCCGGCCGTTAAAAGCCTCTA
ATACCCAAGGTTGACCTCGGATCAGGTAGGAAGACCCGCTGAACTTAAGCATATC
>bTub IBWF 127-08 consensus
TGCTGCTTTCTGGTGTGTTAACCTCCAATCCATCCGAGCCCAAGACAATCAACGCTGACTTCGTCCACAGGCAGA
CCATCTCTGGCGAGCACGGCCTCGACAGCAATGGCGTGTACGTGAATGTCGCCGATTCCGATCGAATACCTGTTC
GCTCACCGCTTCGATAGGTACAATGGCACCTCCGAGCTCCAGCTCGAGCGCATGAACGTCTACTTCAACGAGGTG
AGTGGCATAATACAGTTAGACTCTGTGACACGAAGAGCAAACGGGGTTTGCTGACGAGTGGCTCATCTCCAGGCC
TCCGGCAACAAGTATGTCCCTCGTGCCGTCCTGGTCGATCTGGAGCCCGGCACCATGGACGCCGTCCGCGCTGGT
CCCTTCGGCCAGCTCTTCCGCCCTGACAACTTCGTCTTCGGCCAGTCCGGTGCTGGCAACAACTGGGCCAAGG
```

Sequences shared identities of 100 % (99 % query coverage, 0.0 e-value) and 99.78 % (100 % query coverage, 0.0 e-value) to the ITS and β-tubulin sequences of *Acrophialophora*

levis CBS 484.70 and FMR12780, respectively. To further validate the identity of IBWF 127-08 as *A. levis* chemotaxonomically, the LC-MS profiles of IBWF 127-08 and *A. levis* typestrain CBS 484.70 were compared. Indeed, metabolites produced by the two organisms, especially the constituents of the previously identified bioactive fractions, were identical (Figure S. 2).

Bioinformatic analyses

DNA sequencing was performed by Eurofins Genomics. For the whole genome sequencing a genome sequencer Illumina NovaSeq was used to generate 8,599,340 paired end reads with a length of 150 nucleotides each. The genome was assembled by using the Software SPAdes version 3.15.4[1] to a total length of 3,3045,443 bp in 1,563 contigs with a N50 value of 24. Gene prediction was performed by using AUGUSTUS version 3.5.0[2] and resulted in 11,063 open reading frames. The set of predicted genes was used in antiSMASH version 7.0.0[3] analysis that revealed 35 secondary metabolite biosynthesis gene cluster. Clinker[4] analysis was performed with parameters (sequence identity ≥ 0.3) set to default using the online server available at https://cagecat.bioinformatics.nl/# (last checked: 02.08.2024). The proteins encoded in the *acr* cluster were further analyzed using NCBI BLAST[5] (using Uniprot as a reference database) and InterPro[6].

Plasmid construction

For amplification of DNA fragments, Q5 Hot Start High-Fidelity DNA Polymerase (NEB) was used according to manufacturer's instructions. PCR products were purified with the Monarch PCR & DNA Cleanup Kit (NEB) and fragments assembled into linearized plasmids with the NEBuilder HiFi DNA Assembly (NEB). Primers used in this study are listed in table S. 2.

The KO plasmid for deletion of *pabA* in *A. oryzae* OP12 *pyrG*$^{-}$ was constructed as previously described[7]. Briefly, 5'- and 3'- flanks (947 bp and 798 bp, respectively) were amplified from genomic DNA and assembled into *Sma*I-restricted pUC19, with the primer overhangs creating a *Not*I-restriction site between flanks. The resulting plasmid was then opened with *Not*I and ligated to the *Not*I-excised Ura-cassette of SM-Xpress_Ura using the T4 DNA Ligase (NEB) according to manufacturer's instructions, resulting in the plasmid pKO_AopabA_Ura. The KO plasmid for deletion of *argB* in *A. oryzae* OP12 2Δ was constructed by amplifying 5'- and 3'-flanks from genomic DNA (942 bp and 977 bp, respectively) and the URA-cassette from SM-Xpress_Ura and assembling them into *Sma*I-restricted pUC19, resulting in the plasmid

pKO_AoargB_Ura. To complement arginine auxotrophic strains, the *argB* gene was amplified with its native promoter and terminator in two fragments from *Aspergillus nidulans* FGSC A4 genomic DNA and assembled into *Not*I-restricted SM-Xpress_Ura, exchanging a single base within the CDS (silent) through overlap design to eliminate the *Nco*I-restriction site present in the native CDS of *argB*, resulting in plasmid SM-Xpress_argB(mut).

Expression plasmids for the *acr* genes were cloned by amplifying *acrA*, *acrB*, *acrC*, *acrD*, *acrE* and *acrF* from *A. levis* IBWF 127-08 gDNA and cloning them into *Nco*I-restricted SM-Xpress_Ura[8] (*acrA*, *D*, *E* & *F*), SM-Xpress_paba[7] (*acrB*) and SM-Xpress_argB(mut) (*acrC*).

For construction of the constitutively active expression plasmid pOE_P*gpdA_ptrA*, the *gpdA*-promoter and terminator were amplified from *A. nidulans* genomic DNA, the *ptrA*-cassette was amplified from pPTRI[9] and all fragments assembled into *Sma*I-restricted pUC19, creating an *Eco*RV-restriction site between promoter and terminator. *acrD* was amplified from *A. levis* IBWF 127-08 gDNA and cloned into *Eco*RV-restricted pOE_PgpdA_ptrA to create pOE_acrD_ptrA.

Table S. 2: Primers used in this study

Oligo	Sequence	Purpose
oCW105	ctgcaggtcgactctagaggatccccgGGATATAGAGTTTACCCCTACTG	Cloning of pKO_AopabA for subsequent insertion of URA cassette to yield pKO_AopabA_Ura for deletion of *pabA* in *A. oryzae*
oCW106	GGAAGAATGTGGTCATGCTTTGCGGCCGCCGTATGGATGAACTGTAGC	
oCW107	CTACAGTTCATCCATACGGCGGCCGCAAAGCATGACCACATTCTTCCTC	
oCW108	gacggccagtgaattcgagctcggtacccCCCGGGTCTCAACAAAATGG	
oCW180	gcctgcaggtcgactctagaggatcccc GGGATTGAATACGGTGGCATCC	Cloning of pKO_AoargB_Ura for deletion of *argB* in *A. oryzae*
oCW181	gttgatggtgccaacaatctgcgcggccgcGATGAGATAATTTCCGGTAG	
oCW182	CTCCGCATACTACCGGAAATTATCTCATCgcggccgcgcagattgttgg	
oCW183	CTTCGGTATGGAAAGTCAAACAACGGTCCgcggccgccaggttgtcgag	
oCW184	cgaagagaagctcgacaacctggcggccgcGGACCGTTGTTTGACTTTCC	
oCW185	cggccagtgaattcgagctcggtacccgggCTTCTACTGACAACGCGCGA	
oCW186	ctcgaattcgagctcggtacccgcggccgcATTTCGCGGTTTTTTGGGGT	Cloning of SM-Xpress_argB(mut)
oCW187	ACCGACACGGGCTACAATGCAGGATACCATcGACGAAATGACAACGGAGG	
oCW188	CCTCCGTTGTCATTTCGTCgATGGTATCCTGCATTGTAGCCCGTGTCGGT	
oCW189	ggtcgactctagaggatccccgcggccgcACCTACAGCCATTGCGAAAC	

oCW201	atgcctgcaggtcgactctagaggatccccGAGCTCTGTACAGTGACCGG	Amplification of PgpdA for cloning of pOE_PgpdA_ptrA
oCW202	GGCCATTGGCTTCCGACCTGTTTCGATATCTGTGATGTCTGCTCAAGCGG	
oCW203	CCCCGCTTGAGCAGACATCACAGATATCGAAACAGGTCGGAAGCCAAT	Amplification of gpdAT for cloning of pOE_PgpdA_ptrA
oCW279	GATCCCGTAATCAATTGCCCGCGGCCGCGGACTAAGTATACCCAGATG	
oCW280	CATCTGGGTATACTTAGTCCGCGGCCGCGGGCAATTGATTACGGGATC	Amplification of ptrA for cloning of pOE_PgpdA_ptrA
oCW281	gtgaattcgagctcggtacccGCGGCCGCATGGGGTGACGATGAGCCGC	
oCW301	Catttaacaaacttctcatcacagcaccatgtctcctactgatacccctа	Amplification of acrA for cloning of pSMX_acrA_URA
oCW302	tccgcatctccaacaagatc	
oCW303	gatcttgttggagatgcgga	
oCW304	Ctatacggttcagattgaaatcactgctgcctatttctcgtttgcagcc	
oCW305	Catttaacaaacttctcatcacagcaccatgggttcaattccgaccgaag	Amplification of acrC for cloning of pSMX_acrC_argB(mut)
oCW306	ctatacggttcagattgaaatcactgctgctcagttcttcagcgtcttc	
oCW321	Catttaacaaacttctcatcacagcaccatgccccacaagctcaccatca	Amplification of acrB for cloning of pSMX_acrB_paba(rev)
oCW322	ctatacggttcagattgaaatcactgctgctcaaatctcaacaaccaact	
oCW323	Catttaacaaacttctcatcacagcaccatggcgtacgctctcagtgcca	Amplification of acrE for cloning of pSMX_acrE_URA
oCW324	ctatacggttcagattgaaatcactgctgcttattgcgcttggcgcttgg	
oCW341	catttaacaaacttctcatcacagcaccatgacagtcaacgaaccaaccg	Amplification of acrF for cloning of pSMX_acrF_URA
oCW342	ctatacggttcagattgaaatcactgctgctcaagcggccccggtcttga	
oCW359	catttaacaaacttctcatcacagcaccatggccgaacccggagagcca	Amplification of acrD for cloning of pSMX_acrD_URA
oCW360	ctatacggttcagattgaaatcactgctgctcaagccgagttggcagt	
oCW361	Cagctaccccgcttgagcagacatcacaatggccgaacccggagagcc	Amplification of acrD for cloning of pOE_acrD_ptrA
oCW362	Ctcctggccattggcttccgacctgtttctcaagccgagttggcagtcg	
ITS1F	CTTGGTCATTTAGAGGAAGTAA	sequencing barcode ITS region

ITS4	TCCTCCGCTTATTGATATGC	
Bt2a	GGTAACCAAATCGGTGCTGCTTTC	Sequencing barcode β-tubulin
Bt2b	ACCCTCAGTGTAGTGACCCTTGGC	

Fungal transformation

Aspergillus oryzae OP12 was transformed as previously described[8]. In brief, OP12 *pyrG*$^{-}$ or 3Δ were inoculated into 50 mL YEPD (1 % yeast extract, 2 % peptone, 0.5 % glucose, pH 6.5) supplemented according to autotrophies and incubated shaking at 150 rpm for 18–24 h at 30 °C. The mycelia was harvested, rinsed with and transferred to 25 mL of citrate-phosphate buffer (90 mM, pH 7.3) supplemented with 10 mM DTT and incubated gently shaking at 70 rpm for 1 h at 30 °C. Mycelia was harvested, rinsed with osmotic solution (0.6 M KCl, 10 mM phosphate buffer, pH 5.7) and transferred to 20 mL lysing enzyme solution (1.3 g VinoTaste Pro and 0.1 g lysing enzymes from *Trichoderma harzianum* dissolved in osmotic solution) and incubated shaking at 70 rpm for 2–4 h at 30 °C. Protoplast formation was monitored microscopically. Protoplasts were harvested by straining the solution through miracloth and centrifugation at 4000 rpm for 8 minutes at 4 °C. Protoplasts were subsequently washed twice with washing solution (0.6 M KCl, 0.1 M Tris/HCl, pH 7.0) and solution A (0.6 M KCl, 10 mM Tris/HCl, 50 mM $CaCl_2$, pH 7.5), respectively. Protoplasts were suspended in solution A at a concentration of ~5x10^7 protoplasts/mL. 100 µL of protoplasts and 25 µL of PEG solution (25 % PEG 8000, 10 mM Tris/HCl, 50 mM $CaCl_2$, pH 7.5) were added to 2–5 µg of linearized plasmid DNA (dissolved in ≤ 15 µL) and the mix incubated on ice. After 25 minutes, another 500 µL of PEG solution was added and gently mixed by pipetting. After additional 5 minutes, 1 mL of solution A was added and the mix inverted three times. 600 µL, 500 µL and 400 µL were added to 12 mL of GG10S1.2 (GG10, 1.2 M sorbitol) top agar (cooled to ~45 °C before addition of protoplasts), mixed by inverting two times and poured onto pre-poured GG10S1.2 bottom agar plates. Plates were allowed to dry and then incubated at 30 °C for 4–6 days. Colonies grown on transformation plates were replica-plated twice on GG10 before further analysis.

Counterselection

In between successive transformations, uridine auxotrophy was restored by counterselecting the URA-Blaster cassette as previously described[8]. Therefore, 1x10^5–1x10^6 conidia of *pyrG*$^{+}$

strains were plated on GG10 supplemented with 50 mM HEPES (pH 7.0), 20 mM uridine and 2 mg/mL 5-fluoroorotic acid. The URA cassette is flanked by direct tandem repeats homologous to one another. Homologous recombination of these tandem repeats eliminates the URA cassette, rendering the organism resistant towards 5-FOA, which is otherwise converted to the toxic metabolite 5-FU by *pyrG*. Arising colonies were replica-plated onto GG10 plates either containing or lacking 10 mM uridine to evaluate uridine auxotrophy. Auxotrophic strains were then again subjected to metabolite screening to assure the metabolites of interest were still being produced. Producing strains were then subjected to the next set of transformations.

Construction of OP12 3Δ

In order to obtain a triple-auxotrophic strain for simultaneous transformation of multiple plasmids, *pabA* and *argB* were sequentially deleted in *Aspergillus oryzae* OP12 *pyrG*$^{-}$. Deletion of *pabA* was carried out as previously described[7]. Mutants were selected on media supplemented with 0.0001 % PABA and replica-picked twice on media supplemented with or without PABA to assess auxotrophy. Multiple auxotrophic mutants were counterselected by plating on media supplemented with PABA, 20 mM uridine, 50 mM HEPES (pH 7.0) and 2 mg/mL 5-FOA. These plates were incubated up to 10 days. Colonies were replica-picked on media supplemented with PABA & uridine or only PABA to assess reobtained uridine auxotrophy. The resulting strain OP12 2Δ was then used for transformation of the *argB* knock-out plasmid pKO_AoargB_Ura. Transformants were selected on media supplemented with 0.05 % arginine and PABA and replica-picked twice on media supplemented with PABA and with or without arginine to assess auxotrophy. To reobtain uridine auxotrophy, multiple mutants were again counterselected on plates supplemented with 0.0001 % PABA, 0.05 % arginine, 20 mM uridine, 50 mM HEPES (pH 7.0) and 2 mg/mL 5-FOA. Colonies were replica-picked on media supplemented with PABA, arginine and uridine or without uridine to assess uridine auxotrophy.

Fermentation, extraction, HPLC-MS analysis and metabolite purification

Initial fermentation of *A. levis* for preliminary testing was conducted in 500 mL YMG shaking at 120 rpm at rt for 11 days. For comparing *A. levis* IBWF 127-08 and CBS 484.70, both were cultivated in 500 mL YMG shaking at 120 rpm at rt for 5 days.

Aspergillus oryzae mutant strains were cultivated in 50 mL 2 % starch media (inducing expression) shaking at 150 rpm at 30 °C for 2 days. After fermentation, the culture broth was

separated from the mycelium and both extracted separately. The culture broth was liquid-liquid extracted with a 1:1 ratio of ethyl acetate, the mycelium was extracted by overlaying with MeOH:acetone (1:1) and shaking for at least 2 hours. Crude extracts were dried *in vacuo* at 45 °C and resuspended in MeOH.

For HPLC-MS analysis, samples were applied to a LiChrospher 100 RP-18 (125 mm x 2 mm, 4 µm, Merck KGaA) column connected to Agilent DAD 1260 and Quadrupole LC/MS 6130 modules. For analytical runs a gradient of 0.1 % formic acid and acetonitrile (ACN) from 1 % to 100 % ACN was run in 20 minutes at a flow rate of 0.4 mL/min followed by 4 minutes of 100 % ACN flushing.

To identify the bioactive components of *A. levis* extracts, fractioning was carried out using the previously stated analytical HPLC gradient on a LiChrospher 100 RP-18 column (125 mm x 4 mm, 5 µm, Merck KGaA) at a flow rate of 1 mL/min, collecting 92 fractions into a 96 well plate during the first 23 minutes of the run. The plate was dried *in vacuo* before bioactivity testing (Figure S. 1).

For isolation of **1**, **2**, **4** and **5**, *A. levis* IBWF 127-08 was cultivated in 20 L of YMG media in a bioreactor at 3 L/min aeration, 120 rpm and 37 °C for 6 days. The culture broth was separated from the mycelium and extracted twice with 20 L ethyl acetate. The mycelium was lyophilized and subsequently extracted twice with 2 L MeOH:acetone (1:1) shaking overnight. The crude extracts were dried *in vacuo*, pre-fractioned by SPE (Bond Elut C18, Agilent) and compounds purified by preparative HPLC (Sunfire C18 column [100 Å, 5 µm, 19 mm x 250 mm, Waters GmbH]; 17 mL/min; 0.1 % formic acid and ACN as eluents). Gradients for purification are listed in table S. 3. Preparative HPLC yielded 8.2 mg of **1**, 7.5 mg of **2**, 3.7 mg of **4** and 3 mg of **5**. All compounds were obtained as off-white amorphous solids.

Table S. 3: Preparative HPLC gradients for purification of **1**, **2**, **4** and **5**

	Gradient	
Compounds	Time [min]	% ACN
1, 2	0	67.7
	0.32	67.7
	20.32	88.9
	20.33	100

	23	100
4	0	35
	0.3	35
	28	90
	32	100
	34	100
5	0	1
	0.3	1
	20	100
	28	100

Analytical methods for natural product elucidation

Thin layer chromatography

Analytical thin-layer chromatography (TLC), 0.25 mm silica plates (60 F254) from Merck were used, and the detection was reached by fluorescence quenching under UV light (λ = 254 nm) or by staining with potassium permanganate reagent (solution of $KMnO_4$ (3 g), K_2CO_3 (20 g), 5 % NaOH (5 mL), and H_2O (300 mL)) followed by heating at 400 °C.

NMR spectra

Unless otherwise mentioned, measured NMR spectra were recorded at 296 K on a 600 MHz Bruker Avance-III 600 spectrometer. After prior referencing to the residual solvent signal (DMSO-d_6: 2.50 ppm & 39.52 ppm for ^{1}H NMR and ^{13}C NMR, respectively), all chemical shifts (δ) are reported relative to residual solvent[10]. Coupling constants were reported in Hz and the signal multiplicities were abbreviated as follows: s (singlet), d (doublet), t (triplet), q (quartet), qd (quartet of doublet), m (multiplett). Structural assignments were made with additional information from gCOSY, gHSQC, and gHMBC experiments.

Infrared spectra

Infrared spectroscopy was performed on a Bruker Tensor 27 FTIR spectrometer including a diamond ATR unit and are reported in terms of absorption frequency $\bar{\nu}$ [cm^{-1}].

Mass spectra

HRMS was conducted on an Agilent G6545A Q-ToF with ESI, APCI or APPI source coupled with an Agilent 1260 Infinity II HPLC system. If not describe otherwise, spectra were recorded using positive ionization mode.

Optical rotations

Optical rotation measurements were accomplished with a Perkin-Elmer 241MC polarimeter at λ = 589nm. The instrument was blanked with the solvent used prior to the measurement[11].

Bioactivity assays

To test for antifungal activity, conidia of *Magnaporthe oryzae* 70-15, *Botrytis cinerea* DSM 0877, *Fusarium graminearum* DSM 21727, *Aspergillus oryzae* RIB40 and the mutant *Aspergillus oryzae* RIB40_OE:*acrD* were harvested from properly grown agar plates and diluted in 2 % malt extract media to a final concentration of $1x10^5$ conidia/mL. 200 µL of the solution were added to wells of a 96 well plate containing different concentrations of compounds. The plates were then incubated overnight at room temperature and conidia germination evaluated using a microscope. Ciclopirox served as positive control.

To assess activity against *Candida albicans* ATCC90028, fresh colonies grown on Sabouraud (Difco) plates were suspended in H_2O, diluted 1:20 in Sabouraud media and cultivated shaking at room temperature for 18–24h; growth inhibition was assessed macroscopically. Ciclopirox served as positive control.

To assess activity against *Phytophtora infestans* CBS 430.90, 2 ml of a 2-week-old liquid PDA culture were shredded using a FastPrep twice for 20 s, diluted with 5 mL of H_2O and filtered through miracloth. The filtrate was diluted 1:20 with KGA media and 200 µL distributed in 96-well test plates. Plates were incubated gently shaking at room temperature for 1 week; growth inhibition was assessed macroscopically.

To assess antibacterial activity, *Aneurinibacillus migulanus* ATCC9999 and *Enterobacter cloacae subsp. dissolvens* LMG2683 nutrient broth (Difco) precultures were inoculated and grown overnight shaking at 37 °C and 27 °C, respectively. Precultures were diluted 1:100 in fresh nutrient broth and 200 µL distributed in 96-well test plates. Tetracycline and Streptomycin served as positive controls.

Media and Recipes

Table S. 4: Media composition. For solid media, 2% agar were added before autoclaving.

Media	**Composition (per L)**
YMG	0.4 % yeast extract, 1 % malt extract, 1 % glucose
YEPD	1 % yeast extract, 2 % peptone, 0.5 % glucose, pH 6.5
GG10	50 mM glucose, 10 mM glutamine, 50 mL salt stock, 1 mL Hutners trace elements
GG10S1.2	GG10 + 1.2 M sorbitol
2% Starch	2 % soluble starch, 20 mM glutamine, 50 mL salt stock, 1 mL Hutners trace elements
20x salt stock	3.04 % KH_2PO_4, 1.04 % KCl, 1.04 % $MgSO_4 \cdot 7\ H_2O$

II. Supplementary Figures and Tables

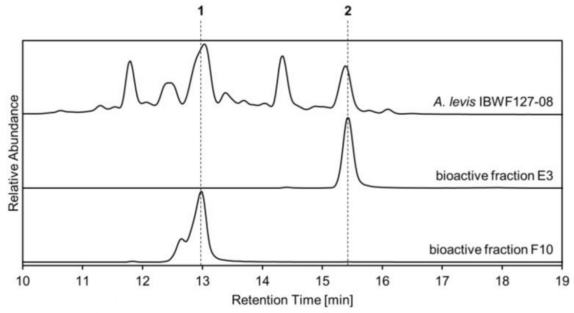

Figure S. 1: Bioactive fractions of *A. levis* extract contain compounds **1** and **2**. TICs of *Acrophialophora levis* IBWF 127-08 culture filtrate extract and bioactive fractions E3 and F10.

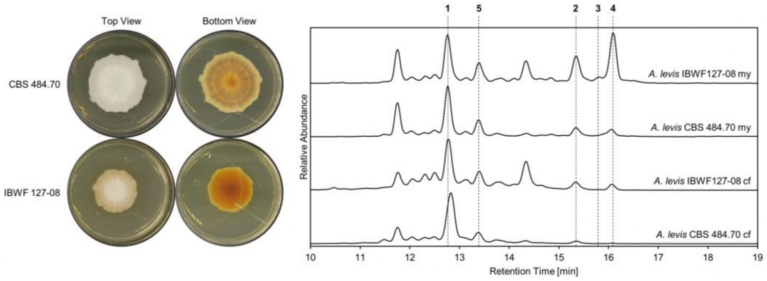

Figure S. 2: Chemotaxonomic comparison of *A. levis* strains IBWF 127-08 and CBS 484.70. Growth morphology of *A. levis* strains grown on YMG agar at 37 °C for 7 days (left). TICs of culture filtrate (cf) and mycelium (my) extracts of *A. levis* cultures grown for 5 days in 500 mL shaking at rt (right).

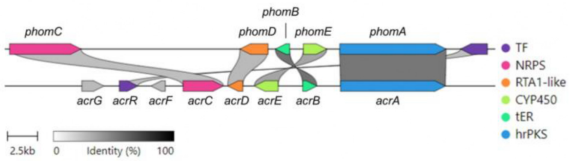

Figure S. 3: Clinker[4] comparison of *acr* and *phom* clusters.

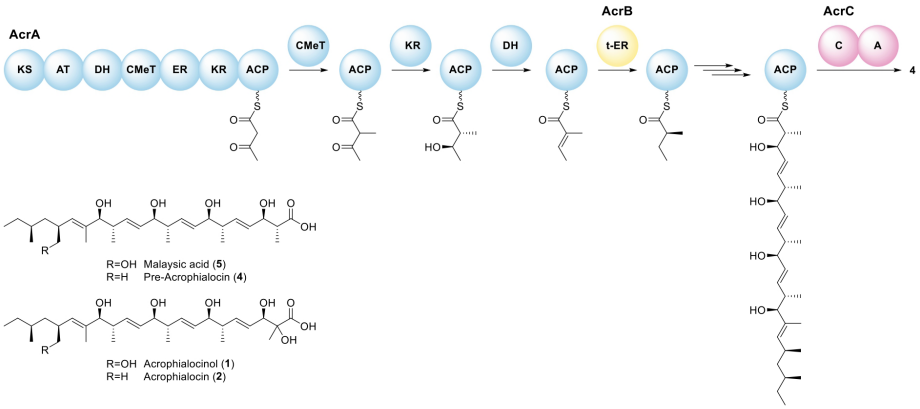

Figure S. 4: Putative stereochemistry of compounds **1**, **2**, **4** and **5** if the canonical stereochemical rule for polyketide biosynthesis proposed by Takino *et al.*[12] applies to **1** biosynthesis. The scheme representatively depicts the tailoring steps occurring during the first elongation cycle and the resulting stereochemistry of the nascent polyketide. Reduction of the achiral α-methyl-β-ketone generates R-configured α-methyl and β-hydroxyl groups. Subsequent dehydration produces an achiral intermediate. Lastly, ene-reduction facilitated by the t-ER AcrB results in formation of a S-configured α-methyl group. The subsequent elongation cycles proceed analogously, with some of the domains being skipped. Finally, the finished polyketide scaffold is hydrolysed by the trNRPS AcrC. ACP, acyl carrier protein domain; AT, acyl transferase domain; C, condensation domain; A, adenylation domain; CMeT, C-methyl transferase domain; DH, dehydratase domain; ER, enoyl reductase domain; KR, ketoreductase domain; KS, ketosynthase domain; t-ER, trans-acting enoyl reductase

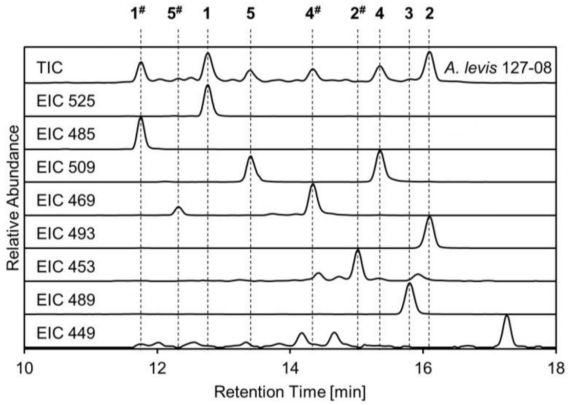

Figure S. 5: EICs of *A. levis* IBWF 127-08 mycelium extract. #Presumed degradation products of compounds **1-5**. The degradation product of **3** is not present in this mycelium extract (the EIC449 peaks do not correspond to **3**#).

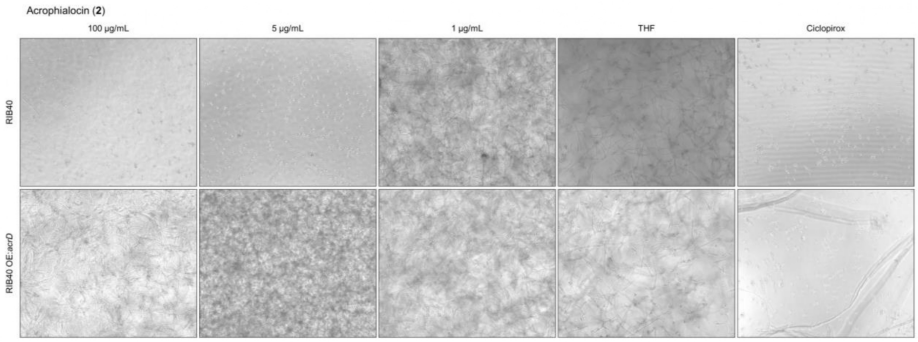

Figure S. 6 Germination inhibition assay comparing susceptibility of RIB40 and RIB40 OE:*acrD* to acrophialocin (**2**). **2** was dissolved in THF. THF served as negative control, ciclopirox served as positive control.

Scheme S. 1: Pharmaceuticals containing tertiary alcohol moiety (highlighted in red).

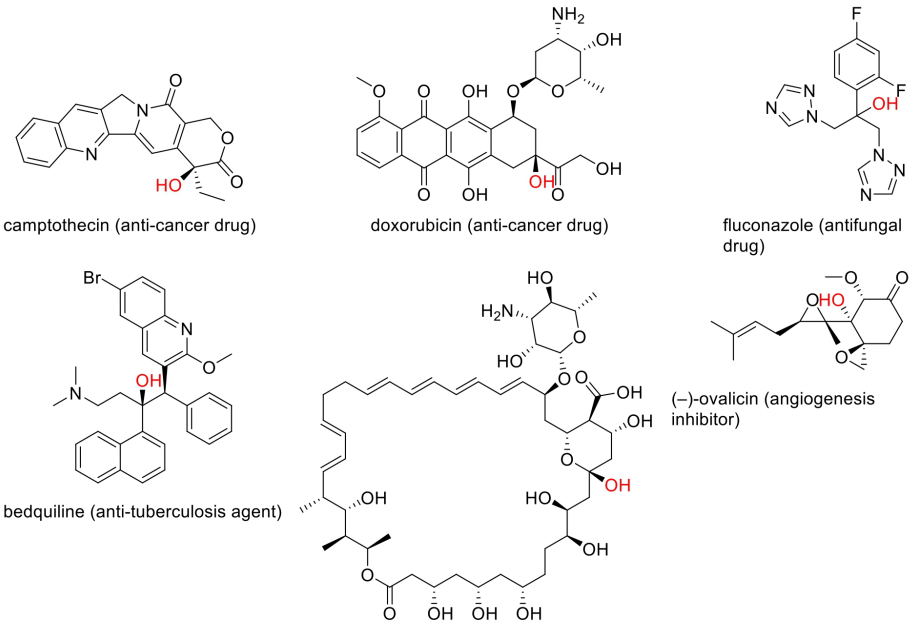

Table S. 5: Genes encoded in the *acr* cluster

Gene	Size (aa)	BlastP hit*	Identity (%)	E-value	Proposed protein function
acrG	514	A0A8K1AW52.1	28.42	2E-63	MFS transporter
acrR	422	E5AE39.1	44.58	3E-112	transcription factor
acrF	341	Q2TXF3.1	25.61	6E-10	αKG-dependent dioxygenase
acrC	1015	P9WEV1.1	33.2	2E-132	truncated NRPS (C-A)
acrD	341	E5AE43.1	57.96	2E-120	RTA1-like protein
acrE	601	E5AE41.1	44.54	2E-180	CYP450 monooxygenase
acrB	356	E5AE42.1	62.95	2E-166	t-ER
acrA	2539	E5AE40.1	61.32	0.0	hrPKS (KS-AT-DH-CMeT-ER-KR-ACP)

*Uniprot for reference database, manually curated choice (best, characterized fungal hit)

III. Analytical data

(4*E*,8*E*,12*E*,16*E*)-3,7,11,15-tetrahydroxy-2,6,10,14,16,18,20-heptamethyldocosa-4,8,12,16-tetraenoic acid (4/Pre-Acrophialocin)

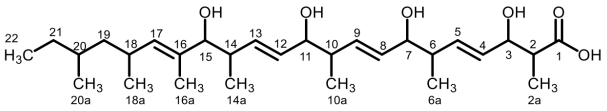

$[\alpha]_D^{21}$ +41.4 (*c* 0.07, MeOH).

R_f 0.87 (MeOH).

IR (ATR): $\tilde{\nu}$ [cm^{-1}] 3394, 3341, 2957, 2925, 1718, 1123, 1071, 1017, 977, 968.

^{1}H NMR, COSY (600 MHz, DMSO-d_6) δ_H 5.59 (dd, *J* = 15.5, 7.1 Hz, 1H, 13-C*H*), 5.57–5.50 (m, 2H, 9-C*H*, 5-C*H*), 5.37–5.32 (m, 1H, 12-C*H*), 5.32–5.25 (m, 2H, 8-C*H*, 4-C*H*), 4.95 (dd, *J* = 9.6, 1.6 Hz, 1H, 17-C*H*), 4.54 (s_{br}, 1H, O*H*), 4.41 (s_{br}, 1H, O*H*), 3.95–3.87 (m, 1H, 3-C*H*), 3.78–3.72 (m, 2H, 11-C*H*, 7-C*H*), 3.46 (d, *J* = 8.4 Hz, 1H, 15-C*H*), 2.47–2.40 (m, 1H, 18-C*H*), 2.20–2.10 (m, 4H, 14-C*H*, 10-C*H*, 6-C*H*, 2-C*H*), 1.52 (d, *J* = 1.3 Hz, 3H, 16-CH_3), 1.31–1.16 (m, 3H, 21-C$H_{2\text{-A}}$, 20-C*H*, 19-C$H_{2\text{-A}}$), 1.10 (dq, *J* = 14.0, 7.3 Hz, 1H, 21-C$H_{2\text{-B}}$), 1.00 (ddd, *J* = 13.6, 9.1, 4.6 Hz, 1H, 19-C$H_{2\text{-B}}$), 0.91–0.88 (m, 6H, 18-CH_3, 2-CH_3), 0.88–0.84 (m, 6H, 10-CH_3, 6-CH_3), 0.80 (t, *J* = 7.3 Hz, 3H, 22-CH_3), 0.79 (d, *J* = 6.3 Hz, 3H, 20-CH_3), 0.75 (d, *J* = 6.8 Hz, 3H, 14-CH_3) ppm.

^{13}C NMR, HSQC, HMBC (151 MHz, DMSO-d_6) δ_C 176.4 (1C, 1-*C*OOH), 135.0 (1C, 16-C_q), 134.2 (1C, 13-*C*H), 134.0 (1C, 5-*C*H), 133.3 (1C, 9-*C*H), 132.8 (1C, 17-*C*H), 131.1 (1C, 4-*C*H), 131.0 (1C, 8-*C*H), 130.9 (1C, 12-*C*H), 81.2 (1C, 15-*C*H), 75.1 (1C, 11-*C*H), 74.9 (1C, 7-*C*H), 73.9 (1C, 3-*C*H), 45.9 (1C, 2-*C*H), 44.5 (1C, 19-*C*H$_2$), 42.5 (1C, 10-*C*H), 42.2 (1C, 6-*C*H), 39.5 (1C, 14-*C*H), 31.9 (1C, 20-*C*H), 29.8 (1C, 21-*C*H$_2$), 29.1 (1C, 18-*C*H), 21.8 (1C, 18-*C*H$_3$), 18.9 (1C, 20-*C*H$_3$), 17.0 (1C, 14-*C*H$_3$), 15.8 (1C, 10-*C*H$_3$), 15.5 (1C, 6-*C*H$_3$), 13.6 (1C, 2-*C*H$_3$), 11.3 (1C, 22-*C*H$_3$), 11.1 (1C, 16-*C*H$_3$) ppm.

HRMS (ESI) *m*/*z*: $[M+Na]^+$ Calcd for $C_{29}H_{50}O_6Na$ 517.3499; Found 517.3493.

(4*E*,8*E*,12*E*,16*E*)-2,3,7,11,15-pentahydroxy-2,6,10,14,16,18,20-heptamethyldocosa-4,8,12,16-tetraenoic acid (2/Acrophialocin)

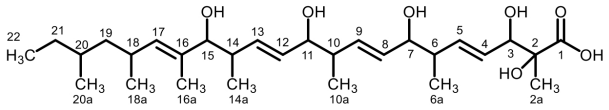

$[\alpha]_D^{21}$ +50.2 (*c* 0.10, MeOH).

R_f 0.79 (MeOH).

IR (ATR): $\tilde{\nu}$ [cm^{-1}] 3395, 3338, 2957, 2926, 2870, 1722, 1454, 1371, 1071, 1016, 974.

^{1}H NMR, COSY (600 MHz, DMSO-d_6) δ_H 5.61–5.58 (m, 1H, 13-C*H*), 5.58–5.51 (m, 2H, 9-C*H*, 5-C*H*), 5.41 (ddd, *J* = 15.7, 7.8, 1.2 Hz, 1H, 4-C*H*), 5.37–5.29 (m, 2H, 12-C*H*, 8-C*H*), 4.95 (d, *J* = 9.4 Hz, 1H, 17-C*H*), 4.58–4.47 (m, 2H, 2 x O*H*), 4.39 (d, *J* = 4.1 Hz, 1H, O*H*), 3.94 (d, *J* = 7.8 Hz, 1H, 3-C*H*), 3.79–3.72 (m, 2H, 11-C*H*, 7-C*H*), 3.46 (dd, *J* = 8.3, 3.6 Hz, 1H, 15-C*H*), 2.48–2.40 (m, 1H, 18-C*H*), 2.20–2.11 (m, 3H, 14-C*H*, 10-C*H*, 6-C*H*), 1.52 (d, *J* = 1.3 Hz, 3H, 16-CH_3), 1.27–1.16 (m, 3H, 21-C$H_{2\text{-A}}$, 20-C*H*, 19-C$H_{2\text{-A}}$), 1.14–1.07 (m, 1H, 21-C$H_{2\text{-B}}$), 1.07 (s, 3H, 2-CH_3), 1.03–0.96 (m, 1H, 19-C$H_{2\text{-B}}$), 0.89 (d, *J* = 6.6 Hz, 3H, 18-CH_3), 0.87 (d, *J* = 6.8 Hz, 3H, 6-CH_3), 0.87 (d, *J* = 6.8 Hz, 3H, 10-CH_3), 0.80 (t, *J* = 7.3 Hz, 3H, 22-CH_3), 0.79 (d, *J* = 6.3 Hz, 3H, 20-CH_3), 0.75 (d, *J* = 6.8 Hz, 3H, 14-CH_3) ppm.

^{13}C NMR, HSQC, HMBC (151 MHz, DMSO-d_6) δ_C 177.0 (1C, 1-*C*OOH), 135.8 (1C, 5-*C*H), 135.0 (1C, 16-C_q), 134.2 (1C, 13-*C*H), 133.4 (1C, 9-*C*H), 132.8 (1C, 17-*C*H), 130.9 (2C, 12-*C*H, 8-*C*H), 128.3 (1C, 4-*C*H), 81.1 (1C, 15-*C*H), 76.9 (1C, 3-*C*H), 76.3 (1C, 2-C_q), 75.1 (1C, 11-*C*H), 74.9 (1C, 7-*C*H), 44.5 (1C, 19-*C*H_2), 42.4 (1C, 10-*C*H), 42.4 (1C, 6-*C*H), 39.4 (1C, 14-*C*H), 31.8 (1C, 20-*C*H), 29.8 (1C, 21-*C*H_2), 29.1 (1C, 18-*C*H), 22.4 (1C, 2-*C*H_3), 21.8 (1C, 18-*C*H_3), 19.0 (1C, 20-*C*H_3), 17.0 (1C, 14-*C*H_3), 15.7 (1C, 10-*C*H_3), 15.3 (1C, 6-*C*H_3), 11.3 (1C, 22-*C*H_3), 11.1 (1C, 16-*C*H_3) ppm.

HRMS (ESI) *m*/*z*: $[M+Na]^+$ Calcd for $C_{29}H_{50}O_7Na$ 533.3449; Found 533.3461.

(4*E*,8*E*,12*E*,16*E*)-3,7,11,15-tetrahydroxy-18-(hydroxymethyl)-2,6,10,14,16,20-hexamethyldocosa-4,8,12,16-tetraenoic acid (5/Malaysic acid)

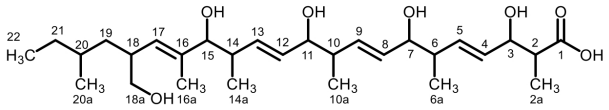

$[\alpha]_D^{21}$ +13.6 (*c* 0.05, MeOH).

R_f 0.70 (MeOH).

IR (ATR): $\tilde{\nu}$ [cm^{-1}] 3391, 3326, 2959, 2926, 2854, 1735, 1672, 1570, 1457, 1330, 1073, 1019, 967.

^{1}H NMR, COSY (600 MHz, DMSO-d_6) δ_H 5.62–5.56 (m, 1H, 13-C*H*), 5.56–5.51 (m, 2H, 9-C*H*, 5-C*H*), 5.37–5.25 (m, 3H, 12-C*H*, 8-C*H*, 4-C*H*), 4.92 (d, *J* = 9.8 Hz, 1H, 17-C*H*), 4.58–4.49 (m, 1H, O*H*), 4.46–4.33 (m, 2H, 2 x O*H*), 3.93–3.85 (m, 1H, 3-C*H*), 3.80–3.70 (m, 2H, 11-C*H*, 7-C*H*), 3.49 (t, *J* = 8.2 Hz, 1H, 15-C*H*), 3.25 (dd, *J* = 10.4, 5.9 Hz, 1H, 18-C$H_{2\text{-A}}$), 3.17 (dd, *J* = 10.4, 6.9 Hz, 1H, 18-C$H_{2\text{-B}}$), 2.48–2.40 (m, 1H, 18-C*H*), 2.21–2.09 (m, 4H, 14-C*H*, 10-C*H*, 6-C*H*, 2-C*H*), 1.52 (d, *J* = 1.3 Hz, 3H, 16-CH_3), 1.23–1.17 (m, 3H, 21-C$H_{2\text{-A}}$, 20-C*H*, 19-C$H_{2\text{-A}}$), 1.17–1.10 (m, 2H, 21-C$H_{2\text{-B}}$, 19-C$H_{2\text{-B}}$), 0.89 (d, *J* = 7.0 Hz, 3H, 2-CH_3), 0.88–0.84 (m, 6H, 10-CH_3, 6-CH_3), 0.80 (t, *J* = 7.3 Hz, 3H, 22-CH_3), 0.79 (d, *J* = 6.0 Hz, 3H, 20-CH_3), 0.75 (d, *J* = 6.9 Hz, 3H, 14-CH_3) ppm.

^{13}C NMR, HSQC, HMBC (151 MHz, DMSO-d_6) δ_C 176.4 (1C, 1-*C*OOH), 137.5 (1C, 16-C_q), 134.2 (1C, 13-*C*H), 133.9 (1C, 5-*C*H), 133.2 (1C, 9-*C*H), 131.0 (1C, 4-*C*H), 130.9 (1C, 8-*C*H), 130.9 (1C, 12-*C*H), 129.0 (1C, 17-*C*H), 81.3 (1C, 15-*C*H), 75.2 (1C, 11-*C*H), 74.8 (1C, 7-*C*H), 74.0 (1C, 3-*C*H), 65.4 (1C, 18-*C*H$_2$), 45.9 (1C, 2-*C*H), 42.5 (1C, 10-*C*H), 42.2 (1C, 6-*C*H), 39.5 (1C, 14-*C*H), 38.5 (1C, 19-*C*H$_2$), 38.2 (1C, 18-*C*H), 31.6 (1C, 20-*C*H), 30.3 (1C, 21-*C*H$_2$), 18.8 (1C, 20-*C*H$_3$), 16.9 (1C, 14-*C*H$_3$), 15.8 (1C, 10-*C*H$_3$), 15.4 (1C, 6-*C*H$_3$), 13.7 (1C, 2-*C*H$_3$), 11.5 (1C, 22-*C*H$_3$), 11.4 (1C, 16-*C*H$_3$) ppm.

HRMS (ESI) *m*/*z*: $[M–H]^-$ Calcd for $C_{29}H_{49}O_7$ 509.3484; Found 509.3489.

The analytical data are in accordance with the literature[13].

(4*E*,8*E*,12*E*,16*E*)-2,3,7,11,15-pentahydroxy-18-(hydroxymethyl)-2,6,10,14,16,20-hexamethyldocosa-4,8,12,16-tetraenoic acid (1/Acrophialocinol)

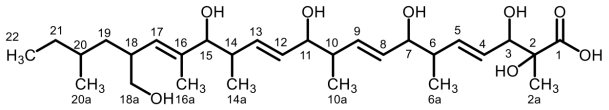

$[\alpha]_D^{21}$ +29.9 (*c* 0.11, MeOH).

R_f 0.79 (MeOH).

IR (ATR): $\tilde{\nu}$ [cm^{-1}] 3393, 3332, 2958, 2925, 2853, 1734, 1455, 1371, 1022, 970.

^{1}H NMR, COSY (600 MHz, DMSO-d$_6$) δ_H 5.62–5.51 (m, 3H, 13-C*H*, 9-C*H*, 5-C*H*), 5.41 (ddd, *J* = 15.6, 7.7, 1.2 Hz, 1H, 4-C*H*), 5.37–5.29 (m, 2H, 12-C*H*, 8-C*H*), 4.92 (d, *J* = 10.0 Hz, 1H, 17-C*H*), 4.60–4.48 (m, 2H, 2 x O*H*), 4.42–4.29 (m, 2H, 2 x O*H*), 3.92 (d, *J* = 7.7 Hz, 1H, 3-C*H*), 3.81–3.71 (m, 2H, 11-C*H*, 7-C*H*), 3.48 (dd, *J* = 8.2, 3.4 Hz, 1H, 15-C*H*), 3.28–3.22 (m, 1H, 18-C$H_{2\text{-A}}$), 3.21–3.13 (m, 1H, 18-C$H_{2\text{-B}}$), 2.47–2.40 (m, 1H, 18-C*H*), 2.21–2.10 (m, 3H, 14-C*H*, 10-C*H*, 6-C*H*), 1.54 (d, *J* = 1.3 Hz, 3H, 16-CH_3), 1.29–1.18 (m, 3H, 21-C$H_{2\text{-A}}$, 20-C*H*, 19-C$H_{2\text{-A}}$), 1.16–1.10 (m, 2H, 21-C$H_{2\text{-B}}$, 19-C$H_{2\text{-B}}$), 1.07 (s, 3H, 2-CH_3), 0.87 (pseudo-d, *J* = 6.8 Hz, 6H, 10-CH_3, 6-CH_3), 0.80 (t, *J* = 7.3 Hz, 3H, 22-CH_3), 0.78 (d, *J* = 6.0 Hz, 3H, 20-CH_3), 0.76 (d, *J* = 6.9 Hz, 3H, 14-CH_3) ppm.

^{13}C NMR, HSQC, HMBC (151 MHz, DMSO-d$_6$) δ_C 177.0 (1C, 1-*C*OOH), 137.5 (1C, 16-C_q), 135.6 (1C, 5-*C*H), 134.2 (1C, 13-*C*H), 133.4 (1C, 9-*C*H), 130.9 (1C, 8-*C*H), 130.9 (1C, 12-*C*H), 129.0 (1C, 17-*C*H), 128.5 (1C, 4-*C*H), 81.3 (1C, 15-*C*H), 76.9 (1C, 3-*C*H), 76.2 (1C, 2-C_q), 75.2 (1C, 11-*C*H), 74.9 (1C, 7-*C*H), 65.4 (1C, 18-*C*H$_2$), 42.4 (1C, 6-*C*H), 42.4 (1C, 10-*C*H), 39.4 (1C, 14-*C*H), 38.5 (1C, 19-*C*H$_2$), 38.2 (1C, 18-*C*H), 31.6 (1C, 20-*C*H), 30.3 (1C, 21-*C*H$_2$), 22.6 (1C, 2-*C*H$_3$), 18.8 (1C, 20-*C*H$_3$), 17.0 (1C, 14-*C*H$_3$), 15.8 (1C, 10-*C*H$_3$), 15.3 (1C, 6-*C*H$_3$), 11.4 (1C, 22-*C*H$_3$), 11.4 (1C, 16-*C*H$_3$) ppm.

HRMS (ESI) *m*/*z*: [M+Na]$^+$ Calcd for $C_{29}H_{50}O_8Na$ 549.3398; Found 549.3404.

The analytical data are in accordance with the literature[14].

IV. ^{1}H- and ^{13}C{^{1}H}-NMR Spectra

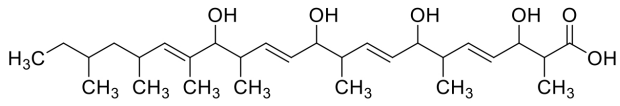

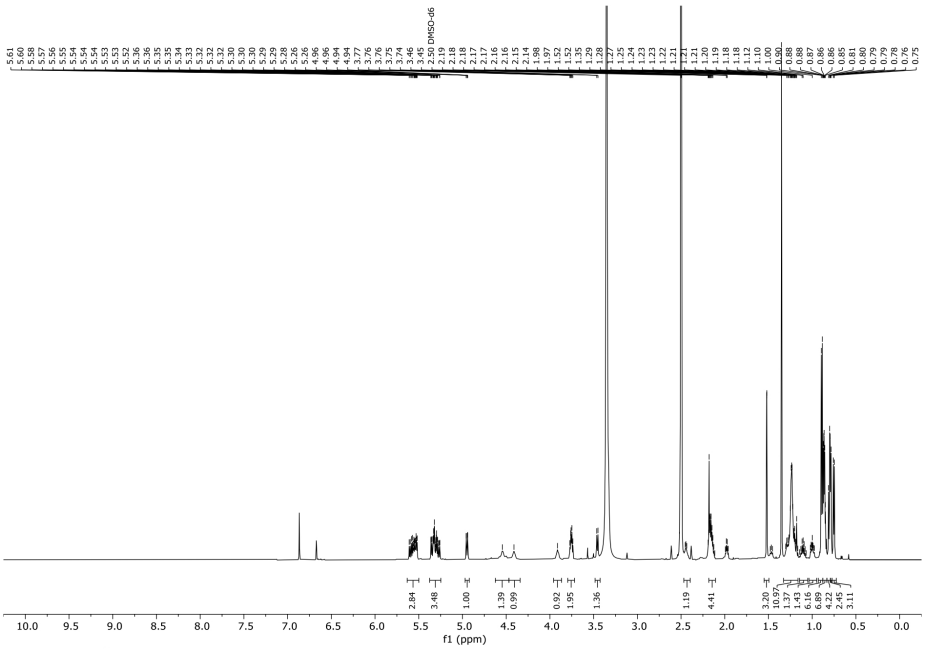

Figure S. 7: ^{1}H-NMR spectrum (DMSO-d_6, 600 MHz, 294 K) of Pre-Acrophialocin (**4**).

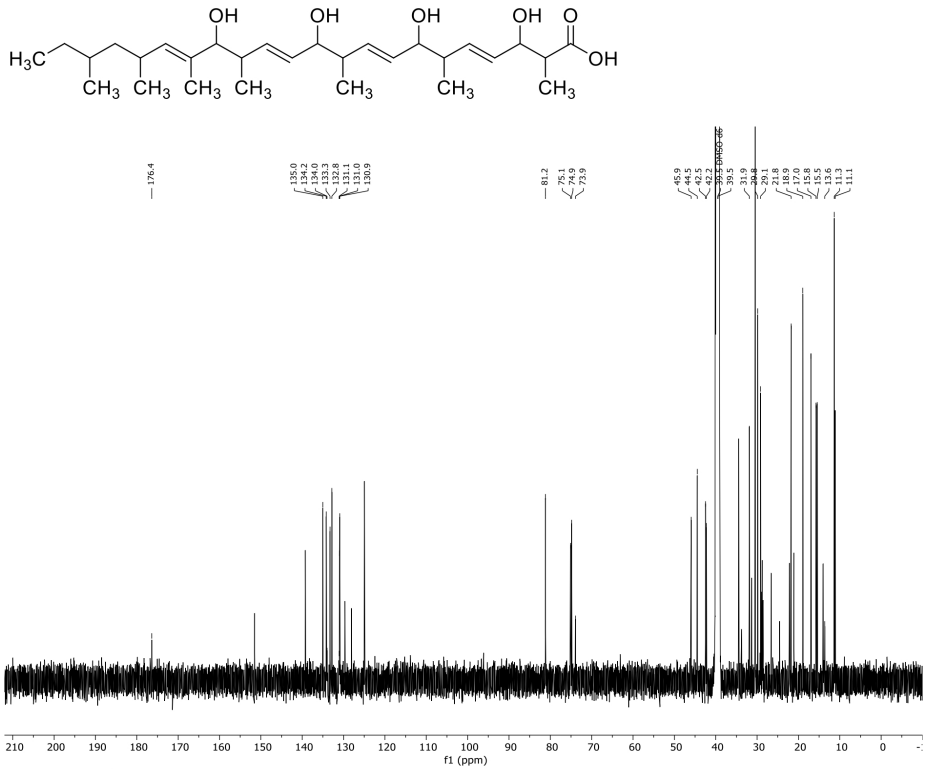

Figure S. 8: $^{13}C\{^{1}H\}$-NMR spectrum (DMSO-d_6, 151 MHz, 294 K) of Pre-Acrophialocin (**4**).

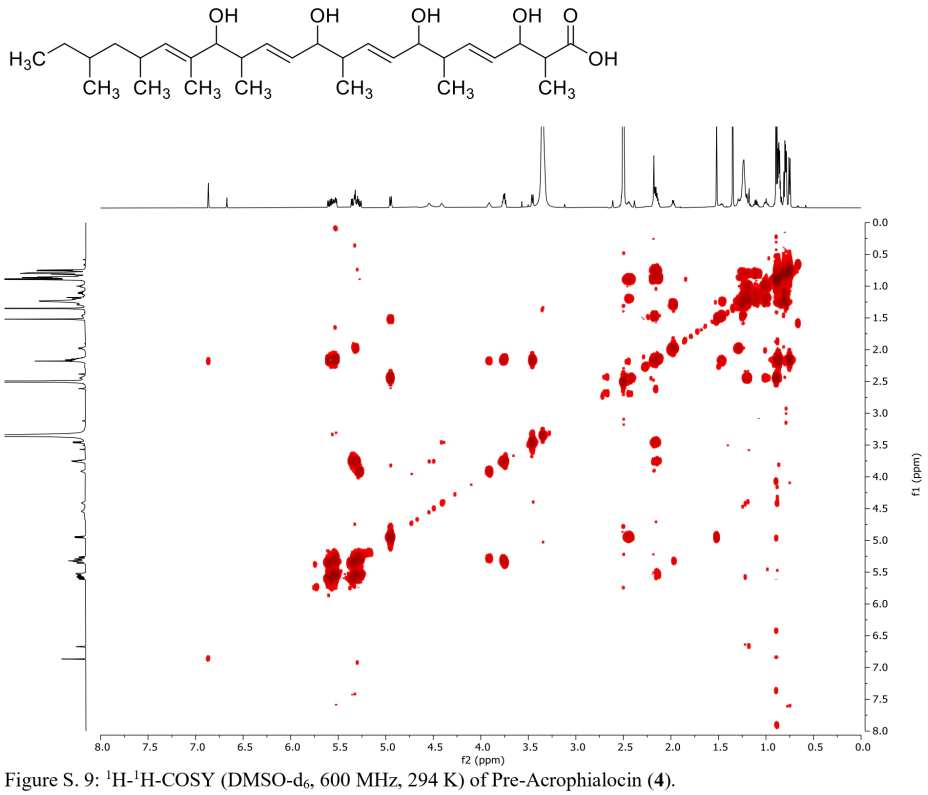

Figure S. 9: ^{1}H-^{1}H-COSY (DMSO-d_6, 600 MHz, 294 K) of Pre-Acrophialocin (**4**).

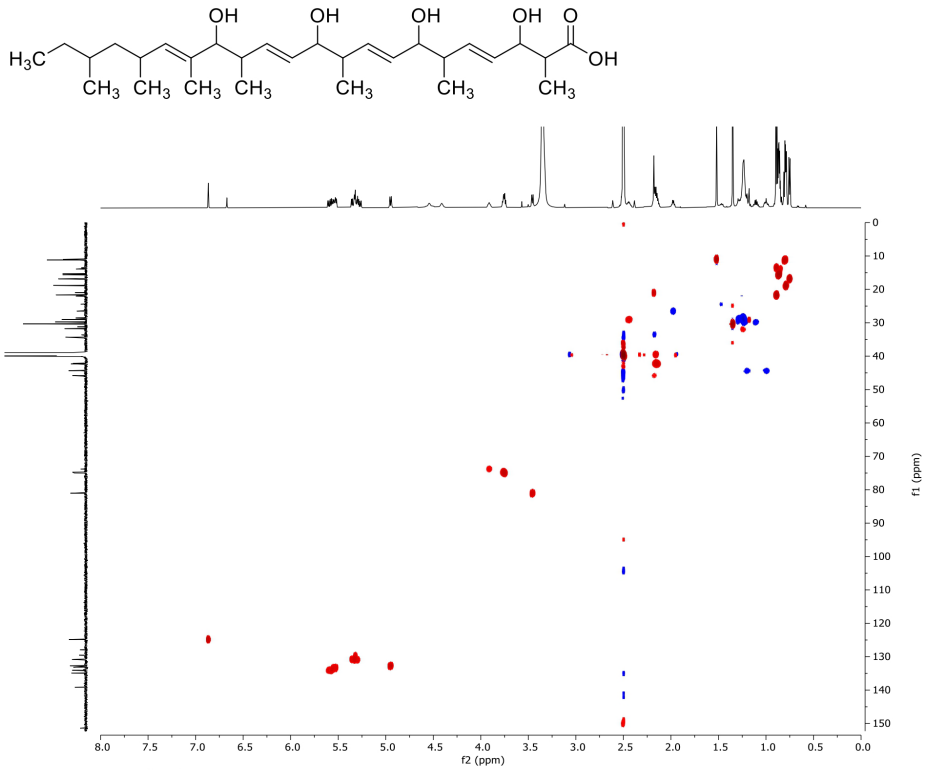

Figure S. 10: ^{1}H-$^{13}C\{^{1}H\}$-HSQC (DMSO-d_6, 600 MHz, 294 K) of Pre-Acrophialocin (**4**).

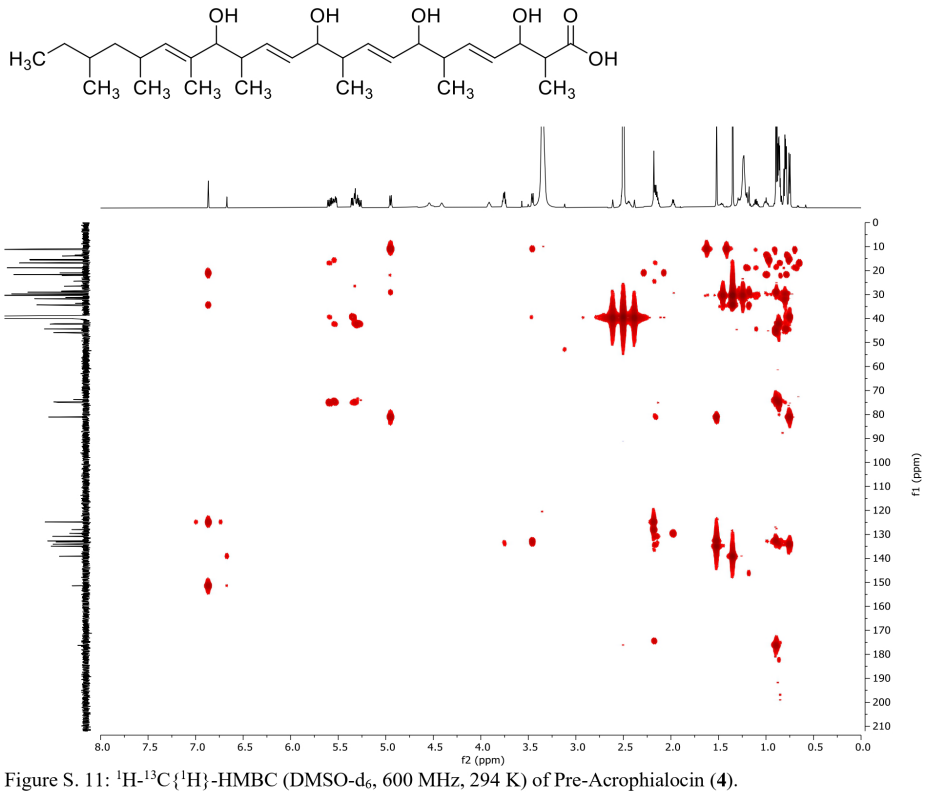

Figure S. 11: ^{1}H-$^{13}C\{^{1}H\}$-HMBC (DMSO-d_6, 600 MHz, 294 K) of Pre-Acrophialocin (**4**).

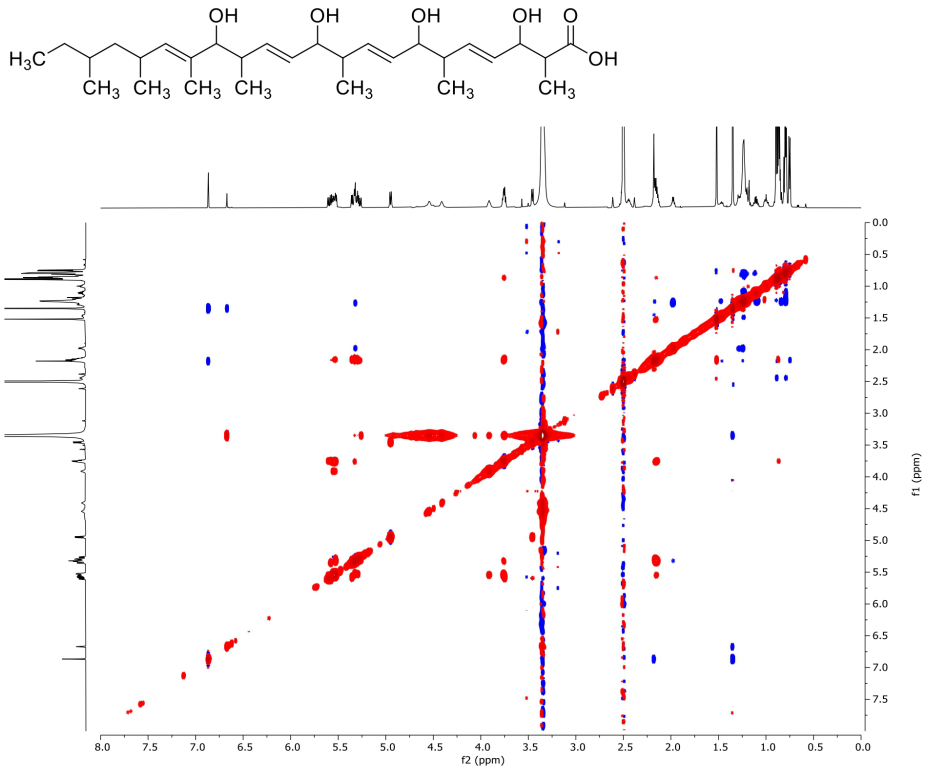

Figure S. 12: ^{1}H-^{1}H-NOESY (DMSO-d_6, 600 MHz, 294 K) of Pre-Acrophialocin (**4**).

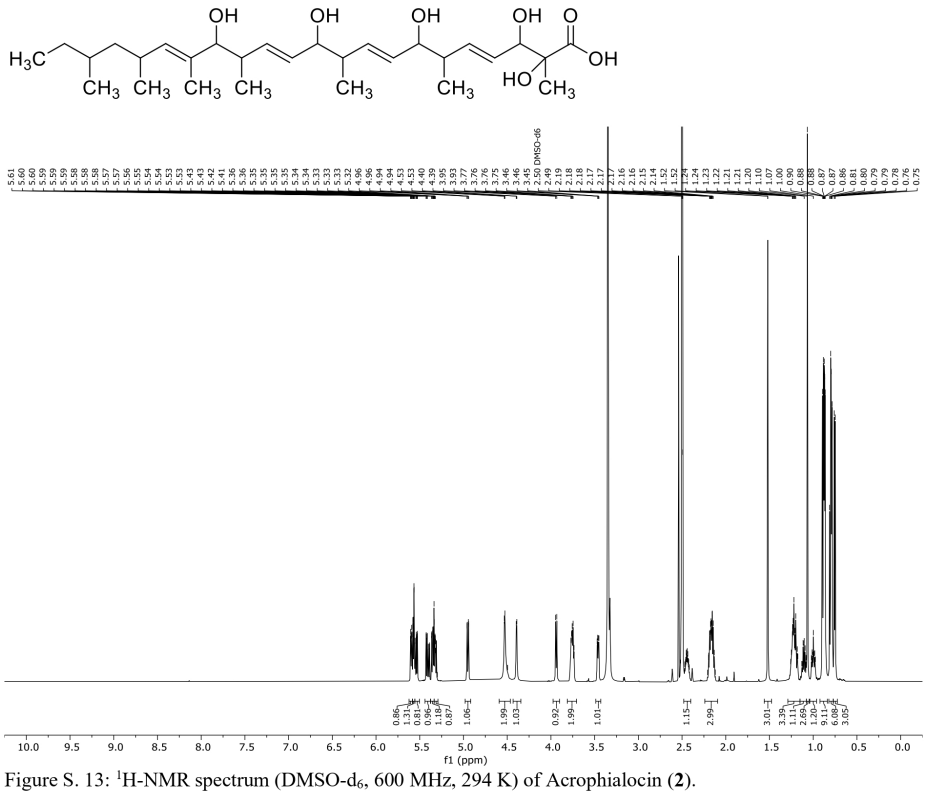

Figure S. 13: ^{1}H-NMR spectrum (DMSO-d_6, 600 MHz, 294 K) of Acrophialocin (**2**).

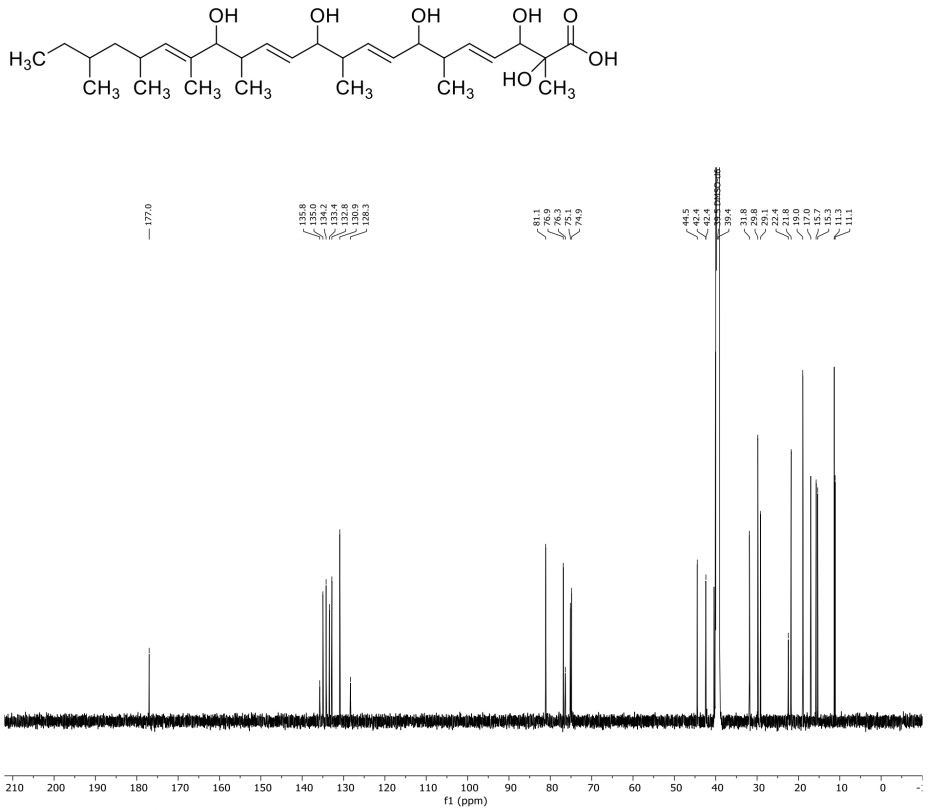

Figure S. 14: $^{13}C\{^{1}H\}$-NMR spectrum (DMSO-d_6, 151 MHz, 294 K) of Acrophialocin (**2**).

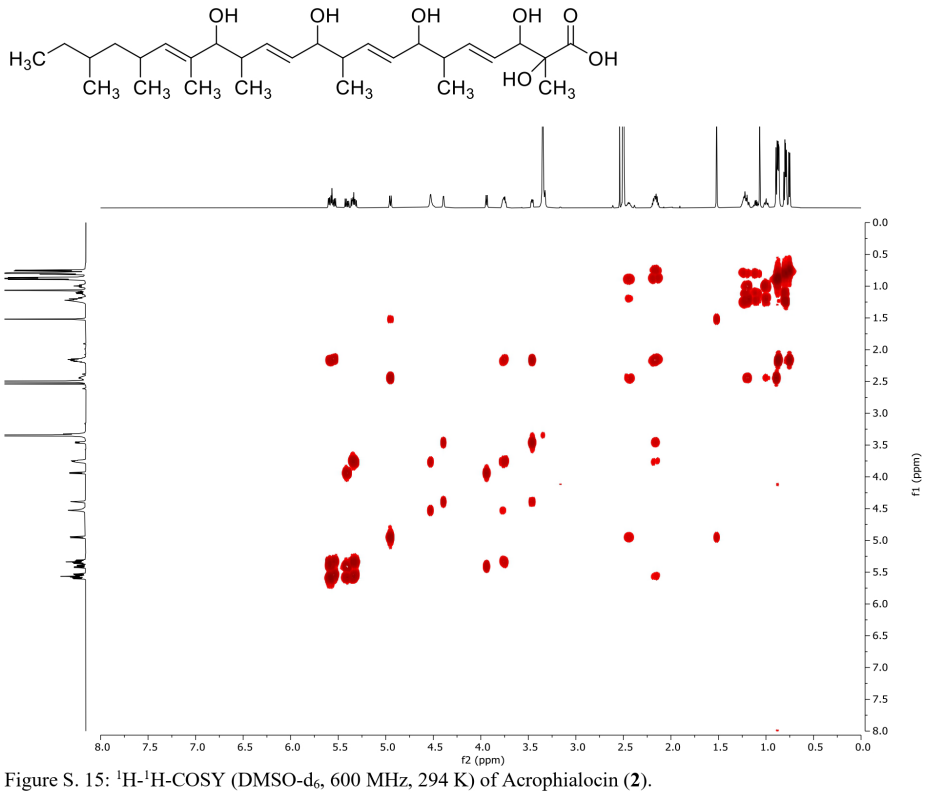

Figure S. 15: ^{1}H-^{1}H-COSY (DMSO-d_6, 600 MHz, 294 K) of Acrophialocin (**2**).

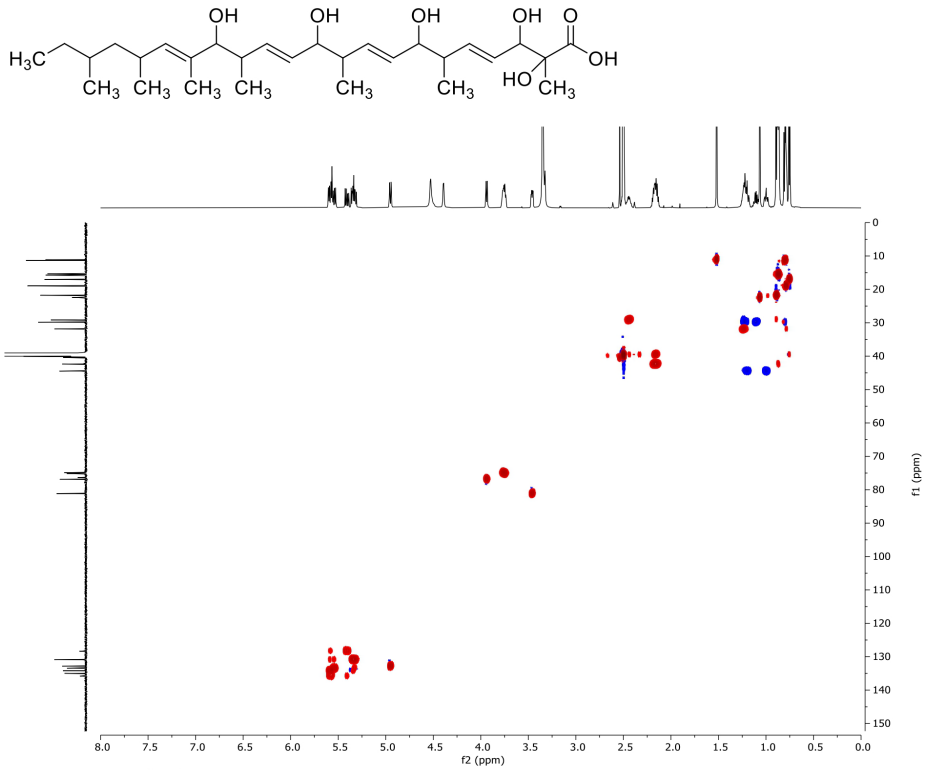

Figure S. 16: ^{1}H-$^{13}C\{^{1}H\}$-HSQC (DMSO-d_6, 600 MHz, 294 K) of Acrophialocin (**2**).

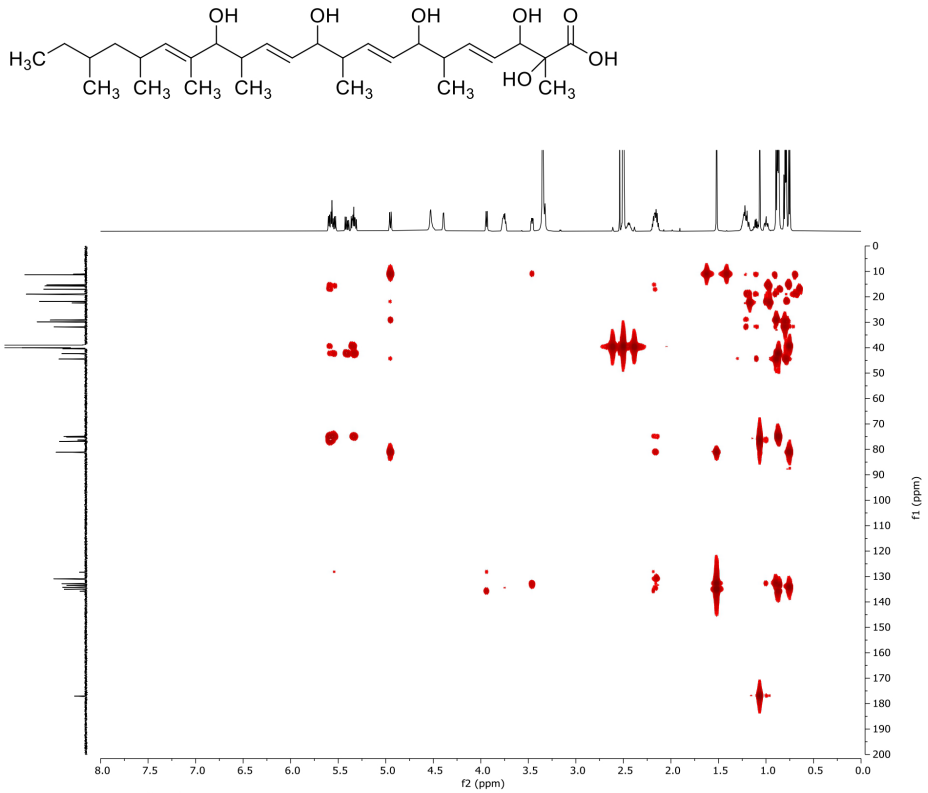

Figure S. 17: ^{1}H-^{13}C{^{1}H}-HMBC (DMSO-d_6, 600 MHz, 294 K) of Acrophialocin (**2**).

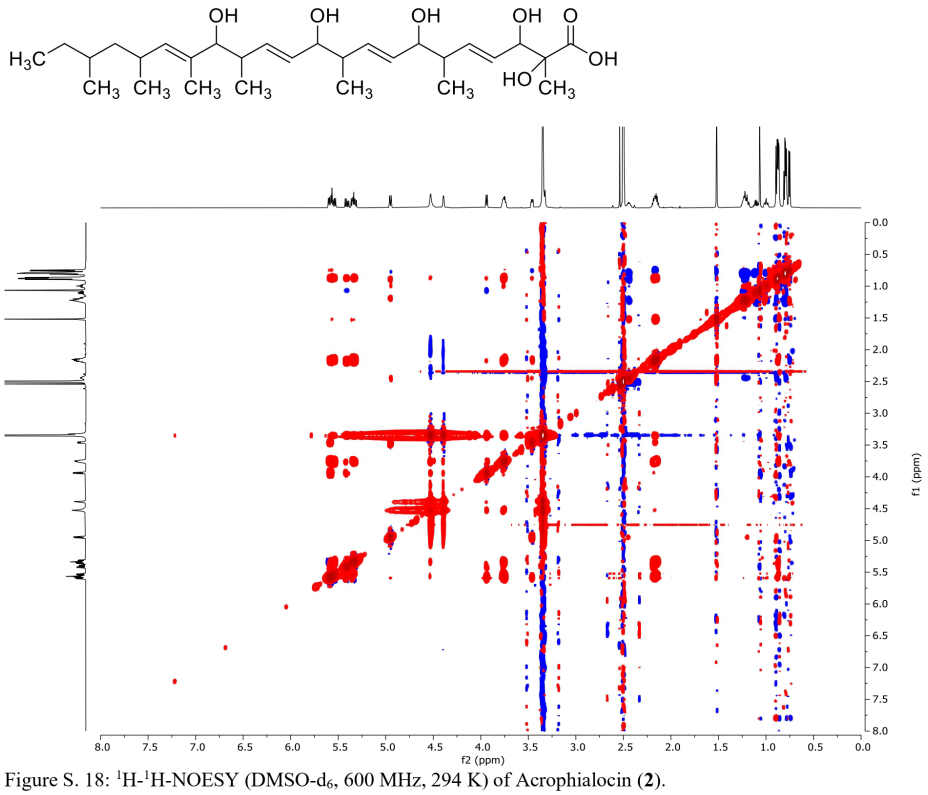

Figure S. 18: ^{1}H-^{1}H-NOESY (DMSO-d_6, 600 MHz, 294 K) of Acrophialocin (**2**).

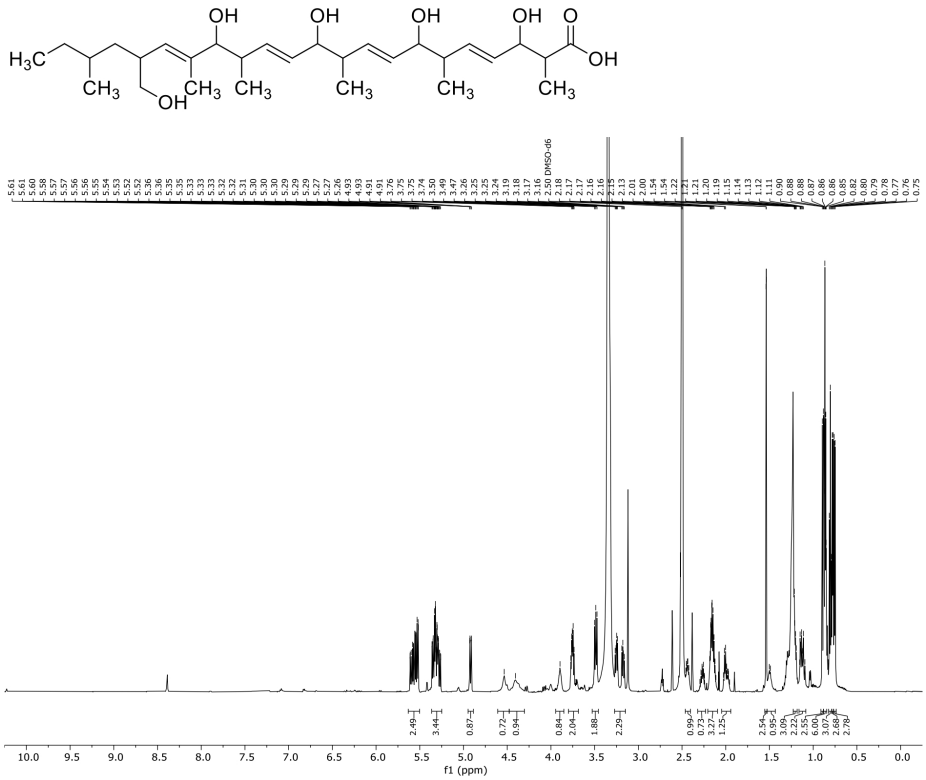

Figure S. 19: ^{1}H-NMR spectrum (DMSO-d_6, 600 MHz, 294 K) of Malaysic acid (**5**).

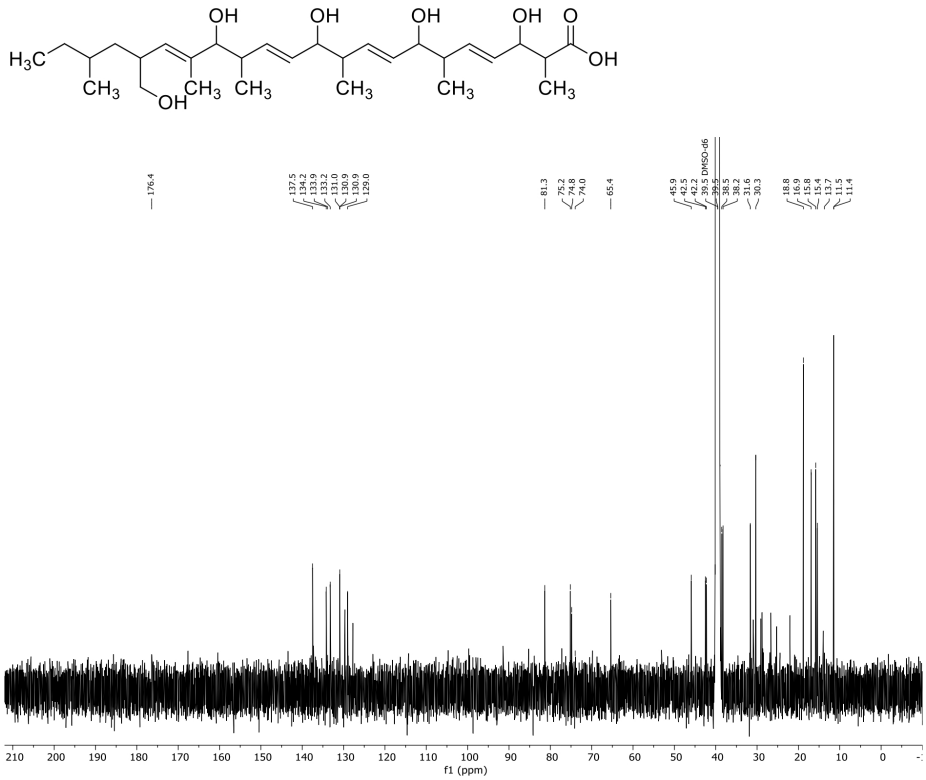

Figure S. 20: $^{13}C\{^{1}H\}$-NMR spectrum (DMSO-d_6, 151 MHz, 294 K) of Malaysic acid (**5**).

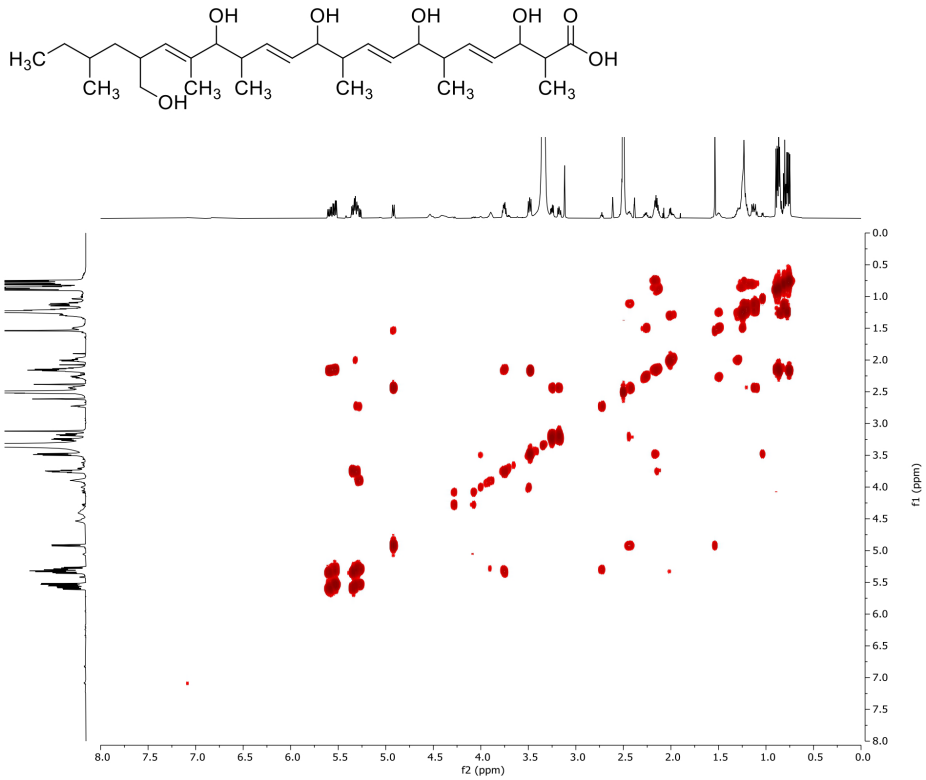

Figure S. 21: ^{1}H-^{1}H-COSY (DMSO-d_6, 600 MHz, 294 K) of Malaysic acid (**5**).

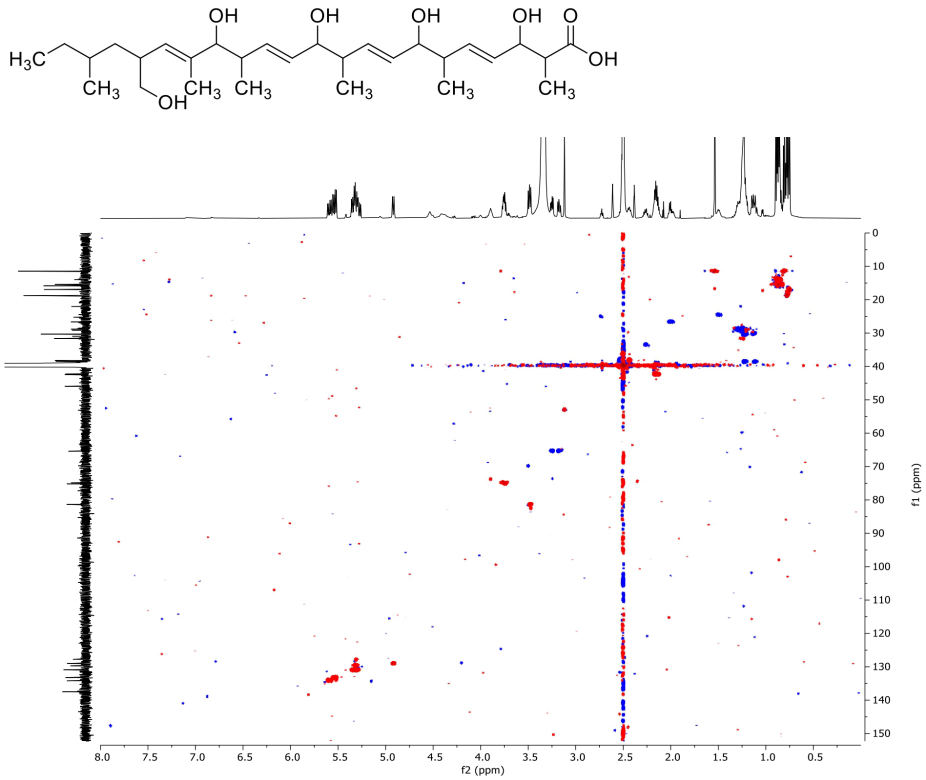

Figure S. 22: ^{1}H-$^{13}C\{^{1}H\}$-HSQC (DMSO-d_6, 600 MHz, 294 K) of Malaysic acid (**5**).

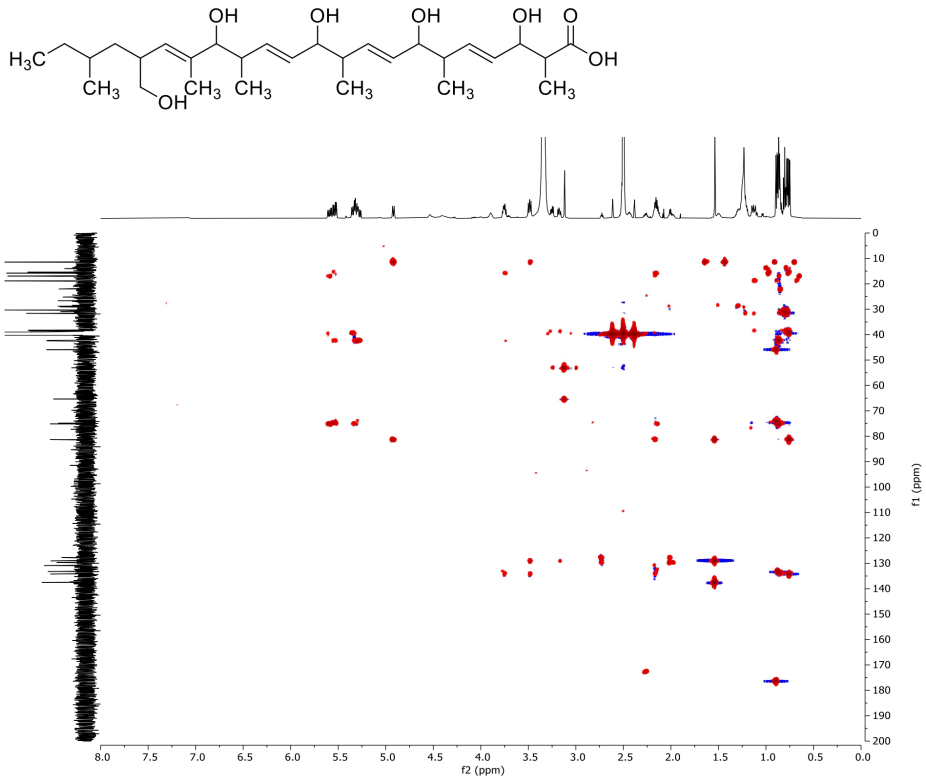

Figure S. 23: ^{1}H-^{13}C{^{1}H}-HMBC (DMSO-d_6, 600 MHz, 294 K) of Malaysic acid (**5**).

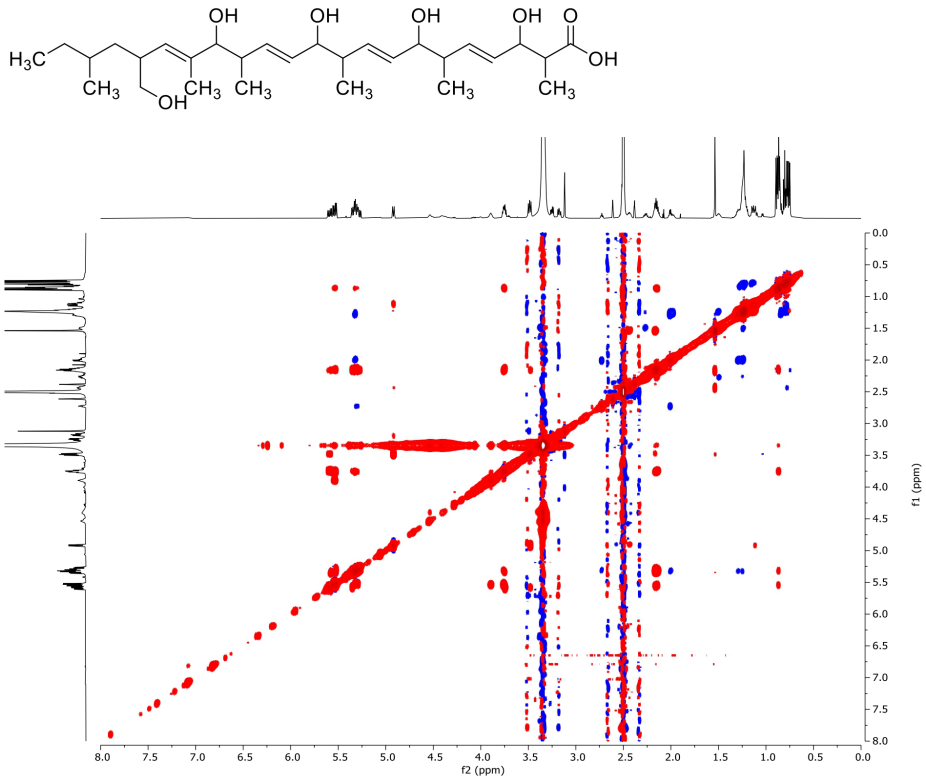

Figure S. 24: ^{1}H-^{1}H-NOESY (DMSO-d_6, 600 MHz, 294 K) of Malaysic acid (**5**).

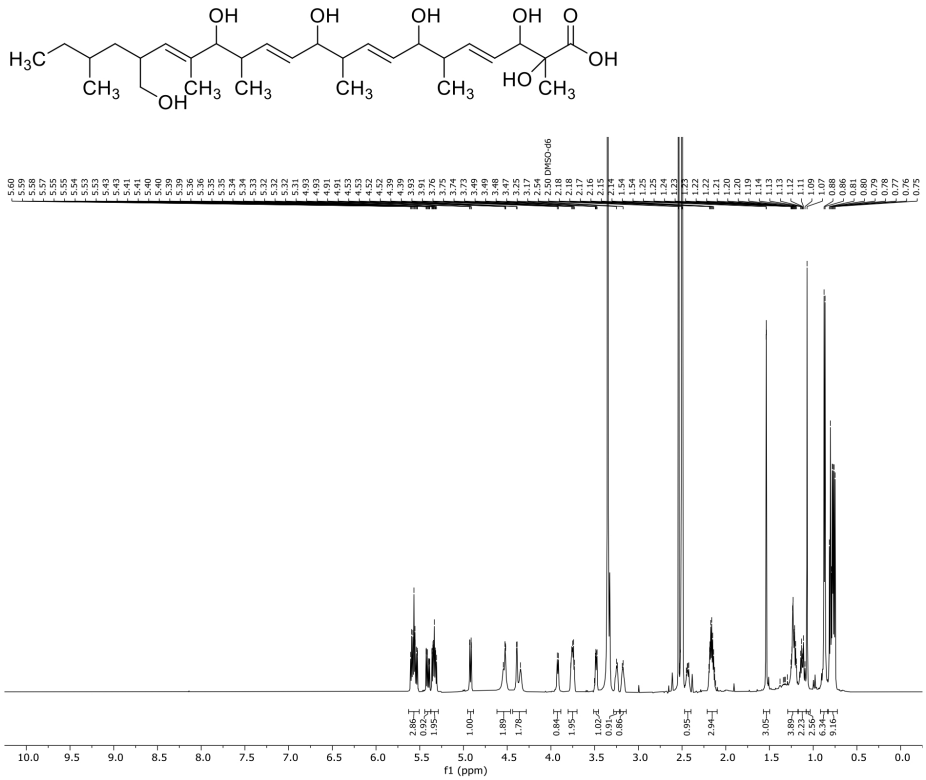

Figure S. 25: ^{1}H-NMR spectrum (DMSO-d_6, 600 MHz, 294 K) of Acrophialocinol (**1**).

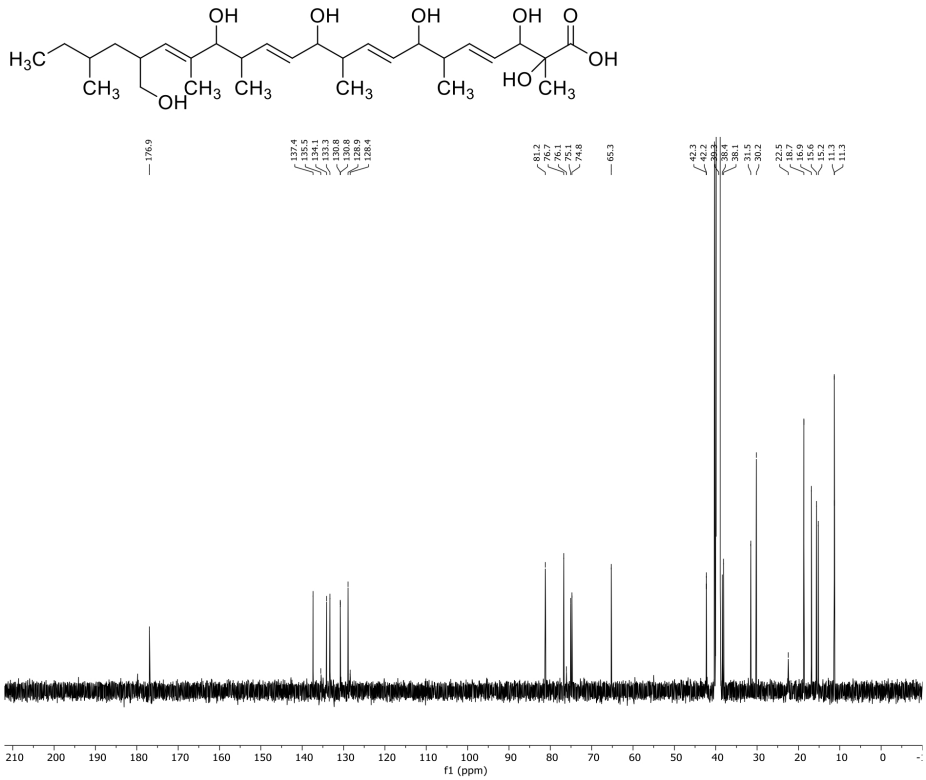

Figure S. 26: $^{13}C\{^{1}H\}$-NMR spectrum (DMSO-d_6, 151 MHz, 294 K) of Acrophialocinol (**1**).

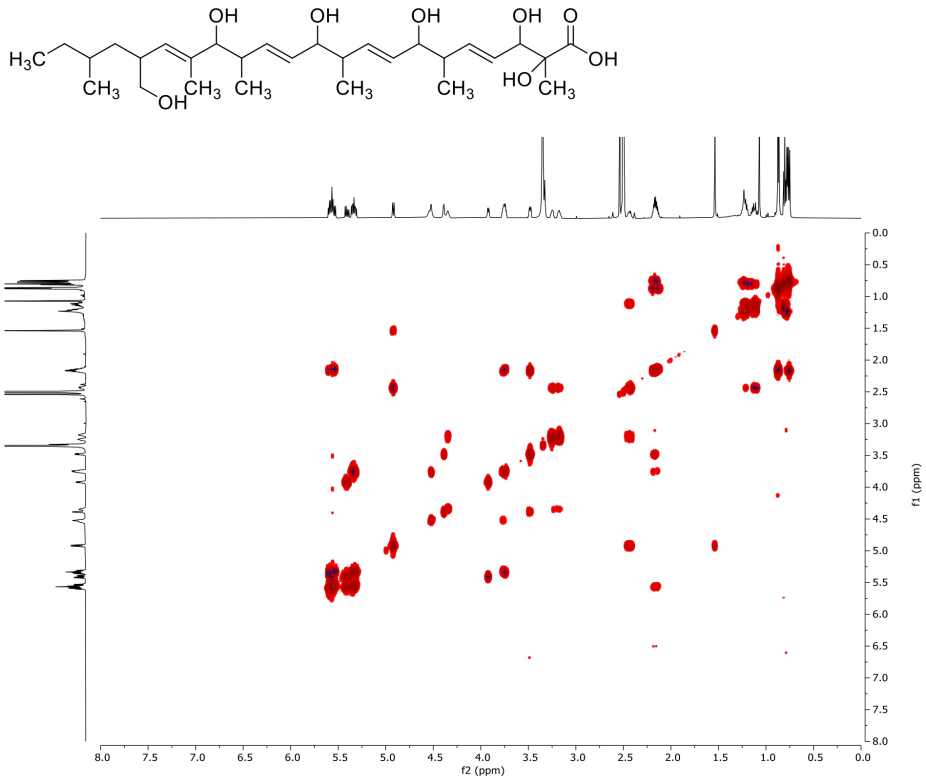

Figure S- 27: ^{1}H-^{1}H-COSY (DMSO-d_6, 600 MHz, 294 K) of Acrophialocinol (**1**).

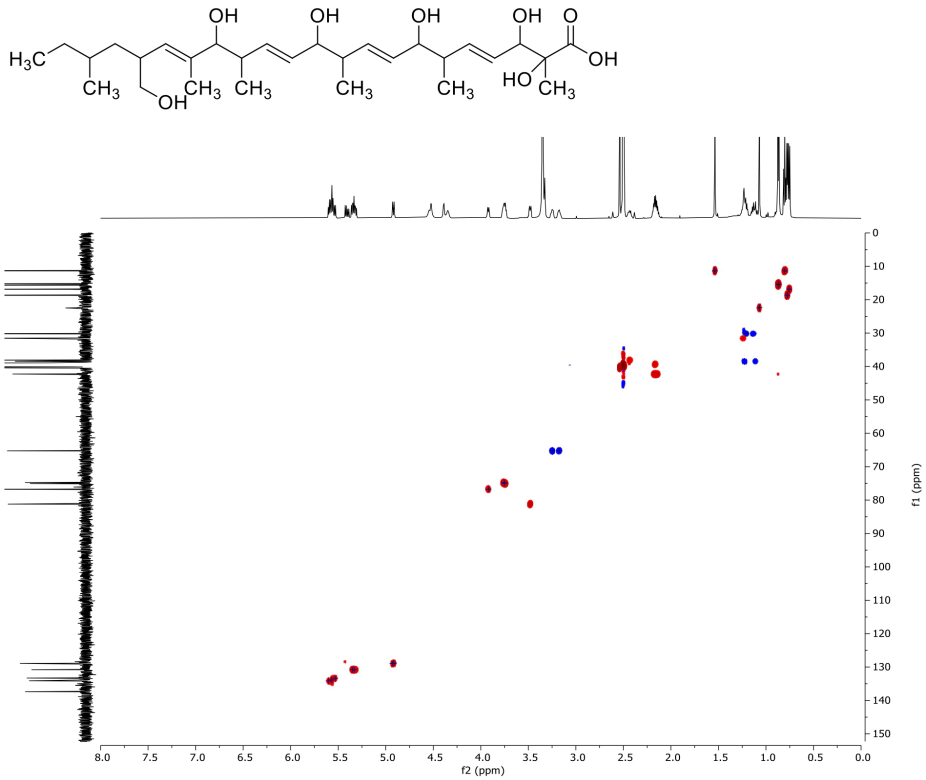

Figure S. 28: ^{1}H-$^{13}C\{^{1}H\}$-HSQC (DMSO-d_6, 600 MHz, 294 K) of Acrophialocinol (**1**).

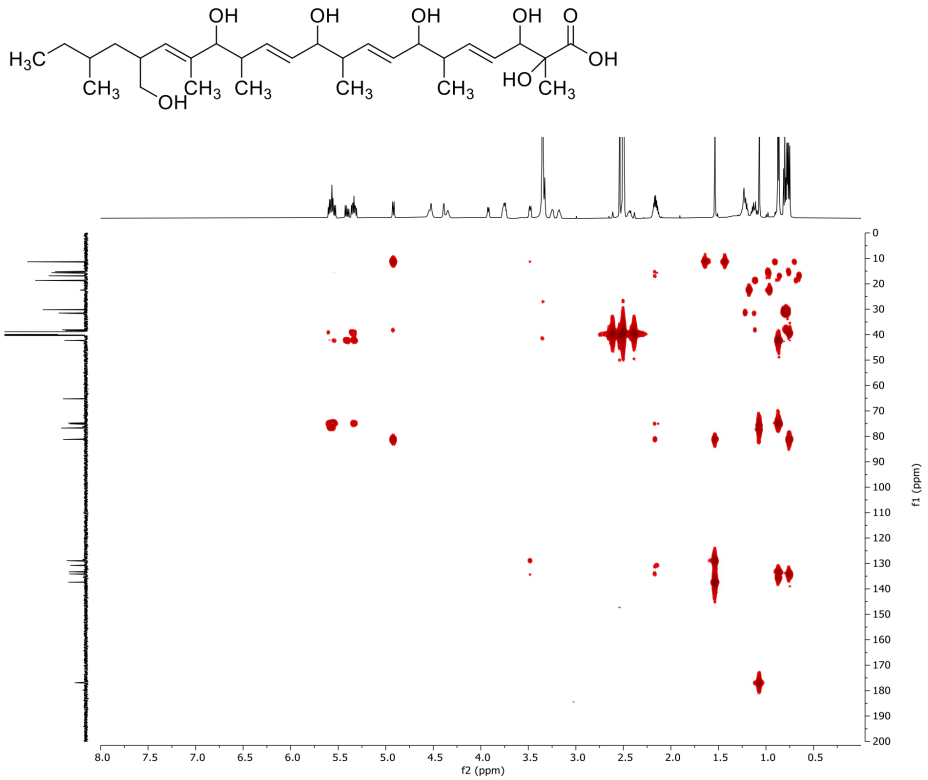

Figure S. 29: ^{1}H-$^{13}C\{^{1}H\}$-HMBC (DMSO-d_6, 600 MHz, 294 K) of Acrophialocinol (**1**).

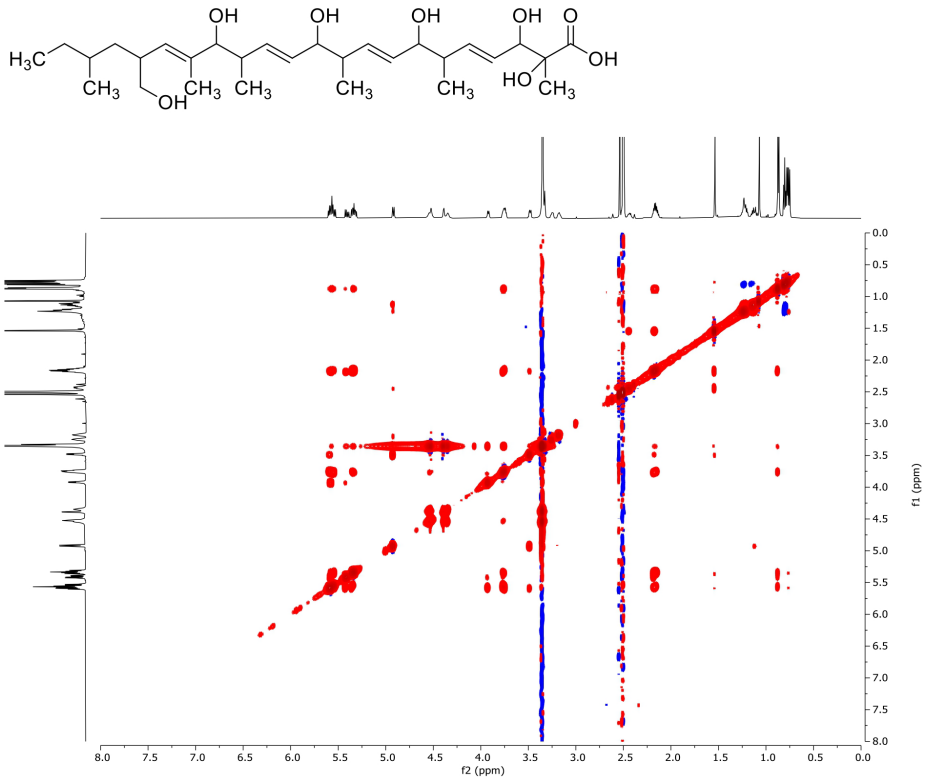

Figure S. 30: ^{1}H-^{1}H-NOESY (DMSO-d_6, 600 MHz, 294 K) of Acrophialocinol (**1**).

V. References

(1) Prjibelski, A. D.; Vasilinetc, I.; Bankevich, A.; Gurevich, A.; Krivosheeva, T.; Nurk, S.; Pham, S.; Korobeynikov, A.; Lapidus, A.; Pevzner, P. A. ExSPAnder: a universal repeat resolver for DNA fragment assembly. *Bioinformatics (Oxford, England)* **2014**, *30* (12), i293-301. DOI: 10.1093/bioinformatics/btu266.
(2) Stanke, M.; Diekhans, M.; Baertsch, R.; Haussler, D. Using native and syntenically mapped cDNA alignments to improve de novo gene finding. *Bioinformatics (Oxford, England)* **2008**, *24* (5), 637–644. DOI: 10.1093/bioinformatics/btn013. Published Online: Jan. 24, 2008.
(3) Blin, K.; Shaw, S.; Augustijn, H. E.; Reitz, Z. L.; Biermann, F.; Alanjary, M.; Fetter, A.; Terlouw, B. R.; Metcalf, W. W.; Helfrich, E. J. N.; van Wezel, G. P.; Medema, M. H.; Weber, T. antiSMASH 7.0: new and improved predictions for detection, regulation, chemical structures and visualisation. *Nucleic acids research* **2023**, *51* (W1), W46-W50. DOI: 10.1093/nar/gkad344.
(4) Gilchrist, C. L. M.; Chooi, Y.-H. clinker & clustermap.js: automatic generation of gene cluster comparison figures. *Bioinformatics (Oxford, England)* **2021**, *37* (16), 2473–2475. DOI: 10.1093/bioinformatics/btab007.
(5) Altschul, S. F.; Gish, W.; Miller, W.; Myers, E. W.; Lipman, D. J. Basic local alignment search tool. *Journal of molecular biology* **1990**, *215* (3), 403–410. DOI: 10.1016/S0022-2836(05)80360-2.
(6) Paysan-Lafosse, T.; Blum, M.; Chuguransky, S.; Grego, T.; Pinto, B. L.; Salazar, G. A.; Bileschi, M. L.; Bork, P.; Bridge, A.; Colwell, L.; Gough, J.; Haft, D. H.; Letunić, I.; Marchler-Bauer, A.; Mi, H.; Natale, D. A.; Orengo, C. A.; Pandurangan, A. P.; Rivoire, C.; Sigrist, C. J. A.; Sillitoe, I.; Thanki, N.; Thomas, P. D.; Tosatto, S. C. E.; Wu, C. H.; Bateman, A. InterPro in 2022. *Nucleic acids research* **2023**, *51* (D1), D418-D427. DOI: 10.1093/nar/gkac993.
(7) Wieder, C.; Da Peres Silva, R.; Witts, J.; Jäger, C. M.; Geib, E.; Brock, M. Characterisation of ascocorynin biosynthesis in the purple jellydisc fungus Ascocoryne sarcoides. *Fungal biology and biotechnology* **2022**, *9* (1), 8. DOI: 10.1186/s40694-022-00138-7. Published Online: Apr. 27, 2022.
(8) Geib, E.; Baldeweg, F.; Doerfer, M.; Nett, M.; Brock, M. Cross-Chemistry Leads to Product Diversity from Atromentin Synthetases in Aspergilli from Section Nigri. *Cell chemical biology* **2019**, *26* (2), 223-234.e6. DOI: 10.1016/j.chembiol.2018.10.021. Published Online: Dec. 6, 2018.
(9) Kubodera, T.; Yamashita, N.; Nishimura, A. Pyrithiamine resistance gene (ptrA) of Aspergillus oryzae: cloning, characterization and application as a dominant selectable marker for transformation. *Bioscience, biotechnology, and biochemistry* **2000**, *64* (7), 1416–1421. DOI: 10.1271/bbb.64.1416.
(10) Fulmer, G. R.; Miller, A. J. M.; Sherden, N. H.; Gottlieb, H. E.; Nudelman, A.; Stoltz, B. M.; Bercaw, J. E.; Goldberg, K. I. NMR Chemical Shifts of Trace Impurities: Common Laboratory Solvents, Organics, and Gases in Deuterated Solvents Relevant to the Organometallic Chemist. *Organometallics* **2010**, *29* (9), 2176–2179. DOI: 10.1021/om100106e.
(11) Lippke, G.; Thaler, H. Die spezifische Drehung des Sorbits und des Sorbit-Molybdat-Komplexes. *Starch - Stärke* **1970**, *22* (10), 344–351. DOI: 10.1002/star.19700221005.
(12) Takino, J.; Kotani, A.; Ozaki, T.; Peng, W.; Yu, J.; Guo, Y.; Mochizuki, S.; Akimitsu, K.; Hashimoto, M.; Ye, T.; Minami, A.; Oikawa, H. Biochemistry-Guided Prediction of the Absolute Configuration of Fungal Reduced Polyketides. *Angewandte Chemie (International*

ed. in English) **2021**, *60* (43), 23403–23411. DOI: 10.1002/anie.202110658. Published Online: Sep. 14, 2021.
(13) ADEBOYA MO. Metabolites of the higher fungi. Part 27. Berteric acid, cameronic acid and malaysic acid, three new polysubstituted fatty acids related to cubensic acid from species of the fungus genus Xylaria. *J Chem Res Syn* **1995**, *9*, 356–357.
(14) Tsukamoto, M.; Kushida, H.; Nakajima, S.; Uchiyama, S.; Nukaga, Y.; Kondo, H.; Suda, H.; Ojiri, K.; Nagashima, M. ANTIFUNGAL SUBSTANCE BE-54753 AND ITS PRODUCTION. JP19980089230 19980317.

Second Publication

Allantofuranone Biosynthesis and Precursor-Directed Mutasynthesis of Hydroxylated Analogues

Carsten Wieder[1,2], Claudia Simon-Sánchez[1], Johannes Liermann[3], Rainer Wiechert[3], Karsten Andresen[1], Eckhard Thines[1,2], Till Opatz[3], Anja Schüffler[2]

[1] Institute of Molecular Physiology, Johannes Gutenberg-University, Hanns-Dieter-Huesch Weg 17, D-55128 Mainz, Germany

[2] Institut für Biotechnologie und Wirkstoff-Forschung gGmbH, Mainz, Hanns-Dieter-Huesch Weg 17, D-55128 Mainz, Germany

[3] Department of Chemistry, Johannes Gutenberg-University, Duesbergweg 10–14, D-55128 Mainz, Germany

Type of authorship:	First author
Type of article:	Research article
Share of work:	70 %
Contribution:	Conceived project and designed experiments; fermentation; natural product purification; genome mining; cloning of plasmids; generation of mutant strains; HPLC analysis; bioactivity assays; analysis and interpretation of data; writing and editing of the manuscript
Journal:	Journal of Natural Products
Date of publication:	18.04.2025
DOI:	10.1021/acs.jnatprod.5c00197

JOURNAL OF NATURAL PRODUCTS

pubs.acs.org/jnp

Article

Allantofuranone Biosynthesis and Precursor-Directed Mutasynthesis of Hydroxylated Analogues

Carsten Wieder,* Claudia Simon-Sánchez, Johannes C. Liermann, Rainer Wiechert, Karsten Andresen, Eckhard Thines, Till Opatz, and Anja Schüffler*

Cite This: *J. Nat. Prod.* 2025, 88, 1191−1200

Read Online

ACCESS | Metrics & More | Article Recommendations | Supporting Information

ABSTRACT: Genome mining and heterologous reconstitution of biosynthetic genes in *Aspergillus oryzae* enabled elucidation of the hitherto elusive biosynthetic route that produces allantofuranone (**1**), a bioactive natural product originally isolated from *Allantophomopsis lycopodina*. The core non-ribosomal peptide synthetase (NRPS)-like enzyme AlfA of the *alf* BGC produces polyporic acid (**2**) from phenylpyruvic acid. In subsequent reactions, compound **2** is reductively dehydrated by the bifunctional enzyme AlfC and methylated by AlfD to produce terferol (**6**). In a final step, the quinol moiety of compound **6** is oxidatively cleaved and contracted by the aromatic ring cleavage dioxygenase AlfB. Using combinatorial biosynthesis, we were able to manipulate the biosynthetic route to yield hydroxylated pathway congeners, most notably the new natural products deoxyascocorynin (**10**), hydroxyterferol (**11**), and hydroxyallantofuranone (**12**).

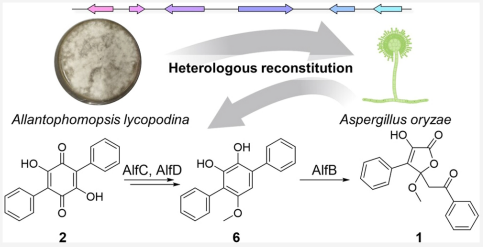

Non-ribosomal peptide synthetases (NRPSs) are multimodular multidomain enzymes that catalyze the ribosome-independent assembly of peptides from proteinogenic and non-proteinogenic amino acids as well as some other keto, hydroxy, and fatty acids.[1] Canonical NRPS modules are composed of at least an adenylation (A), thiolation (T), and condensation (C) domain that catalyze substrate activation, tethering and peptide bond formation of adjacent T-domain-bound substrates, respectively.[1] In contrast to canonical NRPSs, NRPS-like enzymes lack a C-domain and can be distinguished into reducing and non-reducing types, harboring either a terminal reductase (R) or thioesterase (TE) domain, respectively.[2,3] Reducing NRPS-like enzymes are often involved in the reductive tailoring of natural products as in, e.g., the biosynthesis of ascofuranone,[4] but can also produce metabolites of their own as is the case in the biosynthesis of aspergillic and neoaspergillic acid.[5] Non-reducing NRPS-like enzymes catalyze the condensation of two identical aromatic α-keto acids, facilitated by the terminal TE domain, to form various different cyclic core structures, i.e., benzoquinones,[6−10] furanones[11−13] and dioxolanones[14,15] (Figure 1). To this date, no non-reducing type NRPS-like enzyme has been reported that deviates from the aforementioned substrate scope, which limits the diversity of resulting products. Instead, diversification of NRPS-like enzyme derived metabolites is achieved through downstream modifications introduced by tailoring enzymes.

The biosynthesis of terrequinone A, the first natural product reported to derive from an NRPS-like enzyme, was characterized in 2007 by Balibar et al. through *in vitro* reconstitution of the biosynthetic enzymes[6] (Figure 1). The NRPS-like enzyme TdiA produces the benzoquinone didemethylasterriquinone D from two molecules of indolepyruvate, which are provided for the reaction by the L-tryptophan aminotransferase TdiD. Next, the quinone reductase TdiC reduces the quinone core which is subsequently prenylated twice by the prenyltransferase TdiB. While the exact function of TdiE is not quite clear, it is required for formation of the diprenylated product and preventing formation of a mono-*O*-prenylated shunt product.

More recently, Janzen et al. characterized the biosynthesis of the dibenzofurans uscandidusin A/B by first introducing the entire *ucd* BGC into the heterologous host *Aspergillus nidulans* and subsequently deleting biosynthetic genes to study their function and isolate biosynthetic intermediates[16] (Figure 1). The *ucd* BGC encodes an aminotransferase UcdG that is proposed to provide 4-hydroxyphenylpyruvate from L-tyrosine for the NRPS-like enzyme UcdA which produces the benzoquinone atromentin (**8**). Next, the quinone core is proposed to be reductively dehydrated by a bifunctional

Received: February 13, 2025
Revised: April 4, 2025
Accepted: April 8, 2025
Published: April 18, 2025

https://doi.org/10.1021/acs.jnatprod.5c00197
J. Nat. Prod. 2025, 88, 1191−1200

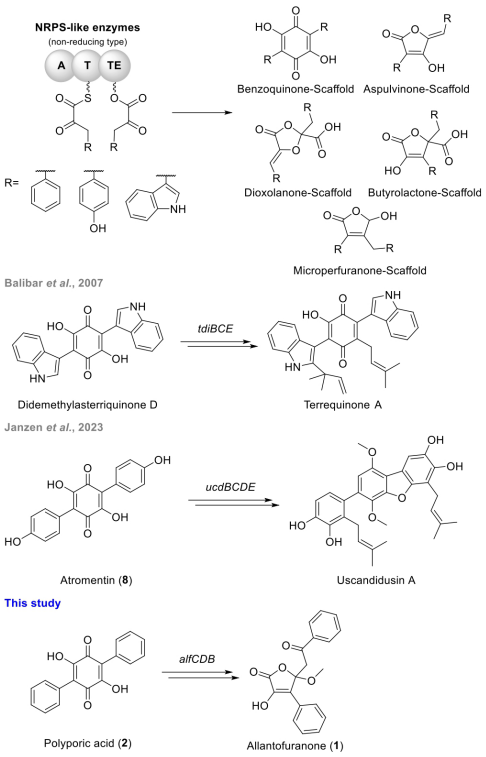

Figure 1. NRPS-like enzyme derived natural products. NRPS-like enzymes catalyze the condensation of two identical aromatic α-keto acids to afford various cyclic products. Increased product diversity is achieved by subsequent tailoring as exemplified by the diversification of benzoquinones.

enzyme UcdB resulting in formation of a 2,3,5-trihydroxyterphenyl intermediate, however, no biosynthetic intermediate could be observed. This proposed intermediate is subsequently dimethylated, prenylated and hydroxylated in a series of reactions catalyzed by UcdC, UcdD and UcdE to give rise to the intermediates usterphenyllins A/B. These then undergo spontaneous dibenzofuran formation to yield the final products, which seems to be dependent on the *m*-hydroxylation of the phenyl rings.

Furthermore, multiple other NRPS-like biosynthetic pathways have been elucidated including the biosynthesis of aspulvinone H,[12] butyrolactone I[3,12] and ascocorynin.[10] On the other hand, many further natural products have been proposed to derive from NRPS-like enzyme pathways, but their biosynthesis has remained enigmatic as is the case for involutin,[17] thelephoric acid,[18] variegatic acid[19] and guignardic acid.[20] It is noteworthy, that the physiology of the host can play a crucial role in the production of NRPS-like enzyme derived products, as exemplified by the enzymatic or non-enzymatic modification of benzoquinones in *Aspergillus niger*[7] and *A. nidulans*.[9]

Allantofuranone (**1**) is produced by *Allantophomopsis lycopodina* and was first reported in 2009.[21] It was initially isolated because of its moderate antifungal activity against some fungal species. Structurally, compound **1** resembles butyrolactone IIa, however it is differently substituted at the C5 position. In a previous study, the biosynthesis of compound **1** was investigated by means of ^{13}C-labeling and feeding of a difluorinated precursor, which hinted toward compound **1** originating from the benzoquinone polyporic acid (**2**)[22] (Figure 1), which, similar to didemethylasterriquinone D and atromentin (**8**), is also the product of NRPS-like enzymes such as AcyN and CorA.[10,18] Therefore, the furanone moiety in compound **1** is proposedly produced via post-synthesis ring contraction which is in contrast to the direct furanone formation in butyrolactone IIa and aspulvinone E. The genetic basis of allantofuranone (**1**) biosynthesis has so far been elusive and especially the unique ring contraction sparked our interest. To our knowledge, no enzymes involved in the ring contraction of NRPS-like enzyme derived natural products have been reported to date.

Here, we report the identification of the BGC responsible for allantofuranone (**1**) biosynthesis in *A. lycopodina*. Heterologous reconstitution of biosynthetic genes in *Aspergillus oryzae* OP12 allowed for the elucidation of the biosynthetic pathway, which involves dioxygenase-catalyzed ring contraction to produce the furanone moiety found in compound **1**. By employing precursor-directed combinatorial mutasynthesis, it was furthermore possible to produce a new hydroxylated analogue of compound **1** and other mono- and dihydroxylated pathway intermediates.

RESULTS AND DISCUSSION

Identification of a Candidate Biosynthetic Gene Cluster. The genome of *A. lycopodina* was sequenced in order to investigate the biosynthetic origin of allantofuranone (**1**). antiSMASH[23] analysis revealed two biosynthetic gene clusters containing non-reducing NRPS-like enzymes, one of which was investigated due to the predicted functions of adjacent genes. Besides the NRPS-like enzyme *alfA*, the *alf* cluster (accession number PQ256815) encodes a 3-deoxy-D-arabinoheptulosonate-7-phosphate (DAHP)-synthase (*alfS*),

Table 1. Proposed Function of *alf* Cluster Genes

gene	size (aa)	BlastP hit[a]	identity (%)	*E* value	proposed protein function
alfS	387	C9K7C8.1	54.25	1×10^{-140}	DAHP synthase
alfB	278	A0A0F7CUE8.1	36.27	3.00×10^{-45}	aromatic ring cleavage dioxygenase
alfR	519	B8N0F0.1	25.71	2.00×10^{-30}	C6-TF
alfA	930	P9WES4.1	69.58	0.0	NRPS-like enzyme (A-T-TE)
alfC	306	P63936.1	24.26	3.00×10^{-7}	dehydrogenase
alfD	433	Q0CS95.1	41.96	3.00×10^{-117}	*O*-methyltransferase

[a]Uniprot as reference database, manually curated choice (best, characterized fungal hit if possible).

https://doi.org/10.1021/acs.jnatprod.5c00197
J. Nat. Prod. 2025, 88, 1191−1200

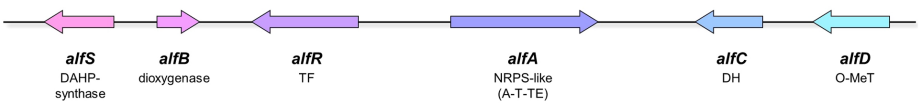

Figure 2. Scheme of *alf* cluster. A, adenylation domain; DAHP, 3-deoxy-D-arabinoheptulosonate-7-phosphate; DH, dehydrogenase; O-MeT, *O*-methyltransferase; T, thiolation domain; TE, thioesterase domain; and TF, transcription factor.

an aromatic ring cleavage dioxygenase (*alfB*), a zinc-binding transcription factor (*alfR*), a dehydrogenase (*alfC*), and an *O*-methyltransferase (*alfD*) (Table 1 and Figure 2).

Elucidation of Allantofuranone Biosynthesis. In order to elucidate the biosynthesis of allantofuranone (**1**), genes encoded in the *alf* cluster were sequentially reconstituted in the heterologous host *Aspergillus oryzae* OP12.[7] The resulting mutant strains were analyzed for the production of metabolites absent from the empty plasmid control strain and their respective parental strains (Figure 3). Newly produced metabolites were purified for structure elucidation.

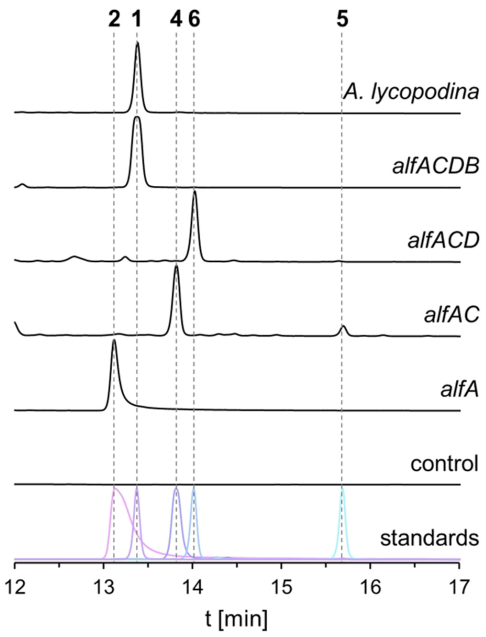

Figure 3. Heterologous reconstitution of allantofuranone (**1**) biosynthesis in *A. oryzae* OP12. Chromatograms (250 nm) of culture filtrate extracts of OP12 mutant strains expressing *alf* genes, *A. lycopodina*, and standards. Control, OP12 transformed with empty plasmid.

Heterologous expression of solely the NRPS-like encoding gene *alfA* resulted in the production of polyporic acid (**2**), the presumed precursor of allantofuranone (**1**),[22] reinforcing the hypothesis, that the *alf* cluster is indeed involved in the biosynthesis of allantofuranone (**1**). Next, coexpression of *alfA* and the predicted dehydrogenase gene *alfC* resulted in formation of the major product deoxypolyporic acid (**4**) and the 5,5-linked symmetric deoxypolyporic acid dimer (**5**), which has not been reported in literature before. We hypothesized that production of compound **4** likely proceeds via the unstable 2,3,5-trihydroxyterphenyl intermediate **3**, which either reoxidizes or dimerizes in the presence of O_2 (Figure S.4). Indeed, reduction and dehydration of compound **2** to compound **3** as well as the spontaneous reoxidation of compound **3** to compound **4** has previously been reported in the biosynthesis of bacterial echosides, where these reactions are catalyzed by two distinct but collaborating enzymes[24,25] (Figure S.5). By comparison, *alfC* combines both these functionalities, catalyzing the reductive dehydration of compound **2** to compound **3**. Analogously, reductive dehydration of the related benzoquinone atromentin (**8**) was previously proposed in the biosynthesis of uscandidusins catalyzed by UcdB (accession number KIA75357.1; Figure S.5),[16] which shares 41.16% homology with AlfC (*E* value: 3.00×10^{-76}).

Additional coexpression of the *O*-methyltransferase coding gene *alfD* alongside *alfAC* resulted in the production of terferol (**6**), an *O*-methylated derivative of the proposed intermediate **3**. The methylation seems to stabilize the reactive *p*-terphenyl core, as apparent by the absence of dimeric shunt products. Lastly, additional coexpression of the aromatic ring cleavage dioxygenase encoding gene *alfB* resulted in the production of allantofuranone (**1**), which implies the oxidative cleavage of compound **6** and subsequent rearrangement of the linear intermediate into the furanone scaffold. Based on these findings the biosynthetic pathway of compound **1** is proposed as depicted in Scheme 1.

Aromatic ring cleavage dioxygenases are frequently encountered in catabolic pathways for the degradation of aromatic compounds,[26,27] but to our knowledge have not been reported in natural product biosynthesis as of yet. These enzymes catalyze the ring fission of catecholic substrates by cleaving the aromatic ring either *ortho* (intradiol dioxygenases) or *meta* (extradiol dioxygenases) to the hydroxyl functionalities[26,27] (Figure S.6). Based on the cleavage pattern AlfB can be categorized as an extradiol-dioxygenase and the cleavage of compound **6** can be compared to the cleavage of polychlorinated-biphenyls by the extradiol-dioxygenase BphC from *Pseudomonas* sp.[28] (Figure S.6).

In the *β*-ketoadipate pathway the intradiol-cleavage of catecholic substrates results in formation of linear muconic acid intermediates, which are subsequently lactonized by cycloisomerases prior to further degradation.[27,29] These muconolactones structurally resemble the scaffold of allantofuranone (**1**) (Figure S.6) and indeed the muconolactone moiety can be found in a variety of other natural products as well, such as pochoniolides,[30] terphyl (di-) acid[31] and terphenolide.[32] Therefore, the adoption of aromatic ring cleavage dioxygenases into secondary metabolism does not seem to be unique to allantofuranone (**1**) biosynthesis. Whether or not the lactonization of compound **1** from the proposed linear intermediate occurs spontaneously or is

https://doi.org/10.1021/acs.jnatprod.5c00197
J. Nat. Prod. 2025, 88, 1191−1200

Scheme 1. Proposed Biosynthetic Pathway for Allantofuranone (1) in *A. lycopodina*

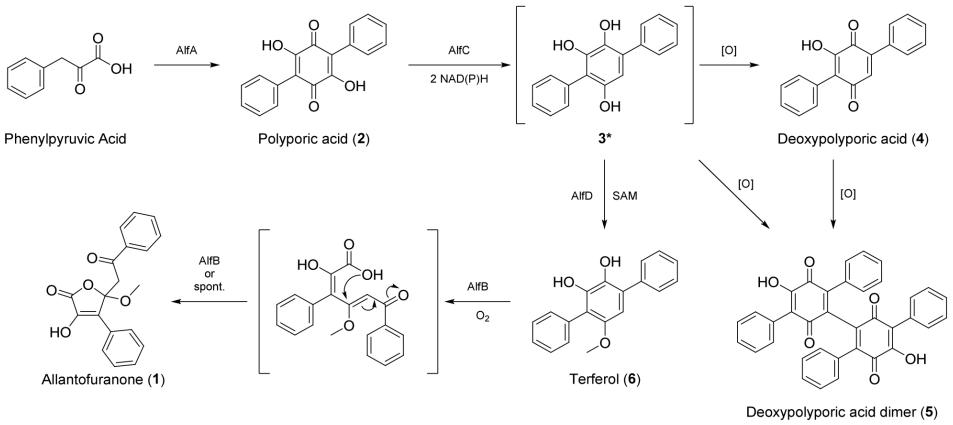

*Product not observed, structure proposed.

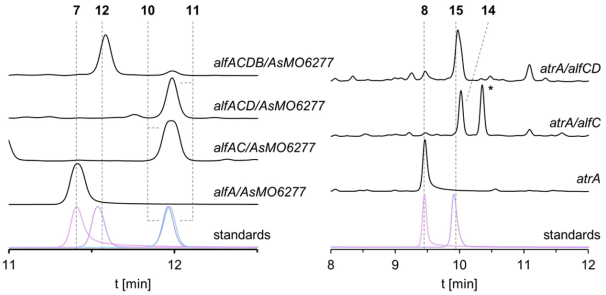

Figure 4. Combinatorial biosynthesis of hydroxylated allantofuranone (**1**) analogues in *A. oryzae* OP12. Chromatograms (250 nm) of culture filtrate extracts of OP12 mutant strains expressing *alf* genes and either *AsMO6277* or *atrA* and standards. (*) Uncharacterized dimer.

favored by AlfB remains elusive. Notably, muconolactones can be spontaneously formed from 2- or 4-alkyl-substituted phenols via their respective muconic acid intermediates when phenols are oxidatively degraded with H_2O_2 (Figure S.6).[33]

An interesting aspect of the allantofuranone (**1**) biosynthetic pathway is the high reactivity of the biosynthetic intermediate **3**, resulting in the formation of various dimers in the heterologous host. Similarly, this likely also gives rise to the hybrid terphenyl-naphthalene pigments reportedly produced by *A. lycopodina*.[34] This exemplifies a novel type of fungal pigment that is based on the product of an NRPS-like enzyme. While many fungi produce pigments that are based on polymerization of DHN, YWA1, or L-DOPA, *Aspergillus terreus* has previously also been reported to produce a non-canonical conidial pigment derived through activation and polymerization of the NRPS-like enzyme product aspulvinone E.[11] Therefore, the biosynthetic pathway of allantofuranone (**1**) might serve an additional purpose in *A. lycopodina* i.e., protection against ultraviolet (UV) light through production of off-pathway hybrid pigments.

Lastly, it is noteworthy that the isolated yield of compound **1** from OP12_*alfACDB* (110 mg/1 L) exceeded the isolated yield from the natural producer previously reported (191.3 mg/20 L) by 11-fold,[21] showcasing the power of heterologous expression for natural product synthesis.

Combinatorial Mutasynthesis of Allantofuranone Analogues. In previous studies it was demonstrated, that the diversity of NRPS-like enzyme derived products can be expanded by employing combinatorial biosynthesis.[3,15,35] Inspired by these approaches, we attempted to exploit the *alf* biosynthetic genes for precursor-directed mutasynthesis to yield new natural products (Figures 4 and Scheme 2). Since it was previously shown that difluorinated compound **2** can be converted into difluorinated compound **1**,[22] we hypothesized that the tailoring enzymes downstream of AlfA might also accept ascocorynin (**7**) and atromentin (**8**), mono- and dihydroxylated congeners of compound **2**, resulting in the formation of hydroxylated analogues of the natural pathway intermediates. To this end, the polyporic acid monooxygenase coding gene *AsMO6277* from *Ascocoryne sarcoides*, which was previously reported to convert compound **2** to compound **7**,[10] was introduced into all previously established OP12_*alf* mutants. Additionally, OP12 mutants harboring the atromentin (**8**) synthetase *atrA*[36] from *A. terreus* instead of *alfA* alongside the other *alf* genes were constructed. Again, all resulting mutant strains were analyzed for the production of

https://doi.org/10.1021/acs.jnatprod.5c00197
J. Nat. Prod. 2025, 88, 1191−1200

Scheme 2. Proposed Mutasynthetic Pathway for Hydroxylated Allantofuranone (1) Analogues

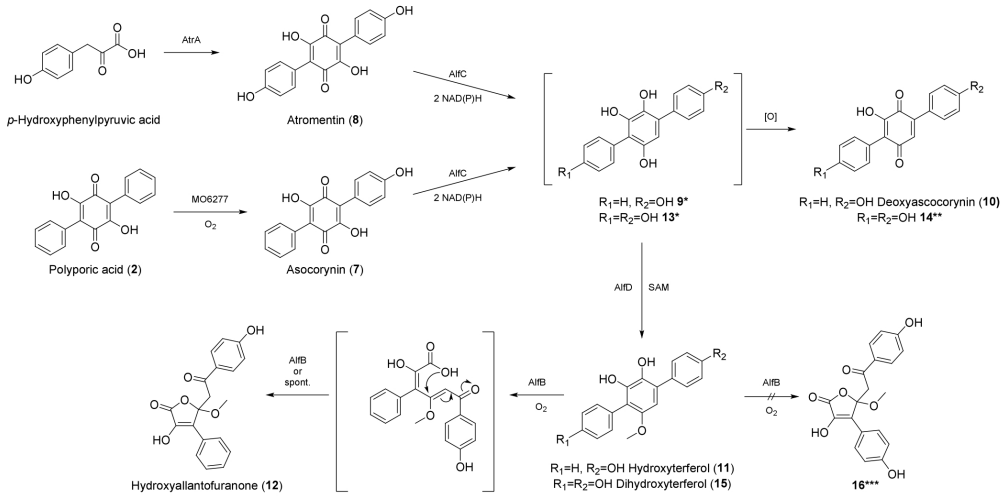

*Product not observed, structure proposed. **Product observed, structure proposed. ***Hypothetical product, not produced, structure proposed.

metabolites and new products were purified for structure elucidation.

As already previously reported, the coexpression of *alfA* and *AsMO6277* in OP12 led to the production of ascocorynin (**7**).[10] Coexpression of *AsMO6277* alongside *alfAC* led to the production of the new natural product deoxyascocorynin (**10**), which is a monohydroxylated congener of compound **4**. Interestingly, only one position isomer of compound **10** is produced, suggesting AlfC either preferring or only accepting one orientation of substrate **7**. Production of compound **10** is proposed to proceed via the unstable intermediate **9** and similar to OP12_*alfAC*, OP12_*alfAC*/*AsMO6277* also produced dimers. The mutant strain OP12_*alfACD*/*AsMO6277* produced the new natural product hydroxyterferol (**11**), which as expected is a monohydroxylated analogue of compound **6**. Finally, additional coexpression of *alfB* resulted in the production of the new monohydroxylated allantofuranone analogue hydroxyallantofuranone (**12**). The allantofuranone (**1**) biosynthetic machinery was shown to be promiscuous enough to accept ascocorynin (**7**), a monohydroxylated analogue of the first biosynthetic intermediate polyporic acid (**2**), which allowed for the production of the new-to-nature natural products **10**, **11**, and **12** (Scheme 2).

Next, we reconfirmed that expression of solely *atrA* in OP12 did result in the production of atromentin (**8**) as previously reported.[36] Coexpression of *atrA* with *alfC* resulted in the production of compound **14**. Unfortunately, despite multiple attempts, we were not able to purify compound **14** for structure elucidation, as it was extremely unstable, decomposing and/or dimerizing during the extraction/purification workflow. The identity of compound **14** is proposed as the dihydroxylated congener of compound **4**, which is in line with the detected mass of 307 Da [M − H^+] and the similarity of the ultraviolet/visible (UV/vis) spectra of compounds **14** and **10** (Figure S.1).

Successful conversion of compound **8** to compound **14** was unexpected, as previously only one position isomer of compound **10** was produced from compound **7** by AlfC. Therefore, while the hydroxyl moieties in either position do not seem to hinder conversion, AlfC might have a stronger affinity toward one substrate orientation when presented with compound **7**. Again, we propose production of compound **14** to proceed via oxidation of intermediate **13**, which seems to be even more unstable compared to proposed intermediates**3** and **9**. Interestingly, while the biosynthesis of uscandidusins A/B is proposed to progress via intermediate **13**, production of compound **14** was not observed in the heterologous host *A. nidulans*.[16] This might be due to the high reactivity of compound **13**, which in the presence of other molecules might result in the formation of insoluble or undetectable conjugates in analogy to the formation of terphenyl-naphthalene hybrid pigments in *A. lycopodina* discussed earlier.

Additional coexpression of *alfD* along *atrA* and *alfC* did successfully result in the production of dihydroxyterferol (**15**), a compound which had previously only been produced synthetically[37] but not described as a natural product. Unfortunately, OP12_*atrA*/*alfCDB* did not produce a dihydroxylated analogue (**16**) of allantofuranone (**1**) (Figure S.7), therefore the substrate promiscuity of AlfB seems to be limited. The discrepancy between conversion of monohydroxylated intermediate **11** but non-conversion of dihydroxylated intermediate **15** was unexpected, as difluorinated compound **2** was previously reported to be converted to difluorinated compound **1**.[22] However, oxygen is both bigger in size and more prone to polar interactions, which might interfere with the catalytic activity of AlfB. This bottleneck could be overcome in the future by additionally employing enzyme engineering. Similarly, engineering of AlfC might allow for accessing the other position isomers of compounds **10**, **11**, and **12**.

https://doi.org/10.1021/acs.jnatprod.5c00197
J. Nat. Prod. 2025, 88, 1191−1200

Table 2. Antimicrobial Activity of Purified Compounds[a]

	MIC (μg/mL)										
organism	1	2	4	5	6	7	8	10	11	12	15
Magnaporthe oryzae (H_2O)[b]	50	–	–	50	5	50	–	50	50	–	–
Magnaporthe oryzae (CM)[b]	50	50	>100	50	10	50	–	10	50	–	–
Botrytis cinerea[b]	>100[d]	>100	>100	–	100	–	–	10	100	–	>100
Fusarium graminearum[b]	–[e]	–	–	–	10	–	–	50	50	–	–
Aspergillus oryzae[b]	>100	–	–	–	–	–	–	100	–	–	–
Candida albicans[c]	–	–	>100	–	100	–	–	10	100	–	–
Phytophthora infestans[c]	>100	100	5	–	50	–	–	5	50	–	–
Staphylococcus aureus[c]	–	50	–	–	50	–	–	100	50	–	100
Pseudomonas aeruginosa[c]	–	–	–	–	–	–	–	–	–	–	–
Aneurinibacillus migulanus[c]	–	–	10	50	50	–	–	50	50	–	50
Enterobacter cloacae subsp. *dissolvens*[b]	–	–	–	–	–	–	–	–	–	–	–

[a]Ciclopirox (100 μg/mL) was used as a positive control, fully inhibiting germination and growth of all tested fungi and oomycetes. Streptomycin (100 μg/mL) and tetracycline (100 μg/mL) were used as positive controls (separately), fully inhibiting the growth of all tested bacteria. [b]Inhibition of conidial germination. [c]Inhibition of growth. [d]Partially inhibited at maximum test concentration. [e]No activity at 100 μg/mL.

Notably, the yield of atromentin (**8**) derived analogues were far lower as compared to the natural allantofuranone (**1**) pathway intermediates. This is likely due to a decreased availability of the substrate 4-hydroxyphenylpyruvic acid as compared to phenylpyruvic acid in the heterologous host. In future efforts this limitation could be overcome by additionally coexpressing a tyrosine transaminase such as *ucdG*. Indeed, deletion of *ucdG* from the uscandidusin BGC in the heterologous host *A. nidulans* led to a slight decrease in metabolite production.[16] Multiple other NRPS-like BGCs have been reported to encode specific transaminases for providing α-keto acids to the NRPS-like enzymes such as TdiD in the terrequinone A BGC of *A. nidulans*[6] and AtrD in the atromentin (**8**) BGC of *Tapinella panuoides*.[8]

Lastly, there are numerous other benzoquinone and terphenyl natural products that contain unique modifications, the biosynthetic origin of which have not been characterized as of yet, but once elucidated can potentially also be harnessed for combinatorial biosynthesis in the future. Among others, these include various methylations, hydroxylations, *C*- and *O*-prenylations, cyclized prenyl moieties and the previously mentioned proximal muconolactone moieties.[38−47]

Structure Elucidation of Purified Compounds. All purifed compounds have been characterized using one-dimensional (1D) and two-dimensional (2D) nuclear magnetic resonance (NMR) as well high-resolution electrospray ionization mass spectrometry (HRESIMS). Allantofuranone (**1**) and six more compounds (**2**, **4**, **6**−**8**, and **15**) have previously been described and their analytical data is in accordance with the literature.

Deoxypolyporic acid dimer (**5**) was found to have a molecular formula of $C_{36}H_{22}O_6$ by HRESIMS. The NMR spectra were very similar to those of deoxypolyporic acid (**4**). The molecular formula and the high similarity indicated a symmetrical homodimer of compound **4**. This was confirmed by the lacking of the quinone methine group (δ_H 6.88, δ_C 133.4) and an additional quaternary carbon atom (δ_C 140.0). Deoxyascocorynin (**10**) had an elemental formula of $C_{18}H_{12}O_4$ according to HRESIMS. Again, the NMR spectra showed similarity to those of compound **4**. The molecular formula indicated an additional hydroxyl group and one phenyl residue gave an AA′BB′ spin system. Thus, it could be concluded that one of the phenyl residues was *p*-hydroxylated. Characteristic ^3J heteronuclear multiple bond correlations (HMBCs) (6.78 → 123.1, 7.47 → 141.7) and an nuclear Overhauser effect (NOE) (6.78 ↔ 7.47) showed that the aryl residue was facing the quinone methine group. Hydroxyterferol (**11**, $C_{19}H_{16}O_4$) was analyzed analogously to compound **10**. The central ring of the terphenyl scaffold could be exhaustingly characterized by HMBC correlations from 3-OH (8.17 → 117.0, 144.9, 136.1), 4-OH (7.91 → 144.9, 136.1, 127.8), and 1-OMe (3.59 → 150.3). Again, ^3J HMBC correlations (6.35 → 129.5) and NOE (6.35 ↔ 7.42) proved a substitution pattern corresponding to compound **10**. Hydroxyallantofuranone (**12**) had an elemental formula of $C_{19}H_{16}O_6$ according to HRESIMS. The spectra showed high similarity to those of allantofuranone (**1**) with one phenyl residue again giving an AA′BB′ spin system. Together with the molecular formula, it could be concluded again that one phenyl residue was *p*-hydroxylated. Its location was determined by HMBC to be connected to the ketone (7.72 → 192.3) while the other phenyl residue showed a correlation into the furanone ring (7.83 → 121.3).

Biological Activity of Purified Compounds. The antimicrobial activity of the purified compounds was assessed in routine bioassays, covering germination inhibition of filamentous ascomycetes including various plant pathogenic species, growth inhibition of dimorphic human pathogenic yeast *Candida albicans*, potato blight oomycete *Phytophthora infestans* and some bacterial strains including human pathogenic *Staphylococcus aureus* and *Pseudomonas aeruginosa* (Table 2). Ciclopirox (100 μg/mL) was used as an experiment positive control, fully inhibiting germination and growth of all tested fungi and *P. infestans*. Streptomycin (100 μg/mL) and tetracycline (100 μg/mL) were used as experiment positive controls, fully inhibiting growth of all tested bacteria. Apart from compound **12**, all compounds exhibited some, mostly mild bioactivity in the performed assays. The most noteworthy activities include the anti-*Phytophthora* activity of compound **4** at an MIC of 5 μg/mL, the germination inhibitory activity of compound **6** against *Fusarium graminearum* at a MIC of 10 μg/mL and the anti-*Candida* and anti-*Phytophthora* activity of compound **10** with MICs of 10 and 5 μg/mL, respectively. However, as these compounds are not only active against one species, but broadly active instead (even across domains), none of the purified compounds poses a valuable drug lead. Interestingly, comparing compounds **4** and **10**, hydroxylation did improve activity in some assays up to 10-fold (antifungal activity against *C. albicans*) and decreased activity in others,

https://doi.org/10.1021/acs.jnatprod.5c00197
J. Nat. Prod. 2025, 88, 1191−1200

showcasing the effect of even minor molecular changes on bioactivity.

SUMMARY

In summary, the allantofuranone (**1**) biosynthetic gene cluster was identified in *A. lycopodina* through genome mining and biosynthesis was elucidated through heterologous reconstitution in *A. oryzae* OP12. Our results confirm the previous finding that the biosynthesis of compound **1** progresses via polyporic acid (**2**) as the first intermediate. The bifunctional enzyme AlfC catalyzes benzoquinone to *p*-terphenyl conversion through reductive dehydration. The unstable intermediate **3** either spontaneously reoxidizes to compound **4**, dimerizes to compound **5**, reacts with naphthalene-compounds to form a novel type of hybrid pigment, or is stabilized through O-methylation by AlfD. In a final reaction, AlfB oxidatively cleaves the *p*-terphenyl core of intermediate **6** which is subsequently rearranged to afford the final furanone scaffold in compound **1**. Additionally, we report combinatorial mutasynthesis of new hydroxylated analogues of natural pathway intermediates (**10**, **11**, and **12**), highlighting the potential of engineering biosynthetic pathways in accessing non-natural chemical diversity.

EXPERIMENTAL SECTION

General Experimental Procedures. Optical rotation measurements were accomplished with a PerkinElmer 241MC polarimeter at λ = 589 nm. A solvent-filled cuvette was used for instrument calibration.[48] UV/vis spectra of compounds were extracted from high-performance liquid chromatography (HPLC) runs (Figure S.1). Infrared spectroscopy was performed on a Bruker Tensor 27 FTIR spectrometer including a diamond ATR unit and is reported in terms of absorption frequency $\bar{\nu}$ (cm^{-1}). NMR spectra were recorded at 294 K on a 600 MHz Bruker Avance-III 600 spectrometer equipped with a 5 mm TCI cryoprobe. ^{1}H and ^{13}C chemical shifts are given relative to tetramethylsilane (TMS). ^{1}H shifts were calibrated using the residual solvent signal ($CDCl_3$: 7.26 ppm; DMSO-d_6: 2.50 ppm).[49] ^{13}C shifts were calibrated using absolute reference from the ^{1}H spectra. HRMS was conducted on an Agilent G6545A Q-ToF with ESI, APCI or APPI source coupled with an Agilent 1260 Infinity II HPLC system. For analytical thin-layer chromatography (TLC) 0.25 mm silica plates (60 F254) from Merck were used, and the detection was reached by fluorescence quenching under UV light (λ = 254 nm) or by staining with potassium permanganate reagent (solution of $KMnO_4$ (3 g), K_2CO_3 (20 g), 5% NaOH (5 mL), and H_2O (300 mL)) followed by heating at 400 °C. HPLC−MS analysis was performed using a LiChrospher 100 RP-18 column (125 × 2 mm, 4 μm, Merck KGaA) attached to an Agilent DAD 1260 module and a Quadrupole LC/MS 6130 module. For analytical runs, 0.1% formic acid in H_2O and acetonitrile (ACN) were used as eluents, running a gradient from 1% to 100% ACN in 20 min followed by 100% ACN for 4 min at 0.4 mL/min flow before re-equilibrating. Preparative HPLC was performed using a Sunfire C18 column (100 Å, 5 μm, 19 × 250 mm, Waters GmbH) running on isocratic flow using 0.1% formic acid in H_2O and ACN as eluents at 17 mL/min flow.

Fungal Strains and Cultivation Conditions. *A. lycopodina* IBWF58B-05A and *A. oryzae* OP12 were routinely cultivated on YMG (0.4% yeast extract, 1% malt extract, and 1% glucose at pH 5.5) and GG10 (50 mM glucose, 10 mM glutamine, 0.52 g/L KCl, 0.52 g/L $MgSO_4{\cdot}7H_2O$, and 1.52 g/L KH_2PO_4; 1 mL/L Hutner's trace elements; pH 6.5), respectively. Media for auxotrophic mutants were supplemented with 10 mM uridine (OP12 *pyrG*$^-$ and counterselected mutants) or 10 mM uridine, 0.0001% *p*-aminobenzoic acid (PABA) and 0,05% arginine (OP12 3Δ). For induction of expression, OP12 mutant strains were cultivated in 2% starch media (2% soluble starch, 20 mM glutamine, 0.52 g/L KCl, 0.52 g/L $MgSO_4{\cdot}7H_2O$, and 1.52 g/L KH_2PO_4; 1 mL/L Hutner's trace elements; pH 6.5). All mutant strains used in this study are listed in Table S.1.

Genome Sequencing and Bioinformatic Analysis. For isolation of genomic DNA, lyophilized mycelium of *A. lycopodina* was extracted with the GeneJET Plant Genomic DNA Purification Kit (Thermo Scientific) according to the manufacturer's instructions. Whole genome sequencing was performed by the Institut für Molekulargenetik NGS-Einheit, Mainz, Germany, using a genome sequencer Illumina HiSeq 2500 to generate 5 929 011 paired end reads with a length of 150 nucleotides each. The genome was assembled by using the Software SPAdes[50] version 3.15.4 to a total length of 39284797 bp in 4383 contigs with an N50 value of 73. Gene prediction was performed by using AUGUSTUS version 3.4.0[51] and resulted in 8752 open reading frames. The set of predicted genes was used in antiSMASH version 6.1.1[23] analysis that revealed 39 BGCs. The *alf* BGC was further analyzed using BLAST[52] and Interpro.[53]

Plasmid Construction. Q5 Hot Start High-Fidelity DNA Polymerase (NEB) was used for all PCR amplifications according to the manufacturer's instructions, PCR products were purified with Monarch PCR & DNA Cleanup Kit (NEB) and plasmids assembled using NEBuilder HiFi DNA Assembly (NEB). Oligonucleotides for all amplification reactions are listed in Table S.2. Coding sequences of *alfA*, *alfB*, *alfC*, *alfD*, *AsMO6277*, and *atrA* were amplified from genomic DNA of *A. lycopodina*, *A. sarcoides* DSM 4705, and *A. terreus* FGSC A1156 and assembled into *Nco*I restricted SM-Xpress_Ura.[7] Additionally, *alfC* and *alfD* amplicons were assembled into *Nco*I SM-Xpress_paba[10] and SM-Xpress_argB(mut),[54] respectively. The general cloning strategy is schematically depicted in Figure S.2. *Escherichia coli* DH5α cells (NEB) were used to propagate assembled plasmids. Plasmids were isolated using the Monarch Plasmid Miniprep Kit (NEB) and correct assembly was confirmed by enzymatic restriction.

Construction of *A. oryzae* OP12 Mutant Strains. *A. oryzae* OP12 (*pyrG*$^-$ and 3Δ) protoplast transformations were carried out as previously described.[7,54] Mutants were constructed by sequentially introducing one plasmid at a time. The URA-cassette in the SM-Xpress_Ura plasmid complements the uridine auxotrophy of OP12, therefore allowing for selection of prototrophic mutants. In between transformations mutant strains were counterselected to reobtain uridine auxotrophy to allow reuse of the same selection marker. Despite multiple efforts, we were unable to counterselect OP12_*atrA*/*alfCD* while maintaining production of compound **15**. Therefore, we reconstructed OP12_*atrA*/*alfCD* in the triple auxotrophic strain OP12 3Δ (*pyrG*$^-$, Δ*pabA*, Δ*argB*)[54] by simultaneously introducing *atrA*, *alfC*, and *alfD* resulting in strain OP12(3Δ)_ *atrA*/*alfCD*, which we were able counterselect to subsequently obtain the strain OP12(3Δ)_ *atrA*/*alfCDB*. Integration of genes was confirmed by diagnostic PCR using the Phire Green Hot Start II PCR Master Mix (Thermo Fisher) (Figure S.3).

Counterselection. Uridine prototrophic (*pyrG*$^+$) mutants were counterselected on 5-FOA plates (GG10 supplemented with 2 mg/mL FOA, 50 mM HEPES at pH 7.0, and 20 mM uridine) as previously described.[54] Resulting uridine auxotrophic (*pyrG*$^-$) mutants were then again analyzed for secondary metabolite production before subsequent transformations.

Fermentation, Extraction, and Metabolite Purification. For screening metabolite production *A. oryzae* OP12 mutant spores were inoculated into 50 mL 2% starch media and cultivated shaking at 150 rpm for 2 days at 30 °C. Cultures were then filtered over miracloth, and the culture filtrate acidified with HCl (helps with solvent solubility of benzoquinones and terphenyls) before liquid/liquid extraction with an equal amount of ethyl acetate. The organic layer was filtered through anhydrous Na_2SO_4 and dried under reduced pressure at 45 °C. Extracts were dissolved in MeOH, centrifuged and applied to HPLC−MS analysis.

For product isolation, mutant spores were first inoculated into 50 mL YEPD media (1% yeast extract, 2% peptone, and 0.5% glucose at pH 6.5) and incubated shaking at 150 rpm overnight at 30 °C. The mycelium was then rinsed with sterile water and transferred to a 1 L 2% starch media main culture and incubated shaking at 120 rpm for

https://doi.org/10.1021/acs.jnatprod.5c00197
J. Nat. Prod. 2025, 88, 1191−1200

another 3 days at 28 °C. Culture filtrate was extracted as previously described. For purification of compound **10**, the media was supplemented with 10 g of HP20 resin to prevent excessive dimerization and decomposition. Instead of extracting the culture filtrate, in this case, the mycelium and resin were extracted instead by submersion in ethyl acetate and shaking for 2 h. Dried extracts were dissolved in DMSO and applied to preparative HPLC. Eluent composition for purification of different compounds is listed alongside pure substance yields in Table 3. Fractions containing the compounds of interest were combined and dried under reduced pressure at 45 °C.

Table 3. Eluent Composition Preparative HPLC and Compound Yields

compound	ACN (%)	yield (mg)
1	55	110.0
2	70	5.2
4	55	19.2
5	55	17.4
6	50	31.3
7	45	50.8
8	30	14.0
10	40	26.2
11	40	28.2
12	40	54.5
15	30	5.3

Allantofuranone (**1**): off-white yellowish amorphous solid; $[\alpha]_D^{21}$ = +1.3 (c = 0.15, MeOH); R_f 0.21 (cHex/EtOAc 3:1); IR (ATR): $\tilde{\nu}$ [cm^{-1}] 2935, 1763, 1681, 1597, 1448, 1388, 1359, 1302, 1177, 1145; HRESIMS *m/z* 323.0934 $[M - H]^-$ (calcd for $[C_{19}H_{15}O_5]^-$ 323.0925); ^1H and ^{13}C NMR see Table S.3. The analytical data are in accordance with the literature.[21]

Polyporic acid (**2**): red/brown/bronze amorphous solid; R_f 0.16 (DCM/MeOH/AcOH 10:1:0.5); IR (ATR) $\tilde{\nu}$ [cm^{-1}] 3306, 2916, 2851, 1613, 1595, 1524, 1497, 1399, 1248, 1002; HRESIMS *m/z* 291.0668 $[M - H]^-$ (calcd for $[C_{18}H_{11}O_4]^-$ 291.0663); ^1H and ^{13}C NMR, see Table S.5. The analytical data are in accordance with the literature.[55]

Deoxypolyporic acid (**4**): vibrant red powder; R_f 0.35 (cHex/EtOAc 3:1); IR (ATR) $\tilde{\nu}$ [cm^{-1}] 3358, 2920, 1665, 1625, 1520, 1493, 1440, 1397, 1116, 1023; HRESIMS *m/z* 275.0721 $[M - H]^-$ (calcd for $[C_{18}H_{11}O_3]^-$ 275.0714); ^1H and ^{13}C NMR, see Table S.5. The analytical data are in accordance with the literature.[56]

Deoxypolyporic acid dimer (**5**): red/brown amorphous solid; R_f 0.13 (cHex/EtOAc 3:1); IR (ATR) $\tilde{\nu}$ [cm^{-1}] 3366, 2923, 1659, 1526, 1493, 1440, 1369, 1297, 1133, 1019; HRESIMS *m/z* 549.1342 $[M - H]^-$ (calcd for $[C_{36}H_{21}O_6]^-$ 549.1344); ^1H and ^{13}C NMR, see Table S.5.

Terferol (**6**): purple oil; R_f 0.40 (cHex/EtOAc 3:1); IR (ATR) $\tilde{\nu}$ [cm^{-1}] 3355, 2929, 2851, 1598, 1414, 1371, 1304, 1227, 1106, 1068; HRESIMS *m/z* 291.1037 $[M - H]^-$ (calcd for $[C_{19}H_{15}O_3]^-$ 291.1027); ^1H and ^{13}C NMR, see Table S.4. The analytical data are in accordance with the literature.[57]

Ascocorynin (**7**): green/gold powder; R_f 0.23 (DCM/MeOH/AcOH 10:1:0.5); IR (ATR) $\tilde{\nu}$ [cm^{-1}] 3308, 2922, 1610, 1517, 1319, 1310, 1242, 997, 946, 721; HRESIMS *m/z* 307.0624 $[M - H]^-$ (calcd for $[C_{18}H_{11}O_5]^-$ 307.0612); ^1H and ^{13}C NMR, see Table S.5. The analytical data are in accordance with the literature.[58]

Atromentin (**8**): red/brown/bronze amorphous solid; R_f 0.08 (DCM/MeOH/AcOH 10:1:0.5); IR (ATR) $\tilde{\nu}$ [cm^{-1}] 2922, 2851, 1606, 1581, 1516, 1437, 1404, 1377, 1236, 1017; HRESIMS (ESI) *m/z* 323.0566 $[M - H]^-$ (calcd for $[C_{18}H_{11}O_6]^-$ 323.0561); ^1H and ^{13}C NMR, see Table S.5. The analytical data are in accordance with the literature.[59]

Deoxyascocorynin (**10**): red/brown amorphous solid; R_f 0.11 (cHex/EtOAc 3:1); IR (ATR) $\tilde{\nu}$ [cm^{-1}] 3251, 2929, 1660, 1625, 1514, 1494, 1439, 1365, 1347, 1113; HRESIMS *m/z* 291.0673 $[M - H]^-$ (calcd for $[C_{18}H_{11}O_4]^-$ 291.0663); ^1H and ^{13}C NMR, see Table S.5.

Hydroxyterferol (**11**): brown/bronze amorphous solid; R_f 0.11 (cHex/EtOAc 3:1); IR (ATR) $\tilde{\nu}$ [cm^{-1}] 3313, 1611, 1517, 1412, 1271, 1233, 1065, 1015, 951, 700; HRESIMS *m/z* 307.0986 $[M - H]^-$ (calcd for $[C_{19}H_{15}O_4]^-$ 307.0976); ^1H and ^{13}C NMR, see Table S.4.

Hydroxyallantofuranone (**12**): off-white amorphous solid; $[\alpha]_D^{21}$ = +0.6 (c = 0.48, MeOH); R_f 0.06 (cHex/EtOAc 3:1); IR (ATR) $\tilde{\nu}$ [cm^{-1}] 2935, 1760, 1688, 1601, 1582, 1287, 1223, 1169, 1016, 951; HRESIMS *m/z* 339.0883 $[M - H]^-$ (calcd for $[C_{19}H_{15}O_6]^-$ 339.0874); ^1H and ^{13}C NMR, see Table S.3.

Dihydroxyterferol (**15**): off-white/gray amorphous solid; R_f 0.33 (cHex/EtOAc 1:1); IR (ATR) $\tilde{\nu}$ [cm^{-1}] 3220, 1610, 1514, 1437, 1269, 1232, 1173, 1015, 951, 835; HRESIMS *m/z* 323.0933 $[M - H]^-$ (calcd for $[C_{19}H_{15}O_5]^-$ 323.0925); ^1H and ^{13}C NMR, see Table S.4. The analytical data are in accordance with the literature.[37]

Bioactivity Assays. *Germination Inhibition of Ascomycete Fungi.* Conidia of *Magnaporthe oryzae* 70-15, *Botrytis cinerea* DSM 0877, *Fusarium graminearum* DSM 21727, and *A. oryzae* RIB40 were harvested from properly grown agar plates and diluted in 2% malt extract media to a final concentration of 1×10^5 conidia/mL. A total of 200 μL of the solution were added to wells of a 96-well plate containing different concentrations of compounds. The plates were then incubated overnight at room temperature and conidia germination evaluated using a microscope. Ciclopirox (100 μg/mL) served as positive control.

Growth Inhibition of Dimorphic Yeast C. albicans. Fresh colonies of *C. albicans* ATCC90028, grown on Sabouraud (Difco) plates, were suspended in H_2O, diluted 1:20 in Sabouraud media, 200 μL distributed in 96-well test plates and cultivated shaking at room temperature for 18−24 h; growth inhibition was assessed macroscopically. Ciclopirox (100 μg/mL) served as positive control.

Growth Inhibition of Oomycete P. infenstans. A total of 2 mL of a 2-week-old liquid PDA culture of *P. infenstans* CBS 430.90 were shredded using a FastPrep twice for 20 s, diluted with 5 mL of H_2O, and filtered through miracloth. The filtrate was diluted 1:20 with PDB media (Difco) and 200 μL distributed in 96-well test plates. Plates were incubated gently shaking at room temperature for 1 week; growth inhibition was assessed macroscopically. Ciclopirox (100 μg/mL) served as positive control.

Growth Inhibition of Bacteria. Nutrient broth (Difco) precultures of *Staphylococcus aureus* ATCC11632 (37 °C), *Pseudomonas aeruginosa* ATCC15442 (37 °C), *Aneurinibacillus migulanus* ATCC9999 (37 °C), and *Enterobacter cloacae* subsp. *dissolvens* LMG2683 (27 °C) were grown overnight shaking. Precultures were diluted 1:100 in fresh nutrient broth and 200 μL were distributed in 96-well test plates. Plates were cultivated shaking at 37 or 27 °C for 18−24 h and growth inhibition was assessed macroscopically. Tetracycline (100 μg/mL) and streptomycin (100 μg/mL) served as positive controls.

■ ASSOCIATED CONTENT

Data Availability Statement

All data underlying this study is available in this article and the Supporting Information. The allantofuranone (*alf*) biosynthetic gene cluster has been deposited at NCBI (accession number PQ256815). The analytical data (NMR spectra, MS spectra, and IR spectra) for all purified compounds has been deposited at Chemotion Repository (10.14272/collection/JCL_2025-02-05).

Supporting Information

The Supporting Information is available free of charge at https://pubs.acs.org/doi/10.1021/acs.jnatprod.5c00197.

Supplementary tables (oligonucleotides and mutant strains), UV/vis spectra of compounds, cloning strategy scheme, mutant strain validation, chromatograms for

https://doi.org/10.1021/acs.jnatprod.5c00197
J. Nat. Prod. 2025, 88, 1191−1200

OP12_*atrA*/*alf CDB*, NMR assignments, and NMR spectra (PDF)

AUTHOR INFORMATION

Corresponding Authors

Carsten Wieder − *Microbiology and Biotechnology, Johannes Gutenberg University, D-55128 Mainz, Germany; Institut für Biotechnologie und Wirkstoff-Forschung gGmbH, D-55128 Mainz, Germany;* orcid.org/0009-0008-7991-5524; Email: cawieder@uni-mainz.de

Anja Schüffler − *Institut für Biotechnologie und Wirkstoff-Forschung gGmbH, D-55128 Mainz, Germany*; Email: schueffler@ibwf.de

Authors

Claudia Simon-Sánchez − *Microbiology and Biotechnology, Johannes Gutenberg University, D-55128 Mainz, Germany*

Johannes C. Liermann − *Department of Chemistry, Johannes Gutenberg University, D-55128 Mainz, Germany*

Rainer Wiechert − *Department of Chemistry, Johannes Gutenberg University, D-55128 Mainz, Germany;* orcid.org/0009-0009-1385-4738

Karsten Andresen − *Microbiology and Biotechnology, Johannes Gutenberg University, D-55128 Mainz, Germany;* orcid.org/0000-0003-1790-325X

Eckhard Thines − *Microbiology and Biotechnology, Johannes Gutenberg University, D-55128 Mainz, Germany; Institut für Biotechnologie und Wirkstoff-Forschung gGmbH, D-55128 Mainz, Germany*

Till Opatz − *Department of Chemistry, Johannes Gutenberg University, D-55128 Mainz, Germany;* orcid.org/0000-0002-3266-4050

Complete contact information is available at: https://pubs.acs.org/10.1021/acs.jnatprod.5c00197

Author Contributions

C.W. conceived the study. C.W. designed the experiments. C.W. and C.S.S. conducted the biological experiments. K.A. performed bioinformatic analysis. C.W. performed metabolite purification. J.C.L. and R.W. collected analytical data. J.C.L. performed structure elucidation of purified compounds. A.S., T.O., and E.T. supervised the experiments. All authors reviewed and interpreted the obtained data and results. C.W. wrote the manuscript. All authors contributed to editing and revising of the manuscript as well as read and approved the final version of the manuscript.

Funding

This work was supported by the Rhineland-Palatinate Center for Natural Products Research.

Notes

The authors declare no competing financial interest.

ACKNOWLEDGMENTS

A. oryzae strain OP12 *pyrG*$^{-}$, plasmids SM-Xpress_Ura and SM-Xpress_paba, and genomic DNA of *A. terreus* were kindly provided by Matthias Brock (University of Nottingham, Nottingham, U.K.). The authors thank Christopher Kampf (Johannes Gutenberg University, Mainz, Germany) for mass spectrometric analyses. Parts of the graphic abstract were created with BioRender.com.

REFERENCES

(1) Zhang, L.; Wang, C.; Chen, K.; Zhong, W.; Xu, Y.; Molnár, I. *Natural product reports* **2023**, *40* (1), 62−88.
(2) Noriler, S.; Navarro-Muñoz, J. C.; Glienke, C.; Collemare, J. *Genomics* **2022**, *114* (6), No. 110525.
(3) van Dijk, J. W. A.; Guo, C.-J.; Wang, C. C. C. *Org. Lett.* **2016**, *18* (24), 6236−6239.
(4) Araki, Y.; Awakawa, T.; Matsuzaki, M.; Cho, R.; Matsuda, Y.; Hoshino, S.; Shinohara, Y.; Yamamoto, M.; Kido, Y.; Inaoka, D. K.; Nagamune, K.; Ito, K.; Abe, I.; Kita, K. *Proc. Natl. Acad. Sci. U.S.A.* **2019**, *116* (17), 8269−8274.
(5) Lebar, M. D.; Mack, B. M.; Carter-Wientjes, C. H.; Wei, Q.; Mattison, C. P.; Cary, J. W. *Frontiers in fungal biology* **2022**, *3*, No. 1029195.
(6) Balibar, C. J.; Howard-Jones, A. R.; Walsh, C. T. *Nat. Chem. Biol.* **2007**, *3* (9), 584−592.
(7) Geib, E.; Baldeweg, F.; Doerfer, M.; Nett, M.; Brock, M. *Cell chemical biology* **2019**, *26* (2), 223−234.e6.
(8) Schneider, P.; Bouhired, S.; Hoffmeister, D. *Fungal genetics and biology* **2008**, *45* (11), 1487−1496.
(9) Seibold, P. S.; Lawrinowitz, S.; Raztsou, I.; Gressler, M.; Arndt, H.-D.; Stallforth, P.; Hoffmeister, D. *Fungal biology and biotechnology* **2023**, *10* (1), 14.
(10) Wieder, C.; Peres da Silva, R.; Witts, J.; Jager, C. M.; Geib, E.; Brock, M. *Fungal biology and biotechnology* **2022**, *9* (1), 8.
(11) Geib, E.; Gressler, M.; Viediernikova, I.; Hillmann, F.; Jacobsen, I. D.; Nietzsche, S.; Hertweck, C.; Brock, M. *Cell chemical biology* **2016**, *23* (5), 587−597.
(12) Guo, C.-J.; Sun, W.-W.; Bruno, K. S.; Oakley, B. R.; Keller, N. P.; Wang, C. C. C. *Chemical science* **2015**, *6* (10), 5913−5921.
(13) Yeh, H.-H.; Chiang, Y.-M.; Entwistle, R.; Ahuja, M.; Lee, K.-H.; Bruno, K. S.; Wu, T.-K.; Oakley, B. R.; Wang, C. C. C. *Applied microbiology and biotechnology* **2012**, *96* (3), 739−748.
(14) Sun, W.-W.; Guo, C.-J.; Wang, C. C. C. *Fungal genetics and biology* **2016**, *89* (89), 84−88.
(15) Hühner, E.; Öqvist, K.; Li, S.-M. *Org. Lett.* **2019**, *21* (2), 498−502.
(16) Janzen, D. J.; Zhou, J.; Li, S.-M. *Org. Lett.* **2023**, *25* (34), 6311−6316.
(17) Shah, F.; Schwenk, D.; Nicolás, C.; Persson, P.; Hoffmeister, D.; Tunlid, A. *Applied and environmental microbiology* **2015**, *81* (24), 8427−8433.
(18) Lawrinowitz, S.; Wurlitzer, J. M.; Weiss, D.; Arndt, H.-D.; Kothe, E.; Gressler, M.; Hoffmeister, D. *Microbiology spectrum* **2022**, *10* (5), No. e0106522.
(19) Tauber, J. P.; Gallegos-Monterrosa, R.; Kovács, Á. T.; Shelest, E.; Hoffmeister, D. *Microbiology* **2018**, *164* (1), 65−77.
(20) Buckel, I.; Andernach, L.; Schüffler, A.; Piepenbring, M.; Opatz, T.; Thines, E. *Sci. Rep.* **2017**, *7* (1), 8926.
(21) Schüffler, A.; Kautz, D.; Liermann, J. C.; Opatz, T.; Anke, T. *Journal of antibiotics* **2009**, *62* (3), 119−121.
(22) Schüffler, A.; Liermann, J. C.; Opatz, T.; Anke, T. *ChemBioChem* **2011**, *12* (1), 148−154.
(23) Blin, K.; Shaw, S.; Augustijn, H. E.; Reitz, Z. L.; Biermann, F.; Alanjary, M.; Fetter, A.; Terlouw, B. R.; Metcalf, W. W.; Helfrich, E. J. N.; van Wezel, G. P.; Medema, M. H.; Weber, T. *Nucleic acids research* **2023**, *51* (W1), W46−W50.
(24) Zhu, J.; Liu, M.; Deng, J.; Chen, W.; Zhu, D.; Duan, J.; Li, Y.; Wang, H.; Shen, Y. *Biochemical and biophysical research communications* **2021**, *559* (559), 62−69.
(25) Clinger, J. A.; Zhang, Y.; Liu, Y.; Miller, M. D.; Hall, R. E.; van Lanen, S. G.; Phillips, G. N.; Thorson, J. S.; Elshahawi, S. I. *ACS Chem. Biol.* **2021**, *16* (12), 2816−2824.
(26) Vaillancourt, F. H.; Bolin, J. T.; Eltis, L. D. *Crit. Rev. Biochem. Mol. Biol.* **2006**, *41* (4), 241−267.
(27) Harwood, C. S.; Parales, R. E. *Annual review of microbiology* **1996**, *50*, 553−590.
(28) Furukawa, K.; Miyazaki, T. *Journal of bacteriology* **1986**, *166* (2), 392−398.

(29) Martins, T. M.; Hartmann, D. O.; Planchon, S.; Martins, I.; Renaut, J.; Silva Pereira, C. *Fungal genetics and biology* **2015**, *74*, 32−44.
(30) Miyano, R.; Matsuo, H.; Nonaka, K.; Mokudai, T.; Niwano, Y.; Shiomi, K.; Takahashi, Y.; Ōmura, S.; Nakashima, T. *J. Biosci. Bioeng.* **2018**, *126* (5), 661−666.
(31) Liu, S.-S.; Zhao, B.-B.; Lu, C.-H.; Huang, J.-J.; Shen, Y.-M. *Natural Product Communications* **2012**, *7* (8), 1057−1062.
(32) Guo, Z. K.; Yan, T.; Guo, Y.; Song, Y. C.; Jiao, R. H.; Tan, R. X.; Ge, H. M. *J. Nat. Prod.* **2012**, *75* (1), 15−21.
(33) Giurg, M.; Kowal, E.; Muchalski, H.; Syper, L.; Młochowski, J. *Synth. Commun.* **2008**, *39* (2), 251−266.
(34) Andernach, L.; Sandjo, L. P.; Liermann, J. C.; Schlämann, R.; Richter, C.; Ferner, J.-P.; Schwalbe, H.; Schüffler, A.; Thines, E.; Opatz, T. *J. Nat. Prod.* **2016**, *79* (10), 2718−2725.
(35) van Dijk, J. W. A.; Wang, C. C. C. *Org. Lett.* **2018**, *20* (17), 5082−5085.
(36) Hühner, E.; Backhaus, K.; Kraut, R.; Li, S.-M. *Applied microbiology and biotechnology* **2018**, *102* (4), 1663−1672.
(37) Zhang, X.-Q.; Mou, X.-F.; Mao, N.; Hao, J.-J.; Liu, M.; Zheng, J.-Y.; Wang, C.-Y.; Gu, Y.-C.; Shao, C.-L. *European journal of medicinal chemistry* **2018**, *146*, 232−244.
(38) Nakagawa, F.; Takahashi, S.; Naito, A.; Sato, S.; Iwabuchi, S.; Tamura, C. *Journal of antibiotics* **1984**, *37* (1), 10−12.
(39) Marchelli, R.; Vining, L. C. *Journal of antibiotics* **1975**, *28* (4), 328−331.
(40) Yan, W.; Wuringege; Li, S.-J.; Guo, Z.-K.; Zhang, W.-J.; Wei, W.; Tan, R.-X.; Jiao, R.-H *Bioorganic & medicinal chemistry letters* **2017**, *27* (1), 51−54.
(41) Li, W.; Gao, W.; Zhang, M.; Li, Y.-L.; Li, L.; Li, X.-B.; Chang, W.-Q.; Zhao, Z.-T.; Lou, H.-X. *J. Nat. Prod.* **2016**, *79* (9), 2188−2194.
(42) Xu, K.; Gao, Y.; Li, Y.-L.; Xie, F.; Zhao, Z.-T.; Lou, H.-X. *J. Nat. Prod.* **2018**, *81* (9), 2041−2049.
(43) El-Elimat, T.; Figueroa, M.; Raja, H. A.; Graf, T. N.; Adcock, A. F.; Kroll, D. J.; Day, C. S.; Wani, M. C.; Pearce, C. J.; Oberlies, N. H. *J. Nat. Prod.* **2013**, *76* (3), 382−387.
(44) Lacey, H. J.; Vuong, D.; Pitt, J. I.; Lacey, E.; Piggott, A. M. *Aust. J. Chem.* **2016**, *69* (2), 152.
(45) Takahashi, C.; Yoshihira, K.; Natori, S.; Umeda, M. *Chemical & pharmaceutical bulletin* **1976**, *24* (4), 613−620.
(46) Ji, L.; Tan, L.; Shang, Z.; Li, W.; Mo, X.; Yang, S.; Yu, G. *Journal of agricultural and food chemistry* **2024**, *72* (10), 5247−5257.
(47) Zhou, G.; Chen, X.; Zhang, X.; Che, Q.; Zhang, G.; Zhu, T.; Gu, Q.; Li, D. *J. Nat. Prod.* **2020**, *83* (1), 8−13.
(48) Lippke, G.; Thaler, H. *Starch/Staerke* **1970**, *22* (10), 344−351.
(49) Fulmer, G. R.; Miller, A. J. M.; Sherden, N. H.; Gottlieb, H. E.; Nudelman, A.; Stoltz, B. M.; Bercaw, J. E.; Goldberg, K. I. *Organometallics* **2010**, *29* (9), 2176−2179.
(50) Prjibelski, A. D.; Vasilinetc, I.; Bankevich, A.; Gurevich, A.; Krivosheeva, T.; Nurk, S.; Pham, S.; Korobeynikov, A.; Lapidus, A.; Pevzner, P. A. *Bioinformatics* **2014**, *30* (12), i293−301.
(51) Stanke, M.; Steinkamp, R.; Waack, S.; Morgenstern, B. *Nucleic acids research* **2004**, *32*, W309−W312.
(52) Altschul, S. F.; Gish, W.; Miller, W.; Myers, E. W.; Lipman, D. J. *Journal of molecular biology* **1990**, *215* (3), 403−410.
(53) Paysan-Lafosse, T.; Blum, M.; Chuguransky, S.; Grego, T.; Pinto, B. L.; Salazar, G. A.; Bileschi, M. L.; Bork, P.; Bridge, A.; Colwell, L.; Gough, J.; Haft, D. H.; Letunić, I.; Marchler-Bauer, A.; Mi, H.; Natale, D. A.; Orengo, C. A.; Pandurangan, A. P.; Rivoire, C.; Sigrist, C. J. A.; Sillitoe, I.; Thanki, N.; Thomas, P. D.; Tosatto, S. C. E.; Wu, C. H.; Bateman, A. *Nucleic acids research* **2023**, *51* (D1), D418−D427.
(54) Wieder, C.; Künzer, M.; Wiechert, R.; Seipp, K.; Andresen, K.; Stark, P.; Schüffler, A.; Opatz, T.; Thines, E. *Org. Lett.* **2025**, *27* (4), 1036−1041.
(55) Jokela, R.; Lounasmaa, M. *Planta medica* **1997**, *63* (4), 381−383.
(56) Colson, K. L.; Jackman, L. M.; Jain, T.; Simolike, G.; Keeler, J. *Tetrahedron Lett.* **1985**, *26* (38), 4579−4582.
(57) Sawayama, Y.; Tsujimoto, T.; Sugino, K.; Nishikawa, T.; Isobe, M.; Kawagishi, H. *Bioscience, biotechnology, and biochemistry* **2006**, *70* (12), 2998−3003.
(58) Puder, C.; Wagner, K.; Vettermann, R.; Hauptmann, R.; Potterat, O. *J. Nat. Prod.* **2005**, *68* (3), 323−326.
(59) Nagao, H.; Ninomiya, M.; Sugiyama, H.; Itabashi, A.; Uno, K.; Tanaka, K.; Koketsu, M. *Bioorganic & medicinal chemistry letters* **2022**, *76*, No. 128992.

https://doi.org/10.1021/acs.jnatprod.5c00197
J. Nat. Prod. 2025, 88, 1191−1200

Supporting Information

Allantofuranone Biosynthesis and Precursor-Directed Mutasynthesis of Hydroxylated Analogues

Carsten Wieder[1,2,*], Claudia Simon-Sánchez[1], Johannes C. Liermann[3], Rainer Wiechert[3], Karsten Andresen[1], Eckhard Thines[1,2], Till Opatz[3], Anja Schüffler[2,*]

[1] Institute of Molecular Physiology, Johannes Gutenberg-University, Hanns-Dieter-Hüsch Weg 17, D-55128 Mainz, Germany

[2] Institut für Biotechnologie und Wirkstoff-Forschung gGmbH, Mainz, Hanns-Dieter-Hüsch Weg 17, D-55128 Mainz, Germany

[3] Department of Chemistry, Johannes Gutenberg-University, Duesbergweg 10–14, D-55128 Mainz, Germany

*Correspondence: cawieder@uni-mainz.de, schueffler@ibwf.de

Table of contents

Supplementary Tables

Table S. 1: *Aspergillus oryzae* mutant strains used in this study

Strain	Parental Strain	Genotype	Produces	Source
OP12 *pyrG*$^-$	See ref.	PamyB:terR_ptrA; *pyrG*$^-$	/	1
OP12 3Δ	See ref.	PamyB:terR_ptrA; *pyrG*$^-$, *ΔpabA*, *ΔargB*	/	2
OP12 empty plasmid	OP12 *pyrG*$^-$	PamyB:terR_ptrA, *pyrG*$^+$	/	This study
OP12 3Δ empty plasmids	OP12 3Δ	PamyB:terR_ptrA, *pyrG*$^+$, *pabA*$^+$, *argB*$^+$	/	2
OP12_*alfA*	OP12 *pyrG*$^-$	PamyB:terR_ptrA; PterA:alfA_URA	**2**	This study
OP12_*alfA pyrG*$^-$	OP12_*alfA*	PamyB:terR_ptrA; PterA:alfA_URA, *pyrG*$^-$	**2**	This study
OP12_*alfAC*	OP12_*alfA pyrG*$^-$	PamyB:terR_ptrA; PterA:alfA_URA, PterA:alfC_URA	**4, 5**	This study
OP12_*alfAC pyrG*$^-$	OP12_*alfAC*	PamyB:terR_ptrA; PterA:alfA_URA, PterA:alfC_URA, *pyrG*$^-$	**4, 5**	This study
OP12_*alfACD*	OP12_*alfAC pyrG*$^-$	PamyB:terR_ptrA; PterA:alfA_URA, PterA:alfC_URA, PterA:alfD_URA	**6**	This study
OP12_*alfACD pyrG*$^-$	OP12_*alfACD*	PamyB:terR_ptrA; PterA:alfA_URA, PterA:alfC_URA, PterA:alfD_URA, *pyrG*$^-$	**6**	This study
OP12_*alfACDB*	OP12_*alfACD pyrG*$^-$	PamyB:terR_ptrA; PterA:alfA_URA, PterA:alfC_URA, PterA:alfD_URA, PterA:alfB_URA	**1**	This study
OP12_*alfACDB pyrG*$^-$	OP12_*alfACDB*	PamyB:terR_ptrA; PterA:alfA_URA, PterA:alfC_URA, PterA:alfD_URA, PterA:alfB_URA, *pyrG*$^-$	**1**	This study
OP12_*alfA/AsMO6277*	OP12_*alfA pyrG*$^-$	PamyB:terR_ptrA; PterA:alfA_URA, PterA:AsMO6277_URA	**7**	This study
OP12_*alfAC/AsMO6277*	OP12_*alfAC pyrG*$^-$	PamyB:terR_ptrA; PterA:alfA_URA, PterA:alfC_URA, PterA:AsMO6277_URA	**10**	This study
OP12_*alfACD/AsMO6277*	OP12_*alfACD pyrG*$^-$	PamyB:terR_ptrA; PterA:alfA_URA, PterA:alfC_URA, PterA:alfD_URA, PterA:AsMO6277_URA	**11**	This study
OP12_*alfACDB/AsMO6277*	OP12_*alfACDB pyrG*$^-$	PamyB:terR_ptrA; PterA:alfA_URA, PterA:alfC_URA, PterA:alfD_URA, PterA:alfB_URA, PterA:AsMO6277_URA	**12**	This study
OP12_*atrA*	OP12 *pyrG*$^-$	PamyB:terR_ptrA; PterA:atrA_URA	**8**	This study
OP12_*atrA pyrG*$^-$	OP12_*atrA*	PamyB:terR_ptrA; PterA:atrA_URA, *pyrG*$^-$	**8**	This study
OP12_*atrA/alfC*	OP12_*atrA pyrG*$^-$	PamyB:terR_ptrA; PterA:atrA_URA, PterA:alfC_URA	**13, 14**	This study
OP12_*atrA/alfC pyrG*$^-$	OP12_*atrA/alfC*	PamyB:terR_ptrA; PterA:atrA_URA, PterA:alfC_URA, *pyrG*$^-$	**13, 14**	This study
OP12_*atrA/alfCD*	OP12_*atrA/alfC pyrG*$^-$	PamyB:terR_ptrA; PterA:atrA_URA, PterA:alfC_URA, PterA:alfD_URA	**15**	This study
OP12(3Δ)_*atrA/alfCD*	OP12 3Δ	PamyB:terR_ptrA; PterA:atrA_URA, PterA:alfC_argB, PterA:alfD_paba	**15**	This study
OP12(3Δ)_*atrA/alfCD pyrG*$^-$	OP12(3 Δ)_*atrA/alfCD*	PamyB:terR_ptrA; PterA:atrA_URA, PterA:alfC_argB, PterA:alfD_paba *pyrG*$^-$	**15**	This study
OP12(3Δ)_*atrA/alfCDB*	OP12(3Δ)_*atrA/alfCD pyrG*$^-$	PamyB:terR_ptrA; PterA:atrA_URA, PterA:alfC_URA, PterA:alfD+PtrpC-alfB_URA	**15**	This study

Table S. 2: Oligonucleotides used in this study

Oligo	Sequence	Purpose
oCW77	CATTTAACAAACTTCTCATCACAGCACCATGGAGCCCAAGAATCTTTAT	amplification of
oCW78	CGGTTCAGATTGAAATCACTGCTGCTCACAACCCCCGATCTTG	alfA
oCW88	CATTTAACAAACTTCTCATCACAGCACCATGGCTACTCTCAATGAACTG	amplification of
oCW89	ACGGTTCAGATTGAAATCACTGCTGCTTATGCCTTTACAACCTCAA	alfD
oCW100	CATTTAACAAACTTCTCATCACAGCACCATGGGTTTCTTCAAGCTTGCG	amplification of
oCW192	CTATACGGTTCAGATTGAAATCACTGCTGCTTATTTACTCTCATAGGGCA	alfC
oCW190	CATTTAACAAACTTCTCATCACAGCACCATGACGTCAAAAGGCCATGTA	amplification of
oCW191	CTATACGGTTCAGATTGAAATCACTGCTGCTTACCAAACATATGAACTCA	alfB
oCW91	CATTTAACAAACTTCTCATCACAGCACCATGTCTTTCAAGAACCTCCAA	amplification of
oCW92	ACGGTTCAGATTGAAATCACTGCTGCCTAAATTCCCCGTGCTTC	atrA
oCW213	CATTTAACAAACTTCTCATCACAGCACCATGCATTATTCTCCTCTCACAG	amplification of
oCW214	CTATACGGTTCAGATTGAAATCACTGCTGCTCACTTAAAAATCACTCTGA	AsMO6277

Supplementary Figures

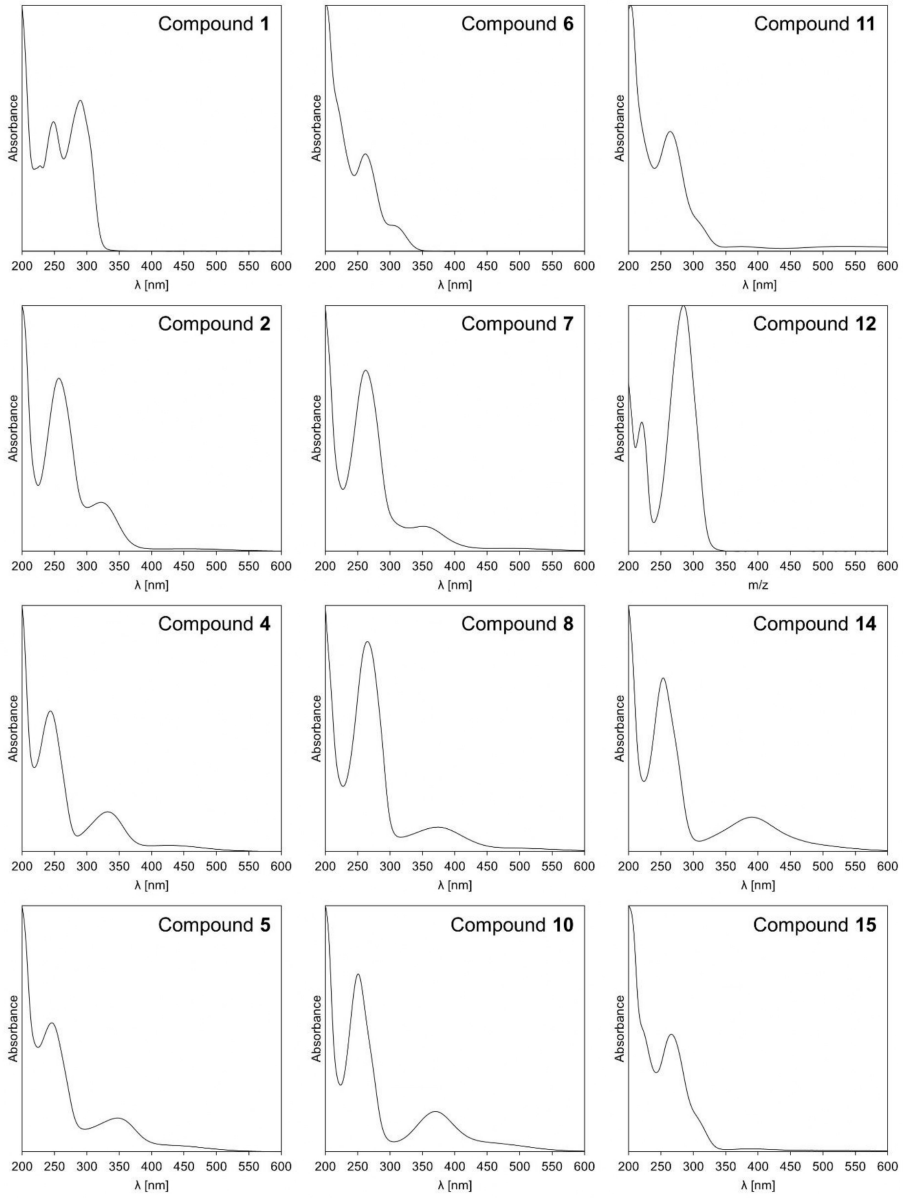

Figure S. 1: UV/Vis-spectra of reported compounds

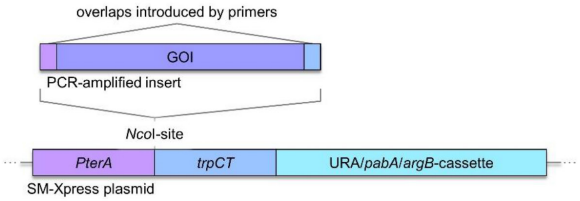

Figure S. 2: Schematic representation of strategy employed for cloning expression plasmids

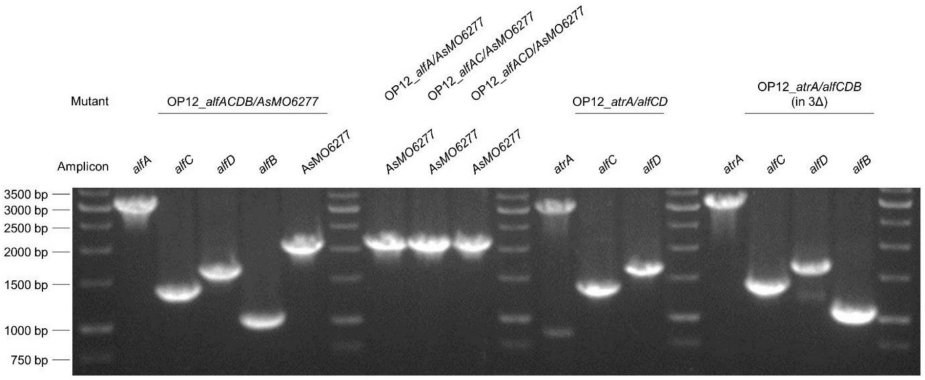

Figure S. 3: Validation of mutant strains. Genomic integration of genes was assessed by diagnostic PCR. Primers and expected amplicon sizes were as follows: *alfA*, oCW75+oCW78, 2993 bp amplicon; *alfC*, oCW75+oCW192, 1368 bp amplicon; *alfD*, oCW75+oCW89, 1632 bp amplicon; *alfB*, oCW75+oCW191, 1042 bp amplicon; *AsMO6277*, oCW75+oCW214, 2075 bp amplicon; *atrA*, oCW75+oCW92, 2964 bp amplicon.

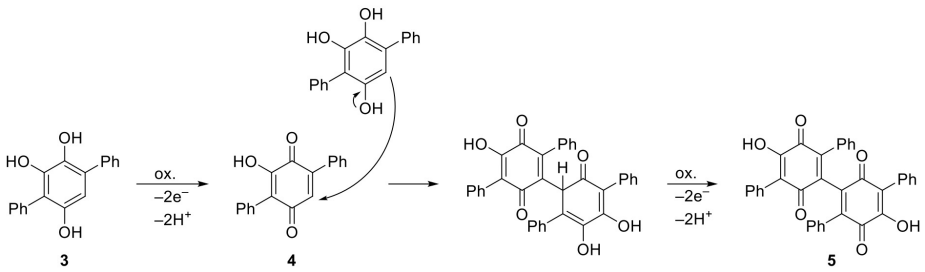

Figure S. 4: Proposed mechanism for formation of compounds **4** and **5** from compound **3**. Based on Hajdok *et al.*[3]

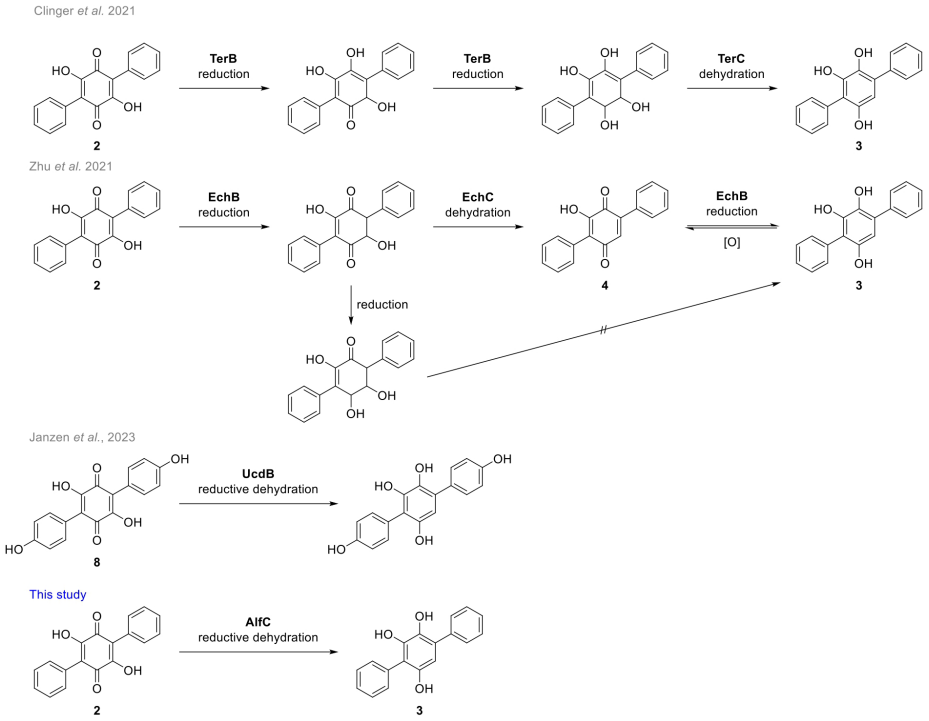

Figure S. 5:Biosynthesis of *p*-terphenyls from benzoquinones in bacteria and fungi[4–6]. Two different routes to **3** have been proposed for the biosynthesis of bacterial echosides.

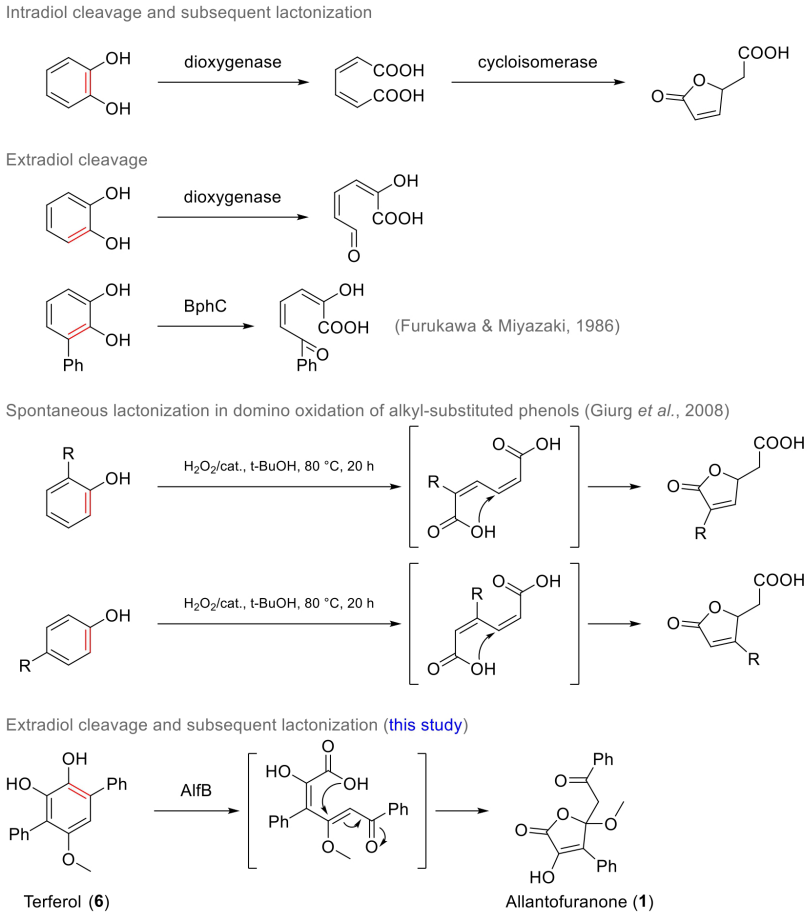

Figure S. 6: Comparison of catechol extra- and intadiol cleavage and different routes to muconolactones[7,8]

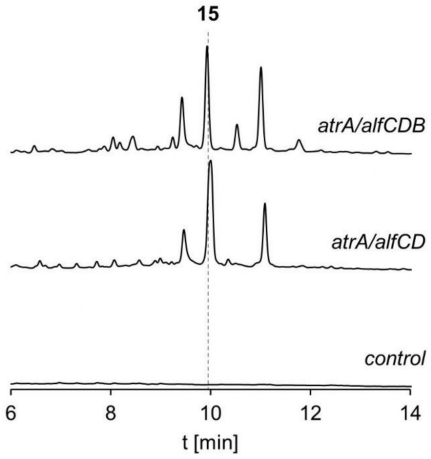

Figure S. 7: Coexpression of *alfB* in OP12(3Δ)_*atrA/alfCD* does not result in production of a dihydroxylated allantofuranone (**1**) analogue. Chromatograms (250 nm) of culture filtrate extracts of OP12 mutant strains. control, OP12 3Δ transformed with empty plasmids

8

NMR Assignments

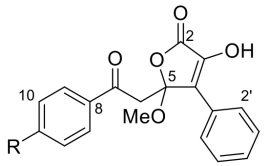

	R	
1	H	Allantofuranone
12	OH	Hydroxyallantofuranone

Table S. 3: NMR Spectroscopic Data (600 MHz) for Allantofuranone (**1**, $CDCl_3$) and Hydroxyallantofuranone (**12**, DMSO-d_6)

Position	Allantofuranone (1) δ_C, type	δ_H (*J* in Hz)	Hydroxyallantofuranone (12) δ_C, type	δ_H (*J* in Hz)
2	167.4, C		166.3, C	
3	140.1, C		142.1, C	
4	122.9, C		121.3, C	
5	107.5, C		106.3, C	
6	43.8, CH_2	3.90 (d, 16.5) 3.67 (d, 16.5)	42.9, CH_2	3.76 (d, 16.4) 3.68 (d, 16.4)
7	193.8, C		192.3, C	
8	136.8, C		128.3, C	
9/13	128.2, CH	7.83 (m)	130.7, CH	7.72 (m)
10/12	128.6, CH	7.40 (m)	115.0, CH	6.75 (m)
11	133.4, CH	7.53 (m)	162.2, C	
1'	129.0, C		129.8, C	
2'/6'	127.6, CH	7.89 (m)	126.7, CH	7.83 (m)
3'/5'	129.1, CH	7.44 (m)	128.7, CH	7.43 (m)
4'	129.3, CH	7.36 (m)	128.2, CH	7.33 (m)
3-OH				11.43 (br s)*
11-OH				10.41 (br s)*

* may be interchanged

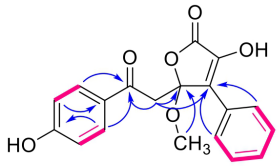

Figure S. 8: Relevant HMBC (→) and COSY (↔) correlations for **12**.

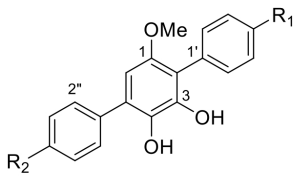

	R_1	R_2	
6	H	H	Terferol
11	H	OH	Hydroxyterferol
15	OH	OH	Dihydroxyterferol

Table S. 4: NMR Spectroscopic Data (600 MHz, DMSO-d_6) for Terferol (**6**), Hydroxyterferol (**11**), and Dihydroxyterferol (**15**)

	Terferol (6)		**Hydroxyterferol (11)**		**Dihydroxyterferol (15)**	
Position	**δ_C, type**	**δ_H (*J* in Hz)**	**δ_C, type**	**δ_H (*J* in Hz)**	**δ_C, type**	**δ_H (*J* in Hz)**
1	150.3, C		150.1, C		150.3, C	
2	117.8, C		117.0, C		117.0, C	
3	145.1, C		145.0, C		144.9, C	
4	136.2, C		136.0, C		136.1, C	
5	128.6, C		128.6, C		127.8, C	
6	103.5, CH	6.44 (s)	103.0, CH	6.38 (s)	103.0, CH	6.35 (s)
1'	134.4, C		134.5, C		124.7, C	
2'/6'	130.8, CH	7.30 (m)	130.8, CH	7.28 (m)	131.8, CH	7.08 (m)
3'/5'	127.4, CH	7.37 (m)	127.4, CH	7.36 (m)	114.3, CH	6.75 (m)
4'	126.3, CH	7.28 (m)	126.8, CH	7.26 (m)	155.8, C	
1"	138.9, C		129.4, C		129.5, C	
2"/6"	129.0, CH	7.61 (m)	130.1, CH	7.43 (m)	130.0, CH	7.42 (m)
3"/5"	128.0, CH	7.43 (m)	114.8, CH	6.82 (m)	114.7, CH	6.80 (m)
4"	126.6, CH	7.33 (m)	156.3, C		156.2, C	
1-OMe	55.6, CH_3	3.62 (s)	55.5, CH_3	3.60 (s)	55.5, CH_3	3.59 (s)
3-OH		8.33 (s)		8.23 (s)		8.17 (br s)
4-OH		8.03 (s)		7.90 (s)		7.91 (br s)
4'-OH						9.33 (br s)
4"-OH				9.45 (s)		9.44 (s)

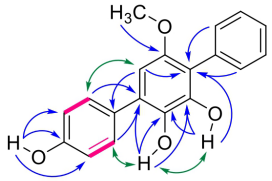

Figure S. 9: Relevant HMBC (→), COSY (↔), and NOESY (↔) correlations for **11**.

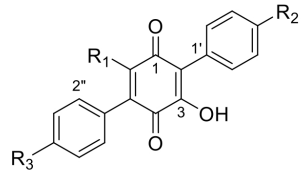

	R_1	R_2	R_3	
2	OH	H	H	Polyporic acid
4	H	H	H	Deoxypolyporic acid
5	Dimer	H	H	Deoxypolyporic acid dimer
7	OH	OH	H	Ascocorynin
8	OH	OH	OH	Atromentin
10	H	OH	H	Deoxyascocorynin

Table S. 5: NMR Spectroscopic Data (600 MHz, DMSO-d_6) for Polyporic acid (**2**), Deoxypolyporic acid (**4**), Deoxypolyporic acid dimer (**5**), Ascocorynin (**7**), Atromentin (**8**), Deoxyascocorynin (**10**)

	Polyporic acid (2)		**Deoxypolyporic acid (4)**		**Deoxypolyporic acid dimer (5)**		**Ascocorynin (7)**		**Atromentin (8)**		**Deoxyascocorynin (10)**	
Position	**δ_C, type**	**δ_H (*J* in Hz)**	**δ_C, type**	**δ_H (*J* in Hz)**	**δ_C, type**	**δ_H (*J* in Hz)**	**δ_C, type**	**δ_H (*J* in Hz)**	**δ_C, type**	**δ_H (*J* in Hz)**	**δ_C, type**	**δ_H (*J* in Hz)**
1	168.0, C[a]		182.7, C		182.0, C		168.2, C[a]		168.3, C[a]		183.3 C	
2	115.4, C		118.7, C		119.3, C		115.5, C		114.5, C		118.4, C	
3	168.0, C[a]		153.4, C		152.8, C		168.2, C[a]		168.3, C[a]		153.3, C	
4	168.0, C[a]		186.2, C		185.2, C		168.2, C[a]		168.3, C[a]		186.2, C	
5	115.4, C		142.2, C		140.4, C		115.2, C		114.5, C		141.7, C	
6	168.0, C[a]		133.4, CH	6.88 (s)	140.0, C		168.2, C[a]		168.3, C[a]		131.2, CH	6.78 (s)
1'	130.8, C		131.0, C		131.2, C		120.9, C		121.6, C		131.1, C	
2'/6'	130.4, CH	7.39 (m)	130.5, CH	7.35 (m)	130.5, CH	7.27 (m)	131.6, CH	7.22 (m)	131.6, CH	7.23 (m)	130.5, CH	7.34 (m)
3'/5'	127.5, CH	7.41 (m)	127.4, CH	7.40 (m)	127.8, CH	7.34 (m)	114.4, CH	6.78 (m)	114.2, CH	6.76 (m)	127.3, CH	7.38 (m)
4'	127.4, CH	7.33 (m)	127.4, CH	7.34 (m)	127.7, CH	7.34 (m)	156.7, C		156.4, C		127.3, CH	7.32 (m)
1"	130.8, C		132.5, C		130.6, C		130.8, C		121.6, C		123.1, C	
2"/6"	130.4, CH	7.39 (m)	129.1, CH	7.59 (m)	128.9, CH	6.75 (m)	130.4, CH	7.37 (m)	131.6, CH	7.23 (m)	130.7, CH	7.47 (m)
3"/5"	127.5, CH	7.41 (m)	128.2, CH	7.48 (m)	127.5, CH	7.39 (m)	127.5, CH	7.40 (m)	114.2, CH	6.76 (m)	115.2, CH	6.85 (m)
4"	127.4, CH	7.33 (m)	129.5, CH	7.48 (m)	128.9, CH	7.39 (m)	127.3, CH	7.32 (m)	156.4, C		159.0, C	
3-OH (6-OH)		11.17 (br s)		10.99 (br s)		11.27 (br s)		10.99 (br s)		10.73 (br s)		10.85 (br s)
4'-OH (4"-OH)								9.56 (s)		9.49 (br s)		9.93 (s)

[a] very broad

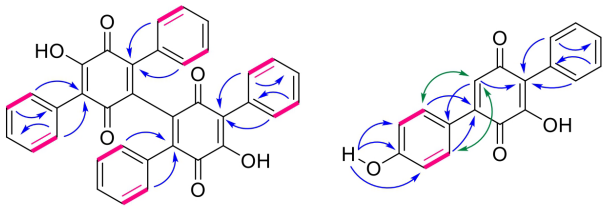

5 **10**

Figure S. 11: Relevant HMBC (→), COSY (↔), and NOESY (↔) correlations for **5** and **10**.

NMR Spectra

NMR spectra (1D and 2D), raw data, and additional analytical data of all compounds can be found free of charge on Chemotion Repository (Table S. 3). Additionally, ^{1}H and ^{13}C NMR spectra of the new compounds are depicted on the following pages.

Table S. 6: Deposited analytical data

	Name	DOI
1	Allantofuranone	https://dx.doi.org/10.14272/ZSQDINYGPVLTCM-UHFFFAOYSA-N.1
2	Polyporic acid	https://dx.doi.org/10.14272/HZKFHDXTSAYOSN-UHFFFAOYSA-N.1
4	Deoxypolyporic acid	https://dx.doi.org/10.14272/GXMJKXBNCXNACS-UHFFFAOYSA-N.1
5	Deoxypolyporic acid dimer	https://dx.doi.org/10.14272/JIJBMATWFKIPNS-UHFFFAOYSA-N.1
6	Terferol	https://dx.doi.org/10.14272/HMCUGCPHZLJKMS-UHFFFAOYSA-N.1
7	Ascocorynin	https://dx.doi.org/10.14272/PNTORJXTFRBTDZ-UHFFFAOYSA-N.1
8	Atromentin	https://dx.doi.org/10.14272/FKQQKMGWCJGUCS-UHFFFAOYSA-N.1
10	Deoxyascocorynin	https://dx.doi.org/10.14272/HLFCRNGNTFLPPX-UHFFFAOYSA-N.1
11	Hydroxyterferfol	https://dx.doi.org/10.14272/NJXLDQMVOFLMIX-UHFFFAOYSA-N.1
12	Hydroxyallantofuranone	https://dx.doi.org/10.14272/LQKBSBWZJOHANT-UHFFFAOYSA-N.1
15	Dihydroxyterferol	https://dx.doi.org/10.14272/HDXIDAAYQIUQQS-UHFFFAOYSA-N.1

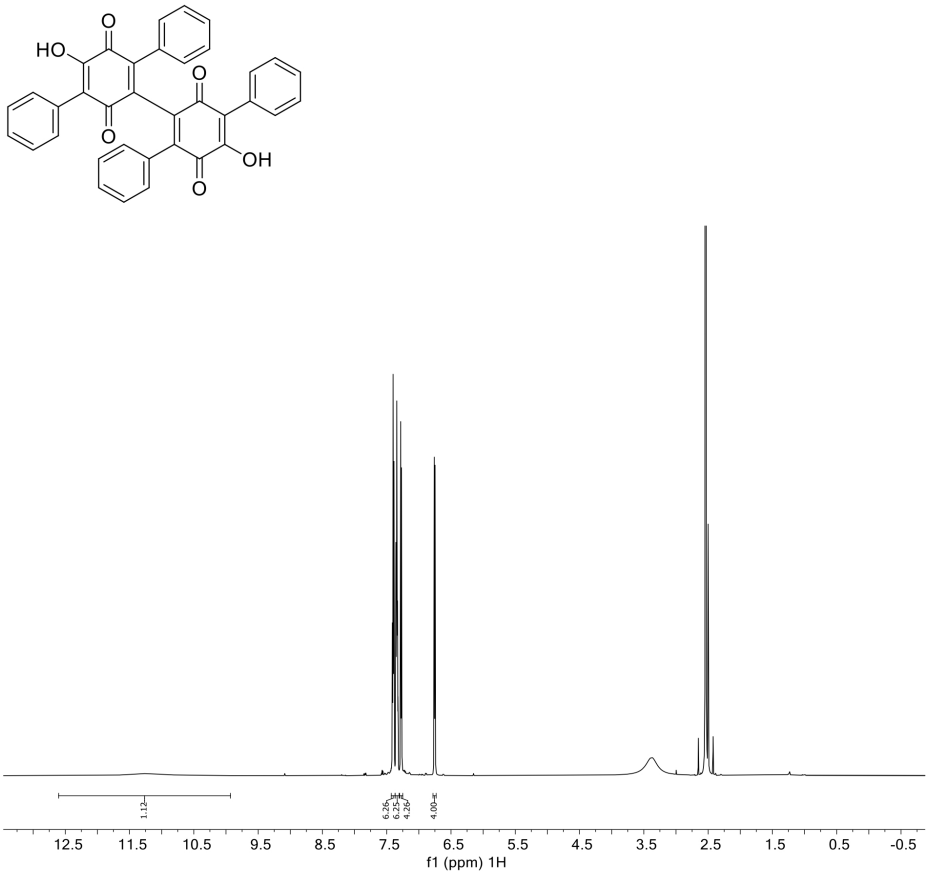

Spectrum S. 1: 1H NMR spectrum (600 MHz, DMSO-d_6) of the new compound deoxypolyporic acid dimer (**5**)

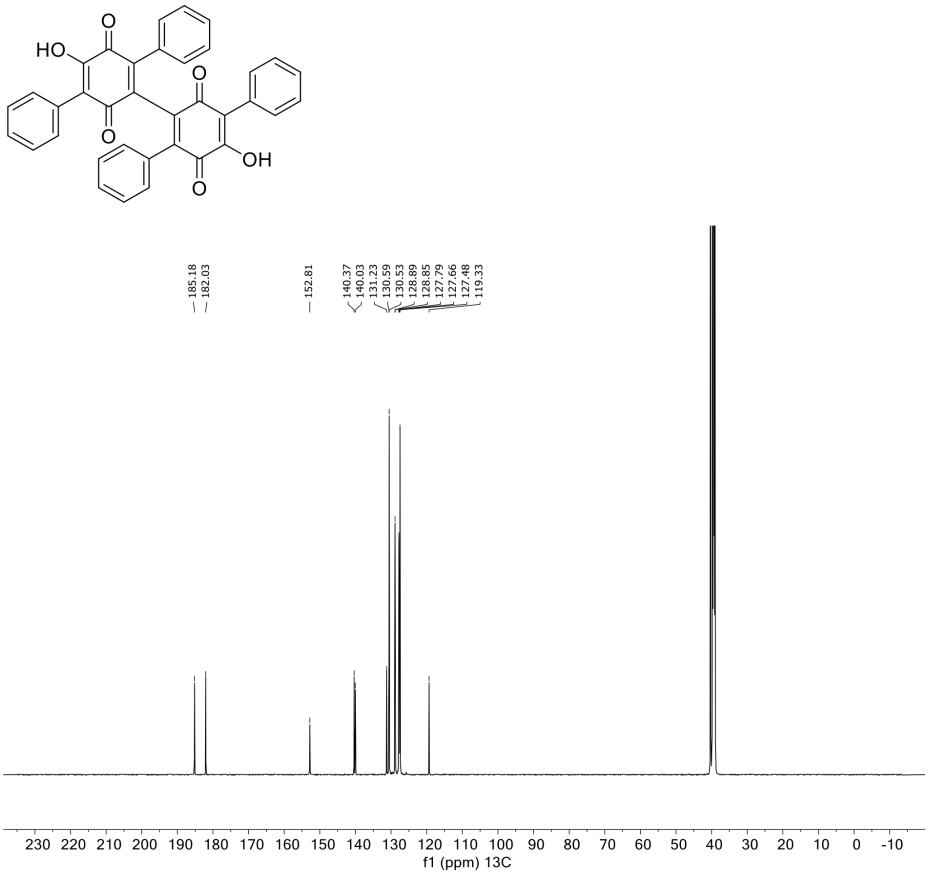

Spectrum S. 2: 13C NMR spectrum (600 MHz, DMSO-d_6) of the new compound deoxypolyporic acid dimer (**5**)

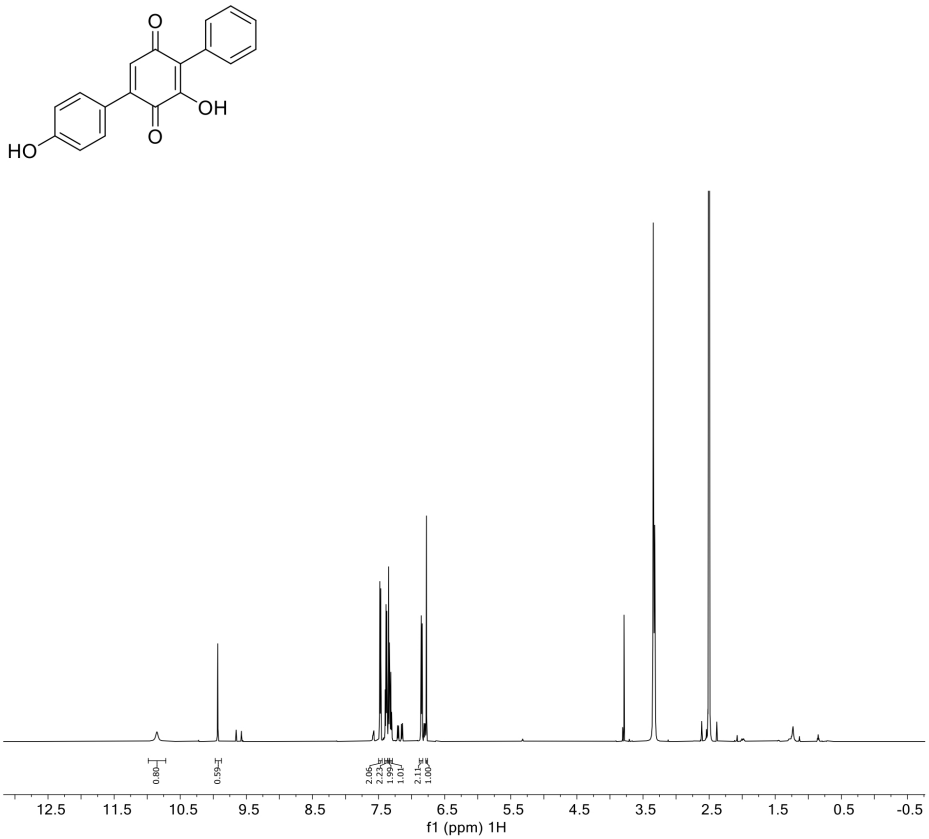

Spectrum S. 3: 1H NMR spectrum (600 MHz, DMSO-d_6) of the new compound deoxyascocorynin (**10**)

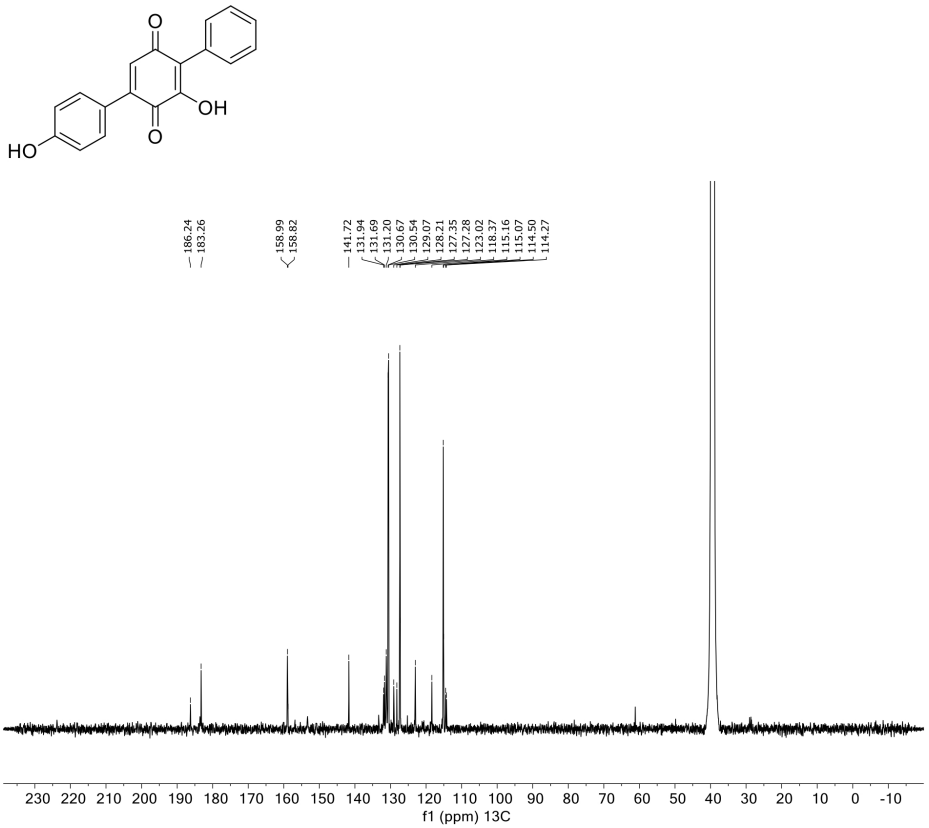

Spectrum S. 4: 13C NMR spectrum (600 MHz, DMSO-d_6) of the new compound deoxyascocorynin (**10**)

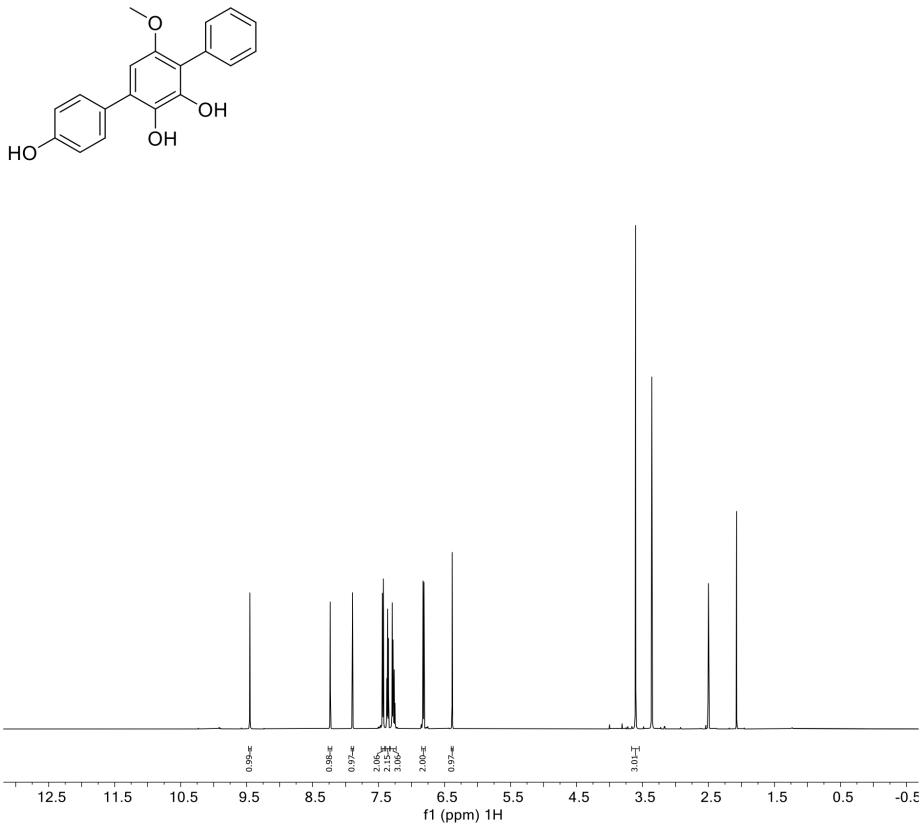

Spectrum S. 5: 1H NMR spectrum (600 MHz, DMSO-d_6) of the new compound hydroxyterferol (**11**)

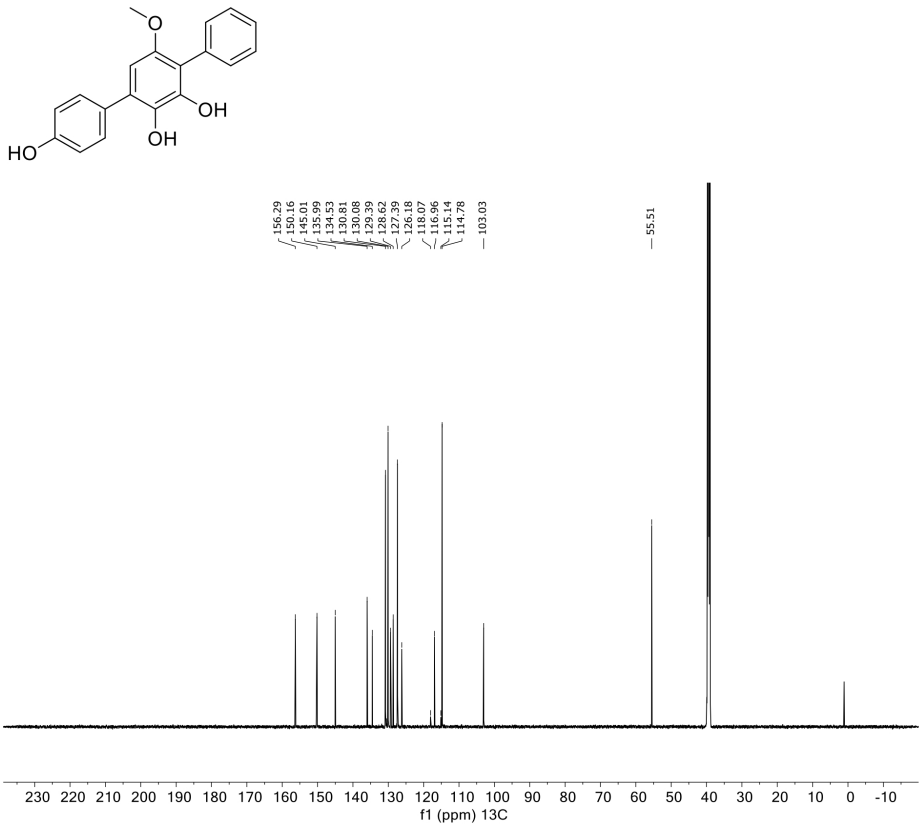

Spectrum S. 6: 13C NMR spectrum (600 MHz, DMSO-d_6) of the new compound hydroxyterferol (**11**)

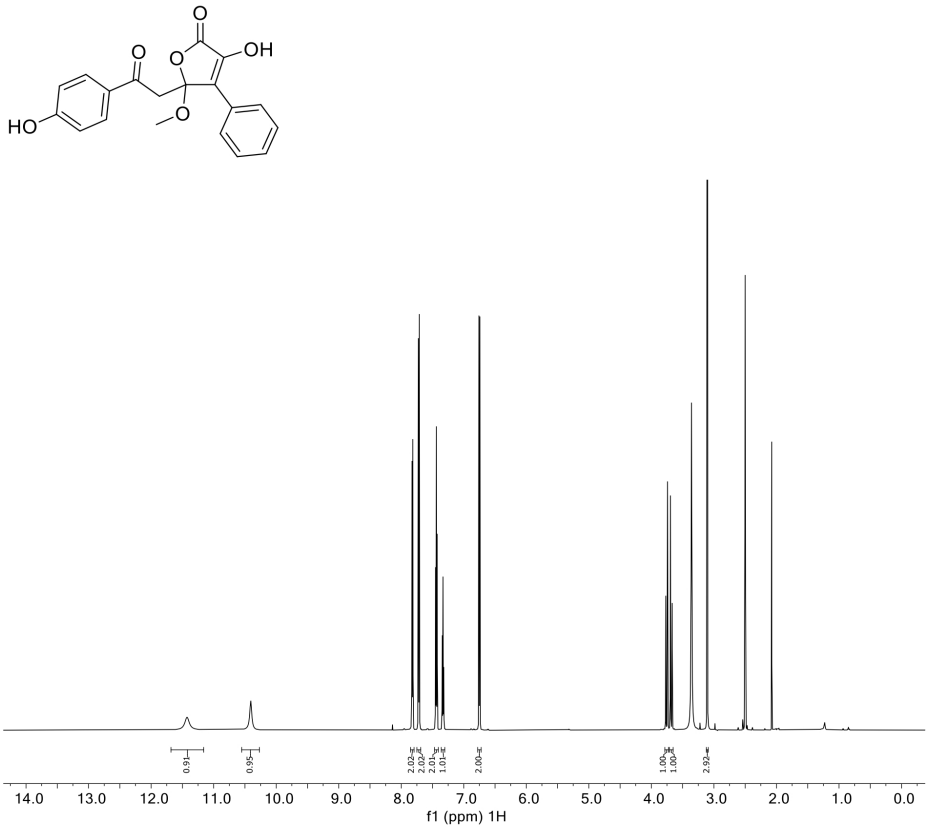

Spectrum S. 7: 1H NMR spectrum (600 MHz, DMSO-d_6) of the new compound hydroxyallantofuranone (**12**)

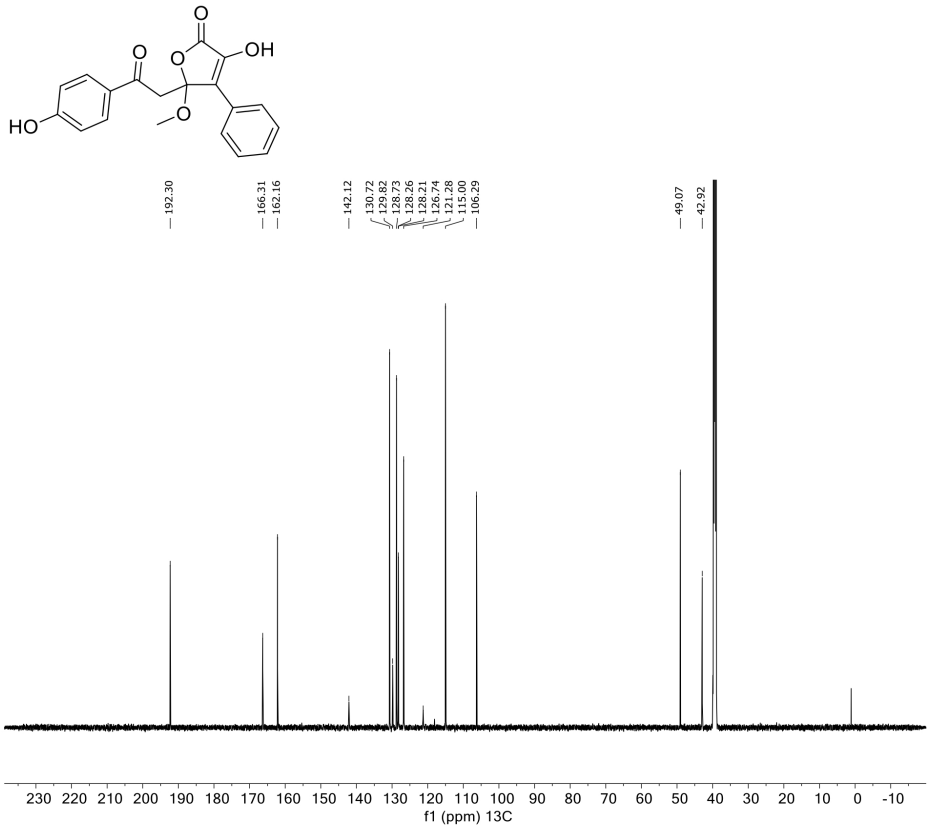

Spectrum S. 8: 13C NMR spectrum (600 MHz, DMSO-d_6) of the new compound hydroxyallantofuranone (**12**)

References

(1) Geib, E.; Baldeweg, F.; Doerfer, M.; Nett, M.; Brock, M. Cross-Chemistry Leads to Product Diversity from Atromentin Synthetases in Aspergilli from Section Nigri. *Cell chemical biology* **2019**, *26* (2), 223-234.e6. DOI: 10.1016/j.chembiol.2018.10.021.

(2) Wieder, C.; Künzer, M.; Wiechert, R.; Seipp, K.; Andresen, K.; Stark, P.; Schüffler, A.; Opatz, T.; Thines, E. Biosynthesis of the Antifungal Polyhydroxy-Polyketide Acrophialocinol. *Organic letters* **2025**, *27* (4), 1036–1041. DOI: 10.1021/acs.orglett.4c04656.

(3) Hajdok, S.; Conrad, J.; Beifuss, U. Laccase-catalyzed domino reactions between hydroquinones and cyclic 1,3-dicarbonyls for the regioselective synthesis of substituted p-benzoquinones. *The Journal of organic chemistry* **2012**, *77* (1), 445–459. DOI: 10.1021/jo202082v.

(4) Clinger, J. A.; Zhang, Y.; Liu, Y.; Miller, M. D.; Hall, R. E.; van Lanen, S. G.; Phillips, G. N.; Thorson, J. S.; Elshahawi, S. I. Structure and Function of a Dual Reductase-Dehydratase Enzyme System Involved in p-Terphenyl Biosynthesis. *ACS chemical biology* **2021**, *16* (12), 2816–2824. DOI: 10.1021/acschembio.1c00701.

(5) Zhu, J.; Liu, M.; Deng, J.; Chen, W.; Zhu, D.; Duan, J.; Li, Y.; Wang, H.; Shen, Y. The coupled reaction catalyzed by EchB and EchC lead to the formation of the common 2',3',5'-trihydroxy-benzene core in echosides biosynthesis. *Biochemical and biophysical research communications* **2021**, *559*, 62–69. DOI: 10.1016/j.bbrc.2021.04.087.

(6) Janzen, D. J.; Zhou, J.; Li, S.-M. Biosynthesis of p-Terphenyls in Aspergillus ustus Implies Enzymatic Reductive Dehydration and Spontaneous Dibenzofuran Formation. *Organic letters* **2023**, *25* (34), 6311–6316. DOI: 10.1021/acs.orglett.3c02234.

(7) Furukawa, K.; Miyazaki, T. Cloning of a gene cluster encoding biphenyl and chlorobiphenyl degradation in Pseudomonas pseudoalcaligenes. *Journal of bacteriology* **1986**, *166* (2), 392–398. DOI: 10.1128/jb.166.2.392-398.1986.

(8) Giurg, M.; Kowal, E.; Muchalski, H.; Syper, L.; Młochowski, J. Catalytic Oxidative Domino Degradation of Alkyl Phenols Towards 2- and 3-Substituted Muconolactones. *Synthetic Communications* **2008**, *39* (2), 251–266. DOI: 10.1080/00397910802369687.

Third Publication

Biosynthesis of the Fungal Cyclic Lipodepsipeptide Pleosporacin, a New Selective Inhibitor of the Phytopathogen *Botrytis cinerea*

Carsten Wieder[1,2], Rainer Wiechert[3], Alexander Yemelin[2], Louis Pergaud Sandjo[4], Eckhard Thines[1,2], Till Opatz[3], Anja Schüffler[2]

[1] Institute of Molecular Physiology, Johannes Gutenberg-University, Hanns-Dieter-Huesch Weg 17, D-55128 Mainz, Germany

[2] Institut für Biotechnologie und Wirkstoff-Forschung gGmbH, Mainz, Hanns-Dieter-Huesch Weg 17, D-55128 Mainz, Germany

[3] Department of Chemistry, Johannes Gutenberg-University, Duesbergweg 10–14, D-55128 Mainz, Germany

[4] Department of Chemistry, Universidade Federal de Santa Catarina, Florianópolis 88040-900, Santa Catarina, Brazil

Type of authorship:	First author
Type of article:	Research article
Share of work:	75 %
Contribution:	Conceived project and designed experiments; isolation of fungal strain; fermentation; natural product purification; Marfey analysis; genome mining; cloning of plasmids; generation of mutant strains; HPLC analysis; bioactivity assays; analysis and interpretation of data; writing and editing of the manuscript
Journal:	ChemBioChem
Date of publication:	09.05.2025
DOI:	10.1002/cbic.202500315

ChemBioChem

Research Article
doi.org/10.1002/cbic.202500315

Chemistry Europe
European Chemical Societies Publishing

www.chembiochem.org

Biosynthesis of the Fungal Cyclic Lipodepsipeptide Pleosporacin, a New Selective Inhibitor of the Phytopathogen *Botrytis cinerea*

Carsten Wieder,* Rainer Wiechert, Alexander Yemelin, Louis Pergaud Sandjo, Eckhard Thines, Till Opatz, and Anja Schüffler*

Bioactivity-guided isolation led to the identification of the cyclic lipodepsipeptide pleosporacin (**1**) from the mycelia extract of fungal strain *Pleosporales* sp. IBWF 020-21, a potent selective inhibitor of the fungal phytopathogen *Botrytis cinerea*. The structure and stereochemistry of **1** were elucidated by NMR and Marfey analysis, respectively. Genome mining identified a candidate biosynthetic gene cluster encoding a hexamodular nonribosomal peptide synthetases, PleA, a fatty acyl-AMP ligase, PleB, and an aspartate decarboxylase, PleC. Reconstitution of *pleABC* allowed for heterologous production of **1** in *Aspergillus oryzae* and confirmed the identity of the *ple* cluster. Based on these findings a biosynthetic route is proposed, with PleB catalyzing lipoinitiation and PleC providing the nonproteinogenic amino acid β-alanine for the assembly of **1**.

1. Introduction

Nonribosomal peptide synthetases (NRPS) are giant multimodular enzyme assembly lines, which facilitate the condensation of amino acids in a ribosome-independent manner. Each module obligatory harbors a minimal set of an adenylation (A), thiolation (T), and condensation (C) domain. These are required for activation of the amino acid building blocks (A-domain), tethering (T-domain), and catalyzing peptide bond formation (C-domain).[1] Synthesis proceeds via repeated condensation of the amine of the T_{n+1}-bound amino acid with the carbonyl of the T_n-bound peptidyl chain. In contrast to ribosomal peptide synthesis, NRPS can also incorporate nonproteinogenic amino acids and hydroxy acids,[2] the latter of which are esterified to yield depsipeptides.[3] Optionally, modules can include tailoring domains, such as *N*-methyltransferase domains and epimerization (E) domains that catalyze L to D stereoinversion of tethered amino acids prior to condensation. In fungal NRPSs, the release of nascent peptides is frequently catalyzed by a terminal condensation (C_T) domain via hydrolysis, lactonization/ lactamization, or Dieckmann cyclization.[4] In the special case of lipopeptides, an additional first step known as lipoinitiation is required to incorporate the fatty acyl moiety. During lipoinitiation in fungal biosynthetic pathways, a free fatty acid is activated by an acyl-AMP ligase and subsequently transferred to an N-terminal T_0-domain to prime the assembly line.[5–7] Elongation of the peptidyl chain then proceeds as described. Many lipopeptides, such as echinocandins, daptomycin, and surfactin, exhibit industrially relevant antimicrobial activity and it was previously shown that the fatty acyl moiety plays an essential role therein.[8] The rise of fungicide resistance in phytopathogenic fungi is a global threat to food production[9] and therefore the nutrition of the steadily growing world population. This necessitates not only the discovery of new lead structures for the development of drugs but also the identification of new molecular targets or mechanisms that circumvent resistance development. Microbial natural products have been a continuous source of drug leads over the last decades.[10] The discovery of selective antimicrobial agents is of particular interest for plant protection, as high selectivity reduces the impact on the environment, which is in line with the European Geen Deal (Directive 2009/128/EC).

Here, we report the bioactivity-guided isolation, characterization, and elucidation of the biosynthesis of a new cyclic lipodepsipeptide pleosporacin (**1**), which exhibits potent selective inhibitory activity against the grey rot pathogen *Botrytis cinerea*.

2. Results and Discussion

In an ongoing effort to identify new antifungal compounds, we isolated fungal strain IBWF 020-21 (Figure S1, Supporting

C. Wieder, E. Thines
Institute of Molecular Physiology
Johannes Gutenberg-University
Hanns-Dieter-Hüsch Weg 17, 55128 Mainz, Germany
E-mail: cawieder@uni-mainz.de

C. Wieder, A. Yemelin, E. Thines, A. Schüffler
Institut für Biotechnologie und Wirkstoff-Forschung gGmbH
Hanns-Dieter-Hüsch Weg 17, 55128 Mainz, Germany
E-mail: schueffler@ibwf.de

R. Wiechert, T. Opatz
Department of Chemistry
Johannes Gutenberg-University
Duesbergweg 10–14, 55128 Mainz, Germany

L. P. Sandjo
Department of Chemistry
Universidade Federal de Santa Catarina
Florianópolis, Santa Catarina 88040-900, Brazil

Supporting information for this article is available on the WWW under https://doi.org/10.1002/cbic.202500315

Information), crude extracts of which exhibit potent conidia germination inhibitory activity against the gray rot pathogen *B. cinerea*. DNA-sequencing of the ITS fungal barcode region (Table S2, Supporting Information) frequently used for species identification[11] did not suffice for species determination; however, the strain can confidently be assigned to the order *Pleosporales*. Bioactivity-guided isolation of the active constituent led to the identification of the new cyclic lipodepsipeptide **1**, which we termed pleosporacin. The structure and stereochemistry of **1** were elucidated by NMR spectroscopy and Marfey analysis, respectively (**Figure 1**). Compound **1** features a macrocyclic scaffold composed of myristic acid (MA), D-Gln_1, L-Ser_2, β-Ala_3, D-Trp_4, L-Ser_5, and D-Tyr_6 with the macrolactone ester bond formed between the β-hydroxy moiety of L-Ser_2 and the carboxyl-moiety of D-Tyr_6. Structurally, **1** is closely related to previously reported cyclic lipodepsipeptides, namely, symbiosin,[12] colisporifungin,[13] verruculin,[14] ophiotine,[15] and aselacin A[16] (Figure S3, Supporting Information). They all share a common macrocyclic scaffold and mainly differ in the fatty acyl moiety. Some of them have been associated with various bioactivities, e.g., colisporifungin was reported to potentiate the activity of caspofungin but does not exhibit antifungal activity of its own.[13] Similarly, symbiosin was reported to boost the activity of necroxime by acting as a biosurfactant while not exhibiting nematicidal activity of its own,[12] whereas ophiotine was reported to exhibit moderate nematicidal activity on its own.[15] The antimicrobial capacity of **1** was evaluated by assaying germination inhibition of various filamentous fungi as well as growth inhibition of the pathogenic yeast *Candida albicans*, the oomycete *Phytophthora infestans*, and various bacteria (**Table 1**). Intriguingly, **1** almost selectively inhibited germination of *B. cinerea* at an MIC of 3 μg mL^{-1} (≈3.2 μM). Germination of *Magnaporthe oryzae* was also partially inhibited however only when assayed in H_2O but not when assayed in media.

When treated with **1**, even at sub-MIC, conidia of *B. cinerea* appear to swell to ≈1.5-fold their usual size (Figure S4, Supporting Information). This has previously been observed when conidia of *B. cinerea* were treated with caspofungin,[17] an echinocandin-type cyclic lipodepsipeptide fungicide known to interfere with cell wall biogenesis by noncompetitively inhibiting the 1,3-β glucan synthase. It is therefore conceivable that the mode of action of **1** might be the inhibition of cell wall biogenesis in *B. cinerea*. As this effect would not be specific to conidia germination but detrimental to the fungus in general, an agar disc assay was performed (Figure S5, Supporting Information), which confirmed that **1** also inhibits the vegetative growth of *B. cinerea*. Additionally, compound **1** exhibits surfactant properties similar to symbiosin (Figure S6, Supporting Information);[12] therefore, it might additionally be capable of disrupting membrane integrity and/or permeability. The exact mechanism of action of **1** and particularly the selective susceptibility of *B. cinerea* remain elusive and yet to be determined. Furthermore, the physiological function of **1** is also unclear, especially as it is mostly retained in the mycelium of the fungus.

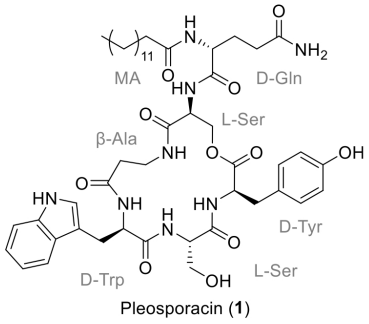

Figure 1. Structure of pleosporacin (**1**).

Table 1. Antimicrobial activity of 1.

Organism	MIC [μg mL^{-1}]
Magnaporthe oryzae (CM/H_2O)[a]	–[c]/>100 [d]
Botrytis cinerea[a]	3 (≈3.2 μM)
Fusarium graminearum[a]	–
Aspergillus oryzae[a]	–
Candida albicans[b]	–
Phytophthora infestans[b]	–
Staphylococcus aureus	–
Pseudomonas aeruginosa	–
Aneurinibacillus migulanus[b]	–
Enterobacter cloacae subsp. *dissolvens*[b]	–

[a]Germination inhibition; [b]Vegetative growth inhibition; [c]No activity up to 100 μg mL^{-1}; [d]Partially inhibited even at 5 μg mL^{-1}, but not fully inhibited even at 100 μg mL^{-1}.

While all the other compounds addressed are of fungal origin, symbiosin is produced by symbiotic endofungal bacteria instead. A plausible candidate biosynthetic gene cluster (BGC) was proposed for symbiosin biosynthesis based on genome mining and in silico analysis; however, validation thereof was not possible as the symbionts were unculturable.[12] In contrast, the biosynthetic pathways of the related fungal cyclic lipodepsipeptides have not been investigated at all, and therefore, we set out to representatively examine the biosynthesis of **1**. To this end, the genome of the fungal strain IBWF 020-21 was sequenced and assembled into 38.3 Mb. The assembly comprised 172 contigs, with an N50 of 0.49 Mb and a GC content of 48.4%. The length of the largest contig was 1.4 Mb. A total of 5 110 840 clean reads were obtained from Illumina sequencing, enabling the prediction of 8158 protein-coding genes with functional annotations. AntiSMASH[18] and FunBGCeX[19] analyses together detected 55 secondary metabolite BGCs including 12 NRPS BGCs, 9 polyketide synthase (PKS) BGCs, 1 hybrid PKS/NRPS BGC, 12 terpene synthase (TPS) BGCs, 15 ribosomally synthesized and post-translationally modified peptide (RiPPs) BGCs, 4 isocyanide synthase (ICS) BGCs, and 2 UbiA-type prenyltransferase (PT) BGCs.

Among the NRPS BGCs, a single-candidate BGC likely responsible for the biosynthesis of **1** was identified. The *ple* cluster (accession number: PV294983) encodes a hexamodular NRPS

Table 2. Proteins encoded in the *ple* cluster.

Gene	Length [aa]	BLASTp[a)]	Identity [%]/*E*-value	Proposed function
pleC	519	E9FCP7.2—L-aspartate decarboxylase dtxS4 [*Metarhizium robertsii*]	44.93/3 E^{-151}	L-Asp decarboxylase
pleA	8396	E9FCP4.2—Nonribosomal peptide synthetase dtxS1 [*Metarhizium robertsii*]	42.81/0.0	NRPS
pleD	1665	P15368.1—Fatty acid synthase subunit alpha [*Penicillium griseofulvum*]	46.57/0.0	FAS α-subunit
pleE	373	P36615.1—Serine/threonine-protein kinase csk1 [*Schizosaccharomyces pombe*]	25.15/2 E^{-04}	Protein kinase
pleF	1281	Q4WTT9.1—ABC-type transporter MDR1 [*Aureobasidium melanogenum*]	49.84/0.0	ABC transporter
pleB	481	S3DB78.1—Acyl-CoA ligase gloD [*Glarea lozoyensis*]	38.29/$7e^{-133}$	Fatty acyl-AMP ligase
pleG	2047	P34229.2—Fatty acid synthase subunit beta [*Yarrowia lipolytica*]	42.80/0.0	FAS β-subunit

[a)]Nearest fungal hit using Uniprot database.

Figure 2. *ple* biosynthetic gene cluster.

PleA, an acyl-AMP ligase PleB, an aspartate decarboxylase PleC, a fatty acid synthase (FAS) α-subunit PleD, a putative protein kinase PleE, an ABC transporter PleF, and a FAS β-subunit PleG (**Table 2**, **Figure 2**). The structure and stereochemistry of **1** are in accord with the number of modules and the arrangement of E-domains in PleA. Moreover, there is an additional T_0-domain in PleA that is likely required for loading of the myristoyl moiety onto the assembly line. PleB is homologous to GloD, the acyl-AMP ligase involved in pneumocandin biosynthesis.[7] GloD catalyzes lipoinitiation by activating polyketide synthase (GloL)-derived 10,12-dimethyl-myristic acid and transferring it to the T_0-domain of GloA. Interestingly, abolishing the production of 10,12-dimethyl-myristic acid via deletion of *gloL* enabled the production of pneumocandin derivatives with alternative fatty acyl moieties, among others MA, suggesting GloD to exhibit some substrate tolerance.[7] This strengthens the hypothesis that PleB catalyzes lipoinitiation in the biosynthesis of **1**, activating and transferring MA to the T_0-domain of PleB. As palmitic and linoleic acid are the most abundant fatty acids in various acsomycetes,[7,20] the FAS subunits PleD and PleG likely collaborate to provide sufficient amounts of MA for the biosynthesis of **1**. PleC is likely to provide β-alanine for the biosynthesis of **1**, as it is homologous to DtxS4, an L-aspartate decarboxylase that converts L-aspartate to β-alanine for the biosynthesis of destruxins.[21]

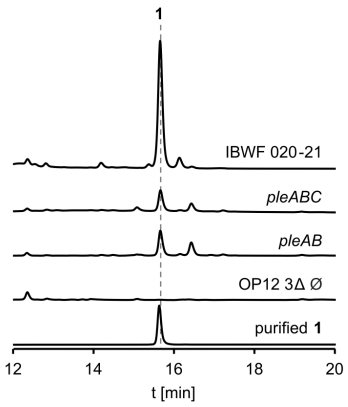

Figure 3. Heterologous reconstitution of pleosporacin (**1**) biosynthesis in *Aspergillus oryzae* OP12. Chromatograms (280 nm) of mycelia extracts of OP12 mutant strains, IBWF 020-21 and purified **1**.

Multimodular NRPS are often challenging to characterize, particularly due to their enormous size and associated difficulties during cloning. Therefore, the biosynthetic pathways of large fungal NRPs are frequently elucidated through gene deletions in native producers instead.[6,21,22] This methodology is, however, limited to organisms that are amenable to genetic manipulation. Consequently, various techniques have been employed to facilitate cloning for subsequent heterologous characterization, ranging from in vivo assembly of plasmids[23] or amplicons[24] to sequential ligation cloning.[25] Due to the slow growth of IBWF 020-21 we also attempted and succeeded in sequentially assembling the ≈25 kb NRPS gene *pleA* into a plasmid for heterologous expression using multistep Gibson assembly. *pleA*, *pleB*, and *pleC* were introduced into the heterologous host *Aspergillus oryzae* OP12 3Δ[26] for subsequent metabolite analysis (**Figure 3**). Indeed, the coexpression of *pleABC* resulted in autonomous production of **1**, albeit at a lower yield as compared to IBWF 020-21. This discrepancy is likely due to a difference in the abundance of the precursor molecule MA. In the original producer IBWF 020-21, MA is likely efficiently provided for the biosynthesis of **1** in a spatiotemporal manner via the action of the FAS encoded by *pleD* and *pleG*. Additionally, multiple other compounds similar in *m/z* and UV were produced by OP12_*pleABC* and also IBWF 020-21 (Figure S7, Supporting Information). These are likely congeners of **1** with altered fatty acyl moieties that derive from promiscuous activity of PleB. Contrary to expectation, the coexpression of solely *pleAB* also results in the autonomous production of **1**. Prototrophic organisms inherently produce β-alanine, as it is,

ChemBioChem
Research Article
doi.org/10.1002/cbic.202500315
Chemistry Europe
European Chemical Societies Publishing

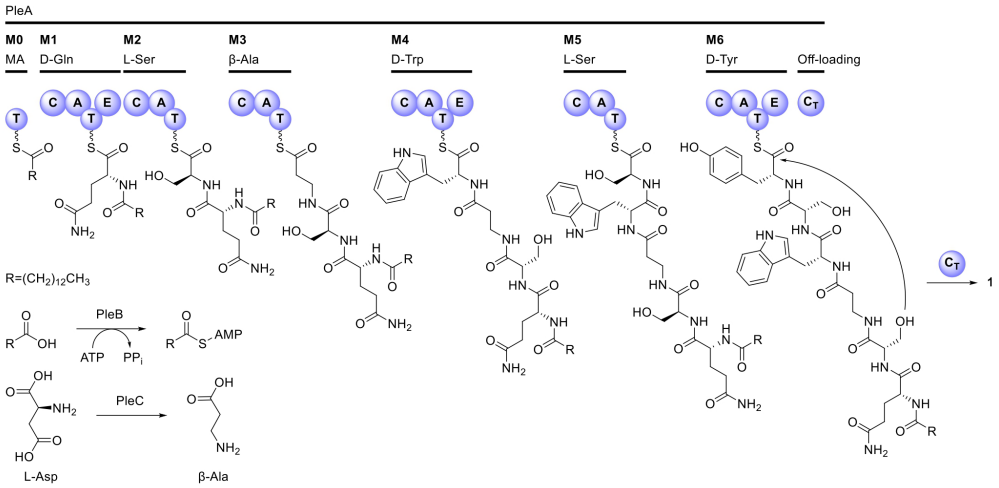

Scheme 1. Proposed biosynthesis of pleosporacin (**1**).

e.g., part of pantothenic acid (vitamin B_5), which is essential for multiple cellular processes including synthesis of coenzyme A. OP12_*pleAB* is apparently able to utilize the intrinsic pool of β-alanine for production of **1**. PleC likely boosts β-alanine supply for higher level production of **1** in the native producer, which is not achieved in OP12_*pleAB* and OP12_*pleABC*, presumably due to insufficient MA supply. Based on these findings the biosynthesis of **1** is proposed to proceed as depicted in **Scheme 1**. The FAS α- and β-subunits PleD and PleG collaborate to synthesize MA, which is subsequently activated by the fatty acyl-AMP ligase PleB and transferred to the T_0 domain of the NRPS PleA. The peptide chain is then elongated with D-Gln_1, L-Ser_2, β-Ala_3 – which is derived from PleC-catalyzed decarboxylation of L-Asp – D-Trp_4, L-Ser_5, and D-Tyr_6. Finally, macrolactonization between the β-hydroxyl moiety of L-Ser_2 and the α-carbonyl of D-Tyr_6 is catalyzed by the terminal C_T-domain, resulting in the release of **1** from the assembly line.

The production of similar cyclic lipodepsipeptides in fungi and bacteria might be indicative of a horizontal gene transfer event. However, the GC content of the *ple* BGC (48.8%) and *pleA* (50.8%) are well in accord with the overall genomic GC content (48.4%). Moreover, PleA and the symbiosin NRPS[12] differ in domain architecture (Figure S8, Supporting Information) and employ different strategies for lipoinitiation and terminal cyclization. Therefore, it can be presumed that the *ple* BGC is truly of fungal origin and was unlikely acquired via horizontal gene transfer.

3. Conclusion

In search for antifungal compounds, we isolated the cyclic lipodepsipeptide pleosporacin (**1**), a new selective inhibitor of *B. cinerea*, from mycelia of the fungal strain *Plepsporales* sp. IBWF 020-21. Although the mechanism remains elusive yet, compound **1** is hypothesized to interfere with the cell wall biogenesis of *B. cinerea*. The discovery and development of more selective antimicrobial agents are crucial for a greener agriculture, as they exhibit fewer nontarget side effects, easing the environmental impact while not compromising crop protection. By investigating the biosynthesis of **1**, it is demonstrated that it is possible and feasible to clone large genes for heterologous characterization, in cases where homologous investigations are not possible. To our knowledge, this is the first characterized biosynthetic pathway of a cyclic lipodepsipeptide related to aselacin A.

Acknowledgements

The authors thank Sri Bühring (IBWF, Mainz) for kindly collecting the freshwater sediment sample from which the fungal strain IBWF 020-21 was isolated and Michael Becker (IBWF, Mainz) for assistance in cloning *pleA*. Plasmids SM-Xpress_Ura and SM-Xpress_pabA were kindly provided by Matthias Brock (University of Nottingham, UK). The authors gratefully acknowledge the financial support provided by BASF SE. This work was supported by the Rhineland-Palatinate Center for Natural Products Research. Parts of the graphic abstract were created with BioRender.com.

Conflict of Interest

The authors declare no conflict of interest.

Data Availability Statement

The data that support the findings of this study are available in the supplementary material of this article.

ChemBioChem
Research Article
doi.org/10.1002/cbic.202500315
Chemistry Europe
European Chemical Societies Publishing

Keywords: biological activity · biosynthesis · cyclic lipodepsipeptides · heterologous expression · natural products · nonribosomal peptide synthetases

[1] L. Zhang, C. Wang, K. Chen, W. Zhong, Y. Xu, I. Molnár, *Nat. Prod. Rep.* **2023**, *40*, 62.
[2] C. T. Walsh, R. V. O'Brien, C. Khosla, *Angew. Chem. Int. Ed.* **2013**, *52*, 7098.
[3] D. A. Alonzo, T. M. Schmeing, *Protein Sci.* **2020**, *29*, 2316.
[4] a) X. Gao, S. W. Haynes, B. D. Ames, P. Wang, L. P. Vien, C. T. Walsh, Y. Tang, *Nat. Chem. Biol.* **2012**, *8*, 823; b) R. F. Little, C. Hertweck, *Nat. Prod. Rep.* **2022**, *39*, 163.
[5] Y.-M. Chiang, E. Szewczyk, T. Nayak, A. D. Davidson, J. F. Sanchez, H.-C. Lo, W.-Y. Ho, H. Simityan, E. Kuo, A. Praseuth, K. Watanabe, B. R. Oakley, C. C. C. Wang, *Chem. Biol.* **2008**, *15*, 527.
[6] R. A. Cacho, W. Jiang, Y.-H. Chooi, C. T. Walsh, Y. Tang, *J. Am. Chem. Soc.* **2012**, *134*, 16781.
[7] L. Chen, Y. Li, Q. Yue, A. Loksztejn, K. Yokoyama, E. A. Felix, X. Liu, N. Zhang, Z. An, G. F. Bills, *ACS Chem. Biol.* **2016**, *11*, 2724.
[8] a) M. Debono, B. J. Abbott, D. S. Fukuda, M. Barnhart, K. E. Willard, R. M. Molloy, K. H. Michel, J. R. Turner, T. F. Butler, A. H. Hunt, *J. Antibiot.* **1989**, *42*, 389; b) M. Debono, W. W. Turner, L. LaGrandeur, F. J. Burkhardt, J. S. Nissen, K. K. Nichols, M. J. Rodriguez, M. J. Zweifel, D. J. Zeckner, R. S. Gordee, *J. Med. Chem.* **1995**, *38*, 3271; c) L. D. Boeck, D. S. Fukuda, B. J. Abbott, M. Debono, *J. Antibiot.* **1988**, *41*, 1085; d) M. Debono, B. J. Abbott, R. M. Molloy, D. S. Fukuda, A. H. Hunt, V. M. Daupert, F. T. Counter, J. L. Ott, C. B. Carrell, L. C. Howard, *J. Antibiot.* **1988**, *41*, 1093; e) J.-M. Bonmatin, O. Laprévote, F. Peypoux, *Comb. Chem. High Throughput Screening* **2003**, *6*, 541.
[9] M. Hahn, *J. Chem. Biol.* **2014**, *7*, 133.
[10] D. J. Newman, G. M. Cragg, *J. Nat. Prod.* **2020**, *83*, 770.
[11] H. A. Raja, A. N. Miller, C. J. Pearce, N. H. Oberlies, *J. Nat. Prod.* **2017**, *80*, 756.
[12] H. Büttner, S. J. Pidot, K. Scherlach, C. Hertweck, *Chem. Sci.* **2022**, *14*, 103.
[13] F. J. Ortíz-López, M. C. Monteiro, V. González-Menéndez, J. R. Tormo, O. Genilloud, G. F. Bills, F. Vicente, C. Zhang, T. Roemer, S. B. Singh, F. Reyes, *J. Nat. Prod.* **2015**, *78*, 468.
[14] T. Bunyapaiboonsri, S. Yoiprommarat, R. Suntivich, S. Preedanon, S. Komwijit, T. Teerawatananond, J. Sakayaroj, *Tetrahedron* **2020**, *76*, 131497.
[15] S. E. Helaly, S. Ashrafi, R. B. Teponno, S. Bernecker, A. A. Dababat, W. Maier, M. Stadler, *J. Nat. Prod.* **2018**, *81*, 2228.
[16] J. E. Hochlowski, P. Hill, D. N. Whittern, M. H. Scherr, R. R. Rasmussen, S. A. Dorwin, J. B. McAlpine, *J. Antibiot.* **1994**, *47*, 528.
[17] W.-Y. Zhu, G. W. Gooday, *Mycol. Res.* **1992**, *96*, 371.
[18] K. Blin, S. Shaw, H. E. Augustijn, Z. L. Reitz, F. Biermann, M. Alanjary, A. Fetter, B. R. Terlouw, W. W. Metcalf, E. J. N. Helfrich, G. P. van Wezel, M. H. Medema, T. Weber, *Nucleic Acids Res.* **2023**, *51*, W46.
[19] J. Tang, Y. Matsuda, *Nat. Commun.* **2024**, *15*, 4312.
[20] P. D. Stahl, M. J. Klug, *Appl. Environ. Microbiol.* **1996**, *62*, 4136.
[21] B. Wang, Q. Kang, Y. Lu, L. Bai, C. Wang, *PNAS* **2012**, *109*, 1287.
[22] L. Chen, Q. Yue, X. Zhang, M. Xiang, C. Wang, S. Li, Y. Che, F. J. Ortiz-López, G. F. Bills, X. Liu, Z. An, *BMC Genomics* **2013**, *14*, 339; b) G. Wang, Z. Liu, R. Lin, E. Li, Z. Mao, J. Ling, Y. Yang, W.-B. Yin, B. Xie, *PLoS Pathog.* **2016**, *12*, e1005685.
[23] a) A. Yoshimi, S. Yamaguchi, T. Fujioka, K. Kawai, K. Gomi, M. Machida, K. Abe, *Front. Microbiol.* **2018**, *9*, 690; b) X. Wei, T. K. Chan, C. T. D. Kong, Y. Matsuda, *J. Nat. Prod.* **2023**, *86*, 416–422.
[24] L. Kirchgaessner, J. M. Wurlitzer, P. S. Seibold, M. Rakhmanov, M. Gressler, *Fungal Biol. Biotechnol.* **2023**, *10*, 4.
[25] L. Präve, C. E. Seyfert, K. A. J. Bozhüyük, E. Racine, R. Müller, H. B. Bode, *Angew. Chem. Int. Ed.* **2024**, *63*, e202406389.
[26] a) E. Geib, F. Baldeweg, M. Doerfer, M. Nett, M. Brock, *Cell Chem. Biol.* **2019**, *26*, 223.e6; b) C. Wieder, M. Künzer, R. Wiechert, K. Seipp, K. Andresen, P. Stark, A. Schüffler, T. Opatz, E. Thines, *Org. Lett.* **2025**.

Manuscript received: April 14, 2025
Revised manuscript received: May 9, 2025
Version of record online:

Supporting Information

Biosynthesis of the fungal cyclic lipodepsipeptide pleosporacin, a new selective inhibitor of the phytopathogen *Botrytis cinerea*

Carsten Wieder*[a,b], Rainer Wiechert[c], Alexander Yemelin[b], Louis Pergaud Sandjo[d], Eckhard Thines[a,b], Till Opatz[c], Anja Schüffler*[b]

[a] Institute of Molecular Physiology, Johannes Gutenberg-University, Hanns-Dieter-Hüsch Weg 17, D-55128 Mainz, Germany

[b] Institut für Biotechnologie und Wirkstoff-Forschung gGmbH, Mainz, Hanns-Dieter-Hüsch Weg 17, D-55128 Mainz, Germany

[c] Department of Chemistry, Johannes Gutenberg-University, Duesbergweg 10–14, D-55128 Mainz, Germany

[d] Department of Chemistry, Universidade Federal de Santa Catarina, Florianópolis 88040-900, Santa Catarina, Brazil

*Correspondence: cawieder@uni-mainz.de, schueffler@ibwf.de

Table of Contents

I. Experimental Procedures

Fungal strains

Fungal strain IBWF 020-21 was isolated from a freshwater sediment sample taken from the Elbe river (near shoreline, sediment plus freshwater) in Hamburg, Germany, in July 2021 by serial dilution plating on Littmann (1.5 % oxgall, 1 % peptone, 1 % glucose, 0.01 g crystal violet, pH 7.0) agar plates supplemented with 100 µg/mL streptomycin. The strain is deposited at the Institut für Biotechnologie und Wirkstoff-Forschung gGmbH (IBWF), Mainz, Germany and was routinely maintained on YMG (0.4 % yeast extract, 1 % malt extract, 1 % glucose, pH 5.5) agar plates at room temperature. *Aspergillus oryzae* OP12 3Δ was routinely cultivated on GG10 (50 mM glucose, 10 mM glutamine, 0.52 g/L KCl, 0.52 g/L $MgSO_4 \cdot 7\ H_2O$, 1.52 g/L KH_2PO_4; 1 mL/L Hutner's trace elements; pH 6.5) agar plates supplemented with10 mM uridine, 0.0001 % *p*-amino benzoic acid (PABA) and 0.1 % arginine at 30 °C for sporulation and maintained as spore suspension in PBS at 4 °C. All mutant strains used in this study are listed in Table S1.

Table S. 1: Mutant strains used in this study

Mutant	Parental Strain	Genotype	Source
OP12 3Δ	see source	*PamyB:terR_ptrA*; *pyrG*$^-$, *ΔpabA*, *ΔargB*	[1]
OP12 empty plasmid control	OP12 3Δ	*PamyB:terR_ptrA*	[1]
OP12_*pleAB*	OP12 3Δ	*PamyB:terR_ptrA*, *PterA:pleA_URA*, *PterA:pleB_argB*, *ΔpabA*	This study
OP12_*pleABC*	OP12 3Δ	*PamyB:terR_ptrA*, *PterA:pleA_URA*, *PterA:pleB_argB*, *PterA:pleC_pabA*	This study

ITS and whole genome sequencing

Genomic DNA of IBWF 020-21 was prepared from lyophilized mycelium using the GeneJET Plant Genomic DNA Purification Kit (ThermoFisher) according to the manufacturer's instructions. The ITS barcode region was amplified using the ITS1F and ITS4 primers with the Phire Green Hot Start II PCR Mastermix (Thermo Fisher), purified using the Monarch PCR & DNA Cleanup Kit (NEB) and analyzed by Sanger sequencing. The consensus of forward and reverse sequencing was BLASTed against the NCBI ITS database.

Table S. 2: ITS sequence of IBWF 020-21

Fungal strain	ITS sequence	selected BLAST hits	Identity/E-value
IBWF 020-21	AGTAAAAGTCGTAACAAGGTTTCCGTAGGTGAACCTGCGGAAG GATCATTATCAATTTACAGCGGACTTCGGTCCTGTCTGCACCC TTGTCTTTTGCGTACTGTATGTTTCCTTGGTAGGCTTGCCTAC CAATAGGACATCATAAACTCTTTTGTAATTGCAATCAGCGTCA GAAAACTATAATAGTTACAACTTTCAACAACGGATCTCTTGGT TCTGGCATCGATGAAGAACGCAGCGAAATGCGAAAAGTAGTGT GAATTGCAGAATTCAGTGAATCATCGAATCTTTGAACGCACAT TGCGCCCCTTGGTATTCCATGGGGCATGCCTGTTCGAGCGTCA TTTGTACCCTCAAGCTCTGCTTGGTGTTGGGTGTTTGTCCCGC TTATACGCGTGGACTCGCCTTAAAGCAATTGGCAGCCGGCATA CTAGCCTGGGAGCGCAGCACATTTTGCGTTTCTTGCTTTGAAT GTCGACGTCCATCAAGTCAAACATTTTGCTCTTGACCTCGGAT CAGGTAGGGATACCCGCTGAACTTAAGCATATC	GU327433.1 uncultured fungus	99.82%/0.0
		MF795792.1 *Pyrenochaeta nobilis* CBS 407.76	94.75%/0.0
		NR_156358.1 *Neocucurbitaria juglandicola* CBS142390	92.25%/0.0

Whole genome sequencing was performed on Illumina HiSeq 2500 platform resulting in 150 bp paired-end reads. The integrity and quality of raw sequence data were initially assessed using FastQC (v0.12.1)[2]. Reads were subsequently filtered to remove low-quality sequences. De novo assembly was performed using SPAdes (v3.15.2) with k-mer lengths of 77, 99, and 121, along with the --careful and --only-assembler parameters to minimize assembly errors[3]. The assembly command used was as follows:

> /opt/anaconda3/envs/de_novo_assembly/bin/spades.py -1 IBWF/1.fastq.gz -2 IBWF/2.fastq.gz -o IBWF/spades_kmers_set_careful_assembly -t 4 -k 77,99,121 --careful –only-assembler

Quality assessment was performed by the QUAST (v5.0.2) tool[4].The assembly with the highest contiguity, as indicated by the largest N50 and contig lengths, was selected for downstream analyses. Gene prediction was carried out using Augustus with a pretrained fungal models. Functional annotation of predicted genes included BLAST comparisons against Swiss-Prot and InterPro databases. Genome visualization was performed using IGV (v2.14.0)[5]. Secondary metabolite biosynthetic gene clusters (BGCs) detection were carried out using antiSMASH (v7.1.0)[6] and FunBGCeX[7]. Predicted clusters were manually curated and validated by BLASTp comparisons against the NCBI non-redundant protein database to confirm functional annotation and assess cluster architecture.

Construction of plasmids and mutants

pleB and *pleC* were amplified from genomic DNA of IBWF 020-21 using Q5 Hot Start High-Fidelity 2X Master Mix (NEB) and assembled into *Nco*I-restricted SM-Xpress_argB(mut) and SM-Xpress_pabA, respectively, using the HiFi DNA assembly master mix (NEB). The ~25 kb CDS of *pleA* was sequentially assembled into SM-Xpress_Ura in three successive HiFi DNA assembly reactions. Initially, four (of seven) fragments were amplified and assembled into *Nco*I-restricted SM-Xpress_Ura, inserting a *Psp*OMI restriction site after the final fragment for reopening the intermediate plasmid after assembly. We sequenced the resulting plasmid and noticed only partial integration of the fourth fragment, however the *Psp*OMI restriction site was intact. Therefore, we redesigned a primer for amplification of the fourth fragment accounting for the new overlap and inserted new fragment four and fragment five into the *Psp*OMI-restricted intermediate plasmid, again inserting a new *Psp*OMI after the fifth fragment. Finally, fragments six and seven were assembled into the *Psp*OMI-restricted second intermediate plasmid and the integrity of the final plasmid validated by whole plasmid sequencing. All oligonucleotides used in this study are listed in Table S3. For construction of OP12_*pleAB* and OP12_*pleABC*, protoplast transformation of OP12 3Δ was carried out as previously described[1]. Integration of *pleB* and *pleC* was confirmed by diagnostic PCR using the 2× Phire Green Hot Start II PCR Master Mix (Thermo) (Figure S. 9).

Table S. 3: Oligonucleotides used in this study

Oligo	Sequence	Purpose
oCW282	catttaacaaacttctcatcacagcaccatgaatgaaataggtgaaagag	Amplification of *pleA* fragments for sequential cloning of SMX_*pleA*_Ura
oCW283	gtgcatcgcgtttatcgtca	
oCW347	gcggtcttcctacaggttga	
oCW522	ctcagtcggatcctgacctt	
oCW523	attgaacttccgttttcagg	
oCW350	tggctgggatatgacttgct	
oCW288	tattcacgacctgatcgctg	
oCW296	ggttcagattgaaatcactgctgcgggcccacttgctagcctagtcgaag	
oCW530	agatgacgtacaacgagcta	
oCW351	ttacaatgagctggatgaaa	
oCW531	ggttcagattgaaatcactgctgcgggccccttaacatacctcggttgg	
oCW525	gtttccaggaaggtcaagat	
oCW526	tagtgaggatctcatcaata	
oCW294	tcctacgctttcgatgcttg	
oCW295	ctatacggttcagattgaaatcactgctgctcaagtaaatgctggcaag	
oCW549	catttaacaaacttctcatcacagcaccatggtcttcactactcccgc	Amplification of *pleB* fragments for cloning of SMX_*pleB*_argB(mut)
oCW313	ccactcacgatattgtccac	
oCW314	gtggacaatatcgtgagtgg	
oCW298	ctatacggttcagattgaaatcactgctgcctacggcatctcattcgac	
oCW299	Catttaacaaacttctcatcacagcaccatggttgtagaaaagtttccta	Amplification of pleC for cloning of SMX_*pleC*_paba
oCW300	Ctatacggttcagattgaaatcactgctgcctacattatgaaggactgg	
oCW75	gcgcaaagacacatgatg	Used for diagnostic PCRs, anneals in the P*terA* promoter
ITS1F	cttggtcatttagaggaagtaa	Amplification of the ITS barcode region
ITS4	tcctccgcttattgatatgc	

Fermentation, extraction, HPLC-MS analysis, extract fractioning and isolation of pleosporacin

In an initial screening, fungal strain IBWF 020-21 was cultivated in 500 mL of YMG media (0.4 % yeast extract, 1 % malt extract, 1 % glucose) for 20 days shaking at 120 rpm at rt. OP12 mutant strains were cultivated in 50 mL 2 % starch media (2 % soluble starch, 10 mM glutamine, 0.52 g/L KCl, 0.52 g/L $MgSO_4 \cdot 7\ H_2O$, 1.52 g/L KH_2PO_4; 1 mL/L Hutner's trace elements; pH 6.5) for 3 days shaking at 150 rpm at rt. Mycelia was harvested by vacuum filtration and extracted with MeOH:actetone (1:1) shaking for 30-60 minutes at rt. The suspension was filtered and dried under reduced pressure. Crude extracts were redissolved in MeOH and analyzed by LC-MS using a LiChrospher 100 RP-18 column (125 mm × 2 mm, 4 µm, Merck KGaA) connected to Agilent DAD 1260 and Quadrupole LC/MS 6130 modules for detection, running a gradient of 1 to 100 % of ACN in H_2O + 0.1 % formic acid in 20 minutes at a flow rate of 0.4 mL/min.

To identify the active ingredient in the mycelia extract of IBWF 020-21, the extract was fractioned using HPLC. The resulting fractions were then re-assessed for germination inhibitory activity against *B. cinerea* and only fractions containing compound **1** exhibited activity.

For isolation of compound **1**, IBWF 020-21 was cultivated in a 20 L bioreactor (YMG media) stirring at 120 rpm at room temperature for 9 days. The mycelium was separated from the culture broth and lyophilized. The mycelium (132 g) was subsequently extracted with 2 L MeOH:actetone (1:1) overnight three times. The dried crude extract (25.6 g) was prefractionated using silica gel chromatography (CH→EE→MeOH; target fraction: 3.1 g) and SPE (Bond Elut C18 Cartridge, Agilent, H_2O→ACN). Half of the SPE fraction containing most **1** (65% ACN fraction, 0.46 g total) was applied to preparative HPLC on a Sunfire C18 column (100 Å, 5 µm, 19 mm × 250 mm, Waters GmbH) running at 17 mL/min (isocratic elution, 62 % ACN, 38 % H_2O + 0.1 % formic acid), yielding 54.4 mg of pure **1** as an off-white amorphous solid.

Analytical chemistry for structure elucidation

Thin layer chromatography

Analytical thin-layer chromatography (TLC), 0.25 mm silica plates (60 F254) from Merck were used, and the detection was reached by fluorescence quenching under UV light (λ = 254 nm) or by staining with potassium permanganate reagent (solution of $KMnO_4$ (3 g), K_2CO_3 (20 g), 5 % NaOH (5 mL), and H_2O (300 mL)) followed by heating to 400 °C.

NMR spectra

Measured NMR spectra were, unless otherwise mentioned, recorded at 296 K on a 600 MHz Bruker Avance-III 600 spectrometer with a 5 mm TCI cryoprobe. After prior referencing to the residual solvent signal (Acetone-d_6: 2.05 & 29.84 ppm for ^{1}H NMR and ^{13}C NMR, respectively), all chemical shifts (δ) are reported relative to residual solvent[8]. Coupling constants were reported in Hz and the signal multiplicities were abbreviated as follows: s (singlet), d (doublet), t (triplet), q (quartet), qd (quartet of doublet), m (multiplet), br (broad).

Infrared spectra

Infrared spectroscopy was performed on a Bruker Tensor 27 FTIR spectrometer including a diamond ATR unit and are reported in terms of absorption frequency $\bar{\nu}$[cm^{-1}].

Mass spectra

HRMS and MS/MS were conducted on an Agilent G6545A Q-ToF with ESI, APCI or APPI source coupled with an Agilent 1260 Infinity II HPLC system. If not described otherwise, spectra were recorded using positive ionization mode.

Optical rotations

Optical rotation measurements were accomplished with a Perkin-Elmer 241MC polarimeter at λ = 589nm. A solvent-filled cuvette was used for instrument calibration[9].

Marfey analysis for determining the stereochemistry of pleosporacin

Marfey analysis was adapted from Büttner *et al.*[10]. Briefly, 1 mg of **1** was hydrolyzed in 2 mL of 6 M HCl at 110 °C overnight or alternatively for 1 h only to prevent degradation of tryptophan[11]. The hydrolysate was dried under a N_2 stream and subsequently redissolved in 500 µL 1 M $NaHCO_3$. 50 µL of a 1 % solution of L-FDAA in acetone was added to 100 µL of the hydrolysate and the reaction heated to 50 °C for 1 h. The reaction was quenched by the addition of 50 µL of 2 M HCl and subsequently diluted with 200 µL of ACN/H_2O (1:1). 200 µg of each amino acid (D- and L-, Gln, Ser, Trp, Tyr) were derivatized in the same way. 5 µL of the references or 20 µl of the **1** hydrolysate were analyzed using LC-MS, running a gradient of H_2O + 0.1 % formic acid and ACN as follows: 1–25 % ACN in 30 min, isocratic 25 % ACN for 10 min, 25–70 % ACN in 20 min, 70–100 % ACN in 1 min, isocratic 100 % ACN for 4 min. Stereochemistry was assigned by comparison of the hydrolysate and amino acid reference chromatograms.

Bioactivity Assays

Germination inhibition of ascomycete fungi

Conidia of *Magnaporthe oryzae* 70-15, *Botrytis cinerea* DSM 0877, *Fusarium graminearum* DSM 21727 and *Aspergillus oryzae* RIB40 were harvested from agar plates and diluted in 2 % malt extract media to a final concentration of $1x10^5$ conidia/mL. 200 µL of the solution were added to wells of a 96-well plate containing different concentrations of the purified compounds. The plates were then incubated overnight at room temperature. Conidia germination was evaluated using a microscope. Ciclopirox (100 µg/mL) served as positive control.

Vegetative growth inhibition of Botrytis cinerea

For assessing whether **1** was fungicidal or merely inhibited germination of *B. cinerea*, antibiotic assay discs were placed on a YMG agar plate and 20 µg, 10 µg, 5 µg, 1 µg **1** or MeOH were added to them. Then, *B. cinerea* was spotted in the middle of the plate and allowed to grow for 7 days at rt. The growth inhibitory activity was visually assessed.

Growth inhibition of dimorphic yeast Candida albicans

Candida albicans ATCC90028 was grown on Sabouraud (Difco) plates. Fresh colonies were suspended in H_2O, diluted 1:20 in Sabouraud media, 200 µL distributed in 96-well test plates and cultivated shaking at room temperature for 18–24h; growth inhibition was assessed macroscopically. Ciclopirox (100 µg/mL) served as positive control.

Growth inhibition of oomycete Phytophthora infestans

2 mL of a 2-week-old liquid PDA (Difco) culture of *Phytophthora infestans* CBS 430.90 were shredded using a FastPrep twice for 20 s, diluted with 5 mL of H_2O and filtered through miracloth. The filtrate was diluted 1:20 with KGA media and 200 µL distributed in 96-well test plates. Plates were incubated gently shaking at room temperature for 1 week; growth inhibition was assessed macroscopically. Ciclopirox (100 µg/mL) served as positive control.

Growth inhibition of bacteria

Nutrient broth (Difco) precultures of *Staphylococcus aureus* ATCC11632 (37 °C), *Pseudomonas aeruginosa* ATCC15442 (37 °C), *Aneurinibacillus migulanus* ATCC9999 (37 °C) and *Enterobacter cloacae* subsp. *dissolvens* LMG2683 (27 °C) were grown shaking overnight. Precultures were diluted 1:100 in fresh nutrient broth and 200 µL were distributed in 96-well test plates. Plates were cultivated shaking at 37 °C or 27 °C for 18–24h and growth inhibition was assessed macroscopically. Tetracycline (100 µg/mL) and Streptomycin (100 µg/mL) served as positive controls.

II. Supplementary Figures

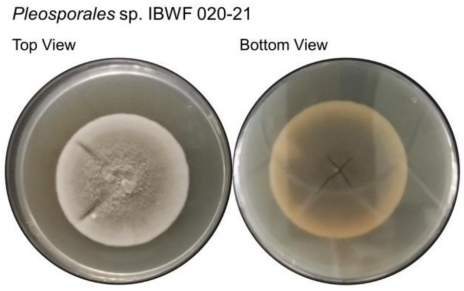

Figure S.: 1Morphology of *Pleosporales* sp. IBWF 020-21 grown on YMG media for 22 days at rt.

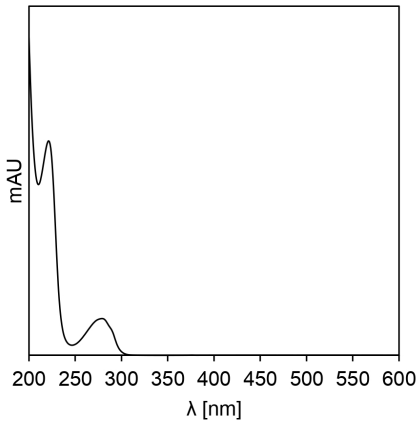

Figure S. 2: UV/Vis spectrum of pleosporacin (**1**).

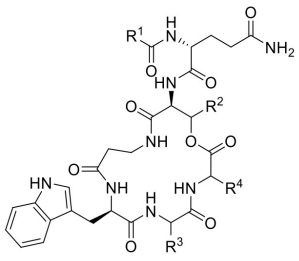

R^1=myristic acid	R^2=L-Ser	R^3=L-Ser	R^4=D-Tyr	Pleosporacin (**1**)
R^1=(*R*)-3-hydroxymyristic acid	R^2=L-Thr	R^3=L-Ser	R^4=D-Tyr	Symbiosin
R^1=dodecanoic acid	R^2=L-Thr	R^3=L-Ser	R^4=D-Phe	Colisporifungin
R^1=dodecanoic acid	R^2=L-Thr	R^3=L-Ser	R^4=D-Tyr	Verruculin
R^1=decanoic acid	R^2=L-Thr	R^3=L-Ser	R^4=D-Phe	Ophiotine
R^1=9-hydroxyoctadeca-10,12-dienoic acid	R^2=L-Thr	R^3=D-Ser	R^4=Gly	Aselacin A

Figure S. 3: Structures of pleosporacin (**1**) and related cyclic lipodepsipeptides[10,12].

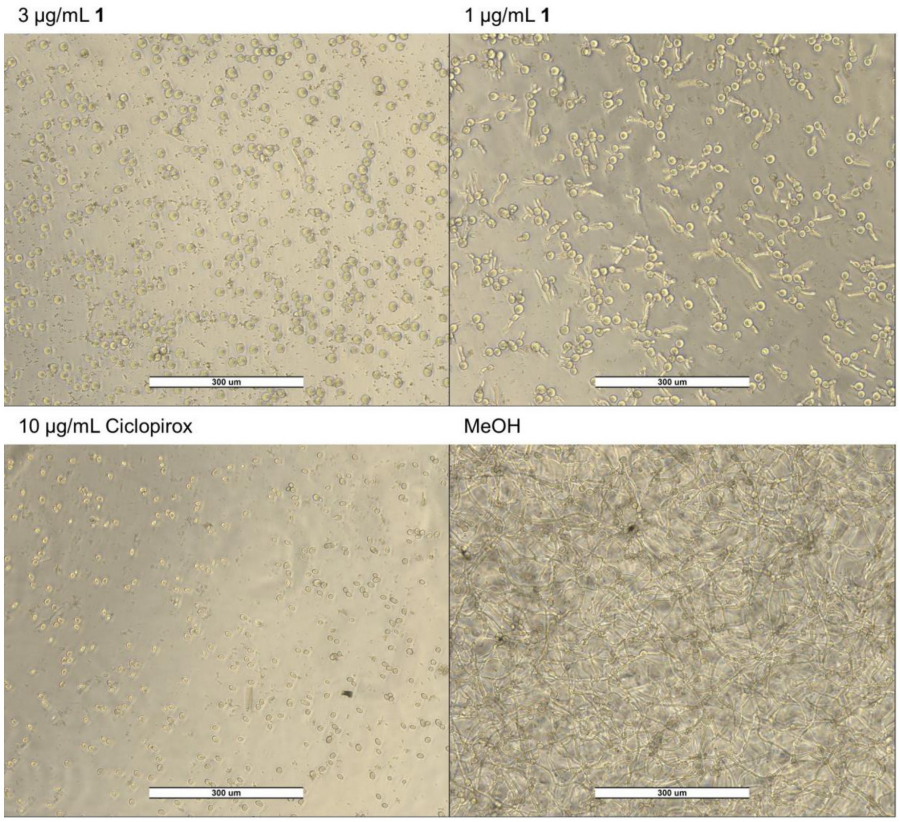

Figure S. 4: Germination inhibitory activity of **1** against *Botrytis cinerea*. Ciclopirox and MeOH served as positive and negative controls for inhibition. Sub-MIC germination is only partially inhibited, i.e., some short germ tubes are being formed. Conidia treated with **1** appear to be bloated (roughly 1.5-fold larger in size). Some media impurities are seen in the background.

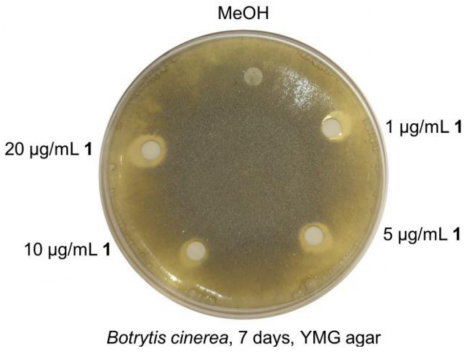

Figure S. 5: Vegetative growth inhibitory activity of **1** against *Botrytis cinerea*. Inhibition zone Ø: 8–11 mm (measured from center of the discs).

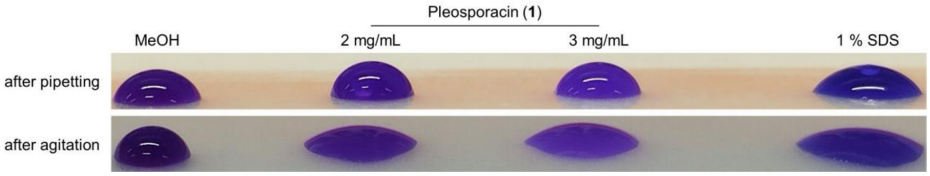

Figure S. 6: Drop Collapse Assay. Carried out as previously described by Büttner *et al.* [10]. After pipetting the drops containing pleosporacin (**1**) do not immediately collapse. However, upon agitation, the drops collapse similar to the 1 % SDS control. The surface tension of the MeOH control is not disturbed even after agitation.

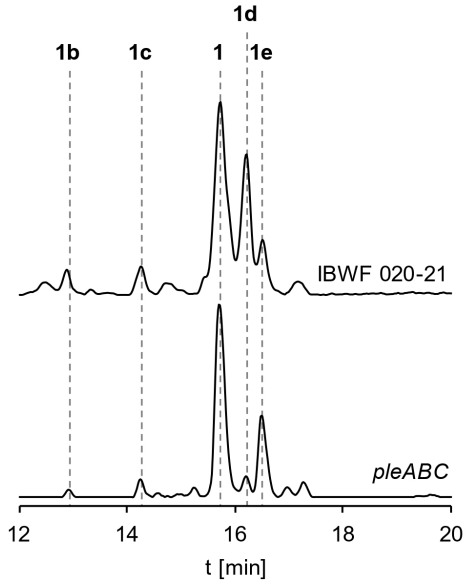

Figure S. 7: Extracted ion chromatograms (800–1000 *m/z*, recorded in negative mode) of IBWF 020-21 and OP12_*pleABC* mycelia extracts. Some of the putative **1** congeners produced are highlighted as **1b** (875 *m/z*), **1c** (903 *m/z*), **1d** (915 *m/z*) and **1e** (945 *m/z*). Presumably, these congeners harbor different length fatty acyl chains, namely (in order) decanoic acid, dodecanoic acid, tridecanoic acid and pentadecanoic acid.

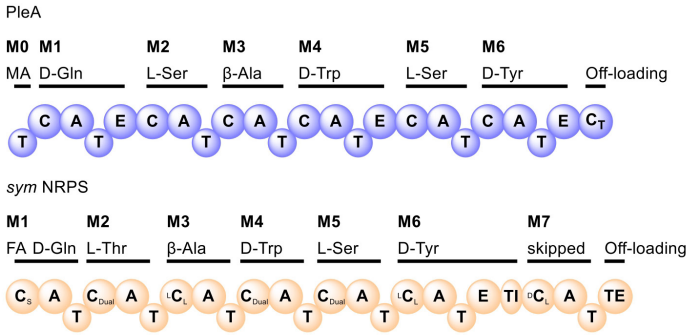

Figure S. 8: Comparison of domain architecture between PleA and *sym* NRPS (Accession No.: UUM22377.1). A, adenylation domain; C, condensation domain (S, starter; Dual, condensation/epimerization), E, epimerization domain; FA, fatty acid (3-hydroxy-myristic acid); MA, myristic acid; T, thiolation domain; TE, thioesterase domain; TI, TIGR01720 domain.

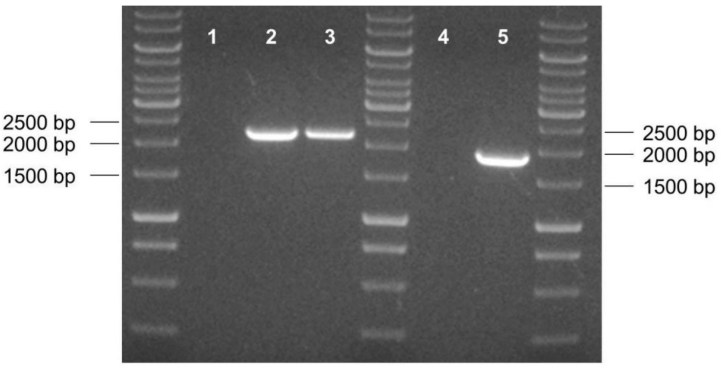

Figure S. 9: Diagnostic PCR confirming integration of *pleB* (left, Primers oCW75 + oCW298, expected amplicon: 1860 bp) and *pleC* (right, Primers oCW75 + oCW300, expected amplicon: 2163 bp). 1 and 4: OP12_empty plasmids; 2: OP12_*pleAB*; 3 and 5: OP12_*pleABC*

III. Analytical Data

Table S. 4: NMR assignment ^{1}H (600 MHz, Acetone-d_6) and ^{13}C NMR (151 MHz, Acetone-d_6)

Unit	Position	δ C, type	δ 1H, mult (Hz)	Unit	Position	δ C, type	δ 1H, mult (Hz)
D-Gln	1	171.2, q	-	TDA	1	173.4, q	-
	2	53.0, CH	4.53 (q, 7.0, 1H)		2	34.2, CH_2	2.28 –, 2.23 (t, 7.5, 2H)
	3	25.1, CH_2	2.00 – 1.95 (m, 2H)		3	24.5, CH_2	1.58 (tp, 13.8, 7.0, 2H)
	4	30.2, CH_2	2.44 – 2.29 (m, 2H)		4-11	28.6, 28.5, 28.5, 28.5, 28.3[d]	1.26 – 1.17 (m, 16H)
	5	172.9, q	-		12	30.8	1.26 – 1.17
	NH		7.96 (d, 5.3, 1H)		13	21.5, CH_2	1.31 – 1.26 (m, 2H)
	NH2		7.02 (br, 1H)[a],6.35 (s, 1H)		14	12.5, CH_3	0.87 (t, 7.0, 3H)
L-Ser-1	1	167.8, q	-	L-Ser-2	1	169.5, q	-
	2	50.3, CH	4.75 (dt, 10.0, 2.5, 1H)		2	56.9, CH	4.19 (q, 5.5, 1H)
	3	64.2, CH_2	4.86 (dd, 10.8, 2.5, 1H), 3.85 (dd, 10.8, 2.5, 1H)		3	60.3, CH_2	3.61 (d, 11.9, 1H), 3.59 – 3.51 (m, 1H)[b]
	NH		8.65 (d, 10.0, 1H)		NH		8.10 (d, 5.6, 1H)
					Oh		3.87 (br, 1H)
β-Ala	1	171.0, q	-	D-Trp	1	173.2, q	-
	2	33.5, CH_2	2.68 (ddd, 14.5, 10.9, 4.2, 1H), 2.26 – 2.23 (m, 1H)		2	53.3, CH	4.69 (q, 7.1, 1H)
	3	36.1, CH_2	3.59 – 3.51 (m, 1H)[b], 3.11 – 3.04 (m, 1H)		3	26.8, CH_2	3.20 – 3.09 (m, 2H)[c]
	NH		7.46 (br d, 6.3, 1H)		NH	-	7.82 (s, 1H)
					NH^{Ind}	-	10.15 – 10.12 (m, 1H)
D-Tyr	1	169.5, q			2^{Ind}	122.9, CH	7.22 (d, 2.2, 1H)
	2	54.2, CH	3.76 (s, 1H)		3^{Ind}	108.5, q	-
	3	32.7, CH_2	3.20 – 3.09 (m, 2H)[c]		$3a^{Ind}$	126.6, q	-
	NH		7.91 (d, 7.4, 1H)		4^{Ind}	117.4, CH	7.55 (d, 7.9, 1H)
	1’	128.2, q			5^{Ind}	117.8, CH	7.03 (d, 6.1, 1H)[a]
	2’, 6’	114.0, 2C, CH	7.01 (d, 6.6, 2H)[a]		6^{Ind}	120.3, CH	7.09 (ddd, 8.1, 7.0, 1.1, 1H)
	3’, 5’	129.5, 2C, CH	6.71 – 6.66 (m, 2H)		7^{Ind}	110.3, CH	7.37 (dt, 8.1, 0.9, 1H)
	4’	154.9, q			$7a^{Ind}$	135.6, q	-
	OH	-	8.26 (s, 1H)				

[a] overlapping signals, [b] overlapping signals, [c] overlapping signals, [d] partially covered by solvent signals.

$[\alpha]_D^{21}$ +47.8 (MeOH) (c=0.23)

IR (ATR): $\tilde{\nu}$ [cm^{-1}] 3292, 2926, 2854, 1741, 1659, 1651, 1644, 1633, 1539, 1517, 1456, 1342, 1232, 1173.

LRMS (ESI) m/z (%): 933.5 (33) $[M+H]^+$.

HRMS (ESI) *m/z*: $[M+Na]^+$ Calcd for $[C_{48}H_{67}N_8NaO_{11}]^+$ 955.4900; Found. 955.4889.

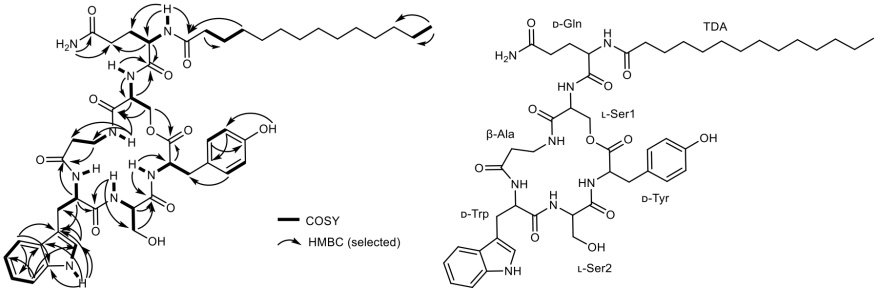

Figure S. 10: Key COSY and HMBC correlations of the NMR structure analysis.

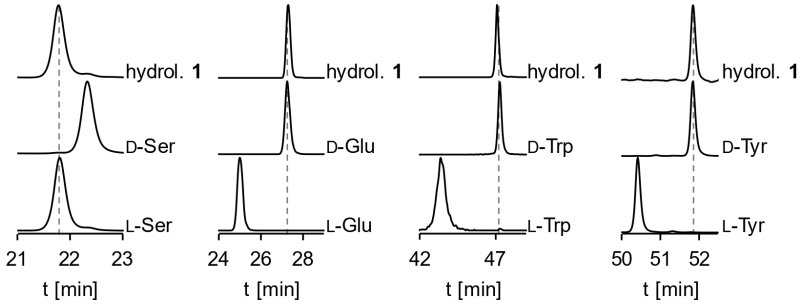

Figure S. 11: Marfey analysis for determining the stereochemistry of **1**. Gln was detected as Glu (conversion during hydrolysis). 300 nm chromatograms are shown for Ser and Tyr. EICs are shown for Glu and Trp (398 m/z and 455 m/z, respectively) due to unrelated overlapping UV/Vis peaks.

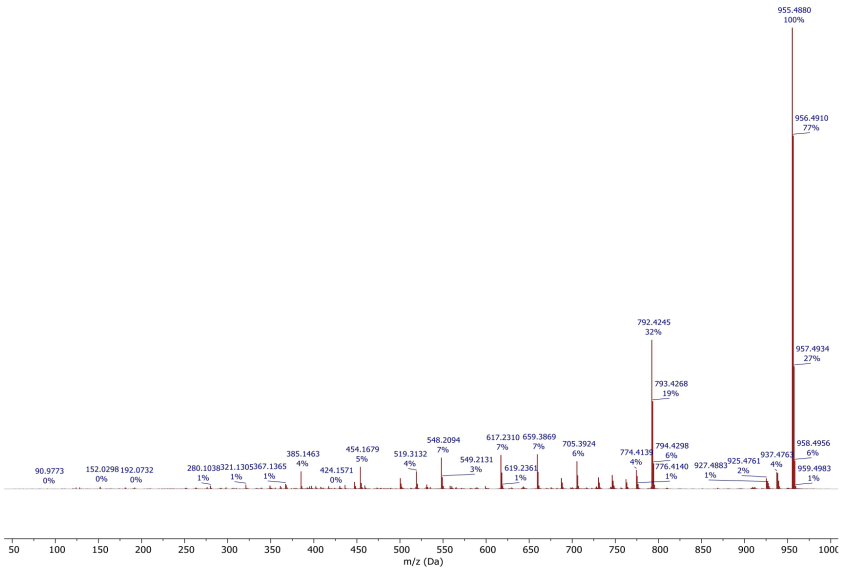

Figure S. 12: MS^2 spectrum of pleosporacin (**1**) recorded with 50 V collision energy.

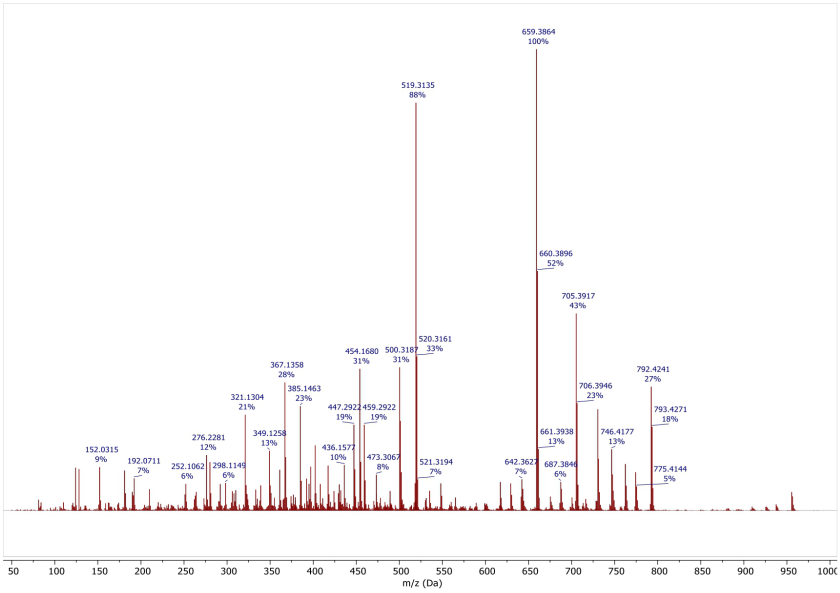

Figure S. 13: MS^2 spectrum of pleosporacin (**1**) recorded with 75 V collision energy.

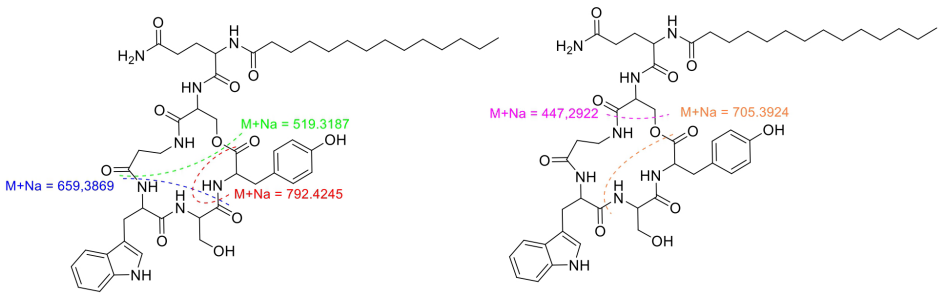

Figure S. 14: Proposed fragmentation of pleosporacin (**1**) for some of the major ion fragments observed.

IV. ^{1}H- and ^{13}C{^{1}H}-NMR Spectra

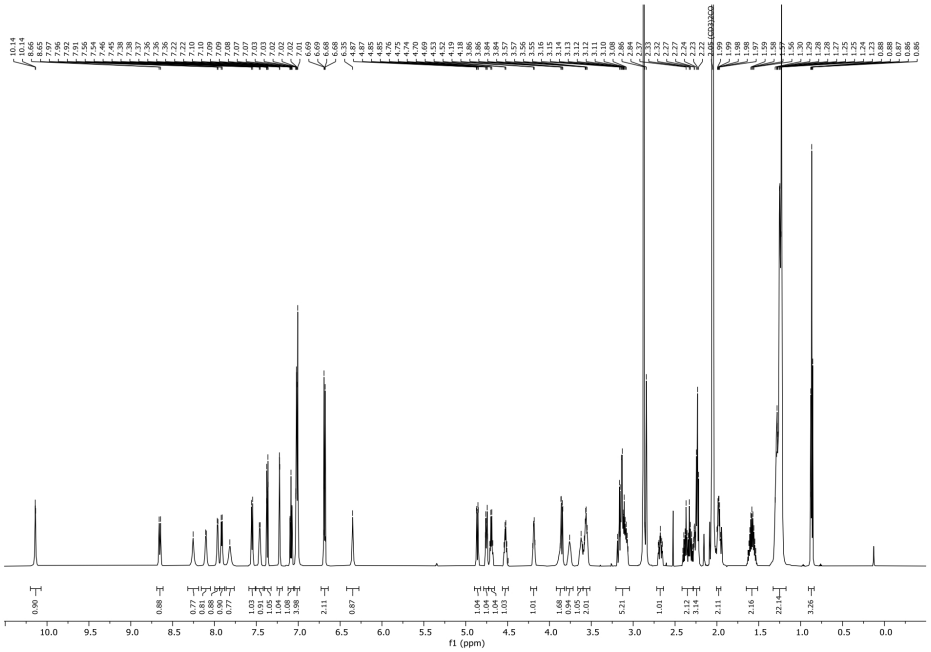

Spectrum S. 1: ^{1}H-NMR spectrum (Acetone-d_6, 600 MHz, 294 K) of pleosporacin (**1**).

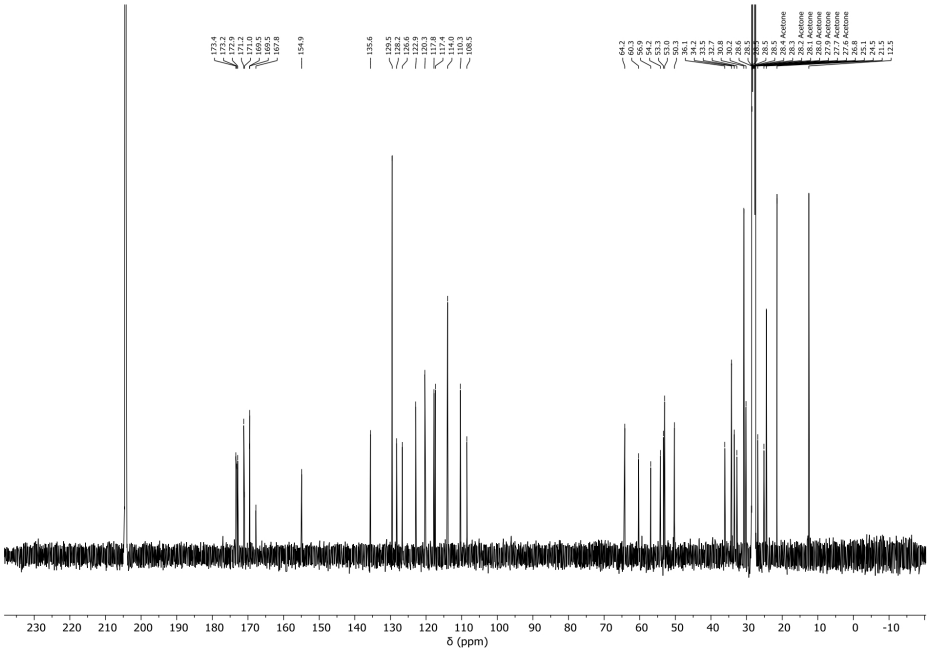

Spectrum S. 2: ^{13}C{^{1}H}-NMR spectrum (Acetone-d_6, 151 MHz, 294 K) of pleosporacin (**1**).

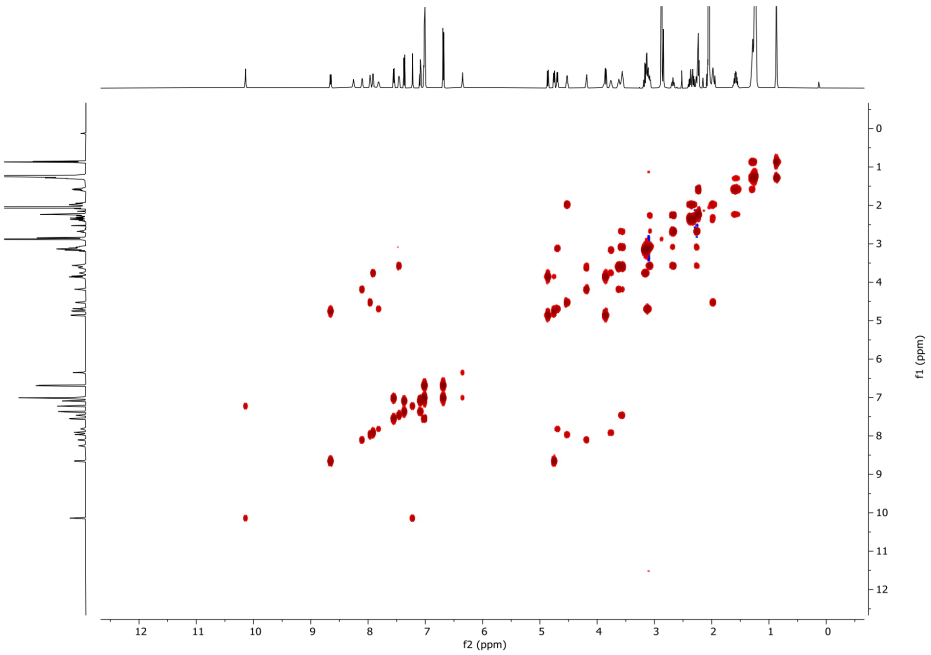

Spectrum S. 3: ^{1}H-^{1}H-COSY (Acetone-d_6, 600 MHz, 294 K) of pleosporacin (**1**).

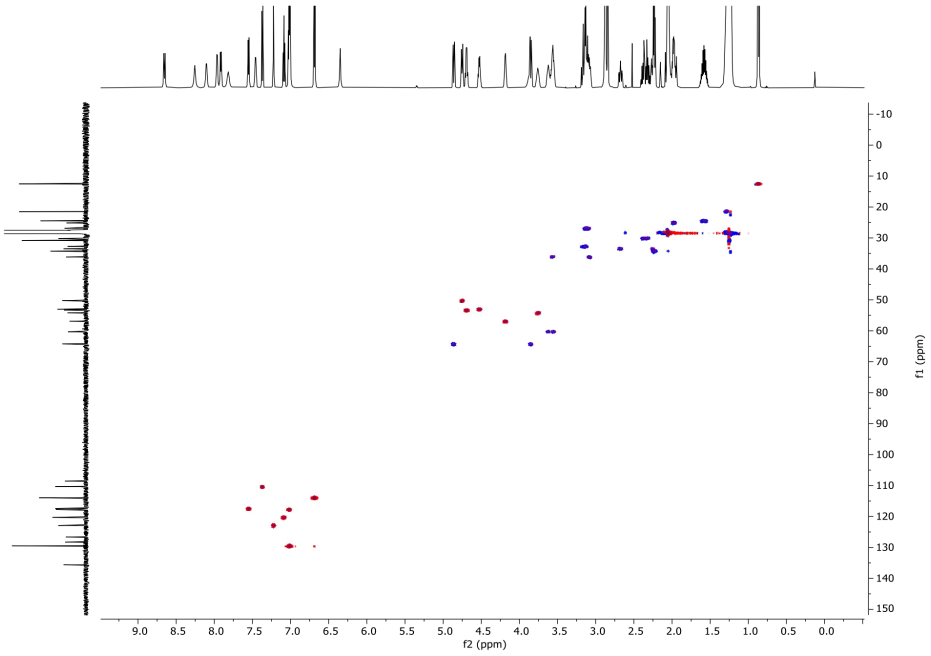

Spectrum S. 4: ^{1}H-^{13}C{^{1}H}-HSQC (Acetone-d_6, 600 MHz, 294 K) of pleosporacin (**1**).

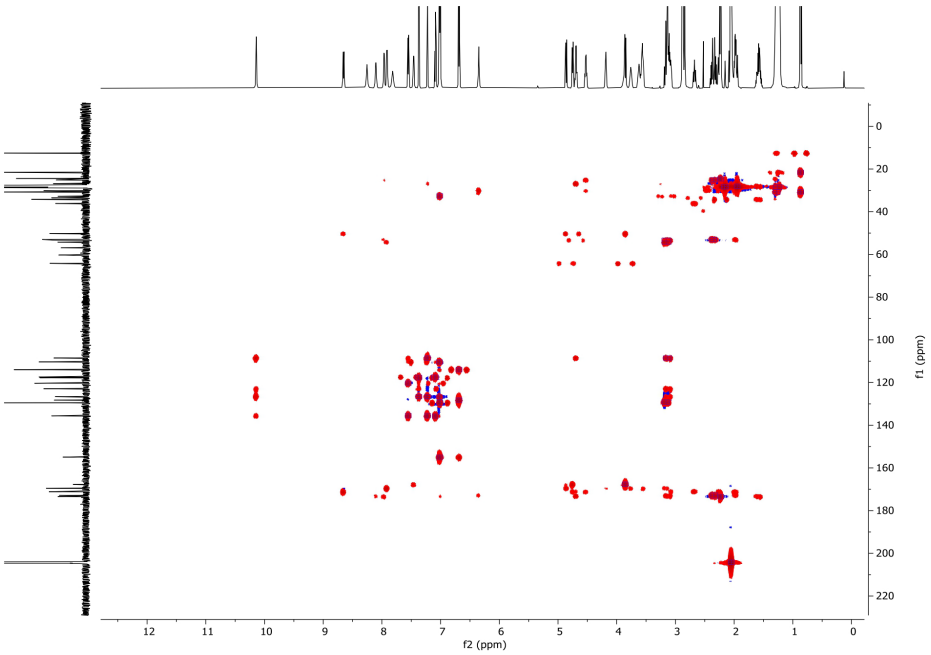

Spectrum S. 5: ^{1}H-^{13}C{^{1}H}-HMBC (Acetone-d$_6$, 600 MHz, 294 K) of pleosporacin (**1**).

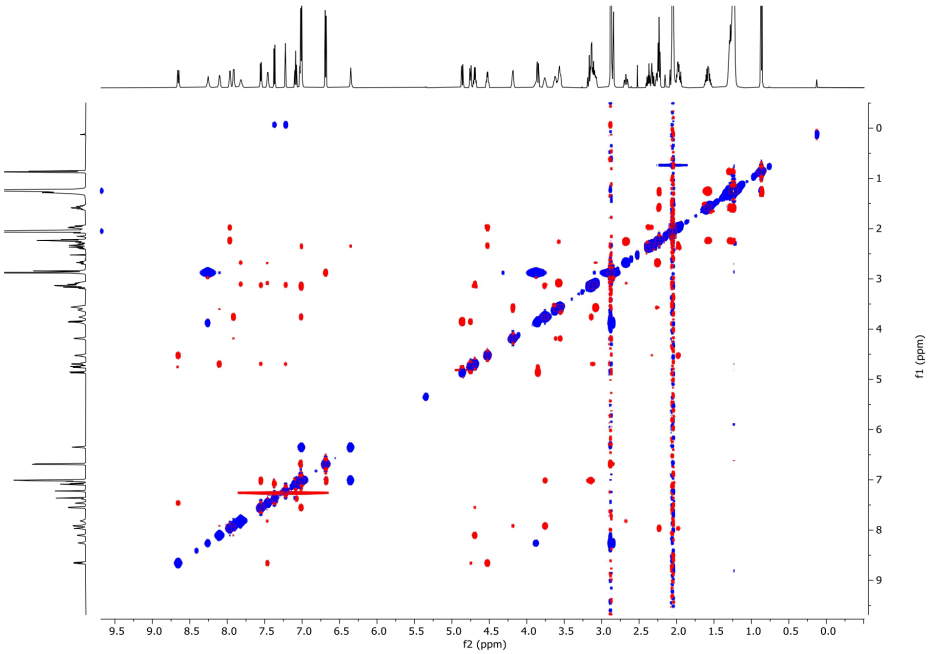

Spectrum S. 6: ^{1}H-^{1}H-NOESY (Acetone-d$_6$, 600 MHz, 294 K) of pleosporacin (**1**).

V. References

[1] C. Wieder, M. Künzer, R. Wiechert, K. Seipp, K. Andresen, P. Stark, A. Schüffler, T. Opatz, E. Thines, *Org. Lett.* **2025**.

[2] S. Andrews, "FastQC: a quality control tool for high throughput sequence data", to be found under https://www.bioinformatics.babraham.ac.uk/projects/fastqc/, **2010**.

[3] A. Bankevich, S. Nurk, D. Antipov, A. A. Gurevich, M. Dvorkin, A. S. Kulikov, V. M. Lesin, S. I. Nikolenko, S. Pham, A. D. Prjibelski et al., *J. Comput. Biol.* **2012**, *19*, 455–477.

[4] A. Gurevich, V. Saveliev, N. Vyahhi, G. Tesler, *Bioinformatics (Oxford, England)* **2013**, *29*, 1072–1075.

[5] H. Thorvaldsdóttir, J. T. Robinson, J. P. Mesirov, *Briefings Bioinf.* **2013**, *14*, 178–192.

[6] K. Blin, S. Shaw, H. E. Augustijn, Z. L. Reitz, F. Biermann, M. Alanjary, A. Fetter, B. R. Terlouw, W. W. Metcalf, E. J. N. Helfrich et al., *Nucleic Acids Res.* **2023**, *51*, W46-W50.

[7] J. Tang, Y. Matsuda, *Nat. Commun.* **2024**, *15*, 4312.

[8] G. R. Fulmer, A. J. M. Miller, N. H. Sherden, H. E. Gottlieb, A. Nudelman, B. M. Stoltz, J. E. Bercaw, K. I. Goldberg, *Organometallics* **2010**, *29*, 2176–2179.

[9] G. Lippke, H. Thaler, *Starch - Starke* **1970**, *22*, 344–351.

[10] H. Büttner, S. J. Pidot, K. Scherlach, C. Hertweck, *Chem. Sci.* **2022**, *14*, 103–112.

[11] K. Fujii, Y. Yahashi, T. Nakano, S. Imanishi, S. F. Baldia, K. Harada, *Tetrahedron* **2002**, *58*, 6873–6879.

[12] a) J. E. Hochlowski, P. Hill, D. N. Whittern, M. H. Scherr, R. R. Rasmussen, S. A. Dorwin, J. B. McAlpine, *J. Antibiot.* **1994**, *47*, 528–535; b) S. E. Helaly, S. Ashrafi, R. B. Teponno, S. Bernecker, A. A. Dababat, W. Maier, M. Stadler, *J. Nat. Prod.* **2018**, *81*, 2228–2234; c) T. Bunyapaiboonsri, S. Yoiprommarat, R. Suntivich, S. Preedanon, S. Komwijit, T. Teerawatananond, J. Sakayaroj, *Tetrahedron* **2020**, *76*, 131497; d) F. J. Ortíz-López, M. C. Monteiro, V. González-Menéndez, J. R. Tormo, O. Genilloud, G. F. Bills, F. Vicente, C. Zhang, T. Roemer, S. B. Singh et al., *J. Nat. Prod.* **2015**, *78*, 468–475;

Fourth Publication

Biosynthesis of the *Paecilomyces marquandii* conidial pigment saintopin

Carsten Wieder[1,2], Sarah Galwas[1], Rainer Wiechert[3], Kevin Seipp[3], Alexander Yemelin[2], Anja Schüffler[2], Till Opatz[3], Eckhard Thines[1,2]

[1] Institute of Molecular Physiology, Johannes Gutenberg-University, Hanns-Dieter-Huesch Weg 17, D-55128 Mainz, Germany

[2] Institut für Biotechnologie und Wirkstoff-Forschung gGmbH, Mainz, Hanns-Dieter-Huesch Weg 17, D-55128 Mainz, Germany

[3] Department of Chemistry, Johannes Gutenberg-University, Duesbergweg 10–14, D-55128 Mainz, Germany

Type of authorship:	First author
Type of article:	Research article
Share of work:	70 %
Contribution:	Conceived project and designed experiments; isolation of fungal strain; fermentation; natural product purification; genome mining; cloning of plasmids; generation of mutant strains; HPLC analysis; bioactivity assays; analysis and interpretation of data; writing and editing of the manuscript
Journal:	Fungal Biology and Biotechnology
Date of publication:	05.06.2025
DOI:	10.1186/s40694-025-00199-4

Wieder *et al. Fungal Biology and Biotechnology* (2025) 12:11
https://doi.org/10.1186/s40694-025-00199-4

Fungal Biology
and Biotechnology

RESEARCH Open Access

Biosynthesis of the *Paecilomyces marquandii* conidial pigment saintopin

Carsten Wieder[1,2*], Sarah Galwas[1], Rainer Wiechert[3], Kevin Seipp[3], Alexander Yemelin[2], Eckhard Thines[1,2], Till Opatz[3] and Anja Schüffler[2*]

Abstract

Paecilomyces marquandii IBWF 003–21 produces vibrant purple pigmented conidia, the color of which can be attributed to the naphthacenedione natural product saintopin (**1**). The target compound was previously reported to exhibit potent topoisomerase-inhibitory activity, yet has not been extensively studied nor has the biosynthesis been elucidated. In an effort to elucidate the biosynthesis of **1**, we mined the genome of *Paecilomyces marquandii* for non-reducing polyketide synthases (nrPKS), introduced them into the heterologous host *Aspergillus oryzae* OP12 and identified a prime candidate for the biosynthesis of **1** we termed *stpA*. Deletion of *stpA* in the native producer *P. marquandii* abolished production of **1**, rendering conidia hyaline in color. *stpA* phylogenetically clusters with clade V nrPKS, canonically requiring trans-acting metallo-β-lactamase-like thioesterases (MβL) for product offloading, however, no MβL is encoded in the vicinity of *stpA*. Instead, a BLAST-search revealed a single MβL, *stpB*, encoded elsewhere in the *P. marquandii* genome, accompanied by a flavin-dependent monooxygenase (FMO), *stpC*, and an *O*-methyltransferase, *stpD*. Heterologous coexpression of *stpA* and *stpC* sufficed for reconstituting **1** biosynthesis in *A. oryzae* OP12 even without additional coexpression of *stpB*. Coexpression of *stpC* alongside the decaketide-synthase *adaA* involved in TAN-1612 biosynthesis also resulted in the production of **1**, which implies that the formation of **1** proceeds *via* a decaketide precursor that is subsequently shortened. While the structure and biosynthesis of **1** are unique compared to other fungal naphthacenediones, further research is necessary to elucidate the elusive mechanism underlying the formation of **1**.

Introduction

Fungal polyketides have been extensively studied for their structural diversity and promising biological activities exploitable for medicinal and agricultural applications. Notable examples include the blockbuster cholesterol-lowering drug lovastatin [1], the antifungal agent strobilurin A produced by *Strobilurus tenacellus* that was used as the lead structure for the development of β-methoxyacrylate agri-fungicides [2, 3] as well as the fungistatic drug griseofulvin commonly used for treatment of onychomycosis [4, 5]. Most fungal polyketides are synthesized by type I iterative polyketide synthases (PKS), multidomain enzymes that catalyze repeated decarboxylative Claisen condensation to produce polyketides of varying modifications and chain length [6–8].

PKS are divided into reducing and non-reducing types based on their inherent set of domains. All PKS share essential ketosynthase (KS), acyltransferase (AT) and acyl-carrier protein (ACP) domains and can include additional optional *C*-methyltransferase (CMeT), reductase

*Correspondence:
Carsten Wieder
cawieder@uni-mainz.de
Anja Schüffler
schueffler@ibwf.de

Full list of author information is available at the end of the article

Graphical abstract

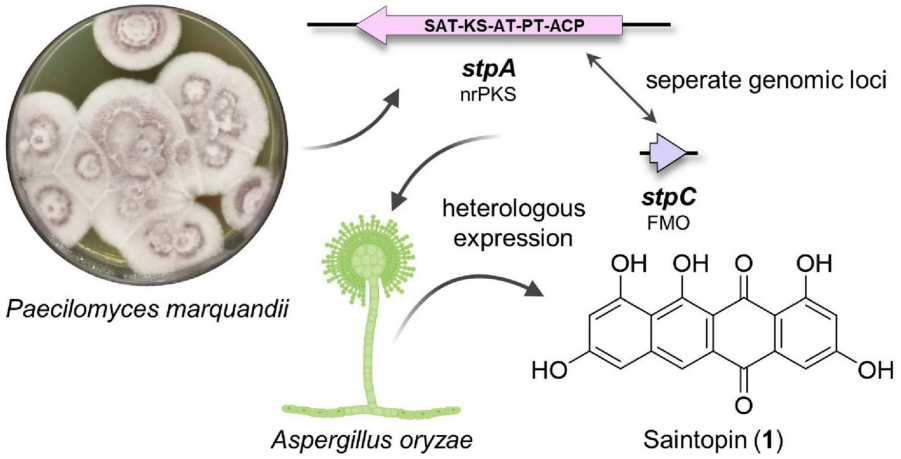

Keywords Natural products, Conidial pigment, Non-reducing polyketide synthase, Biosynthesis, Heterologous expression

(R) or thioesterase (TE) domains. Non-reducing PKS additionally canonically harbor a starter acyltransferase (SAT) [9] and product template (PT) [10] domain responsible for initial substrate loading and product cyclization, respectively, but lack reductive domains found in reducing PKS. The function of the SAT domain is essential in some cases, particularly when loading unusual starter units such as hexanoyl-CoA [9] or in hr/nrPKS hybrid pathways [11], but has been shown to be dispensable without compromising function in recently described basidiomycete nrPKS [12]. The product template domain has been suggested to act as a substrate tunnel that prefolds the nascent polyketide to facilitate aldol-condensation mediated cyclization [13], therefore being responsible for the (poly-)cyclic structure of non-reduced polyketide products.

Phylogenetically, nrPKS cluster into 12 distinct clades, each clade sharing characteristic features in domain architecture, polyketide length and cyclization pattern [12–15]. In contrast to most other nrPKS, clade V nrPKS lack a terminal R- or TE-domain for product offloading, the function of which is commonly complemented by a metallo-β-lactamase-like TE (MβL) protein encoded in the genomic vicinity of clade V nrPKS, firstly described in atrochrysone carboxylic acid biosynthesis [16]. Furthermore, clade V has recently been subdivided into three subclades (V-I, V-II and V-III) [12, 15]. While clade V-I and clade V-III PKS produce octaketides such as atrochrysone/endocrocin [16] and unusual heptaketides such as alternariol [17] and the benzophenone precursor of griseofulvin [18], clade V-II PKS produce nona- and decacetides such as asperthecin [19, 20], TAN-1612 [20], viridicatumtoxin [21], fumicycline [22], neosartoricin [23] and hancockinone A [24] (Fig. 1). Besides MβL, clade V-II nrPKS additionally cluster with flavin-dependent monooxygenases (FMOs). These FMOs catalyze C2-hydroxylation, which is indispensable for cyclization of the fourth ring in the case of naphthacenediones like TAN-1612, as their absence alternatively results in hydrolytic release of a tricyclic product [20].

The fungal naphthacenedione saintopin (Fig. 1), isolated for the first time in 1990 from *Paecilomyces* sp., has previously been shown to exhibit potent topoisomerase I & II inhibitory activity, making it a promising candidate for development as an anti-tumor agent [25]. Indeed, the structurally related bacterial anthracyclines such as doxorubicin (marketed as Adriamycin®, Fig. 1) are already being used to treat various cancers, albeit at the high risk of cardiotoxicity [26]. Despite the promising activity originally reported, only few studies on saintopin have been conducted since. While saintopin is structurally related to other fungal naphthacenediones it does harbor unique structural features, such as the lack of side chains and the resulting planarity (Fig. 1), implying an alternative or extended biosynthetic route. Here we report the isolation of saintopin from *Paecilomyes marquandii*, which is

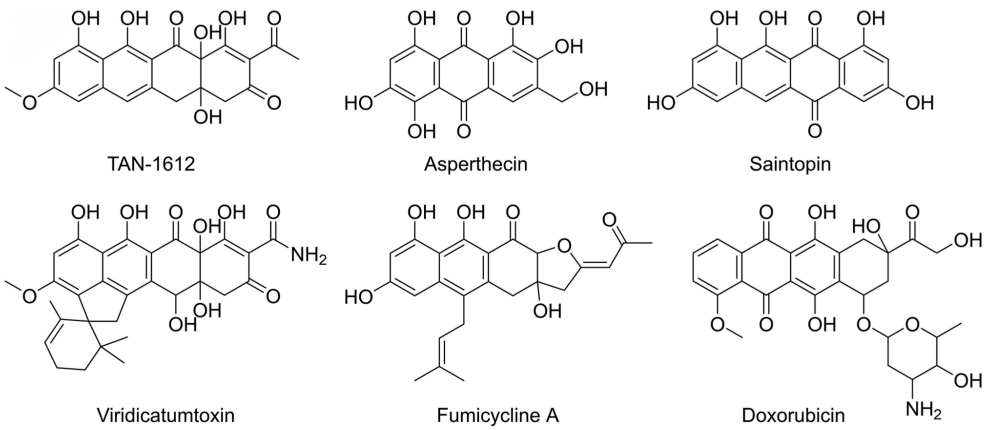

Fig. 1 Selected structures of fungal naphthacenediones and related polyketides

responsible for the conidial pigmentation in the producing organism, as well as identification and heterologous reconstitution of saintopin biosynthetic genes in *Aspergillus oryzae*. Saintopin biosynthesis only requires two enzymes and features an elusive mechanism of polyketide cyclization diverging from other characterized fungal naphthacenedione pathways.

Results

Isolation of the *Paecilomyces marquandii* conidial pigment saintopin

A fungus with vibrant purple conidial pigmentation was isolated from a contaminated agar plate in Mainz, Germany. Sequencing of the barcode ITS region (Table S4) identified the isolate as *Paecilomyces marquandii* (synonym: *Marquandomyces marquandii*) and the strain was deposited at the Institut für Biotechnologie und Wirkstoff-Forschung gGmbH (IBWF, Mainz, Germany) with reference number IBWF 003–21. The major metabolite produced in conidia of *P. marquandii* was identified to be compound **1**, the UV/Vis spectrum of which did align with the purple color of the conidia (Fig. 2). Fortunately, compound **1** was also produced in liquid culture and preparative amounts were obtained from the extraction of the mycelia of *P. marquandii* from a 10 L scale-up fermentation. The purple pigment was isolated from the crude extract using chromatographic techniques and the metabolite identified as saintopin (**1**) by NMR spectroscopy and HRESIMS analysis (Fig. 2).

Heterologous expression of nrPKS genes identifies a prime candidate for saintopin biosynthesis

To identify the biosynthetic origin of saintopin (**1**), the genome of *P. marquandii* IBWF 003–21 was sequenced and assembled into 42.3 Mb, distributed across 406 contigs, with an N50 of 0.7 Mb and a GC content of 51.6%. The length of the largest contig was 2.6 Mb. The results indicated a high-quality genome assembly. A total of 6,617,776 clean reads were obtained from Illumina sequencing, enabling the prediction of 12,761 protein-coding genes, 8,987 of which had functional annotations. AntiSMASH analysis supplemented by manual curation using FunBGCeX results revealed the presence of 81 secondary metabolite (SM) biosynthetic gene clusters (BGCs), comprising 23 nonribosomal peptide synthetases (NRPSs), 16 polyketide synthases (PKSs), 14 terpene synthases (TPSs), 5 hybrid and 23 other BGCs (e.g., ribosomally synthesized and post-translationally-modified peptides (RiPPs), isocyanide synthases (ICS)).

Given the aromatic structure of saintopin (**1**), we hypothesized that its biosynthesis is mediated by a nrPKS. Compound **1** shares structural similarity with other fungal naphthacenediones, such as TAN-1612 and viridicatumtoxin (Fig. 1), however differs in functionalization and substitution, suggesting a different biosynthetic pathway. Among the PKSs identified, seven were categorized as non-reducing. One of these was excluded from further analysis due to high similarity with the sorbicillin BGC of *Acremonium chrysogenum*. The six remaining nrPKS genes were cloned into expression plasmids and introduced into the heterologous host *Aspergillus oryzae* OP12 *pyrG*$^{-}$ [27] to investigate product formation. This strain features a coupled promoter system, which amplifies gene expression and therefore results in higher SM production.

Five out of the six nrPKSs produced detectable products in the heterologous host, as evident from the comparison with the empty plasmid control strain (Fig. 3).

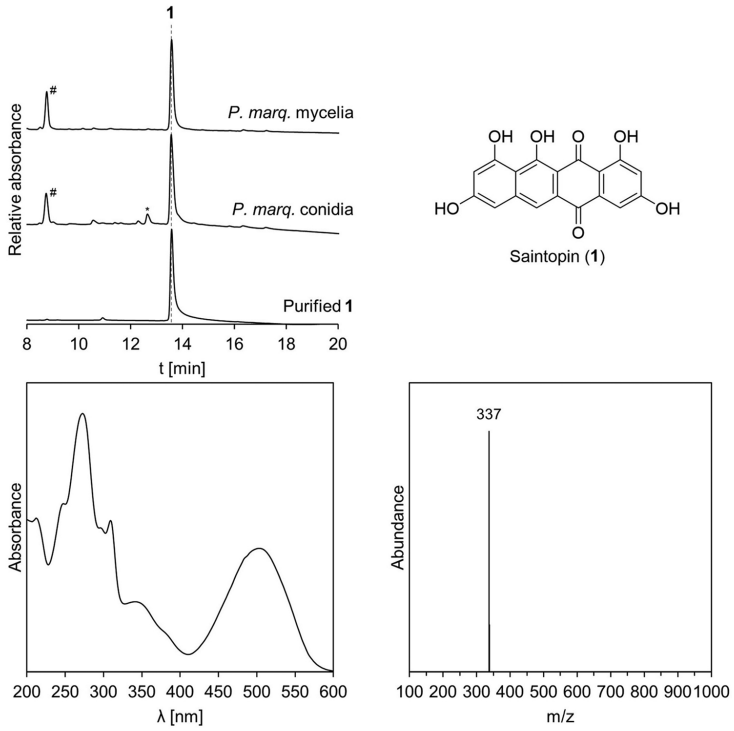

Fig. 2 Saintopin (**1**) is produced in *Paecilomyces marquandii* conidia and mycelia. Chromatograms (250 nm) of *P. marquandii* conidia extract, mycelia extract and purified **1**. Structure, UV/Vis- and neg. ionization mass spectrum of **1**. * corresponds to compound **10**. # unrelated (non-purple colored) compound

Most products were purified from scale-up fermentation of the mutant *A. oryzae* strains and their structures were elucidated by NMR and HRESIMS analysis. While PmPKS1 and PmPKS2 are strictly orsellinic acid (**2**) and nor-toralactone (**3**) synthases, respectively, PmPKS4 and PmPKS6 produced multiple products of different chain lengths. OP12_PmPKS4 predominantly produced 6,8-dihydroxy-3-(2-oxopropyl)-1*H*-2-benzopyran-1-one (**4**), orthosporin (**5**), minor amounts of citreoisocoumarin (**6**) and saccharonol A (**7**). OP12_PmPKS6 produced compounds **2** and **7**. No products were produced by OP12_PmPKS5.

OP12_*stpA* produced only traces of several compounds, the major one being **8** (379 Da [M–H$^+$]) and even smaller amounts of **9** (381 Da [M–H$^+$]), **10** (337 Da [M–H$^+$]) and **11** (355 Da [M–H$^+$]) (Fig. 3, Figure S2). Unfortunately, we were not able to obtain sufficient amounts of the compounds produced by OP12_*stpA* for structure elucidation, as yields were too low and production was not scalable. Compounds **8**, **9** and **10** shared the same UV/Vis spectra, suggesting similar molecular structures (Figure S1). The UV/Vis and identified masses of **8** and **10** align with compounds that were previously identified when the clade V nrPKS AdaA was assayed in vitro [20]. Based on this congruence, we propose the structures of **8** and **10** as the previously reported deca- and nonaketide anthrapyrones (Fig. 3). As compound **9** also shares the same UV/Vis and differs from **8** by only + 2 Da, we propose **9** to be the reduced congener of **8**. The structure of compound **11** remains ambiguous. Interestingly, upon reinvestigation of *P. marquandii* extracts for compounds **2**–**11**, compound **10** could also be detected in the conidia extract of *P. marquandii* (Fig. 2). In conclusion, *stpA* seems to be the only nrPKS encoded in the genome of *P. marquandii* producing polyketides of sufficient chain length required for **1** production, making it the prime candidate for the biosynthesis of **1**.

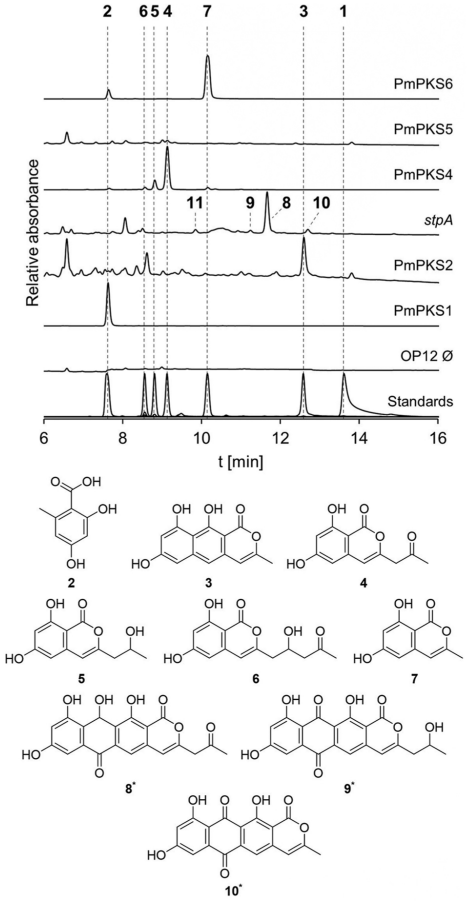

Fig. 3 Heterologous expression of *P. marquandii* nrPKS genes in *A. oryzae* OP12 results in production of different chain length aromatic polyketides. Chromatograms (250 nm) of mutant culture filtrate extracts and purified metabolites. Structures of **2**–**7** were elucidated by NMR and HRESIMS. * Structures of **8**–**10** are proposed. Ø, empty plasmid control strain

Deletion of *stpA* abolishes saintopin production in *P. marquandii*

To assess the involvement of *stpA* in saintopin (**1**) biosynthesis, we first sought to establish a transformation protocol for *P. marquandii*. Fortunately, employing previously established protocols frequently used for protoplasting aspergilli did also successfully yield protoplasts from *P. marquandii* mycelia, albeit after prolonged incubation. However, *P. marquandii* seems highly insensitive to the most commonly used selection agents (as apparent by pre-tests, data not shown, e.g., hygromycin, phleomycin, BASTA, nourseothricin). Despite background growth of untransformed colonies on the transformation plates we eventually succeeded in obtaining a single *ΔstpA* mutant by using geneticin (G418) as a selection agent at 1000 µg/mL (Figure S3). *ΔstpA* exhibits an albino phenotype, lacking conidial pigmentation, which is due to the abolishment of the production of **1** (Fig. 4).

Heterologous reconstitution of saintopin biosynthesis

With *stpA* identified as the core gene involved in the biosynthesis of **1**, we next sought to reconstitute additional accessory genes in *A. oryzae* to elucidate the biosynthetic pathway. StpA has a SAT-KS-AT-PT-ACP domain architecture and phylogenetically clusters with clade V nrPKS, which lack an intrinsic offloading domain and therefore require trans-acting MβL for product offloading. More specifically, StpA belongs to clade V-II enzymes such as AdaA and VrtA, that are involved in the biosynthesis of the fungal naphthacenediones TAN-1612 and viridicatumtoxin, and the respective biosynthetic pathways require action of an FMO for cyclization of the fourth ring. However, neither a MβL nor a FMO are encoded in the vicinity of *stpA*. A BLAST search of the MβL-coding gene *adaB* identified a single homolog in the genome of *P. marquandii* we termed *stpB*. Interestingly, homologs of the FMO *adaC* and the *O*-methyltransferase *adaD* are encoded next to *stpB*, which we consequently termed *stpC* and *stpD*, respectively (Fig. 5; Table 1).

We next performed sqRT-PCR analysis (Figure S4) of all genes surrounding *stpA* and the trans-cluster encoding *stpBCD* with cDNA derived from cultures producing or not producing **1**. Unfortunately, the results did not show any correlation between gene expression and production of **1**, implying an alternative regulatory mechanism, making it difficult to assess genes involved in the biosynthesis of **1**. To experimentally probe accessory genes involved in the biosynthesis of **1**, we co-introduced the homologs necessary for the production of naphthacenediones in other biosynthetic pathways, namely *stpABC*, into the triple auxotrophic *A. oryzae* OP12 3Δ [28] and performed metabolite analysis as previously.

Coexpression of *stpA* and *stpB* did not yield any new compounds, other than those already produced by solely *stpA*, namely trace amounts of **8**, **9**, **10** and **11** (Fig. 6). Intriguingly, the coexpression of *stpABC* but also *stpAC* resulted in the production of **1** (Fig. 6) and various other, presumably shunt products (**13**–**18**, Figure S5). Compounds **10** and **11** were still produced in OP12_*stpAC* and OP12_*stpABC*, whereas compounds **8** and **9** could not be detected. An additional compound **12** (323 Da [M–H$^+$]) was detected predominantly in culture filtrate extracts of OP12_*stpAC* and OP12_*stpABC*. Attempts towards purifying **12** were unsuccessful, since all fractions purified by preparative HPLC additionally

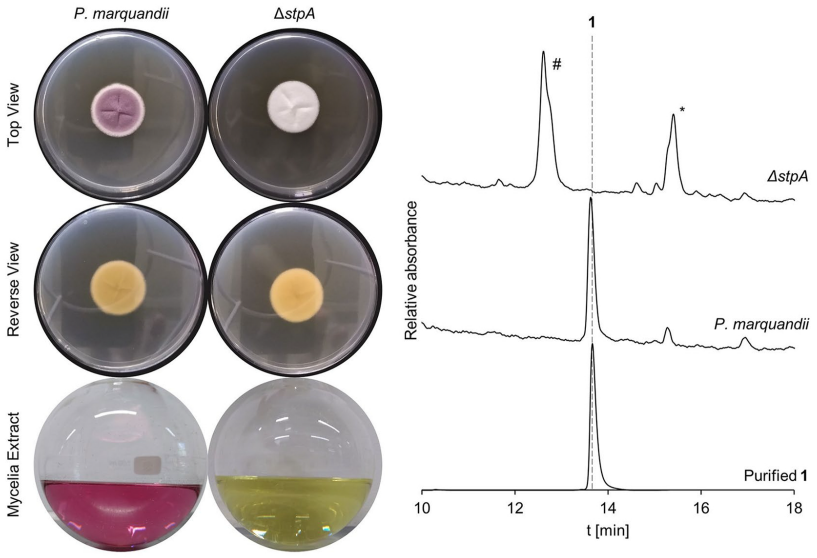

Fig. 4 Deletion of *stpA* results in the loss of conidial pigmentation and abolishment of **1** production. Morphology of *P. marquandii* and *ΔstpA* cultures with their respective mycelia extracts and chromatograms (250 nm). * Presumably trichodimerol by comparison to an internal standard. # Unidentified compound

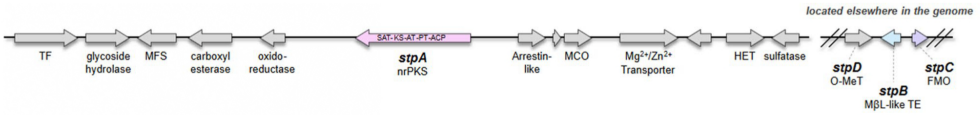

Fig. 5 Scheme of the *stp* BGC

Table 1 Proposed function of *stp* genes

Gene	Size (aa)	BlastP hit*	Identity (%)	E-value	Proposed protein function
stpA	1824	D7PHZ2.1	69.01	0.0	nrPKS (SAT-KS-AT-PT-ACP)
stpB	319	Q4WA58.1	60.00	1e-141	metallo-β-lactamase-like thioesterase
stpC	421	D7PHZ9.1	59.40	0.0	FAD-dependent monooxygenase
stpD	244	D7PHZ7.1	60.99	3e-100	*O*-methyltransferase

*Uniprot as reference database

contained **1**. The mass difference of 14 Da between **12** and **1** might indicate spontaneous oxidation of a non-quinone precursor we termed presaintopin (**12**) in the presence of oxygen to afford the quinone moiety in saintopin (**1**). This would explain the presence of **1** in purified fractions of **12**. During preparation of mycelia extracts, compounds are exposed to atmospheric oxygen for a longer period of time as compared to culture filtrate extracts, resulting in complete oxidation of **12** to **1**, and non-detection of **12** in mycelia extracts. Indeed, during the preparation of mycelia extracts of *P. marquandii*, OP12_*stpAC* or OP12_*stpABC*, the extracts are initially orange-colored and will only turn increasingly purple with prolonged incubation, indicative of conversion of **12** to **1**.

The mechanism underlying the formation of saintopin (**1**) is elusive as the reaction catalyzed by StpC is not readily apparent from the structure of **1**. To gain first mechanistic insights into the formation of **1**, *stpC* was introduced alongside either the decaketide synthase *adaA* or the nonaketide synthase *aptA* into *A. oryzae* OP12 3Δ (Fig. 6). Expression of *aptA* and *aptA*/*stpC* resulted in the production of only **11**, with no apparent differences between the two mutants, whereas formation of **1** was not observed (Fig. 6). In contrast, expression of *adaA* and *adaA*/*stpC* resulted in the production of the same compounds observed for *stpA* and *stpAC*, respectively, with *adaA*/*stpC* producing **1** (Fig. 6, Figure S6).

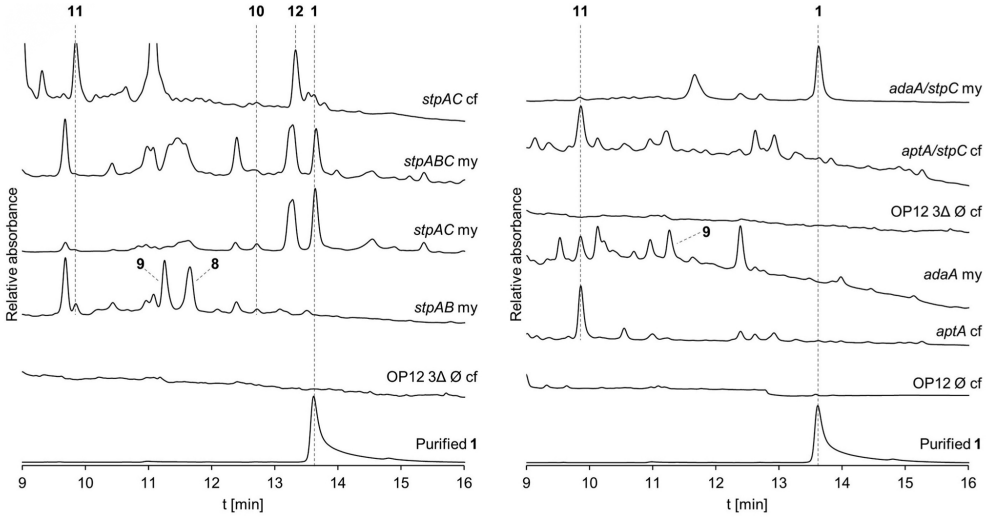

Fig. 6 Heterologous coexpression of *stpAC* suffices to reconstitute saintopin (**1**) biosynthesis in *A. oryzae*. Chromatograms (250 nm) of mutant mycelia and culture filtrate extracts and purified **1**. my, mycelia extract. cf, culture filtrate extract

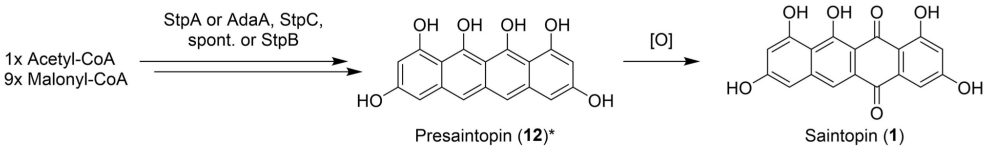

Fig. 7 Proposed biosynthesis of saintopin (**1**). * Structure of **12** is proposed

This implies the necessity of a decaketide precursor for the production of **1**. Based on these findings we propose a biosynthetic scheme for the production of **1** (Fig. 7).

Discussion

In the present study, we successfully linked the purple color of *P. marquandii* conidia to the production of the naphthacenedione polyketide pigment saintopin (**1**). While most fungi produce pigmented conidia, the pigments differ between species. Many fungi produce melanins for conidial pigmentation, oligo-/polymers derived through oxidative polymerization from various monomeric precursors, such as dihydroxynaphthalene (DHN), L-dioxyphenylalanine (DOPA) or the more recently described aspulvinone E [29, 30]. Amongst others, melanins have been associated with photoprotection, they have shown antioxidant properties, they contribute to temperature- and osmo-tolerance and they are vital for cell development and virulence in pathogenic fungi [29, 31, 32]. Irrespective of the type of pigment produced, conidial pigmentation plays a vital role in protection against UV-induced DNA damage [33]. It was previously shown for another *Paecilomyces* species that production of the conidial pigment YWA1 increases tolerance towards UV irradiation [34]. Furthermore, bis-naphthopyrone pigments produced by *Fusarium* species display non-toxic antifeedant activity against fungivorous animal predators [35]. While the exact biological and ecological function of **1** in *P. marquandii* remains unclear, it likely plays a similar protective role described for other conidial pigments.

To elucidate the biosynthesis of saintopin (**1**), we first performed heterologous expression of nearly all nrPKS encoded in the genome of *P. marquandii* in the heterologous host *A. oryzae* OP12 [27, 28]. Whereas five of six nrPKS produced different polyketide products of varying chain lengths (**2**–**11**), expression of PmPKS5 did not lead to the production of a polyketide product. This might be due to the involvement in a hybrid/cooperative biosynthetic pathway, where the nrPKS is primed by e.g., hrPKS- or FAS-derived precursors [11, 36]. Production of polyketides of different chain lengths in

varying abundancies from a single nrPKS, as is the case for PmPKS4 and PmPKS6, is frequently observed [37–39]. The reduced polyketides **5**, **6** and **9** are shunt products that likely derive from the action of an endogenous, promiscuous reductive enzyme of *A. oryzae* such as e.g., AoiI, involved in the reduction of **4** to **5** in the *A. oryzae* 8-methyldiaporthin biosynthetic pathway [40]. Moreover, compounds **8**–**10** are proposedly quinones that derived from their respective non-quinone precursors through spontaneous oxidation in the presence of oxygen, similar to the proposed conversion of **12** to **1**. Spontaneous quinone formation has previously been observed for other aromatic polyketides such as e.g., endocrocin [16] and flaviolin [41].

Heterologous expression of PmPKS2, PmPKS3, PmPKS4 and PmPKS6 yielded large amounts of their respective polyketide products, more than sufficient for isolation and structure elucidation. In contrast, heterologous expression of *stpA* only led to production of trace amounts of the nona-/decaketides **8**–**11**. Since clade V nrPKS do not harbor an intrinsic offloading domain, product release from StpA likely only occurs *via* slow spontaneous hydrolysis or α-pyrone formation in the absence of a trans-acting offloading enzyme. The low yield of **8**–**11** hindered the production of sufficient amounts for isolation and structure elucidation. While the structures of **8**–**10** were proposed based on previously reported products produced by AdaA in vitro [20], the structure of **11** remains ambiguous. Nevertheless, **11** is assumed to be a nonaketide, as it was also produced by OP12 expressing *aptA*, which reportedly is a nonaketide synthase [20]. As the compounds produced by OP12_*stpA* are the only polyketides sufficiently similar in size to **1**, we deleted *stpA* in the native producer. This resulted in the loss of conidial pigmentation and abolished the production of **1**, which unequivocally linked the biosynthesis of saintopin (**1**) to the nrPKS *stpA*.

As *stpA* does not suffice for **1** production, we aimed to investigate the accessory genes required for biosynthesis. Homologs of the MβL *adaB*, FMO *adaC* and *O*-methyltransferase *adaD* involved in TAN-1612 biosynthesis [20] were found located elsewhere in the genome of *P. marquandii* instead of clustered alongside *stpA*. While encountered only infrequently in fungi, there are reports on BGCs that are split across multiple loci in the genome, such as e.g., the austinol biosynthetic genes in *Aspergillus nidulans* [42]. As no correlation between **1** production and expression of *stpABCD* and any of the genes encoded in the vicinity of *stpA* was observed in sqRT-PCR analysis, *stpBC* were coexpressed alongside *stpA* in an effort to identify biosynthetic intermediates. Unexpectedly, coexpression of *stpAC* did already suffice to reconstitute the production of **1** in *A. oryzae*, whereas additional coexpression of *stpB* did not result in any apparent differences. Apart from **1**, OP12_*stpAC* and OP12_*stpABC* produced various, presumedly shunt products (**13**–**18**) that might arise from **12** or **1** *via* the action of endogenous *A. oryzae* enzymes, which might serve as a strategy to cope with the reported toxicity of **1** [25]. The biosynthesis of **1** is proposed to proceed *via* the non-quinone intermediate **12** that spontaneously undergoes quinone-oxidation in the presence of oxygen.

To gain first insights into the rationale underlying the formation of **1**, the nona- and decaketide synthases *aptA* and *adaA* were heterologously expressed in *A. oryzae* OP12 with and without additional coexpression of *stpC*. Expression of *aptA* and *aptA/stpC* resulted in the production of only **11**, which was contrary to our expectations, as AptA was previously reported to produce **10** in vitro [20]. Heterologous expression of *adaA* resulted in the production of the same nona- and decaketide products that were also produced by *stpA*, and coexpression of *adaA/stpC* similarly resulted in the production of the same compounds produced by *stpAC* and *stpABC*, including **1**. This implies the formation of **1** to proceed *via* a decaketide (C_{20}) precursor, although the structure of **1** contrary suggests a nonaketide (C_{18}) origin. Therefore, the decaketide precursor seems to be deactetylated during the StpC-mediated formation of **1**.

Intriguingly, **1** does not contain a methyl- (e.g., atrochrysone carboxylic acid), acetyl- (e.g., ATHN) or longer chain poly-β-ketone (e.g., YWA1) side chain usually present in non-reduced polyketide scaffolds that arises from the mechanism of terminal cyclization. The only other fungal-derived polyketide sharing this structural feature is the melanin precursor THN. It is usually synthesized from the precursors ATHN [43] or YWA1 [44–46] through enzymatic polyketide shortening (deacetylation or deacetoacetylation) by hydrolases such as Ayg1p [45] (Fig. 8B). However one enzyme, ClPKS1, was described to synthesize THN directly. It was previously assumed that THN is synthesized by ClPKS1 from solely malonyl-CoA [41], facilitating the late decarboxylation of the starter malonate-unit and therefore elimination of the sidechain during second ring cyclization, this hypothesis was however later proven incorrect. Even though ClPKS1 is indeed a true THN synthase, it was shown that ATHN emerges as a bound intermediate, which however is deacetylated by ClPKS1 unique TE domain during Dieckmann cyclization [47] (Fig. 8C). While it was recently shown that basidiomycete nrPKS are capable of synthesizing polyketides solely from malonyl-CoA [12], no enzyme has been reported to date that catalyzes decarboxylation-facilitated terminal cyclization as initially proposed for ClPKS1 [41]. Recently, another intriguing polyketide shortening mechanism has been reported to occur in dichlodiaporthin biosynthesis [50]. The flavin-dependent halogenase (FDH) domain

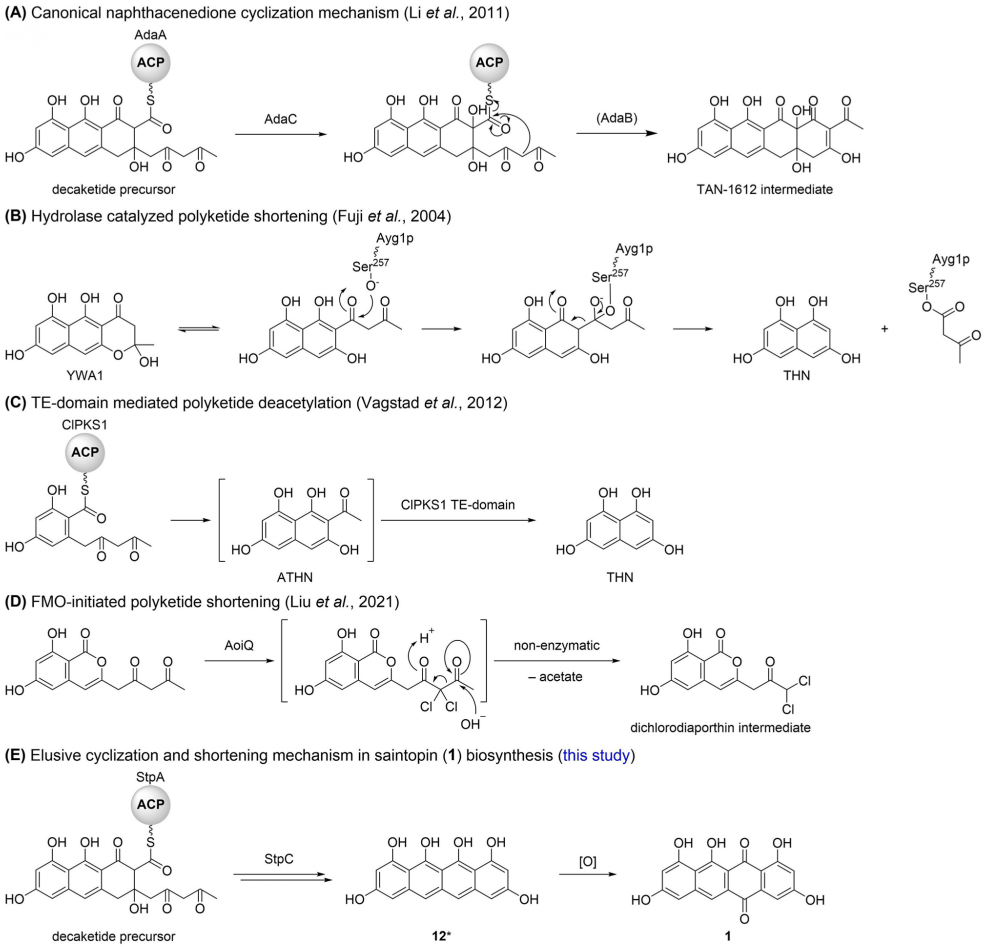

Fig. 8 Cyclization and polyketide shortening mechanisms in polyketide biosynthetic pathways [20, 45, 47, 50]

of the bifunctional enzyme AoiQ *gem*-dichlorinates the 1,3-diketone moiety of a polyketide substrate, resulting in deacetylation facilitated by spontaneous nucleophilic addition of water at the terminal carbonyl moiety and subsequent cleavage [50] (Fig. 8D).

The fungal naphthacenediones reported so far, namely TAN-1612, viridicatumtoxin [21], hypomycetin [48] and anthrotainin [49], all share the same basic scaffold implying a common biosynthetic rationale. While viridicatumtoxin biosynthesis has only been proposed based on the deletion of a few biosynthetic enzymes [21], TAN-1612 biosynthesis has been investigated in detail [20], offering insights into the canonical mechanism for fungal naphthacenedione formation. The nrPKS involved in TAN-1612 biosynthesis, AdaA, belongs to clade V-II nrPKSs. Therefore, AdaA lacks a terminal offloading domain and is dependent on the trans-acting MβL AdaB for product release [16]. First and second ring cyclization in TAN-1612 biosynthesis are catalyzed *via* PT domain mediated aldol condensation whereas the third ring cyclization occurs *via* spontaneous aldol cycloaddition, resulting in the conservation of a hydroxyl moiety at position C15. The cyclization of the fourth ring is in turn catalyzed by the MβL AdaB but requires C2-hydroxylation introduced by the FMO AdaC (Fig. 8A). The other related fungal naphthacenediones also share this structural

feature of C2- and C15- hydroxylation, whereas **1** lacks both hydroxylations. While AdaB is dispensable for TAN-1612 formation, as fourth ring cyclization can also occur spontaneously after C2-hydroxylation, coexpression did substantially improve productivity in the heterologous host *S. cerevisiae* [20]. In contrast, no apparent differences in productivity were observed between *stpABC* and *stpAC*. Although cross-complementation of AdaA with AptB was reported to be unsuccessful [20], it cannot be ruled out that StpA could potentially be cross-complemented by the *A. oryzae* intrinsic (solely encoded) MβL DiaB (AO090701000529), canonically involved in dichlorodiaporthin biosynthesis [50]. Alternatively, StpB might be entirely dispensable for the production of **1**.

The two related fungal decaketides fumicycline and neosatoricin are proposed to be released prior to FMO-catalyzed C2-hydroxylation [22, 23], resulting in the formation of non-naphthacenedione products, which suggests a diverging interaction between the FMOs and nrPKSs (on-line vs. post-synthesis modification). As saintopin (**1**) lacks C2-hydroxylation but formation of **1** is dependent on StpC, the function of StpC might be entirely different from other reported naphthacenedione FMOs. StpC seems to somehow facilitate both polyketide shortening and cyclization of the fourth ring in **1** biosynthesis. Although compound **8** is only produced in traces when only *stpA* is expressed, it cannot yet be ruled out, that oxidative transformation of **8** to **1** (or the non-quinone precursor of **8** to **12**) occurs post-synthesis. While heterologous reconstitution of saintopin (**1**) biosynthesis provides first evidence for a unique biosynthetic pathway (Fig. 8E), further research will be necessary in the future to elucidate the function of StpC and the elusive mechanism underlying saintopin (**1**) formation.

In summary, we identified the conidial pigment produced by *P. marquandii* as saintopin (**1**) *via* purification and structure elucidation. In an effort to unravel the biosynthesis of the unusual naphthacenedione **1**, we performed genome sequencing, genome mining and heterologous expression of nrPKS genes in *A. oryzae*, identifying a candidate nona-/decaketide nrPKS, *stpA*, involved in the biosynthesis of **1**. Establishing the transformation of *P. marquandii* enabled the deletion of *stpA* in the native producer, which led to the loss of conidial pigmentation and the abolishment of the production of **1**, unequivocally linking the biosynthesis of **1** to *stpA*. As no correlation was found between gene expression and the production of **1**, we reverted to heterologous coexpression of candidate accessory genes in *A. oryzae* to identify additional genes involved in the biosynthesis of **1**. Intriguingly, the coexpression of solely *stpA* and the FMO *stpC* led to the production of **1** in the heterologous host. As coexpression of the decaketide synthase *adaA*, but not the nonaketide synthase *aptA*, alongside *stpC* also led to the production of **1**, formation of **1** is proposed to proceed *via* a decaketide intermediate that is subsequently shortened. Although StpC seems to facilitate polyketide shortening and fourth ring cyclization in the biosynthesis of **1**, the underlying mechanism remains elusive as of yet.

Methods

Strains & cultivation

Paecilomyces marquandii strain IBWF 003–21 was isolated from a contaminated agar plate in Mainz, Germany in 2020 and is deposited at the Institut für Biotechnologie und Wirkstoff-Forschung gGmbH (IBWF, Mainz, Germany). *P. marquandii* was routinely cultivated on solid YMG (2% malt extract, 1% glucose, 0.4% yeast extract) agar plates at room temperature. *Aspergillus oryzae* OP12 *pyrG*$^{-}$ and OP12 3Δ were routinely cultivated on GG10 (1% glucose, 10 mM glutamine, 0.152% KH_2PO_4, 0.052% KCl, 0.052% $MgSO_4 \cdot 7\ H_2O$, 1 mL/L Hutners trace elements) supplemented with 10 mM uridine (OP12 *pyrG*$^{-}$) or 10 mM uridine, 0.0001% PABA and 0.05% arginine (OP12 3Δ) at 30 °C. Spore suspensions of fungi were prepared in PBS supplemented with 0.01% Tween 80 and filtered through miracloth. *E. coli* strain NEB DH5α was used for plasmid propagation. All mutant strains used in this study are listed in Table S1.

Bioinformatic analysis

The genomic DNA was sequenced using paired-end Illumina HiSeq 2500 with 2×150 bp reads. Initial quality assessment of the raw sequencing data was performed using FastQC (version 0.11.9) to ensure high data integrity. Following quality assessment, the reads were filtered for quality, and the assembly was carried out using SPAdes (version: 3.15.2). The filtered reads were assembled using SPAdes, with the following command:

```
/opt/anaconda3/envs/de_novo_assembly/bin/spades.py -1 BGC/1.fastq.gz -2 BGC/2.fastq.gz -o BGC/spades_kmers_set_careful_assembly1 -t 4 -k 77,99,121 --careful --only-assembler.
```

The SPAdes assembler was used with k-mer sizes of 77, 99, and 121, along with the *--careful* flag to minimize mismatches. The quality of the assembled contigs was evaluated using QUAST (version: 5.0.2), and the assembly with the highest N50 and largest contigs was selected for further analyses.

For gene prediction, the best assembly was processed using pretrained fungal models in Augustus, as implemented in Blast2GO. Functional annotation was performed by executing BLAST searches against the following databases: NR (NCBI non-redundant protein sequences), InterPro and Swiss-Prot.

IGV (version: 2.14.0) was used to visualize the assembled genome. The resulting GFF file, along with the scaffolds from the best assembly, was then utilized in antiSMASH (version: 7.1.0) analysis by leveraging specific profile hidden Markov models to identify fungal biosynthetic gene clusters (BGCs) encoded within the genome. The results were further compared and supplemented by FunBGCeX (Fungal Biosynthetic Gene Cluster eXtractor), a genome mining tool designed for fungal natural product discovery. FunBGCeX detects biosynthetic proteins by referencing a manually curated database of fungal natural product biosynthetic gene clusters (FunBGCs). Identified secondary metabolite (SM) BGCs were further investigated and characterized through manual curation of gene annotations using NCBI BLASTp analysis.

Plasmid construction

Genomic DNA of fungi was prepared using the GeneJET Plant Genomic DNA Purification Kit (Thermo Fisher). PmPKS1, PmPKS2, *stpA*, PmPKS4, PmPKS5, PmPKS6, *stpB*, *stpC*, *aptA* and *adaA* were amplified from genomic DNA of *P. marquandii* IBWF 003–21, *Aspergillus nidulans* FGSC A4 or *Aspergillus niger* FGSC A1144 using the Q5-HotStart DNA-Polymerase (NEB) and assembled into *Nco*I restricted plasmids his_SM-Xpress_URA [27], SMX-Xpress_Ura [27], SM-Xpress_pabA [51] or SM-Xpress_argB(mut) [28] using the NEBuilder® HiFi DNA Assembly 2 × Master Mix (NEB). For deletion of *stpA*, flanking regions (795 bp and 856 bp, respectively) were amplified from genomic DNA, the G418 resistance cassette was amplified from pC-G418-YR (Addgene plasmid No. 61767) [52] and assembled into *Sma*I-restricted pUC19 to make pKO_*stpA*_G418. The KO-cassette was retrieved from the plasmid using *Not*I prior to transformation. Expression plasmids were linearized prior to transformation using appropriate restriction enzymes. All oligonucleotides used for cloning are listed in Table S2.

sqRT-PCR

RNA of *P. marquandii* was isolated using the RNeasy Plant Mini Kit (Qiagen). DNA was removed from RNA samples using DNaseI, RNAse-free (Thermo Fisher) prior to reverse transcription into cDNA using the RevertAid First Strand cDNA Synthesis Kit (Thermo Fisher). DreamTaq HotStart MM (Thermo Fisher) was used for all sqRT-PCRs according to the manufacturer's instructions. cDNA concentrations were normalized to the signal intensity of the bTub amplicon. All sqRT-PCRs were carried out using the same reaction conditions. All oligonucleotides used for sqRT-PCR are listed in Table S3.

Fungal transformation

Protoplast transformation of *A. oryzae* has been carried out as previously described [27]. *P. marquandii* was transformed analogously however took longer for protoplast formation (~6 h). Transformed *P. marquandii* protoplasts were regenerated on GG10S1.2 (GG10 supplemented with 1.2 M sorbitol) supplemented with 1000 µg/mL geneticin (G418) at room temperature for 10–14 days until single transformant colonies appeared.

Fermentation, metabolite extraction, analysis & purification

After fermentation (see below), cultures were separated into mycelia and culture filtrate through vacuum filtration or filtering over miracloth. Culture filtrates were acidified with a few drops of 6 N HCl (improved solvent solubility of most aromatic polyketides), extracted with an equal amount of ethyl acetate and extracts were dried under vacuum at 45 °C. Mycelia and conidia were extracted with methanol: acetone (1:1) shaking at 120 rpm for one hour before filtration and drying under vacuum at 45 °C. Extracts were redissolved in MeOH and applied to HPLC-MS analysis using a LiChrospher 100 RP-18 (125 mm × 2 mm, 4 µm, Merck KGaA).

For secondary metabolite screening of OP12 mutants, spores were routinely inoculated into 50 mL 2% starch medium (2% soluble starch, 20 mM glutamine, 0.152% KH_2PO_4, 0.052% KCl, 0.052% $MgSO_4 \cdot 7H_2O$, 1 mL/L Hutners trace elements) and incubated shaking at 150 rpm and 30 °C for 2 days.

For isolation of RNA, *P. marquandii* was cultured in 500 mL of YMG, PDB (Difco) and CZ media (3% Sucrose, 0.3% $NaNO_3$, 0.1% K_2PO_4, 0.05% $MgSO_4 \cdot 7\ H_2O$, 0.05% KCl, 0.01% $Fe_2(SO_4)_3$) shaking at 120 rpm at room temperature for 96 h. Samples of each culture were taken after 48 h, 72 h and 96 h, respectively, the mycelia was washed with H_2O and snap-frozen in LN_2. The mycelia was lyophilized and subsequently used for RNA extraction and metabolite extraction.

For comparison of metabolite production, *P. marquandii* WT and *ΔstpA* strain were cultured in 500 mL of YMG media for 4 days shaking at 120 rpm at room temperature.

For the isolation of **1**, *P. marquandii* was cultivated in 5 × 2 L YMG-medium shaking at 120 rpm for 6 days at room temperature. The mycelia was lyophilized and extracted with MeOH: acetone (1:1) overnight twice. The extract was dried *in vacuo* and pre-fractioned *via* SPE on a Bond Elut C18 column (Agilent) before subsequent purification using preparative HPLC.

For the isolation of **2** and **7**, the mycelia of an overnight 250 mL YEPD preculture of OP12 PmPKS6 was transferred into 2.5 L of 2% starch media and incubated shaking at 120 rpm at 28 °C for 3 days. For the isolation of

Table 2 Preparative HPLC eluent composition & compound yields

Compound	% ACN	Yield
Saintopin (**1**)	48	5.8 mg
Orsellinic acid (**2**)	37	42 mg
nor-Toralactone (**3**)	30	7.2 mg
6,8-dihydroxy-3-(2-oxopropyl)-1*H*-2-benzopyran-1-one (**4**)	28	104.7 mg
Orthosporin (**5**)	28	41.8 mg
Citreoisocoumarin (**6**)	28	1.8 mg
Saccharonol A (**7**)	37	71.1 mg

compound **3** the mycelia of overnight 250 mL YEPD precultures of OP12 PmPKS2 was transferred into 2 × 2.5 L of 2% starch media and incubated shaking at 120 rpm at 28 °C for 3 days. For the isolation of compounds **4**–**6** an overnight 250 mL YEPD preculture of OP12 PmPKS4 was inoculated into 2.5 L of 2% starch media and incubated shaking at 120 rpm at 28 °C for 3 days. The culture filtrates were extracted with an equal amount of ethyl acetate and the crude extracts applied to preparative HPLC.

Compounds were purified by preparative HPLC on a Sunfire C18 column (100Å, 5 µm, 19 mm × 250 mm, Waters GmbH) running isocratic flows of ACN and 0.1% formic acid in H_2O at 17 mL/min flow (eluent composition and yields are listed in Table 2). Crude extracts applied to preparative HPLC were dissolved in DMSO.

Analytical chemistry and structure elucidation

Thin layer chromatography

Analytical thin-layer chromatography (TLC), 0.25 mm silica plates (60 F254) from Merck were used, and the detection was reached by fluorescence quenching under UV light (λ = 254 nm) or by staining with potassium permanganate reagent (solution of $KMnO_4$ (3 g), K_2CO_3 (20 g), 5% NaOH (5 mL), and H_2O (300 mL)) followed by heating to 400 °C.

NMR spectra

Measured NMR spectra were, unless otherwise mentioned, recorded at 296 K on a 600 MHz Bruker Avance-III 600 spectrometer with a 5 mm TCI cryoprobe. After prior referencing to the residual solvent signal ($CDCl_3$: 7.26 ppm & 77.16 ppm; DMSO-d_6: 2.50 ppm & 39.52 ppm; DMF-d_7: 2.75 ppm & 29.76 ppm for ^{1}H NMR and ^{13}C NMR, respectively), all chemical shifts (δ) are reported relative to residual solvent [53]. Coupling constants were reported in Hz and the signal multiplicities were abbreviated as follows: s (singlet), d (doublet), t (triplet), q (quartet), qd (quartet of doublet), m (multiplet).

Infrared spectra

Infrared spectroscopy was performed on a Bruker Tensor 27 FTIR spectrometer including a diamond ATR unit and are reported in terms of absorption frequency $\bar{\nu}$ [cm^{-1}].

Mass spectra

HRMS was conducted on an Agilent G6545A Q-ToF with ESI, APCI or APPI source coupled with an Agilent 1260 Infinity II HPLC system. If not described otherwise, spectra were recorded using positive ionization mode.

Optical rotations

Optical rotation measurements were accomplished with a Perkin-Elmer 241MC polarimeter at λ = 589 nm. A solvent-filled cuvette was used for instrument calibration [54].

Supplementary Information

The online version contains supplementary material available at https://doi.org/10.1186/s40694-025-00199-4.

Supplementary Material 1

Acknowledgements

Aspergillus oryzae strain OP12 *pyrG*$^-$ and plasmids SM-Xpress_URA, his_SM-Xpress_URA and SM-Xpress_pabA were kindly provided by Matthias Brock (University of Nottingham, UK). Part of the graphical abstract figure was made with http://www.BioRender.com.

Author contributions

C.W. conceived the study. C.W. designed the experiments. C.W. and S.G. conducted the biological experiments. A.Y. performed bioinformatic analysis. C.W. performed metabolite purification. R.W. and K.S. performed structure elucidation of purified metabolites. A.S., T.O. and E.T. supervised the project. All authors reviewed and interpreted the obtained data and results. C.W. wrote the manuscript. All authors contributed to editing and revising of the manuscript, as well as read and approved the final version of the manuscript.

Funding

Open Access funding enabled and organized by Projekt DEAL.
This work was supported by the Rhineland Palatinate Center for Natural Products Research.

Data availability

No datasets were generated or analysed during the current study.

Declarations

Ethics approval and consent to participate

Not applicable.

Consent for publication

All authors give their consent for publication.

Competing interests

The authors declare no competing interests.

Author details

[1]Institute of Molecular Physiology, Johannes Gutenberg-University, Hanns-Dieter-Hüsch Weg 17, D-55128 Mainz, Germany
[2]Institut für Biotechnologie und Wirkstoff-Forschung gGmbH, Mainz, Hanns-Dieter-Hüsch Weg 17, D-55128 Mainz, Germany
[3]Department of Chemistry, Johannes Gutenberg-University, Duesbergweg 10–14, D-55128 Mainz, Germany

Received: 23 January 2025 / Accepted: 28 April 2025
Published online: 05 June 2025

References

1. Alberts AW, Chen J, Kuron G, Hunt V, Huff J, Hoffman C, et al. Mevinolin: a highly potent competitive inhibitor of hydroxymethylglutaryl-coenzyme A reductase and a cholesterol-lowering agent. Proc Natl Acad Sci U S A. 1980;77:3957–61. https://doi.org/10.1073/pnas.77.7.3957.
2. Anke T, Oberwinkler F, Steglich W, Schramm G. The strobilurins–new antifungal antibiotics from the basidiomycete Strobilurus Tenacellus. J Antibiot (Tokyo). 1977;30:806–10. https://doi.org/10.7164/antibiotics.30.806.
3. Sauter H, Steglich W, Anke T, Strobilurins. Evolution of a new class of active substances. Angew Chem Int Ed. 1999;38:1328–49. https://doi.org/10.1002/(SICI)1521-3773(19990517)38:10%3C1328::AID-ANIE1328%3E3.0.CO;2-1.
4. Oxford AE, Raistrick H, Simonart P. Studies in the biochemistry of microorganisms: Griseofulvin, C(17)H(17)O(6)Cl, a metabolic product of Penicillium griseo-fulvum Dierckx. Biochem J. 1939;33:240–8. https://doi.org/10.1042/bj0330240.
5. Gupta AK, Foley KA, Versteeg SG. New antifungal agents and new formulations against dermatophytes. Mycopathologia. 2017;182:127–41. https://doi.org/10.1007/s11046-016-0045-0.
6. Hertweck C. The biosynthetic logic of polyketide diversity. Angew Chem Int Ed. 2009;48:4688–716. https://doi.org/10.1002/anie.200806121.
7. Cox RJ, Simpson TJ. Fungal type I polyketide synthases. Methods Enzymol. 2009;459:49–78. https://doi.org/10.1016/S0076-6879(09)04603-5.
8. Chooi Y-H, Tang Y. Navigating the fungal polyketide chemical space: from genes to molecules. J Org Chem. 2012;77:9933–53. https://doi.org/10.1021/jo301592k.
9. Crawford JM, Dancy BCR, Hill EA, Udwary DW, Townsend CA. Identification of a starter unit acyl-carrier protein transacylase domain in an iterative type I polyketide synthase. Proc Natl Acad Sci U S A. 2006;103:16728–33. https://doi.org/10.1073/pnas.0604112103.
10. Crawford JM, Thomas PM, Scheerer JR, Vagstad AL, Kelleher NL, Townsend CA. Deconstruction of iterative multidomain polyketide synthase function. Science. 2008;320:243–6. https://doi.org/10.1126/science.1154711.
11. Chiang Y-M, Szewczyk E, Davidson AD, Keller N, Oakley BR, Wang CCC. A gene cluster containing two fungal polyketide synthases encodes the biosynthetic pathway for a polyketide, Asperfuranone, in Aspergillus Nidulans. J Am Chem Soc. 2009;131:2965–70. https://doi.org/10.1021/ja8088185.
12. Löhr NA, Rakhmanov M, Wurlitzer JM, Lackner G, Gressler M, Hoffmeister D. Basidiomycete non-reducing polyketide synthases function independently of SAT domains. Fungal Biol Biotechnol. 2023;10:17. https://doi.org/10.1186/s40694-023-00164-z.
13. Liu L, Zhang Z, Shao C-L, Wang J-L, Bai H, Wang C-Y. Bioinformatical analysis of the sequences, structures and functions of fungal polyketide synthase product template domains. Sci Rep. 2015;5:10463. https://doi.org/10.1038/srep10463.
14. Li Y, Image II, Xu W, Image I, Tang Y. Classification, prediction, and verification of the regioselectivity of fungal polyketide synthase product template domains. J Biol Chem. 2010;285:22764–73. https://doi.org/10.1074/jbc.M110.128504.
15. Throckmorton K, Wiemann P, Keller NP. Evolution of chemical diversity in a group of Non-Reduced polyketide gene clusters: using phylogenetics to inform the search for novel fungal natural products. Toxins (Basel). 2015;7:3572–607. https://doi.org/10.3390/toxins7093572.
16. Awakawa T, Yokota K, Funa N, Doi F, Mori N, Watanabe H, Horinouchi S. Physically discrete beta-lactamase-type thioesterase catalyzes product release in Atrochrysone synthesis by iterative type I polyketide synthase. Chem Biol. 2009;16:613–23. https://doi.org/10.1016/j.chembiol.2009.04.004.
17. Saha D, Fetzner R, Burkhardt B, Podlech J, Metzler M, Dang H, et al. Identification of a polyketide synthase required for alternariol (AOH) and alternariol-9-methyl ether (AME) formation in Alternaria alternata. PLoS ONE. 2012;7:e40564. https://doi.org/10.1371/journal.pone.0040564.
18. Cacho RA, Chooi Y-H, Zhou H, Tang Y. Complexity generation in fungal polyketide biosynthesis: a spirocycle-forming P450 in the concise pathway to the antifungal drug Griseofulvin. ACS Chem Biol. 2013;8:2322–30. https://doi.org/10.1021/cb400541z.
19. Szewczyk E, Chiang Y-M, Oakley CE, Davidson AD, Wang CCC, Oakley BR. Identification and characterization of the asperthecin gene cluster of Aspergillus Nidulans. Appl Environ Microbiol. 2008;74:7607–12. https://doi.org/10.1128/AEM.01743-08.
20. Li Y, Chooi Y-H, Sheng Y, Valentine JS, Tang Y. Comparative characterization of fungal anthracenone and Naphthacenedione biosynthetic pathways reveals an α-hydroxylation-dependent Claisen-like cyclization catalyzed by a Dimanganese thioesterase. J Am Chem Soc. 2011;133:15773–85. https://doi.org/10.1021/ja206906d.
21. Chooi Y-H, Cacho R, Tang Y. Identification of the viridicatumtoxin and Griseofulvin gene clusters from Penicillium aethiopicum. Chem Biol. 2010;17:483–94. https://doi.org/10.1016/j.chembiol.2010.03.015.
22. König CC, Scherlach K, Schroeckh V, Horn F, Nietzsche S, Brakhage AA, Hertweck C. Bacterium induces cryptic meroterpenoid pathway in the pathogenic fungus Aspergillus fumigatus. ChemBioChem. 2013;14:938–42. https://doi.org/10.1002/cbic.201300070.
23. Chooi Y-H, Wang P, Fang J, Li Y, Wu K, Wang P, Tang Y. Discovery and characterization of a group of fungal polycyclic polyketide prenyltransferases. J Am Chem Soc. 2012;134:9428–37. https://doi.org/10.1021/ja3028636.
24. Li H, Shu S, Kalaitzis JA, Shang Z, Vuong D, Crombie A, et al. Genome mining of Aspergillus Hancockii unearths cryptic polyketide hancockinone A featuring a prenylated 6/6/6/5 carbocyclic skeleton. Org Lett. 2021;23:8789–93. https://doi.org/10.1021/acs.orglett.1c03283.
25. Yamashita Y, Saitoh Y, Ando K, Takahashi K, Ohno H, Nakano H. Saintopin, a new antitumor antibiotic with topoisomerase II dependent DNA cleavage activity, from Paecilomyces. J Antibiot (Tokyo). 1990;43:1344–6. https://doi.org/10.7164/antibiotics.43.1344.
26. van der Zanden SY, Qiao X, Neefjes J. New insights into the activities and toxicities of the old anticancer drug doxorubicin. FEBS J. 2021;288:6095–111. https://doi.org/10.1111/febs.15583.
27. Geib E, Baldeweg F, Doerfer M, Nett M, Brock M. Cross-Chemistry leads to product diversity from atromentin synthetases in aspergilli from section Nigri. Cell Chem Biol. 2019;26:223–e2346. https://doi.org/10.1016/j.chembiol.2018.10.021.
28. Wieder C, Künzer M, Wiechert R, Seipp K, Andresen K, Stark P, et al. Biosynthesis of the antifungal Polyhydroxy-Polyketide acrophialocinol. Org Lett. 2025. https://doi.org/10.1021/acs.orglett.4c04656.
29. Langfelder K, Streibel M, Jahn B, Haase G, Brakhage AA. Biosynthesis of fungal melanins and their importance for human pathogenic fungi. Fungal Genet Biol. 2003;38:143–58. https://doi.org/10.1016/S1087-1845(02)00526-1.
30. Geib E, Gressler M, Viediernikova I, Hillmann F, Jacobsen ID, Nietzsche S, et al. A Non-canonical melanin biosynthesis pathway protects Aspergillus terreus conidia from environmental stress. Cell Chem Biol. 2016;23:587–97. https://doi.org/10.1016/j.chembiol.2016.03.014.
31. Jacobson ES. Pathogenic roles for fungal melanins. Clin Microbiol Rev. 2000;13:708–17. https://doi.org/10.1128/cmr.13.4.708-717.2000.
32. Cordero RJ, Casadevall A. Functions of fungal melanin beyond virulence. Fungal Biol Rev. 2017;31:99–112. https://doi.org/10.1016/j.fbr.2016.12.003.
33. Braga GUL, Rangel DEN, Fernandes ÉKK, Flint SD, Roberts DW. Molecular and physiological effects of environmental UV radiation on fungal conidia. Curr Genet. 2015;61:405–25. https://doi.org/10.1007/s00294-015-0483-0.
34. Lim S, Bijlani S, Blachowicz A, Chiang Y-M, Lee M-S, Torok T, et al. Identification of the pigment and its role in UV resistance in Paecilomyces variotii, a Chernobyl isolate, using genetic manipulation strategies. Fungal Genet Biol. 2021;152:103567. https://doi.org/10.1016/j.fgb.2021.103567.
35. Xu Y, Vinas M, Alsarrag A, Su L, Pfohl K, Rohlfs M, et al. Bis-naphthopyrone pigments protect filamentous ascomycetes from a wide range of predators. Nat Commun. 2019;10:3579. https://doi.org/10.1038/s41467-019-11377-5.
36. Watanabe CMH, Townsend CA. Initial characterization of a type I fatty acid synthase and polyketide synthase multienzyme complex NorS in the biosynthesis of aflatoxin B(1). Chem Biol. 2002;9:981–8. https://doi.org/10.1016/S1074-5521(02)00213-2.
37. Löhr NA, Eisen F, Thiele W, Platz L, Motter J, Hüttel W, et al. Unprecedented mushroom polyketide synthases produce the universal anthraquinone precursor. Angew Chem Int Ed Engl. 2022;61:e202116142. https://doi.org/10.1002/anie.202116142.
38. Watanabe A, Ebizuka Y. Unprecedented mechanism of chain length determination in fungal aromatic polyketide synthases. Chem Biol. 2004;11:1101–6. https://doi.org/10.1016/j.chembiol.2004.05.015.
39. Zaehle C, Gressler M, Shelest E, Geib E, Hertweck C, Brock M. Terrein biosynthesis in Aspergillus terreus and its impact on phytotoxicity. Chem Biol. 2014;21:719–31. https://doi.org/10.1016/j.chembiol.2014.03.010.
40. Nakazawa T, Ishiuchi K, Praseuth A, Noguchi H, Hotta K, Watanabe K. Overexpressing transcriptional regulator in Aspergillus oryzae activates a

silent biosynthetic pathway to produce a novel polyketide. ChemBioChem. 2012;13:855–61. https://doi.org/10.1002/cbic.201200107.
41. Fujii I, Mori Y, Watanabe A, Kubo Y, Tsuji G, Ebizuka Y. Enzymatic synthesis of 1,3,6,8-tetrahydroxynaphthalene solely from malonyl coenzyme A by a fungal iterative type I polyketide synthase PKS1. Biochemistry. 2000;39:8853–8. https://doi.org/10.1021/bi000644j.
42. Lo H-C, Entwistle R, Guo C-J, Ahuja M, Szewczyk E, Hung J-H, et al. Two separate gene clusters encode the biosynthetic pathway for the meroterpenoids Austinol and dehydroaustinol in Aspergillus Nidulans. J Am Chem Soc. 2012;134:4709–20. https://doi.org/10.1021/ja209809t.
43. Wheeler MH, Abramczyk D, Puckhaber LS, Naruse M, Ebizuka Y, Fujii I, Szaniszlo PJ. New biosynthetic step in the melanin pathway of Wangiella (Exophiala) dermatitidis: evidence for 2-acetyl-1,3,6,8-Tetrahydroxynaphthalene as a novel precursor. Eukaryot Cell. 2008;7:1699–711. https://doi.org/10.1128/EC.00179-08.
44. Tsai HF, Fujii I, Watanabe A, Wheeler MH, Chang YC, Yasuoka Y, et al. Pentaketide melanin biosynthesis in Aspergillus fumigatus requires chain-length shortening of a heptaketide precursor. J Biol Chem. 2001;276:29292–8. https://doi.org/10.1074/jbc.M101998200.
45. Fujii I, Yasuoka Y, Tsai H-F, Chang YC, Kwon-Chung KJ, Ebizuka Y. Hydrolytic polyketide shortening by ayg1p, a novel enzyme involved in fungal melanin biosynthesis. J Biol Chem. 2004;279:44613–20. https://doi.org/10.1074/jbc.M406758200.
46. Watanabe A, Fujii I, Tsai H, Chang YC, Kwon-Chung KJ, Ebizuka Y. Aspergillus fumigatus alb1 encodes naphthopyrone synthase when expressed in Aspergillus oryzae. FEMS Microbiol Lett. 2000;192:39–44. https://doi.org/10.1111/j.1574-6968.2000.tb09356.x.
47. Vagstad AL, Hill EA, Labonte JW, Townsend CA. Characterization of a fungal thioesterase having Claisen cyclase and deacetylase activities in melanin biosynthesis. Chem Biol. 2012;19:1525–34. https://doi.org/10.1016/j.chembiol.2012.10.002.
48. Breinholt J, Jensen GW, Kjær A, Olsen CE, Rosendahl CN, Romerosa A, et al. Hypomycetin - an antifungal, tetracyclic metabolite from hypomyces aurantius: production, structure and biosynthesis. Acta Chem Scand. 1997;51:855–60. https://doi.org/10.3891/acta.chem.scand.51-0855.
49. WONG S-M, KULLNIG R, DEDINAS J, APPELL KC, KYDD GC, GILLUM AM, et al. Anthrotainin, an inhibitor of substance P binding produced by Gliocladium catenulatum. J Antibiot (Tokyo). 1993;46:214–21. https://doi.org/10.7164/antibiotics.46.214.
50. Liu M, Ohashi M, Hung Y-S, Scherlach K, Watanabe K, Hertweck C, Tang Y. AoiQ catalyzes geminal dichlorination of 1,3-Diketone natural products. J Am Chem Soc. 2021;143:7267–71. https://doi.org/10.1021/jacs.1c02868.
51. Wieder C, Da Peres Silva R, Witts J, Jäger CM, Geib E, Brock M. Characterisation of Ascocorynin biosynthesis in the purple jellydisc fungus Ascocoryne sarcoides. Fungal Biol Biotechnol. 2022;9:8. https://doi.org/10.1186/s40694-022-00138-7.
52. Sidhu YS, Cairns TC, Chaudhari YK, Usher J, Talbot NJ, Studholme DJ, et al. Exploitation of sulfonylurea resistance marker and non-homologous end joining mutants for functional analysis in Zymoseptoria tritici. Fungal Genet Biol. 2015;79:102–9. https://doi.org/10.1016/j.fgb.2015.04.015.
53. Fulmer GR, Miller AJM, Sherden NH, Gottlieb HE, Nudelman A, Stoltz BM, et al. NMR chemical shifts of trace impurities: common laboratory solvents, organics, and gases in deuterated solvents relevant to the organometallic chemist. Organometallics. 2010;29:2176–9. https://doi.org/10.1021/om100106e.
54. Lippke G, Thaler H. Die Spezifische Drehung des sorbits und des Sorbit-Molybdat-Komplexes. Starch Stärke. 1970;22:344–51. https://doi.org/10.1002/star.19700221005.

Publisher's note

Supporting Information

Biosynthesis of the *Paecilomyces marquandii* conidial pigment saintopin

Carsten Wieder [1,2,*], Sarah Galwas [1], Rainer Wiechert [3], Kevin Seipp [3], Alexander Yemelin [2], Eckhard Thines [1,2], Till Opatz [3], Anja Schüffler [2,*]

[1] Institute of Molecular Physiology, Johannes Gutenberg-University, Hanns-Dieter-Hüsch Weg 17, D-55128 Mainz, Germany

[2] Institut für Biotechnologie und Wirkstoff-Forschung gGmbH, Mainz, Hanns-Dieter-Hüsch Weg 17, D-55128 Mainz, Germany

[3] Department of Chemistry, Johannes Gutenberg-University, Duesbergweg 10–14, D-55128 Mainz, Germany

*Correspondence: cawieder@uni-mainz.de, schueffler@ibwf.de

Table of Contents

Additional figures

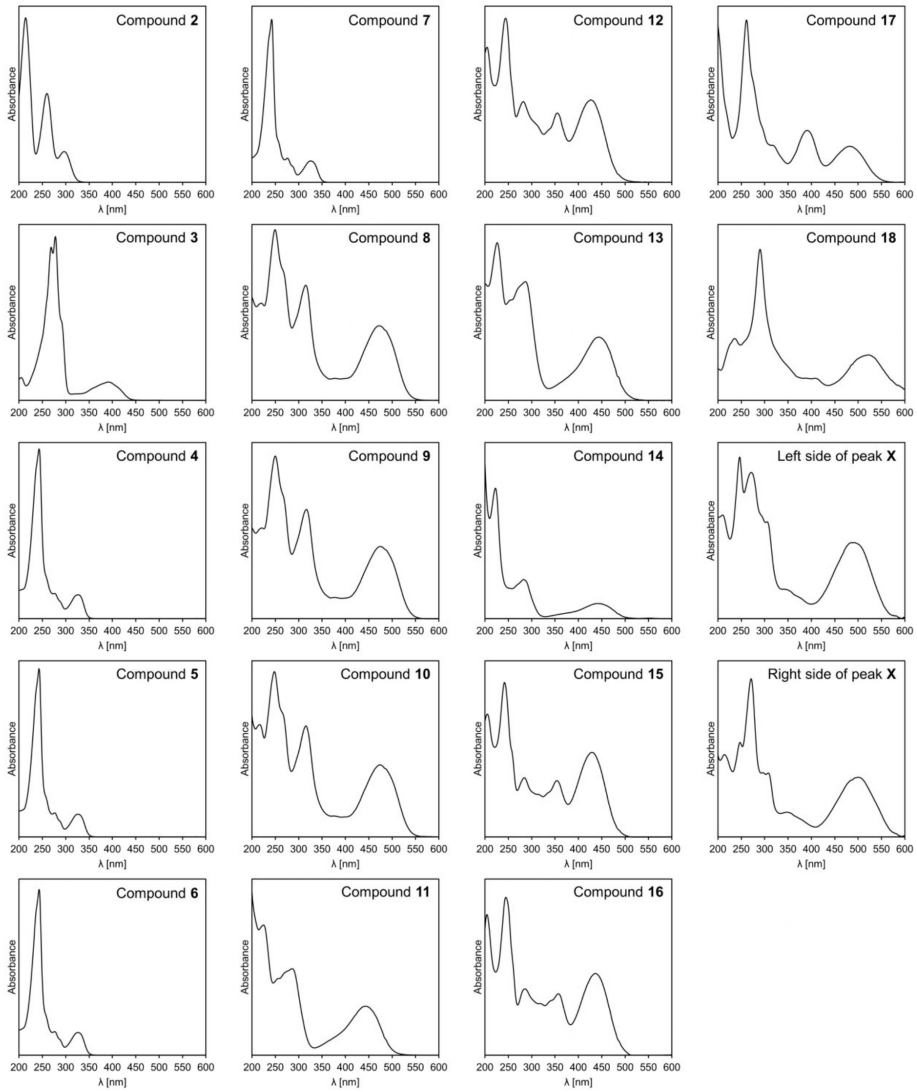

Figure S. 1: UV/Vis-spectra of purified compounds **2**–**7**, detected compounds **8**–**18** and peak **X**

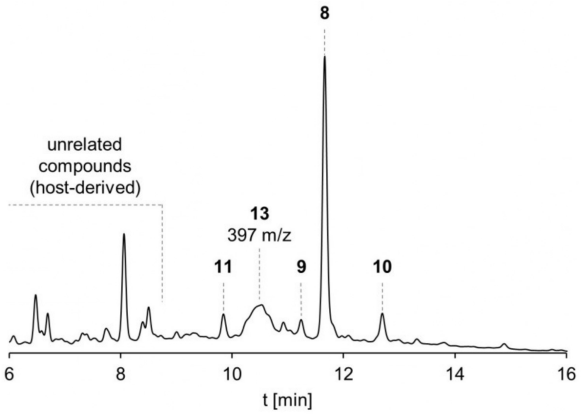

Figure S. 2: Magnified chromatogram (250 nm) of the OP12_*stpA* culture filtrate extract and assignment of an additional presumed shunt product (**13**). Mass data was recorded in negative mode. The UV/Vis spectrum of **13** can be found in Figure S. 1.

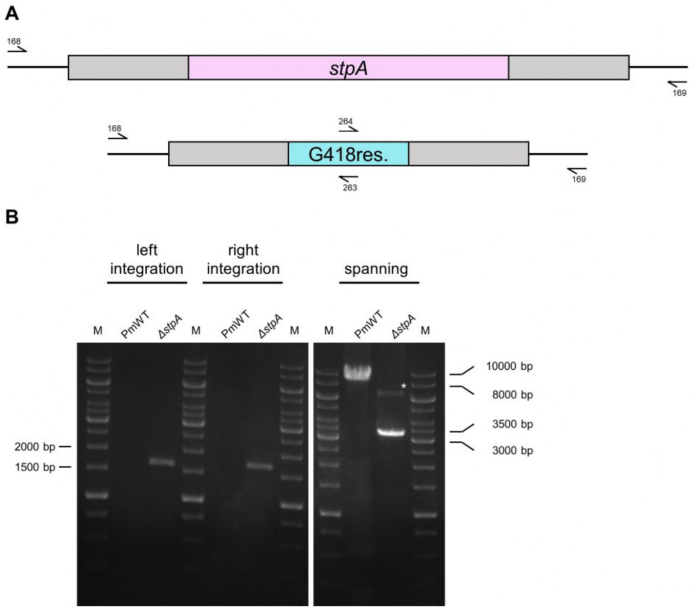

Figure S. 3: Verification of stpA-deletion. (A) PCR-strategy for verification of deletion. The grey boxes represent the flanks used for homology directed deletion of stpA. Primers 5'- and 3'- of the flanks and within the G418 resistance cassette were used to amplify sequences from PmWT and *ΔstpA* DNA. (B) PCR-amplicons observed are in accord with the deletion strategy, confirming identity of the ΔstpA deletion mutant. * denotes an off-target amplicon

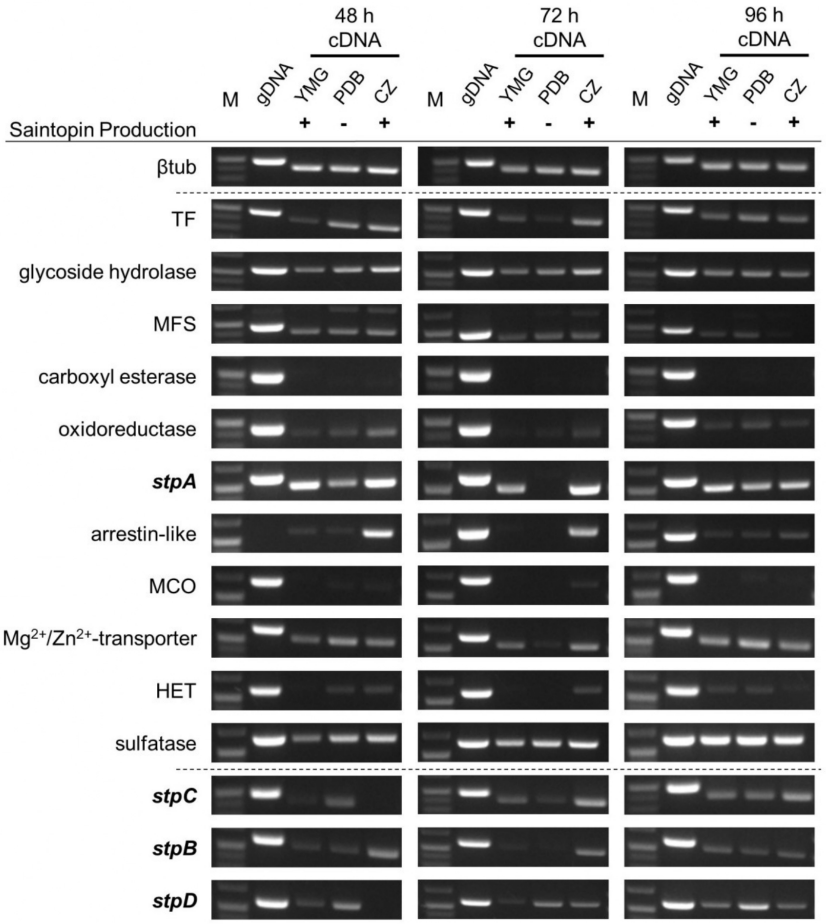

Figure S. 4: sqRT-PCR of stpA clustered and non-clustered genes. *P. marquandii* was inoculated cultivated in either YMG, PDB or CZ media for 4 days shaking at 120 at room temperature. After 48, 72 and 96 hours, 50 mL samples were taken for isolation of RNA and evaluation of saintopin (**1**) production by HPLC. RNA was reverse transcribed into cDNA and cDNA concentrations adjusted to produce similar intensity β-tub signals. Primers were designed intron-spanning as far as possible. Homologs of other napthacenedione biosynthesis genes are highlighted in bold.

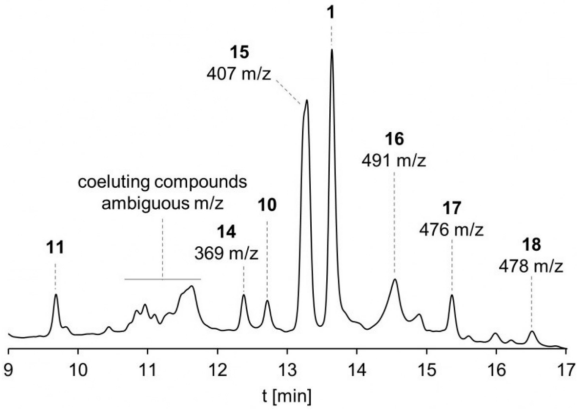

Figure S. 5: Magnified chromatogram (250 nm) of the OP12_*stpAC* mycelia extract and assignment of some additional presumed shunt product (**14**–**18**). Mass data was recorded in negative mode. The UV/Vis spectra of **14**–**18** can be found in Figure S. 1.

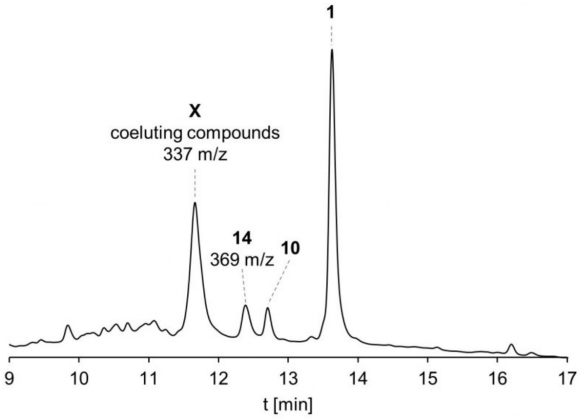

Figure S. 6: Magnified chromatogram (250 nm) of the OP12_ *adaA/stpC* mycelia extract and assignment of some additional presumed shunt product (**14**, Peak **X**). Mass data was recorded in negative mode. The UV/Vis spectra of the left and right side of Peak **X** can be found in Figure S. 1.

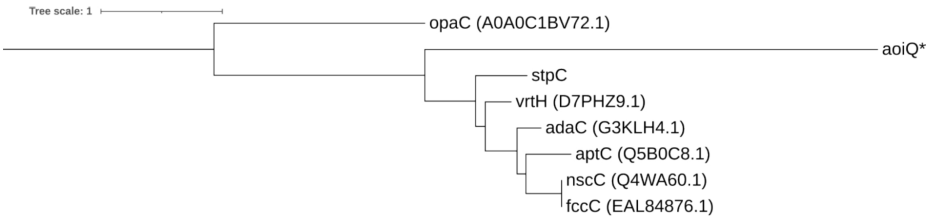

Figure S. 7: Phylogenetic analysis of flavin-dependent monooxygenases involved in naphthacenedione and dichlorodiaporthin biosynthetic pathways. The amino acid sequences of the flavin-dependent monooxygenases were aligned using the MUSCLE algorithm [1] on the EMBL-EBI webpage. A maximum likelihood phylogenetic tree was created using W-IQ-Tree [2] and visualized with iTOL [3], rooting the tree at the midpoint. *opaC* was included as an outgroup. *only the FDH domain [4] of *aoiQ* was used for the alignment

Additional tables

Table S. 1: Mutant strains used in this study

Strain	Genotype	Produces	Source
OP12 *pyrG*$^-$	PamyB:terR_ptrA; *pyrG*$^-$	/	[5]
OP12 3Δ	PamyB:terR_ptrA; *pyrG*$^-$, *ΔpabA*, *ΔargB*	/	[6]
OP12 empty plasmid	PamyB:terR_ptrA, *pyrG*$^+$	/	This study
OP12 3Δ empty plasmids	PamyB:terR_ptrA, *pyrG*$^+$, *pabA*$^+$, *argB*$^+$	/	[6]
OP12_PmPKS1	PamyB:terR_ptrA; PterA:nHis-PmPKS1_URA	**2**	This study
OP12_PmPKS2	PamyB:terR_ptrA; PterA:PmPKS2_URA	**3**	This study
OP12_*stpA*	PamyB:terR_ptrA; PterA:nHis-*stpA*_URA	**8, 9**	This study
OP12_PmPKS4	PamyB:terR_ptrA; PterA:nHis-PmPKS4_URA	**4-7**	This study
OP12_PmPKS5	PamyB:terR_ptrA; PterA:nHis-PmPKS5_URA	/	This study
OP12_PmPKS6	PamyB:terR_ptrA; PterA:nHis-PmPKS6_URA	**2, 7**	This study
OP12_*aptA*	PamyB:terR_ptrA; PterA:*aptA*_URA	**11**	This study
OP12_*adaA*	PamyB:terR_ptrA; PterA:*adaA*_URA	**8, 9**	This study
OP12_*stpAB*	PamyB:terR_ptrA; PterA:nHis-*stpA*_URA, PterA:*stpB*_pabA; *ΔargB*	**8, 9**	This study
OP12_*stpAC*	PamyB:terR_ptrA; PterA:nHis-*stpA*_URA, PterA:*stpC*_argB(mut); *ΔpabA*	**1, 10**	This study
OP12_*stpABC*	PamyB:terR_ptrA; PterA:nHis-*stpA*_URA, PterA:*stpB*_pabA; PterA:*stpC*_argB(mut)	**1, 10**	This study
OP12_*aptA/stpC*	PamyB:terR_ptrA; PterA:*aptA*_URA, PterA:*stpC*_argB(mut); *ΔpabA*	**11**	This study
OP12_*adaA/stpC*	PamyB:terR_ptrA; PterA:nHis-*stpA*_URA, PterA:*stpC*_argB(mut); *ΔpabA*	**1, 10**	This study

Table S. 2: Oligonucleotides used for cloning

Oligo	Sequence	Purpose
oCW126	Accatgcatcatcatcaccatcaccatggagcttacactagccatgtcct	Amplification of PKS1 for cloning
oCW170	cggttcagattgaaatcactgctgttatctcatgttgtgtaagcaatat	
oCW273	catttaacaaacttctcatcacagcaccatgggacatccagggagcttgt	Amplification of PKS2 for cloning
oCW277	ccttacgccttccattcatc	
oCW278	gatgaatggaaggcgtaagg	
oCW143	cggttcagattgaaatcactgctgttatcctaagccatagcctggcgaa	
oCW172	accatgcatcatcatcaccatcaccatggatacgatacggttggcacagc	Amplification of *stpA* for cloning
oCW135	cggttcagattgaaatcactgctgttatcttagcagttctggtcaac	
oCW173	accatgcatcatcatcaccatcaccatggagtcaccgccgcagacgtcgg	Amplification of PKS4 for cloning
oCW174	cggttcagattgaaatcactgctgttatcctataaaaaggcaataatga	
oCW175	accatgcatcatcatcaccatcaccatggagccaagatattttgccacgt	Amplification of PKS5 for cloning
oCW176	cggttcagattgaaatcactgctgttatcttagggcttatcagacatga	
oCW177	accatgcatcatcatcaccatcaccatggatatcgatctgagacaacaga	Amplification of PKS6 for cloning
oCW178	cggttcagattgaaatcactgctgttatctcacttgcctacattattgg	
oCW164	catttaacaaacttctcatcacagcaccatgGCGACACCCAGTCCTCTCG	Amplification of *stpB* for cloning
oCW165	ctatacggttcagattgaaatcactgctgcCTAGTCAGAATCAGACACCA	
oCW249	catttaacaaacttctcatcacagcaccatgGCCATCAAGAGCCCAGCCG	Amplification of *stpC* for cloning
oCW250	ctatacggttcagattgaaatcactgctgcctaagccgtcactgttccgg	
oCW331	Catttaacaaacttctcatcacagcaccatgtctgcccctacgaagctgg	Amplification of *adaA* for cloning
oCW332	ctatacggttcagattgaaatcactgctgctcagcaatactgctccaacc	
oCW333	Catttaacaaacttctcatcacagcaccatgaaagacaatacgcatagca	Amplification of *aptA* for cloning
oCW334	ctatacggttcagattgaaatcactgctgcctaacagtactgctctaacc	
oCW151	aggtcgactctagaggatccccGCGGCCGCgcgaacatgtagattggtgg	Amplification of left flank for pKO_stpA_G418
oCW152	CAAGCCCAAAAAATGCTCCTTCAATATCAGcaacggacttgtcacctctc	
oCW153	ttattataaggagaggtgacaagtccgttgCTGATATTGAAGGAGCATTT	Amplification of G418 cassette for pKO_stpA_G418
oCW154	atggttgaggtgttaccatggttgaccgacCATCATGCAACATGCATGTA	
oCW155	CATCAGACAGTACATGCATGTTGCATGATGgtcggtcaaccatggtaaca	Amplification of right flank for pKO_stpA_G418
oCW156	agtgaattcgagctcggtacccGCGGCCGCgacaagagtccagtccgagt	

Table S. 3: Oligonucleotides used for sqRT-PCR

Oligo	Sequence	sqRT-PCR Amplicon
oCW121	ATGATGGCCGCTTCTGACTT	
oCW122	CTCCTCTTCCTCCTCGTCAA	β-tub
oCW218	ctggattgcattctggct	
oCW219	gatcgaagccggataaga	TF
oCW220	gacgtcaacacatacagc	
oCW221	ccagactgctacgaatct	glycoside hydrolase
oCW222	gcaaaccagaagaagcca	
oCW223	cgtacaagctgaacttgg	MFS
oCW224	gctcaatggatatgcgct	
oCW225	cacgcggttgttcaagaa	carboxyl esterase
oCW226	ggaatcagttgcgtgatg	
oCW227	cggcatcggttcatacat	oxidoreductase
oCW228	gatggcaagtcgatgcat	
oCW229	ctatctcgacaaggtgac	*stpA*
oCW230	gccgccatcgaaattaac	
oCW231	ccttgatagtaggtacgg	arrestin-like
oCW232	gttctcggagatcaacac	
oCW233	ggtatatctcgctctgca	MCO
oCW234	caacatataccgcgccta	
oCW235	gtagtccttgtcgtactc	Mg^{2+}/Zn^{2+}-transporter
oCW236	ccacttatcaacccacga	
oCW237	gtggtagaagtgcatcca	HET
oCW238	ccttccctctcatagtca	
oCW239	cgtttgcccttcatcatg	sulfatase
oCW240	GACGGCTGTGTTTGAGAA	
oCW241	GATACGACGAGAGCTCTT	*stpB*
oCW242	GTCCAGGCTGTTCATGTA	
oCW243	CCTCTGTCTCACGTTGAA	*stpC*
oCW244	GCCAAGGAATCGTACAAG	
oCW245	GCGCCTTCTCAAAGTCAA	*stpD*

Table S. 4: ITS sequence of *P. marquandii* IBWF 003-21

Fungal strain	ITS sequence (ITS1F+ITS4)	BLAST hit	Identity/E-value
IBWF 003-21	GGAAGTAAAAGTCGTAACAAGGTCTCCGTTGGTGAACCAGCGGAGGGATCATTACCGAGTTTTCAA CTCCCAAACCCACTGTGAACATATACCTTTGTTTTCGTTGCCTCGGCGGTTCGCGCCGCCGGGTGA CACCTAAACCCTGATTTTAATTACAGAAGTCTTTCTGAGTAAAAACATTCTAAATGAATCAAAACT TTCAACAACGGATCTCTTGGTTCTGGCATCGATGAAGAACGCAGCGAAATGCGATAAGTAATGTGA ATTGCAGAATTCAGTGAATCATCGAATCTTTGAACGCACATTGCGCCCGCCAGTATTCTGGCGGGC ATGCCTGTTCGAGCGTCATTTCAACCCTCAAGACCCCTTCGGGGGACTTGGTGTTGGGGACCGGCA CAGGGGCCTGCCTGCTTGTCTTGCAGCGCCCTCGCCGCCCCCGAAATGAATTGGCGGCCTCGTCGC GGCCTCCCCTGCGTAGTAGCACAACCTCGCAACGGGAACGTGACGGCGGCCACTGCCGTAAAACAA CCCAAACTTTATTAGAGTTGACCTCGAATCAGGTAGGAATACCCGCTGAACTTAAGCATATC	*Paecilomyces marquandii*	95.77%/ 0.0

Table S. 5: Predicted gene sequences of *P. marquandii* nrPKS and accessory genes. Predicted Introns are underlined

Gene	Predicted gene sequence
stpA	atgtacgatacggttggcacagccatggccgacggcaccccagccaggctcgtgtactttggaaacgagttccccaatgatgatctcagcgatatctttcgcaagctgcaccagcatagcaaggatcggaggttccgcctgctgtctgcttttcttgacgaagtaat tctcgttctgcagcaagaattcgcaaaactcccccaccatgttcgaagccaggtgcctcactttgacaacatcgtgacccttttcagagatgggattccttcgggagctcgggctcggggctgccatggaaagcgctttcctcctcacgctgcaagttggtttgttca ttgggtaagtcaagtcaccatgaacctcaagtcattgtcggcgcgaggctaatgaagaaaacaagacaccacgaggcaaaggatcaagagctcaatctgcccaagggtcccacgatgctggctggtctcggcgtcggactcttcactggcgcatccgtagctctgtc tacctctcttgcagaggtggtcaagaatgcggccgagctgctgagggtttccttcagactcggagtctacattggcgatttcagcagcaagttggagtcgccacagcctgacggcagcctccagagctggtcgcatgtcatcaccggcatgacggaagagtccgtga gcagcgaggcgtctcgactcaacgaagagctcgggagccacgccatctccaagctcttcatcagcgccgccgacaagacatccgtcagtctcagcgggcctccttctcgaatcaaggctgctttccagcactcgagcgagcttcgatactccaagtccatccccctg cctgtctacgatggactttgccacgccaagcacgtctatggccagagggactacgacgccgtcatggacagcgagaactcgctcgttcccatgtcgcgcaagctgcagcttccgctcatctcgcccaggacgggcaagccgttcttggccaccgaggcaggcgacct gatgaaggagattgccagcgagttgatgaccagtgccatctatctcgacaaggtgacggacggcatcctcggccacgtcgactcggtttccaccgccgacgagctctatctcgccacgttccgcacttccatcgccttcaagggcattctgcagactctggagaaca cgttcccagacgtgaaaatcctgaagagcgacatggcggactgggtccatgaagactttggcgacagacggccaggtaatgtcggatgctccaagcttgccattgttggtatggcttgccgcatgcccggaggcggtaatgatcttgaccagttctgggagctcatg gaacagggccgggatgttcacacgactgttccccttgatcgatttgatctggcgactcattacgacccttctggcaacactgggaatgcggctacgacgccgtttggaaactttatcgaccgtcccggctttttcgacgctgcctttttcaacatgtctccaagaga ggtaattcccccccttttccccaatcttcttagcctccaaagtggccgacatcatactaacagcgtctggtgtaggctgagcaaaccgatcccatgcatcgacttgccatcgccactgcctatgaagccatggaaatggccggcatggtcacaggacgcaccgcctc gacacgccgtgagcgcattggcacttactacggccaggccagtgatgattggcgtgagctcaacggcgcgcagaacatcggcacgtacgcagtcccgggcggcgtgcgaggcttcatcgcaggacgcatcaactacttcttcaagttctcgggtccgtccttctgcg tcgataccgcctgctccagctccatggctgccatccagctagcttgcacggcgctctgggccggtgagattgacaccgccgtggccggaggcgtcaacatcatcaccgaccctgacaactactgcggcttgggcaatgcccatttcctgtccaagacggggcagtgc aaggtctgggacaaggacgccgatggctactgcagagccgacgccatcggatccgtggtgctgaagcgcctggaagatgccgaggcggacaacgacaacatccttggtgttgttaccgccgccgcgacgaaccactgcgccgatgccatctccatcacgcatcctca cgcaggacatcagaaggagaactaccgtcgtgtgctccataatgccggcgtgaacccccctcgatgtcagctttattgagatgcacggcacgggaacccaggctggcgatgccatggagtccgagtccgtcttggacgtctttgctcccttgcgacctcgccgccgcg ctgatcagaagctccttctcggcgcggtgaaaagtaacattggacattctgaagcagccgcaggcgtctcctccttgatcaagatgctcctgtgcttcgaaaagagcctgattcctccccacgttggcatcaagacggagatcaacccgcgcatccccaaggacttg gatcgccgcaacgccaacatggccatggagttgacgccgtgggttcgaccagccgggaagaagcgcattgccatggtcaactcgtttggtgctcatggcggcaataccacgctgctgcttgaggatccgtctgagagagatagaccgcgtctcagcctcgagagtgc cgatggtcgtgctttataccccatcgtcatctctgccaagagcaagaagtctctgcaagccaatatcgaaggtcttctcggctacctcgagaagaaccccggattggacctggccgacgtgtcttacaccacctgtgcacgacgcactcactacaatctgcgtgttg caacttcggcttccaccgtttctggactgcagaagttcctccgaaatgctattgacaacaaggtcggcctcgagaccaaggctatcccgcccaatattccctcggtggtgctcacctttaccggccagggtgcttcttacaagggcatccgtcaagacctgtttgac gaggtccccttcttccgtgaccaagtccttcaacttgaccagctcgttcagcgcttgggcttcccatccgttgtcccagccatcactggcagtgatgacgacgaggtccaatctcccgtcattagccagctcagcatcgtggtcttggagattgccctcgctcgatt ctggtcctacatgggcgtgaagccgagtgctgtcatcggccacagcctgggagaatacgccgcccttgccgtcgctggtgtcttgtccgcctcggatgttttgtacctcgttggtcggcgtgcacagattacacaggagctatgcactccttatagccgcgccatgc tgtccgtcctgggagatcttgacgatatcacccaggtgttgaaggctagcccagagaccaaggccgtcgagtacgaggtttcctgccagaatactcatgtcgataacgtgctgggagcttcccgagaggatattgaatctattcaaaaggtcctcgaggccaaggcc ttcaagtgcacgcgtctggaacttccctttgctttccacacttgccagatggacgctgtcattgacgagctcgaggccctggccgagactgttcctttcaaggcaccgagtatccccgttctgtctaccatgcttggaactgccgtgtttgacggaaagaccatcaa cgccaactacctccgccgtcagacacgcaacactgtcagatttgcagacgctattgaggctgctcgtgacatgggcattgttgatgaccaaaccgtctgggttgacgttggtcctcaccccgtctgcgtcggcttcgtgaagaagctcattcctacagcaaggattg gctcgtcttgccgacgcaacgaggacaacatctccaccgtcgtaaagactctggtcaccctgcacgctgccggcatcactccccactggaacgagtactaccgacacaacgagacagcttacactctgttgcatcttcccaagtatgcttggaacgagaccaactac tggattccgtactacggcacgtggacccttgataaggctttcgtcaagttcggacgcaaagacggcagcgtccctgcgcccgtctctgctgctcctagtttccgcacgtcgacgattcaccaagtcaccagtgaaaccatcgaagcctccacggcgtctctccacgt cctctctgatatccagcatcccgagttccttgctgctgtttacggacacacaatgaacaactgcggcgtggccacctcttccatctggacagacatggcatgggccgtgggtgagtacctgtacaagaaactacagcccgacgtcaaggaagtccacatgaacatcc ttgatctcgaggttctccacggccaggtggccagcaagaccaagggcgcctaccagccgctggctctcgaagccaacctggacttggacacgcaaatcatgtcgctggcctggtacgacgtcagtgtcgagactggcgagcgtgacgccgagagcttcgctactgct tccgtacggttcgaggacccggacgtctggacttccgagtggaatcgccagacgcacctggtgcagggacgcatcgagaccctgcagcagctcgccaacgagaacaaggccaaccgcatctccaagcgcatggcctacaccctgttcaagaaactcgtcgactacgc cgagcactaccgcggcatcgacaacatgatcctccacgagtacgaggcagttgcggacatcacgctggcaaatgaccgtcacggcacatggcacactcctcctcactggatcgacagcgtctgccatctcgccggcctcatcatgaacggcagcgacgcgtccaaca ccgacgactacttctacgtcacgcccggtgcggacgcgttccgtctgctgaagcccctcgaggcgggcggcaagtacaggagctacgtgcgcatgttccccgtccccatcgaggcgggaatgcacgccggtgatgtctacatcctgcaagacgacaccatcgtcggt gtcttgacgcagatccgcttccgtcgcgtacaccggctcctgctggaccgcttcttctctgccccaacgggagacaaggtcaagaaccgcgacgctcatcagactcggcccgctgcgtccgcgcctcccaagaagacagctgctcctgcgcccgtgaaagctgcccc tgcccctgcgccggcgcccaagccagcgcccaaggctgccccgctggtcatgcaaatccacgagactgcgagcgtgagcgatagtctgtccagctcttctacgctgtctagcagcgaggcaagccccatgggcaacacgacgcctcaaacgggtaacactacccctc agacgggcaacgttacgcccaagatggaggagctggatacgggtgttgtcggccagtgtctccagatcatgtcccgcgagaccaacctcgagatgagcgagctgtccgccgacgctgcctttacgcatctgggcgtcgactcgctcatgtcgctggtgctgtccgag aagttccgcaacgagctcggtgttgatatcaagagctccttgttcctcgagtgtcctaccgtcggcgagttcaaggagtgggttgaccagaactgctaa
stpB	atggcgacacccagtcctctcgaagaatcattttggcaggagtacctatcagaccaggcggctaaactgccgcctctgtctcacgttgaagatgtaacggaccgggtggttcgtatcatgggtggaaatccaggacgatgaagctccagggcacaaacacatatct cgtcggcacaggacagtctagaattctcatcgacacaggcgaagtatgaaaaaagttcacaaatctctcatcatttcagtacactgacctggtttcagggctccccagagtggattcaacgcctcatccgggtgcttcaagatcgtggcctcgacatctcccatgtc ctactcacccactggcacagagaccacacgggcggcgcgcccgacctcgtagcctttgatcccagcttcgcgcacaggatctacaagaaccagccggaccgtgaccagaaccccatccaagacggacaggtcttcgccgtcgaaggcgccaccatccgcgcccgtctt cacccccggccacgcggtagaccacatgtgcttcctcctggaggaggaaaacgccctcttcacgggcgacaacgtcctcggccacggcttctccgtggtgatggatctggccgtctacatgaacagcctggactacatggccgccaagggatgcgcgacgggatacc cgggccacggcgccaagattgccaacctgcctgccaagatgcacgagtacatccaccacaacgaggttcgtatccagaaggtcctgtctgcgctgacctggaagggcacggggatgaagggcgggatgaccctgcaggagattatacgctccatctacggcgacgtg caggggggacattgcggactatgcgctggcgcccttcttgacgcagatattgtggaagttggcggaggatggcaaggtcgggttctcgccgggggagcccaagaaggcgaggtggttcgggctgggggggtgttcgcaaggcgacttctattgctgcgtcggtggtgtc tgattctgactag
stpC	atggccatcaagagcccagccgccccgtcctcatcatcggcgcaggtttgtcaggcctcgccgccgggcgaattctggcaaaccacggcgtcccaactatcgtgttcgaagagtcctctccggagctcggtgagagctttgccatgggactgcgcgactggtgcta ccagccacttctcgaggctcttggcggcgtgtccctcaagagcatgatcaaggccgtggccccggatcgacacgttggcggaagcggcctggtcgatttctgtatgcgcgacaacgcgactggcaacattctcgtaacaactcccgacgataagaggccggtggtga cgcgggcgaaccgcaatgccgttcgcgcttggctcgccgactgcggcgacgatgacctggatgtgcgataccaccacaagttggcgagcgtatctggcaccctgggaaacatgacggctgtgtttgagaacggagcgcagtacaacggctgtttgatcatcgctgcc gatggtgttgactctgcaggtgagtgacgtgacttacacggtcaaaacttgcctccctggcaactatcaccagacacttttcttacacacttgtacagttcgcactcagctgctgcctggcctcgttccccagattctccctgcggtaatctacaacggcaggttcc agctatcgcgcccaagagttcgaccagcacatcaagccacgcacaaacggctccaacgtcctctcgggcatcggcgacggcttcaacaccaacatcacggtgtgcaacatgaccgacgccaaggtcaacctcgactggtcgtactcgagacgcgctcgcggcgacacc gacgccttgttcgacaactcggaaggcgccaagacccggggcgtgacgggcaccatccccgaagcgctggtggaagagctctcgtcgtatcagctggcggatccttggggccggtacgtcaacgccgaggctatcaagcagcattccgtcttccagtgggtcagccg atgcgtcttcgtccccacggaggaggccaagaagaatggacagcagggcgtggtctttgtgggcgatgcgtggcacacgatgcctgtgttcagcggcgagggggaaacccacggcgttctggatagtgttgagctcgccatggccatcgtggagaaggattcgctgg

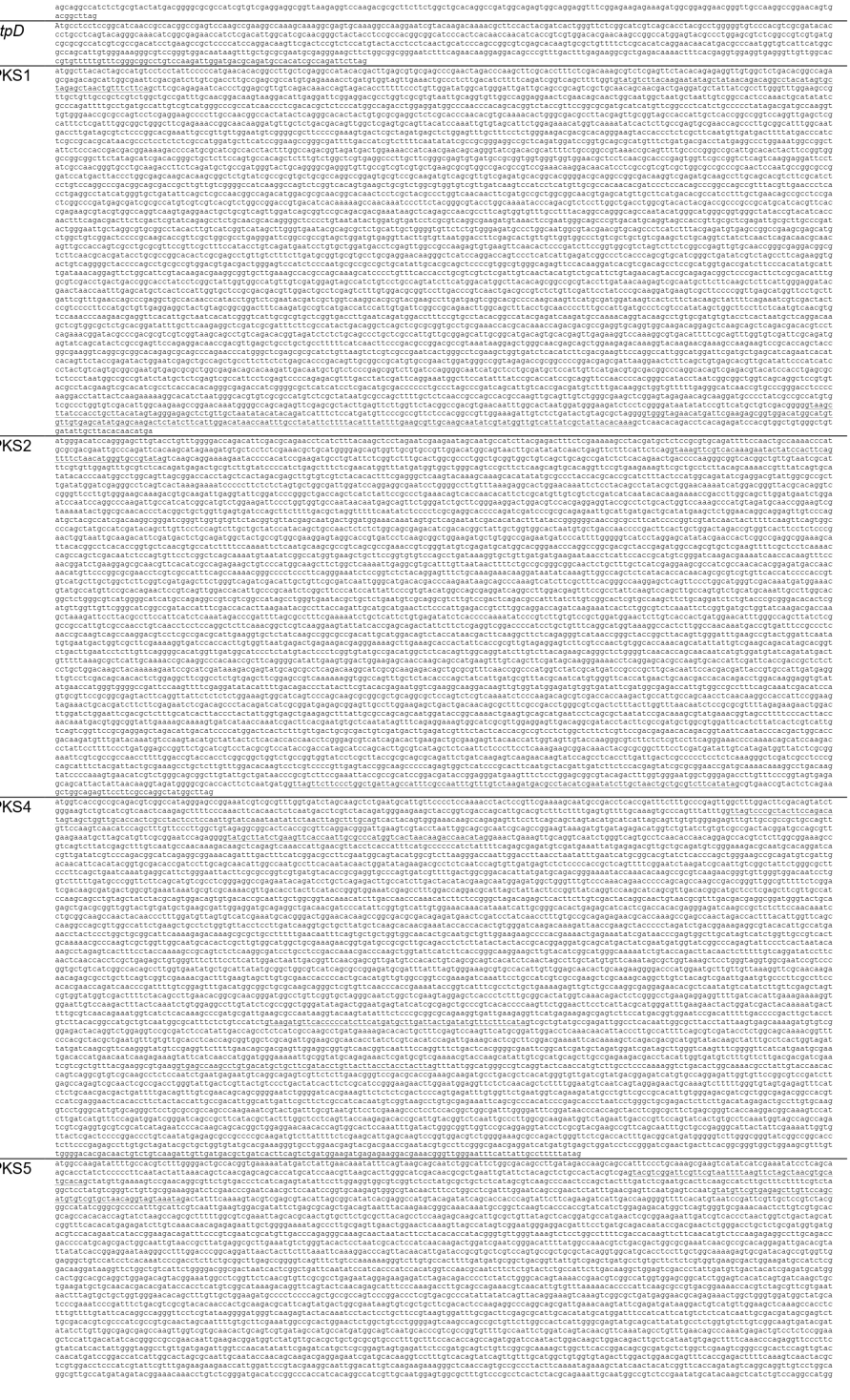
stpD
PKS1
PKS2
PKS4
PKS5

	gccacctggcttgaatgtggcggacctgagtatccaaaaggctcttttgttcgacgacaaggccgatgcccatattcttcattgtaccgttcagactagtggcactggtgaccatgcaagtgtcgtatttcatacgcgcaatgggttgctcaagaatgaacatgcac gctgtacggtatattacggagacttacgtgtgtgggctgccgagttggcaagagtcaactacctcgtcgaggcacgtattgatgcattagcatcaggtaacgctagtcatgcaatctcaaaatacaatcaacctgcggcctaccagagcttcgcgagtttcgtcgac tatggtccccaataccaggggatgaaggaggtgttgttgtgtgctaaatcaggtgaagcgactgcagaactcagtttccaagcaagtaatgaggggaactttttcttcaatccgtattggattgatggctgctgtcatctctcgggattcatccttaatgccaaaga agccgcagattcgtccgaggaggtattcatctcagagggctgggagtctctgaggttcattgagcgtctccgtgagggaactacatatcggtcatacacacgcatgcaaccagtacatgggatgagtttggtcgcaggtgatgtgcacatccttagagacaaatgca tcattggcgtagcaaatggggtgaagttccgttctgttcccaagagggcgcttcatctactactgccaccaaccattacatgtcgcacaagcaactcccagcgtcagtcaattgcagaattggctctacaaactgacaatgtcaacccaaaaattacaaagaaaggg cagggttacgcgacattcccagcgctgtatcgaactacagcacagacctctttgatggatgagtttcttcgaattgtacaagttgaaattggttgcgagactgaagacttgggtgacaatgctacctttacatcccttggctgtgactcactgatggtgttggttat tgctagcagagtgcatgaggagttggagataaatattcgaccccaggcatttctggagtaccctaccattggggatttcaaagaatttctagctagtctgcgtatcacggacactagaagttcggatgcctctacttcgtctacggtatctggtgttaccgacgagc cagatatcggacaattgtcggattccgagagctctacatctcgattaggtgacaagacctgcgaagagcaggaagaaacaaaaaagtctctggatactgcaatggcagacgctccgatcagaacaatcgagagggttgaatgcctcagggatcagtttcccaaccgc aaagccaaatcagttctgcttcaaggaagccgtcagatagcgtttaaaaacctgttcatgattccagatggcagtggctccgcgtattcctacagcgagcttggttcacttggttcagagtgggctatttggggattggtctccccgttcatgaagactcctcacga gtacacctgcggagttgaaggaatagcacgaaagtttcttgaggaaatgaagcaacgccaaccagttggcccatatgttttagcaggttggtccattggcggaactattgcttacgagataacgagacagttaactcggtccgatgaacaagtctcccacttgattc tgatcgacgcaccatgcccccctccttgacgatccattacccagacatttgggccgctggtttgctgatattggaatcatcggctcgaagatgggcgcgagcctctgtattccagactggattcttccacattttgatatgagcgccaaggcattcgcggattataag ccggtacctatctctcgagaccactgtccgatcaccatggctgtttggtgtgaggatggcgtatgtcgaacgcagcaagatccacgcccgcatccatacccgactggccacgctctctttctgctggagaacagagaagactttggtccaaaccgctgggacgagct cctggcttcggaaaagatacagacaaaacgcatgcgcggaaatcattttacaatgatgcgtgaacccttggtatgcttcctgcttcaactgggtacaggtggaaactaattggtctgattagacacaggatttaactgcaattatttatcaggcggtcatgtctgat aagccctaa
PKS6	atgtatcgatctgagacaacagatcggcggacgctcgtcgtgttcggcgaccaaaccagcaatgtaaccagcatcgccaagcaactcttcctgggcgttccccagagcgcagcagccacagagttccttcgcgatgcgagtgcggccctcatggctcagagagatcg tttacggccgtttcagcgcaaccatcttcctgatttcaagaacctccatgacatagcaaggatatacgacgaggccagcggcgtatgccatccatccatcaccagcgtcatgctgtgtgctacacagttgttgcaattgttcaggtcagtaatgttcacagtagcgc cagagcatagcgttgcgtatcagcgtctgacgattcacagatatttcgaagaacatcgcccggggcccaacgagaaccatcacgtcactactgttgggttatgcaccggctcccttgccgcccgcggctttcgcggcctctaacggggtcgaagatctcaggtggttg gccgtcccgactatatccatggcctttcagctcggcctacaagctgctacggcgagcagcatgctctacgaacaagacgccgcgagactgggcagctggtccgtcgcaatacccaacatgcccgaggatgaggctatatctgccttgtccgtgtacgacgccggcca tcatctatcgctgcgtcacagatgcttcgtcagtgccgtcggcctgaaaagtgtcaccatctcaggagctccgcccgcgttgagggccttcaccgacacccttgccgcgtcgcagcctgagcgaaggctcgttgagctacccgtgtttgcagcattccacgctgtcc acattcacccatttctagacttccctagcttcctatccaggtgtggtgtcagccttcccctactggcccgcttcaaacccgtacaccgtctcttgtcgccgttgacgggcgagcctgtcgtagccaacgacgcctttgggctgttcaagacagctgtttgcgagaca ttgcaggcacccttgagactagatcttatagtcgaagggttcgccaagttcatccaggacgaaaagatctcaagcatctctgtcgaagttgtgtctcccacaacggtggcagatggtattgtggctgccctggtacaacaaactcaagccagcgtttcatcgagacc aatcgtggctctgccatccgctggtgagatccggagcaatccccctttcaacaatgtacctctggcaatcgttggcatgtctggacggtttccagacgccgacagtgccgaggcgctctgggaccttttggcccagaaaatcgacgcccatcgtgttgttcccaagg accgcttcgatgtaaatgtacatgttgatcctgctggcaaggctaaaaacacctcctggacgccttatggctgttttattaaccgtcccggcgagtttgaccctcgattcttcaacatgagcccaaaagaagcgcttcaaacagaccctatgcaacgactagcgctc gtgacggcatatgaagctttggagcaggctggctttgtgccagatcgtacccggtcaagtgcgtcgcaccgggttggaactttctacggccagacgagcgacgactaccgagacgtcaattccgcgcaggacattggaacgtactttatcaccggtggcattcgagc ctttggccctgtaagtcgaccctggctgctcctattcctggtcctagactcaaaagcctaacgtgcggtagggccgaataaactactttttcaagttctctgggcccagctactccgtcgacacggcgtgctcctcgagcctcgctgccatccagctcgcttgcact gccatctggaatggtgagtgcgataccgcagtcgccggagggctcagtatcttgacatcgccggacctcttctccggcttgagccggggccagtttctttccaagactggctcatgcaagacttttgacaacgccgcagacggatactgcagagcagacggtatagg aacggtagtcatcaaacgactaaaagacgccgagagcgatcgtgacaatgtgctagctgcggtattaggcgctggcacaaaccattcggcacacgccatctccatcacccatcctcacgccgaaacccaatctgatctctatcgccaggttttgcagcaggccggcg tggatcctcacgatgtttcctacattgaaatgcatgggaccggaacgcaggctggggacggaacggaaatgaagtccgtgagcgatgtgtttgcaccgccgtcatctaaagcccgtgccagcgataatcccctctacgttggggctatcaaatccagcgtgggccac ggtgaagcttcttccggagtcatatcgttgatcaaagccatgaccatcctgaagaagtctctgataccaccccaggccatcaagggcgagttgaacgtcggcttcccggatctgaaggcgcgaaatatccgcattgctaggcacatgacaccctttccagagaggaa ggggatcaagaagacagtgctggtcaacaacttcagtgccgcaggtggcaatacagcactcttgatacaagagcctccagagacccggatcgagcacaacaaggaacctcgaaacgcccatccagtgaccgtctcggggcacactcattcagccatgctcaacaacc ttgatcggctgatcgagttcctggctaataactcggagacatctccgctcgatttgtcctacaccactactgctcgtcgaaggcaccacaacttccgtgccaccgtcgtcgagagctcgactcctcggattctcgctgccctgaagctcaagagggcgtcgctagcg gaaggcacatttatcccgccaaagaaaccacggtccgtcgtgttcacgttcacggggcaaggatctgcatatccagccctggcacgcgagatttacaacacgtccacgcagttcagggctgatgtttggcattttgacggcatcgcccgtcaacaaggattccccac cttccttccgctcatcactgacgccagccttgccgacatcaatgtcctgtctccggctcagacccagattggtcttgtctgcatacaagtcgcgctcgcacgcctctggagctcctttggtatcaagcccagcgccgtcatcggacacagcctcggagaatacgcag cgttgcaagtcgcgggtgtcttgtcggtgagcgatatgattctgcttgtcggctcgagagcgcgtctcatggagagtaaatgcgaaaggaactctcacgcaatgcttgcagtcgccgccccctgggtgttccgtccagtcaatggcagcagagtgtctggatggcgtc gacctggcttgttccaacacgccccgagaatccgtcttcgcaggagaaaagtccaagattgagcagcttgcgcaaaagctgaatgagtgcaagatccgctctactcagctacgcgtgccttatgcctttcactccacccaagtcgacagcatcttggaggactttgg caatattgccagcgtcgtcaacatgggcgtcccgcatacaacagtcataagcccgacgcgcggtagggttttggatgcgggagacaagatagacggtgagtacctgaagcatcactgccgccacacggtacaatttgcccaggcgatagagcacagccgccaagccg gcgtcatcaccgatgcgacgacattgatcgaggtcggaccccatccgatctgtagtggcatggtgagatctacgctgggcgagaaaacgcagactctgtcgacactgaaccggaaagagaacccgtggaatgccattgtaggcagcctggcttcgctgcatgacgcc ggccatactgtgaactggtccgaataccagcgagatttcgagtctgcttgtcgtttgatacacctcccctcttatgctttcgacaacaagaattattggatcgactatcggaacaactggacgctgcgcaagggcgacccttccacggctgcagcagacgcgcagag cgtcgtcgcggaccggagcggcaacgcgaagccatacatctcaagctccgtccatcgcgtggtggaagaggattacaacagcgctcaaccgagggtcgtgtttgagactgacctgtcacacccagacatgcacacggccatgtctggacaccgcgtgaatggctctg cactttgcccttcttctctgtatgccgacattgccttgaccattgcaaagtacattcgggaccaaccaggctcaggactggatcaagatgggcatgacgtctgcgacatggaggtgacgcaacctctgattatcaatcctcaccgcgaccaagagaacagaacgttg cgcgtcgtgacacatgtcgataaaagaagccacatcctgtctttggagtattcctcttacggaccagcaccagcactcaaaactccagtcaagcacgccatgtgccgcgtcgagtttggtaatcggcaaaaatggtcgagacgatgggttcacgacttacacctggt caaggaccgcattgcgggcttgaaggtcgcgacccagtccggcaaagcgagcagcatcacgaagcggcttgcctaccgtctattcgcaaaccttgtcgactatgctccagacttccagcgcatgggtcaagtctggctagatggcgtgggccgcgaagcaaccgccg tcgtctccctcgacagacgagagacggatgccaactttaccttcagcccttaccacctagacggcttactccacctgtcgggcttcatcatgaacggcaacgatgatattgatgccaacgaagcagtgtacatctctcacggctggcaaagtcttcgcttggcagag cctctcgtgccagacaccaactaccatgtctatgtcaagatgcttcccgtcgacaagaccatggttgccggaaacgtctatgtcttgcacgacgacaaggttgttgcattgtgcgaaagcatccgcttccagcgtgtccctcgcgcggtactggacatgctgctccc tccagttccgacgagtcgtcctcgtcgagctgcaggccctgccccggagagatttaaacatggaggcagtccaccagtcgtgaaagtcgctgagcgggtggctccaacaaagaagcagttgccgttggctccagcacaactcccggccacatcagggactgtttcga caccacagtccgagctcttcatgcaggtcatcgccaacgaaatcggactcggcacaggtgaactgaacgtcacagacaacctggtcgacctgggtgtggactccctgatgtcgctggctttggctggacagctagttgagcagttcggagtgaatgttgatcatggc gaattgatgcagtgtgccagcatcaaagacctgctcaggcttctccaagataaacaggagccgccgccggcttccacccagaacgaagaacacgctggcaccagcagcagcagcagcggaagcagtgcgtcttcctcggccggcggcttgggtaccgtgacgccccc caccagagccacaactcctgctgtgaaaccggccgacgacatggggcgtctcgtatactccatcgtcctggaagagacgggcatggaaggagaggacttccagtcttctgccgagctgagtgatctcggggtcgactccctcatgagcctcgctatccttgccaagc ttcgcgaagcaggcgtcgatctgagtccaaccttttttccttgacaaccgtacaatggacgacgtctttcgtacgctcggcaaaggtaaggaccctggcgcagaagaagaacagcaagtgattgacagcaccgcatcgcaggcatccaacctccgctctgaagccgct gaagccactgcagccgctgccgccggctcccgaccccatgcgcagtgtatcctactgcaaaaggcaaccgcatctccggctgggcaatcattgttcctcttcccagatggctcgggctcaccgtttgcctacgcagctctggaaagactagatccaacgctcgacgt ctatgggctcgcctgcccgtttttgaaaagcccgtcagccttcaaagaccatggtattgaagcaacggcggcagagtatatcaagacacttctggccaagtgtcccgcaggctcactccatctcggcggctggtccgtcggtggcgttctcgcgttcgaggcagcaa agcaactgaccgaggtccacggccgccaagtagccagcctggtattgatcgatgcgccctgtccactgaccttgccgcctatgaacgggaggctgattaagttcttggactctcttcaattatttgctcctcctggcgagcggaatgcacgatcccgagcggatacg gaaaagcaccgcatggttttggagcacttcgatgcgactgttgaatgcctcggccgctacaggccggcatcgatggcaatggcaatccggacattggtaatatgggctagtgatggtgttgttggacacggggatgctatcccggaccgcatgttgttggatgatcc catggcaaactggatactccaggatcgagggactcccggccctcacggatgggacaagctcctgccatctcacaacttggagatcgtgacaacgcccggtaatcacttttcgatgatggtgggtggcaatgttcgggcactctcgttgggtttgcaggcgcattttc aaggtttaaatgccaataatgtaggcaagtga

Table S. 6: Predicted protein sequences of *P. marquandii* nrPKS and accessory proteins.

Gene	Predicted protein sequence
stpA	MYDTVGTAMADGTPARLVYFGNEFPNDDLSDIFRKLHQHSKDRRFRLLSAFLDEVILVLQQEFAKLPHHVRSQVPHFDNIVTLSEMGFLRELGLGAAMESAFLLTLQVGLFIGHHEAKDQELNLPKGPTMLAGLGVGLFTGASVALSTSLAEVVKNAAELLRVSFRL GVYIGDFSSKLESPQPDGSLQSWSHVITGMTEESVSSEASRLNEELGSHAISKLFISAADKTSVSLSGPPSRIKAAFQHSSELRYSKSIPLPVYDGLCHAKHVYGQRDYDAVMDSENSLVPMSRKLQLPLISPRTGKPFLATEAGDLMKEIASELMTSAIYLDKVTD GILGHVDSVSTADELYLATFRTSIAFKGILQTLENTFPDVKILKSDMADWVHEDFGDRRPGNVGCSKLAIVGMACRMPGGGNDLDQFWELMEQGRDVHTTVPLDRFDLATHYDPSGNTGNAATTPFGNFIDRPGFFDAAFFNMSPREAEQTDPMHRLAIATAYEAME MAGMVTGRTASTRRERIGTYYGQASDDWRELNGAQNIGTYAVPGGVRGFIAGRINYFFKFSGPSFCVDTACSSSMAAIQLACTALWAGEIDTAVAGGVNIITDPDNYCGLGNAHFLSKTGQCKVWDKDADGYCRADAIGSVVLKRLEDAEADNDNILGVVTAAATNH CADAISITHPHAGHQKENYRRVLHNAGVNPLDVSFIEMHGTGTQAGDAMESESVLDVFAPLRPRRRADQKLLLGAVKSNIGHSEAAAGVSSLIKMLLCFEKSLIPPHVGIKTEINPRIPKDLDRRNANMAMELTPWVRPAGKKRIAMVNSFGAHGGNTTLLLEDPSE RDRPRLSLESADGRALYPIVISAKSKKSLQANIEGLLGYLEKNPGLDLADVSYTTCARRTHYNLRVATSASTVSGLQKFLRNAIDNKVGLETKAIPPNIPSVVLTFTGQGASYKGIRQDLFDEVPFFRDQVLQLDQLVQRLGFPSVVPAITGSDDDEVQSPVISQLS IVVLEIALARFWSYMGVKPSAVIGHSLGEYAALAVAGVLSASDVLYLVGRRAQITQELCTPYSRAMLSVLGDLDDITQVLKASPETKAVEYEVSCQNTHVDNVLGASREDIESIQKVLEAKAFKCTRLELPFAFHTCQMDAVIDELEALAETVPFKAPSIPVLSTML GTAVFDGKTINANYLRRQTRNTVRFADAIEAARDMGIVDDQTVWVDVGPHPVCVGFVKKLIPTARIGSSCRRNEDNISTVVKTLVTLHAAGITPHWNEYYRHNETAYTLLHLPKYAWNETNYWIPYYGTWTLDKAFVKFGRKDGSVPAPVSAAPSFRTSTIHQVTSE TIEASTASLHVLSDIQHPEFLAAVYGHTMNNCGVATSSIWTDMAWAVGEYLYKKLQPDVKEVHMNILDLEVLHGQVASKTKGAYQPLALEANLDLDTQIMSLAWYDVSVETGERDAESFATASVRFEDPDVWTSEWNRQTHLVQGRIETLQQLANENKANRISKRMA YTLFKKLVDYAEHYRGIDNMILHEYEAVADITLANDRHGTWHTPPHWIDSVCHLAGLIMNGSDASNTDDYFYVTPGADAFRLLKPLEAGGKYRSYVRMFPVPIEAGMHAGDVYILQDDTIVGVLTQIRFRRVHRLLLDRFFSAPTGDKVKNRDAHQTRPAASAPPKK TAAPAPVKAAPAPAPAPKPAPKAAPLVMQIHETASVSDSLSSSSTLSSSEASPMGNTTPQTGNTTPQTGNVTPKMEELDTGVVGQCLQIMSRETNLEMSELSADAAFTHLGVDSLMSLVLSEKFRNELGVDIKSSLFLECPTVGEFKEWVDQNC
stpB	MATPSPLEESFWQEYLSDQAAKLPPLSHVEDVTDRVVRIMGGNPGTMKLQGTNTYLVGTGQSRILIDTGEGSPEWIQRLIRVLQDRGLDISHVLLTHWHRDHTGGAPDLVAFDPSFAHRIYKNQPDRDQNPIQDGQVFAVEGATIRAVFTPGHAVDHMCFLLEEENA LFTGDNVLGHGFSVVMDLAVYMNSLDYMAAKGCATGYPGHGAKIANLPAKMHEYIHHNEVRIQKVLSALTWKGTGMKGGMTLQEIIRSIYGDVQGDIADYALAPFLTQILWKLAEDGKVGFSPGEPKKARWFGLGGVRKATSIAASVVSDSD
stpC	MAIKSPAAPVLIIGAGLSGLAAGRILANHGVPTIVFEESSPELGESFAMGLRDWCYQPLLEALGGVSLKSMIKAVAPDRHVGGSGLVDFCMRDNATGNILVTTPDDKRPVVTRANRNAVRAWLADCGDDDLDVRYHHKLASVSGTLGNMTAVFENGAQYNGCLIIAA DGVDSAVRTQLLPGLVPQILPAVIYNGRFQLSRQEFDQHIKPRTNGSNVLSGIGDGFNTNITVCNMTDAKVNLDWSYSRRARGDTDALFDNSEGAKTRGVTGTIPEALVEELSSYQLADPWGRYVNAEAIKQHSVFQWVSRCVFVPTEEAKKNGQQGVVFVGDAWHT MPVFSGEGGNHGVLDSVELAMAIVEKDSLEQAISAYYDGARHRVEEAVKRSKTRFFWLHRPMAEWQEVSEKRKMAEERVAKAGTVTA
stpD	MPPPASTATAESKPKAKAKASAKAKESYKTKRFHYDHWVLGIVSTYAWGCPTSRYTLPQYRANIGENHLDIGIATGYYLRHGGIPLTTNITVVDTNKPAMEYALERLGRRDARAIVADILKPLPIQDKFDSVSMYYLLNCIPAGVEHKCAVFSHIRNNMTPNGVIHG ASIVGKGVRVDNKFAARMRGKLLAAGIFQNKEDSPFDFEKALRQNFHEVEVRVVGTVFLFRAACPRLDDADATSPDS
PKS1	MAYTSHVLLFPHEHTALLEAIHDLSVRARTRPKLRTFLDKASRVLHREVVALTRPERDSIGEFDDLVDLAERHVRKPDVVVETALLTSFQIGQLLVFAENHPGALSDKPVDTFFPVGYGMGLIAAAVAATATTEDAIIALGLEAVAVAARLAADLQRTSKDIEDSED AWSRVIAGVGQEELEQQLAMANANCRPLQTAYIAQILPDAIVVMGPPSTLDTLSHGQTWRMAQPTARSTVPARCIMFGPHLPPIDDAKVVGTAPVLEEAPCQRPLYSGHTTVREALAPNTCKTLGDALRVAVATIAHRPVQVELAFLDLAAGLRETGNKDVALTTVG SSAVTSKLCSILEKHGQNITLAECEPALAAFGNDLDSVSRHEIAVVGMSGRFPESDSLDELWSLLSSGKTTHREVPPSRFNVDDFYDPSRRTHNALLSRHGCFIRKPGDFDHRLFNISPREAAQMDPVQRMFLMTTYEALEMAGYSPTDDGKDPMRIATYFGQTVDD WKTINEQQGIDTHFLPAVNRSFAPGRIAHYFRWAGGFYSIDTGCSSSATALCLAREALASGECDAAVVGGGTLLNAPEWFAGLSQGGFLSPTGACKTFSDAADGYCRGEGVAVVVLKRVADAVRNKDNILAVVAGAARNSNAGAGSMTYPGEQAQAALYRRVLRQAG VRPQDVSVVEMHGTGTQAGDKVEMQALQHVFASPVQARRQRPLVVGAIKASLGHSEAASGVVSLIKSILMLRHNTIPPQPGQPFTLNPHLRPIMGADIQLANGQTWTRNGTTPRYALVNNFDAAGGNVSMLLHDTPSFAEQPPPTRPDERSRHVVVTSGRTVTSQKA NKSLLRAYLAKYPDVSLADLAYTTTARRMHHVHREAYVARSSEELLRQLDQRSADDEISSEPTPSVVFAFTGQGSQYMGMGGGLYRTSPTFRRLLDSYQSLCNAQGLPCNILDVILASGEDVNSEWAARDMQVATVALEIALARYWELLGVRPTLVIGHSLGEYAAL CIAGVFSVGDALAMAYERAALIFTRCEPAEASMLAVGLPASTVRWRLRDSAAVAGCEVTCVNGPSSTVVGGPVAAVEALQVYLNSDNATVATSRLRVPFAFHTCQMNPVLDDLELAAKSVKFNTPDLPVASSLLGRVVQPGEDGVFNARYLRRHTREPVVFLDAVRA CEEQGLIQDQSLIIEIGPHPACIGLISSSLQKVTVRGYPSLRRGRDDWESISQCAAAAYCTQLPVAWAEFHKDHVDSLRMVTDLPTYAFDKQEFWHSYKTKAVLESHASKASPVSPPASSRLSTTCLHSVEQYRRDGSRLLATFGVDLTDRHLSSAIGGHVVDGVAI CPASIFMDMAYTAAAYLDNKSRNASSSSSLGGYELTNLSMLTPLVLRDDVGLPRVFVDAVLDPSTDAVSVRFLSRKDEVASPVEHGSCLIRLNQPEAATTHTWSRIRSLVKARVRSLDESARPKQVHAMDKSLFYKLFSEIVDYSVPFHAVEEATVAADFQDAVMTI HCDSAAELGSFTCNPFAIDALVHIAGFLLNVNVSKPKNEVHIANHIGSLRVLGDLESDGPFRAYTAIRDQDAKTGTSLCDVYLTNAQDKLVALCTDICFKRLDRDFFAILTGSARAVPAKPRTNQTTPRCRWQDRSSSSSDDTSSETDTPDASSVSSLSDTVDLSAA LLAIVAEHCGMTVHELRRSKGVTFSQFGVDSQMSISILAEFQRTTDVELPAAFFINFPTPDAVNKELGNEQLEETKVQERKPRSPHQLPAKVRRGTERSPEPMGSSAHLLSLVAESLGLEAGDLTSSTKFQAIGMDSMLSIRITSQFYRDTGIELPAAFFSEHPTVA AACAELDGPVETAAPDERLRNSSAVSTLHIPIIPTVSAANVSALARQHKIDNAVSRAVLIQGQSCSCDAPLFMTCDGPGTVETYIHLSALPNGRRIYALESPFLESPETFDLSIQEMASIFIRTIRRFQPHGPYLIGGWSAGSVYAYEVAHRLTTQGETIGALIILD MRPPCPSPISIVTDDVFDKAGVFEGINRARDLPKDLLLKKKAHLMGTCRAMSRYNAPAFALNRQPRQVAVVWAKLGVENSKDAPIAAMCRPGVDIGKKPEQMGPAEFERYLSSWFYGRREQFGTNGWEDLLGDNISVHAVDGDHFSMMFPPFSTAVGKIVSDTVALG LNTDLTEIHVAVGCDIAYTT
PKS2	MGHPGSLYLFGDQTFDAEPHLYKLLESKNSNAILRDFLEKAYDALRVQIFQLPKPMRDELPRFTSIEDVLLSKRCMGSSGCVPLDMAVTCIYQLSSFILSQAGKEYPTSEDACILGLCTGALAAVAVSCSRSLTELTPRAVTAVVIAFRVGVCVSQMRLRLVSPSEL SRTWFMMVAGQSASQAVHRFREESSLPLTAKPFISAYTPNGLAVSGPPSSLDELVSSTHFRGLKYKAKHIYAPYHAPHLYSMADIEDVLAPLDMDRGPQSLKKIPLLSSAGDWIQEANPGALFKEALEQILLQPIRWNKIMDGLRTGPGSLWEAKTCKIEVFGSRAD QLIYSALKQSPTHSRMLSSRSSIHKKTDLGSLDESGIQSRPKIAIIGMSGRFPGGANNNEQFWDLLREGLDVHEEVPPLHWSKAHVDATGSRKNTGATPYGCWLSDPASFDARFFNISPREAPQIDPAQRIALMTAYEALEQAGVVPDATPSTRRDRVGVFYGVTSN DWMETNSAQNIDTYFIPGGNRAFIPGRINYFFKFSGPSYAIDTACSSSLAAIHTAANSLWQRDIDTAIAGGTNVLTNPDFTAGLDRGHFLSRTGNCKTFDDSADGYCRGEGVGTVILKRLEDAVAENDPILGVILGAYTNHSAEAESITRPHTGAQRAIFSKILNAS AVSAETVGYVEMHGTGTQAGDATEMASVLEVFAPQNQPARQSPVFLGSAKCNIGHGEAASGVSSLIKVLLMMKNNLIPPHVGIKTKINHKFPTDLKERNVHIAREAVPWQASGSKLRRAFVNNFSAAGGNSALLIEEAPSPTHGDDQQHVPGANLVAISAKTGPSLQ GNLRSLQEFLQRNKDNIKVGQLSYTTTARRVHHPHRVMLAGSSVDELLGQIDIAVRDQLGMTRPKNKQPKVIFAFTGQGAQFPGMGRQMMETYAMFRTELRQLDHIARNLGFPSIIPVYMASEDQALDEFPPIQVQLASVCMQIALARLWASWGIMPEAVVGHSLGE YAALNVAGVLSDSDAIYLVGTRAKLLQDLCTRGTHSMLVVRASADTISTTLKNTPYQIACMNSPIETVLAGPDQEITLASQILGDAGIKTTKLKIPYAFHSSQIDPILAPFEKSAHSVRYLTPKYPVLCPLDGTLVTTDGTFGPAYLGRHCRQPVNLLQALQTARQG SIITEQTILLEVGPHPAVSGMVKATLGQQMTVISALNRKSAKDVLADALKVLYQAGADIAWTVYHNDFKASQRVITGLPAYSWDLKPYWIQYVNDWSLRKGDPPLVVNETEKTREKLESTTIHRVVEESSSNCGTKQHIIVEADIARSDLNPLVQGHMVDGIPLCTP SVYADMALTVGRYLVLQKQGSGVNTSNNHVDVSDMTVFKALIAKPQGPQPLQGHIEVDWKSNQAAMKFVSFDSKGKPQEHAKCTIRFTDRSLLLDKLQKESASIKTSMQRLRQGIAQETAARFNRPMVYRMIRPLAQFHDDYRAIDEVVLDSNTLEASASVSFGAVK KGGQFALHPAIIDAFTQSCGFTMNCNDHTDLDKEVYMNHGWGRFQVFEDIHFDRPYTSYTRMVEGKDKLWYGDVVIFDGETIVAAFQQIDIQCVPRRVLQVILSLESGISPSKRGAAGAPVSSKSPKTASTTKTAIASNLNKATIPEVETARSSSRISTALQIIADE SGVALEELTDNSAFADLGVDSLLGLTISARFREELDLDLEFDALCITYPTIGELKSFIAPAAMDTGKTEVQHESSALISDKAYETVAFSHLPTNDVAVLKSKSDHNQIDFTNVLNIVSEESGIALEELTGDTYFADAGVDSLLSLVIVSRFREELDIDIPMDSLFVD CATVDDLRSFLLTTPSSGSSRSDENTDGNSIPTTGTDKMFDTNVQVHAITLTPPTSGASSDTEDCEELQPLVVVPRASSLVLQGNPKTASKTLFLFPDGAGSASSYASIPTIASSTCVIALNSPFLKEADKLRAAFLDDIVIDGYLAEIRRRQPFGPYHLGGWSAGG ILAYRAAQILIKSQEQVSSLTLIDSPPPLKGLDRLPQHFYDYCESLLLFGHKSSSPLSTGKPPEWLIPHFNATIDLLHEYRAEPMQNKGLTSIPKVNIVWAAACIADNPRLPKLPPHPDDTGGMKFLLERRTDFGGNGWETLFPGSESSITINKVDGAHHFSMMREP YSQKLAEFLRQAMA
PKS4	MVTAADVGHREPEIVAFGDLASSECIVPLQNLLRSKSNADLTDFFARVGFGLRQYLGSLSSSTQELFPNFTTLNDLVYRWEEATGRPALHVFLLSVLQSAQFICHYSGKQAREFPSAASTCIISSCVGEFVAAAASCSKSTSSFVPLAVEAALTAFRTGLKSYLIGS AIAAGSKDVIETWSVSVSPTTDASVEEMLSMFAESRGETESCRSIWVSASTPTGATSLGGKPSVLSSFVNANKDKLRVKPLNVTSPFHAPHLFSERDVDEIMRDVAADVGKDAMHRITLISSQTASEAETDLTFIGRLRMAVHGVLRDQLDLNLIFESCGTYLTQLG SRRCRLTTFTYGATPILAATLANAFTIQLDIEDASQSSVDESLPTAQFSESKIAIVGYSGRFPSAESNEAFWELLRAGRDVHREVPSDRFDWRTHYDADGKIPNTSRVKNGCWVDNPGLFDARFFSMSPREAENTDPAQRLAILTTYEAMEMAGFVPNRTPSSQADR VGVFLGSTSDDWREINASQNVDTYFIPGGNRAFGPGRISYYFRLSGPSISVDTACSSSFVAIQAACSYLRSGQCDTAIAGGTNILTNPNIFSGLDRAHFLSTTGNCNAFDDEADGYCRADAVGTVMLKRLEDAEADNDPIFGVIVETNINHCGHTESITRPHEGDQA ALFQQILRQANYNPLDVSVIEMHGTGTQAGDATEMNSILSTFVPQRERTKAEPTRPLYIGSAKASVGHSEAASGVTSLIKVLLMLKHNEIPPHCGIKTKINRSYPLDLTERGVHIAMKPTPWLRHSKETKRAAFLNNFSAAGGNTAMLLEEAPRKLRNIDNPSGLHS HLVAVTAKTPKSLVGNAHSLVAWLRKNGDAALADLSYTTTARRMQHDYRMMVSAQSIPSLIQSLESLSYQKPQSLKAILPPTKRPKLVFIFTGQGSLYIGMGKNLYQTYNSFCQDILQLNHLAESCGFLSFIGLIDGSTSVDVHTVSAVTSQLALLCVQIALVKLLG RWRIRPGAVIGHSLGEYAALYAAGVISAGDAIYLVGKRATLLEQHCKKGTHGMLVVKGSQQETERLLQSVENDFEVACANHPTAHVVAGPKDQIPAIVAEARKAGLSTVELNVPFAFHTNQINPILSEFDMAAAQAGLVFNPPKIPVISPLLKRVVCQGEENTLNMS YLVRASRGMVDFSTALNTAQRDGLFGARAIWLEVGAHPLCGTMVKQTLGPEEEVLITLKEKVELSKTLLKSVEALYLAGWDIDWNEYHRELPVTPQVLELPHYAWDLKNYWIDYKNDFCVNRNGHLTKPDAIEAPIRYKYISPAAQKVIEEVHEKSESSMTVESDIF DPDLLPVLHGHAVNGAFLCPSSLYAEIGLTIGAYLLSEQKMCRETTGLEVRDLHIDQPLIAKPDEKTHCFRVQVHADWTSNNITLAIFSVDTSGSKTVSHATLNVCVAPHQRWLADWKRNTYLVTSRLKALASDENSQKLRRRMVYKLFASLVDYDQAFKGMSEVLL NSDELEAVSTVNFQVSDSRGEFGIDARWIDSLGQVSGFIMNANDTMNNQEKVFINHGWEKLRYAEKLDASKTYQAYCRMQLAEKTTYIGDVFVLDDDRIVAVYEGVKFIGMGRQVLNHVLPPKRSDTGKTPIVPTPVRRVASLSNLNENVRQSRSLERVRRTESKMP DAHMGVDRMTEIMCQEIGVPASDLEPESQLADLGIDSLLSLTITSRIREELGMEVLSTALLECQSVGELQSLFGCSESFISATTTDFDSLSNSSGESGDHESSLSTPSEICGSEWSEDMPVRRTLWETIAGETATSIEELTPSTTIADIGIDSLLAITMSVSLCEKF SAHIPSTLILGCETLLDIETALCKVLGIVQGSCAASPRNRTDLRNVPRKPSSTAGDLGISDNPPATSALLSGSPRTAKSILIMFPDGSGSAASYATLAPQLPRDTALYGLNCPWRKNGLELTRSSITVPQMVASQIVEVRRIIESHKQHGWRNNTSGTPNLILGGWS AGGILAYEAVQQFAAEGITIRKLVLLDSPDPVNMRAPPRKMSYFLEALSKSGGRLGKAPDWVLDHFDGMMGVLGGYRPAPLPESLVLDTLLVYARKGAWNEYDEPNTCLRANEDHDVSWILRDRTDFTAGGWKRLLGTRQLSVKIVDDADHFSLMEDERRTKRVGNF IIAFL
PKS5	MAKIFCHVFGDCHGEKYDLLNKYFSKQQSGILATALIDQAAISLQSEVISSKYPQQAPISPFNTIKQLNEQHHASNVKHLGIDNALNCILQLCHYVDYVEKSEQAFCDPHQSIFLGGGVGLLCAALIASSPTPATLISNALQAILLSFRLGSYVGSVAERISNPNQR SNPVQEWAYNFPGLDLESAELYLNEFNESNTISKVRRAYISGISRGHVQISAPPSILQKIIDQGVFTCNPIRCSVYGPYRAPHLHSSIEVDDILSAADSNLQERANKCRLKSPTVSSGETWLSGCETTLVVHAATHQYLSQRFLASKLARNCASALTASKSKHCAVI AHGCHELAEELIVTLTGLTSIGFTHERSCQTTERIAGENSPCELNWNSKLAIVGMGGRFPDADNTDELWDLLCDGDDVHRIIPEDRFPVESHVDPEGKATNTSYTPYGCWVKSPGLFDHKFFNMSPREALQTDPMQRLAIVTAYEALEMSGYTPNRTPSTRLDRIGT FYGQTSDDWREINAAQEIDTYYITGGIRAFGPGRINYFFKFKGPSYNIDTACSSSAAALQVACTSLLAKECDTAVVGGLSILTNPDLFCGLSRGQFLSKKGSCATFDDAADGYCRADACASLVVKRLEDAISDKDKVLAVILGTATNHSADSISITHPHGPTQSSLY SAILDKAGVDPIDVDYIEMHGTGTQAGDSTEMASVLNVFAPENRRRDLDRPLYLGTVKPNVGHGGAASGVTSVIKLLKMLQHDTIPPHVGIKTGSVLNRAFPKDLAARNVNIVFKNTPFKRRDGKPRLAFVNNFSAAGGNTALLLEDAPPQLPPVPDPRDAHIISVT GKSKSALMRNAEKLAGWMAMHPEIPISDVAYTTTARRIQYDWRISVAASTLQEAQAAIETSIRDDKDCHVGSSKPPLCFVFTGQGSSYKGMGQEYYKSYSCFRKWICDFERIAHMHGFPSFMSLINCDDSESCDTSPIAVQLAILCFEMAALELWLSWGVKPAAVLG HSLGEYAALYASGVLSASDTIYLVGERAKLVVQHCSRDSHAMMAVNAPVAGVLPILDQYNVQIACLNSPNETVLSGSSIDISRAAEQLKTDGLCCTLLRVPFAFHTSQMDPILDKLDRLAHNVSFSNPEVPFVSSLLGRPVDEIGPTYIRDHARGVVRFSDAVCSAQ KLASPDSAMLWLEVGPHSSCTNMIRTIIGTSAIAIPTARRGESMHKVLCHSISCLHGCGVDLDWNEFHRDFSKSTTLVDLPSYSFEKKNHWIPYEGNWTLSRRKGSTSAALLQNRKLSTTSVHQIVRQVVLAGVAMIDTETNLSRDDIRPTITGHRCNGVALCPASL YAEIAMAVSEYAYKLICPGHGPPGLNVADLSIQKALLFDDKADAHILHCTVQTSGTGDHASVVFHTRNGLLKNEHARCTVYYGDLRVWAAELARVNYLVEARIDALASGNASHAISKYNQPAAYQSFASFVDYGPQYQGMKEVLLCAKSGEATAELSFQASNEGNFF FNPYWIDGCCHLSGFILNAKEAADSSEEVFISEGWESLRFIERLREGTTYRSYTRMQPVHGMSLVAGDVHILRDKCIIGVANGVKFRSVPKRALHLLLPPTITCRTSNSQRQSIAELALQTDNVNPKITKKGQGYATFPALYRTTAQTSLMDEFLRIVQVEIGCETE DLGDNATFTSLGCDSLMVLVIASRVHEELEINIRPQAFLEYPTIGDFKEFLASLRITDTRSSDASTSSTVSGVTDEPDIGQLSDSESSTSRLGDKTCEEQEETKKSLDTAMADAPIRTIERVECLRDQFPNRKAKSVLLQGSRQIAFKNLFMIPDGSGSAYSYSELG SLGSEWAIWGLVSPFMKTPHEYTCGVEGIARKFLEEMKQRQPVGPYVLAGWSIGGTIAYEITRQLTRSDEQVSHLILIDAPCPLLDDPLPRHLGRWFADIGIIGSKMGASLCIPDWILPHFDMSAKAFADYKPVPISRDHCPITMAVWCEDGVCRTQQDPRPHPYPT GHALFLLENREDFGPNRWDELLASEKIQTKRMRGNHFTMMREPLTQDLTAIIYQAVMSDKP
PKS6	MYRSETTDRRTLVVFGDQTSNVTSIAKQLFLGVPQSAAATEFLRDASAALMAQRDRLRPFQRNHLPDFKNLHDIARIYDEASGVCHPSITSVMLCATQLLQLFRYFEEHRPGPNENHHVTTVGLCTGSLAAAAFAASNGVEDLRWLAVPTISMAFQLGLQAATASSM LYEQDAARLGSWSVAIPNMPEDEAISALSVYDAGHHLSLRHRCFVSAVGLKSVTISGAPPALRAFTDTLAASQPERRLVELPVFAAFHAVHIHPFLDFPSFLSRCGVSLPLLARFKPVHRLLSPLTGEPVVANDAFGLFKTAVCETLQAPLRLDLIVEGFAKFIQDE KISSISVEVVSPTTVADGIVAALVQQTQASVSSRPIVALPSAGEIRSNPPFNNVPLAIVGMSGRFPDADSAEALWDLLAQKIDAHRVVPKDRFDVNVHVDPAGKAKNTSWTPYGCFINRPGEFDPRFFNMSPKEALQTDPMQRLALVTAYEALEQAGFVPDRTRSSA SHRVGTFYGQTSDDYRDVNSAQDIGTYFITGGIRAFGPGRINYFFKFSGPSYSVDTACSSSLAAIQLACTAIWNGECDTAVAGGLSILTSPDLFSGLSRGQFLSKTGSCKTFDNAADGYCRADGIGTVVIKRLKDAESDRDNVLAAVLGAGTNHSAHAISITHPHAE TQSDLYRQVLQQAGVDPHDVSYIEMHGTGTQAGDGTEMKSVSDVFAPPSSKARASDNPLYVGAIKSSVGHGEASSGVISLIKAMTILKKSLIPPQAIKGELNVGFPDLKARNIRIARHMTPFFPERKGIKKTVLVNNFSAAGGNTALLIQEPPETRIEHNKEPRNAHP VTVSGHTHSAMLNNLDRLIEFLANNSETSPLDLSYTTTARRRHHNFRATVVESSTPRILAALKLKRASLAEGTFIPPKKPRSVVFTFTGQGSAYPALAREIYNTSTQFRADVWHFDGIARQQGFPTFLPLITDASLADINVLSPAQTQIGLVCIQVALARLWSSFGI KPSAVIGHSLGEYAALQVAGVLSVSDMILLVGSRARLMESKCERNSHAMLAVAAPGCSVQSMAAECLDGVDLACSNTPRESVFAGEKSKIEQLAQKLNECKIRSTQLRVPYAFHSTQVDSILEDFGNIASVVNMGVPHTTVISPTRGRVLDAGDKIDGEYLKHHCRH TVQFAQAIEHSRQAGVITDATTLIEVGPHPICSGMVRSTLGEKTQTLSTLNRKENPWNAIVGSLASLHDAGHTVNWSEYQRDFESACRLIHLPSYAFDNKNYWIDYRNNWTLRKGDPSTAAADAQSVVADRSGNAKPYISSSVHRVVEEDYNSAQPRVVFETDLSHP DMHTAMSGHRVNGSALCPSSLYADIALTIAKYIRDQPGSGLDQDGHDVCDMEVTQPLIINPHRDQENRTLRVVTHVDKRSHILSLEYSSYGPAPALKTPVKHAMCRVEFGNRQKWSRRWVHDLHLVKDRIAGLKVATQSGKASSITKRLAYRLFANLVDYAPDFQRM GQVWLDGVGREATAVVSLDRRETDANFTFSPYHLDGLLHLSGFIMNGNDDIDANEAVYISHGWQSLRLAEPLVPDTNYHVYVKMLPVDKTMVAGNVYVLHDDKVVALCESIRFQRVPRAVLDMLLPPVPTSRPRRAAGPAPERFKHGGSPPVVKVAERVAPTKKQLP LAPAQLPATSGTVSTPQSELFMQVIANEIGLGTGELNVTDNLVDLGVDSLMSLALAGQLVEQFGVNVDHGELMQCASIKDLLRLLQDKQEPPPASTQNEEHAGTSSSSSGSSASSSAGGLGTVTPPTRATTPAVKPADDMGRLVYSIVLEETGMEGEDFQSSAELSD LGVDSLMSLAILAKLREAGVDLSPTFFLDNRTMDDVFRTLGKGKDPGAEEEQQVIDSTASQASNLRSEAAEATAAAAAGSRPHAQCILLQKATASPAGQSLFLFPDGSGSPFAYAALERLDPTLDVYGLACPFLKSPSAFKDHGIEATAAEYIKTLLAKCPAGSLHL GGWSVGGVLAFEAAKQLTEVHGRQVASLVLIDAPCPLTLPPMNGRLIKFLDSLQLFAPPGERNARSRADTEKHRMVLEHFDATVECLGRYRPASMAMAIRTLVIWASDGVVGHGDAIPDRMLLDDPMANWILQDRGTPGPHGWDKLLPSHNLEIVTTPGNHFSMMVG GNVRALSLGLQAHFQGLNANNVGK

9

Analytical data

2,4-Dihydroxy-6-methylbenzoic acid (Orsellinic acid) (2)

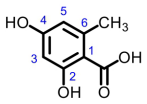

R_f 0.12 (DCM/MeOH, 95:5).

IR (ATR): $\tilde{\nu}$ [cm^{-1}] 3543, 2648, 1615, 1495, 1455, 1353, 1254, 1211, 1171, 995, 891, 825, 796, 728, 624, 582, 471.

^{1}H NMR, COSY (600 MHz, DMSO-d$_6$) δ_H 13.43 (s$_{br}$, 1H, O*H*), 12.12 (s$_{br}$, 1H, O*H*), 10.15 (s, 1H, O*H*), 6.17 (dd, *J* = 2.5, 0.7 Hz, 1H, 5-C*H*), 6.11 (d, *J* = 2.5 Hz, 1H, 3-C*H*), 2.39 (s, 3H, 1-C*H*$_3$).

^{13}C NMR, HSQC, HMBC (151 MHz, DMSO-d$_6$) δ_C 173.3 (1C, 1-*C*OOH), 164.5 (1C, 2-*C*$_q$), 162.0 (1C, 4-*C*$_q$), 142.9 (1C, 1-*C*$_q$), 111.0 (1C, 5-*C*H), 104.8 (1C, 6-*C*$_q$), 100.5 (1C, 3-*C*H), 23.5 (1C, 6-*C*H$_3$).

HRMS (ESI) *m*/*z*: [M–H]$^-$ Calcd for $C_8H_7O_4$ 167.0350; Found 167.0354.

The analytical data are in accordance with the literature [7].

6,8-Dihydroxy-3-methyl-1*H*-isochromen-1-one (Saccharonol A) (7)

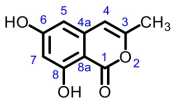

R_f 0.51 (DCM/MeOH, 95:5).

IR (ATR): $\tilde{\nu}$ [cm^{-1}] 3254, 3079, 1680, 1644, 1622, 1573, 1506, 1482, 1383, 1360, 1253, 1236, 1182, 1154, 1106, 1071, 694, 864, 833, 790, 716, 689, 621, 549, 529, 434, 415.

^{1}H NMR, COSY (600 MHz, DMSO-d$_6$) δ_H 10.95 (s$_{br}$, 1H, 8-O*H*), 10.85 (s$_{br}$, 1H, 6-O*H*), 6.47 (d, *J* = 1.0 Hz, 1H, 4-C*H*), 6.33 (d, *J* = 2.2 Hz, 1H, 5-C*H*), 6.30 (d, *J* = 2.2 Hz, 1H, 7-C*H*), 2.20 (d, *J* = 1.0 Hz, 3H, 3-C*H*$_3$).

^{13}C NMR, HSQC, HMBC (151 MHz, DMSO-d$_6$) δ_C 165.7 (1C, 6-*C*$_q$), 165.5 (1C, 1-*C*OO), 162.7 (1C, 8-*C*$_q$), 154.2 (1C, 3-*C*$_q$), 139.8 (1C, 4a-*C*$_q$), 104.3 (1C, 4-*C*H), 102.4 (1C, 5-*C*H), 101.4 (1C, 7-*C*H), 97.9 (1C, 8a-*C*$_q$), 18.9 (1C, 3-*C*H$_3$).

HRMS (ESI) *m*/*z*: [M+H]$^+$ Calcd for $C_{10}H_9O_4$ 215.0855; Found 215.0877.

The analytical data are in accordance with the literature [8].

6,8-Dihydroxy-3-(2-oxopropyl)-1*H*-isochromen-1-one (4)

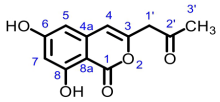

R_f 0.44 (DCM/MeOH, 95:5).

IR (ATR): $\tilde{\nu}$ [cm^{-1}] 3357, 3209, 1714, 1687, 1651, 1609, 1582, 1459, 1411, 1357, 1323, 1287, 1203, 1150, 1059, 1024, 964, 868, 795, 660, 575, 521, 467, 456, 418.

^{1}H NMR, COSY (600 MHz, DMSO-d$_6$) δ_H 10.91 (s$_{br}$, 2H, 8-O*H*, 6-O*H*), 6.56 (s, 1H, 4-C*H*), 6.39 (d, *J* = 2.2 Hz, 1H, 5-C*H*), 6.34 (d, *J* = 2.2 Hz, 1H, 7-C*H*), 3.77 (s, 2H, 1'-CH_2), 2.20 (d, *J* = 1.0 Hz, 3H, 3'-CH_3).

^{13}C NMR, HSQC, HMBC (151 MHz, DMSO-d$_6$) δ_C 203.4 (1C, 2'-*C*O), 165.8 (1C, 6-*C*$_q$), 165.2 (1C, 1-*C*OO), 162.7 (1C, 8-*C*$_q$), 151.2 (1C, 3-*C*$_q$), 139.2 (1C, 4a-*C*$_q$), 106.9 (1C, 4-*C*H), 103.0 (1C, 5-*C*H), 101.9 (1C, 7-*C*H), 98.1 (1C, 8a-*C*$_q$), 47.0 (1C, 1'-*C*H$_2$), 29.8 (1C, 3'-*C*H$_3$).

HRMS (ESI) *m*/*z*: [M+H]$^+$ Calcd for $C_{12}H_{11}O_5$ 235.0601; Found 235.0603.

The analytical data are in accordance with the literature [9].

(*S*)-6,8-Dihydroxy-3-(2-hydroxypropyl)-1*H*-isochromen-1-one ((+)-Orthosporin) (5)

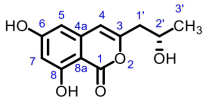

$[\alpha]_D^{21}$ +42.2 (*c* 0.23, MeOH).

R_f 0.34 (DCM/MeOH, 95:5).

IR (ATR): $\tilde{\nu}$ [cm^{-1}] 3460, 3064, 2979, 1678, 1644, 1633, 1575, 1495, 1397, 1283, 1267, 1226, 1173, 1149, 1115, 1065, 1047, 1007, 936, 841, 794, 757, 688, 546, 487.

^{1}H NMR, COSY (600 MHz, DMSO-d$_6$) δ_H 10.99 (s, 1H, 8-O*H*), 10.85 (s$_{br}$, 1H, 6-O*H*), 6.48 (s, 1H, 4-C*H*), 6.36 (d, *J* = 2.2 Hz, 1H, 5-C*H*), 6.30 (d, *J* = 2.2 Hz, 1H, 7-C*H*), 4.82 (d, *J* = 4.9 Hz, 1H, 2'-O*H*), 4.01–3.92 (m, 1H, 2'-C*H*), 2.53 (dd, *J* = 14.4, 5.3 Hz, 1H, 1'-C$H_{2\text{-A}}$), 2.47 (dd, *J* = 14.4, 7.7 Hz, 1H, 1'-C$H_{2\text{-B}}$), 1.13 (d, *J* = 6.2 Hz, 3H, 3'-CH_3).

^{13}C NMR, HSQC, HMBC (151 MHz, DMSO-d$_6$) δ_C 165.7 (1C, 1-*C*OO), 165.6 (1C, 6-*C*$_q$), 162.7 (1C, 8-*C*$_q$), 155.4 (1C, 3-*C*$_q$), 139.7 (1C, 4a-*C*$_q$), 105.4 (1C, 4-*C*H), 102.6 (1C, 5-*C*H), 101.4 (1C, 7-*C*H), 98.2 (1C, 8a-*C*$_q$), 64.0 (1C, 2'-*C*H), 42.7 (1C, 1'-*C*H$_2$), 23.4 (1C, 3'-*C*H$_3$).

HRMS (ESI) *m*/*z*: [M–H]$^-$ Calcd for $C_{12}H_{11}O_5$ 235.0612; Found 235.0620.

The analytical data are in accordance with the literature [10]. The absolute configuration was determined by comparison of the specific rotation with literature data [9].

(*R*)-6,8-Dihydroxy-3-(2-hydroxy-4-oxopentyl)-1*H*-isochromen-1-one

((+)-Citreoisocoumarin) (6)

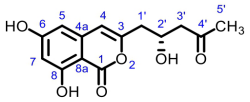

$[\alpha]_D^{21}$ +91.6 (*c* 0.06, MeOH).

R_f 0.37 (DCM/MeOH, 95:5).

IR (ATR): $\tilde{\nu}$ [cm^{-1}] 3165, 2923, 1680, 1622, 1578, 1509, 1462, 1361, 1282, 1238, 1169, 1064, 1025, 987, 669, 852, 798, 716, 694, 649, 619, 595, 574, 548, 531, 504.

^{1}H NMR, COSY (600 MHz, DMSO-d$_6$) δ_H 10.99 (s$_{br}$, 2H, 8-O*H*, 6-O*H*), 6.48 (s, 1H, 4-C*H*), 6.35 (d, *J* = 2.2 Hz, 1H, 5-C*H*), 6.30 (d, *J* = 2.2 Hz, 1H, 7-C*H*), 5.04 (s$_{br}$, 1H, 2'-O*H*), 4.31–4.22 (m, 1H, 2'-C*H*), 2.62–2.52 (m, 3H, 3'-CH_2, 1'-C$H_{2\text{-A}}$), 2.49–2.45 (m, 1H, 1'-C$H_{2\text{-B}}$), 2.10 (s, 3H, 5'-CH_3).

^{13}C NMR, HSQC, HMBC (151 MHz, DMSO-d$_6$) δ_C 207.3 (1C, 4'-*C*O), 165.9 (1C, 6-*C*$_q$), 165.6 (1C, 1-*C*OO), 162.7 (1C, 8-*C*$_q$), 154.6 (1C, 3-*C*$_q$), 139.6 (1C, 4a-*C*$_q$), 105.8 (1C, 4-*C*H), 102.7 (1C, 5-*C*H), 101.5 (1C, 7-*C*H), 98.1 (1C, 8a-*C*$_q$), 64.6 (1C, 2'-*C*H), 50.4 (1C, 3'-*C*H$_2$), 41.0 (1C, 1'-*C*H$_2$), 30.6 (1C, 5'-*C*H$_3$).

HRMS (ESI) *m*/*z*: [M–H]$^-$ Calcd for $C_{14}H_{13}O_6$ 277.0718; Found 277.0720.

The analytical data are in accordance with the literature [11].

7,9,10-Trihydroxy-3-methyl-1*H*-benzo[*g*]isochromen-1-one (nor-Toralactone) (3)

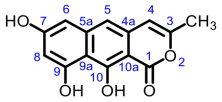

R_f 0.42 (DCM/MeOH, 95:5).

IR (ATR): $\tilde{\nu}$ [cm^{-1}] 3017, 3009, 1679, 1642, 1581, 1511, 1366, 1348, 1285, 1234, 1156, 1103, 1019, 1001, 960, 870, 835, 775, 660, 629, 575, 522, 417.

^{1}H NMR, COSY (600 MHz, DMSO-d$_6$) δ_H 12.92 (s$_{br}$, 1H, O*H*), 10.27 (s, 1H, 7-O*H*), 10.22 (s$_{br}$, 1H, O*H*), 6.96 (s, 1H, 5-C*H*), 6.56 (d, *J* = 1.8 Hz, 1H, 6-C*H*), 6.43 (s, 1H, 4-C*H*), 6.39 (d, *J* = 1.8 Hz, 1H, 8-C*H*), 2.20 (s, 3H, 3-CH_3).

^{13}C NMR, HSQC, HMBC (151 MHz, DMSO-d$_6$) δ_C 166.7 (1C, 1-*C*OO), 162.9 (1C, 10-*C*$_q$), 160.9 (1C, 7-*C*$_q$), 158.6 (1C, 9-*C*$_q$), 152.3 (1C, 3-*C*$_q$), 141.7 (1C, 5a-*C*$_q$), 131.8 (1C, 4a-*C*$_q$), 111.0 (1C, 5-*C*H), 107.1 (1C, 9a-*C*$_q$), 104.2 (1C, 4-*C*H), 101.6 (1C, 8-*C*H), 101.3 (1C, 6-*C*H), 96.7 (1C, 10a-*C*$_q$), 18.9 (1C, 3-*C*H$_3$).

HRMS (ESI) *m*/*z*: [M–H]$^-$ Calcd for $C_{14}H_9O_5$ 257.0455; Found 257.0459.

The analytical data are in accordance with the literature [12].

1,3,8,10,11-Pentahydroxytetracene-5,12-dione (Saintopin) (1)

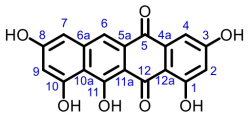

R_f 0.29 (*n*Hex/EtOAc/MeOH/AcOH, 5:5:0.5:0.1).

IR (ATR): $\tilde{\nu}$ [cm^{-1}] 3409, 2924, 2853, 1593, 1383, 1352, 1200, 1110, 768, 619.

^{1}H NMR, COSY (600 MHz, DMF-d$_7$) δ 15.17 (s, 1H, 11-O*H*), 7.45 (s, 1H, 6-H), 7.13 (d, *J* = 2.4 Hz, 1H, 4-H), 6.56 (d, *J* = 2.4 Hz, 1H, 2-H), 6.55 (d, *J* = 2.3 Hz, 1H, 7-H), 6.22 (d, *J* = 2.3 Hz, 1H, 9-H).

^{13}C NMR, HSQC, HMBC (151 MHz, DMF-d$_7$) δ 183.9 (5-C), 183.2 (12-C), 178.8 (11-C), 166.5 (10-C), 165.4 (1-C), 162.6 (3-C), 161.3 (8-C), 138.7 (6a-C), 135.8 (4a-C), 132.3 (5a-C), 115.7 (6-C), 115.1 (10a-C), 112.4 (12a-C), 108.1 (2-C), 107.2 (11a-C), 104.9 (4-C), 103.1 (7-C), 101.4 (9-C).

HRMS (ESI) *m*/*z*: [M+H]$^+$ Calcd for $C_{18}H_{11}O_7$ 339.0499; Found 339.0508.

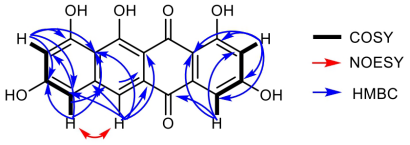

5,12-dioxo-5,12-dihydrotetracene-1,3,8,10,11-pentayl pentaacetate

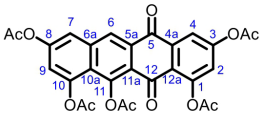

Due to the very poor solubility of saintopin, we additionally recorded NMR spectra after per-acetylation, which increased solubility and the resulting data further validates the conclusions drawn. Therefore, saintopin (3.5 mg) was suspended in DCM (1 mL) and pyridine (1 mL). Acetic anhydride (0.5 mL) was added and the mixture was stirred at room temperature for 3 h. The solution gradually turned from red to yellow. The reaction was quenched by addition of aqueous $NaHCO_3$ solution. The mixture was extracted twice with DCM and the organic layers were dried over $MgSO_4$ and the solvent was removed under reduced pressure. The crude was purified by flash column chromatography (silica, DCM/EtOAc 19:1) to yield 1.4 mg of saintopin pentaacetate as a yellow solid.

R_f 0.62 (DCM/EtOAc, 9:1).

IR (ATR): $\tilde{\nu}$ [cm^{-1}] 2925, 1771, 1680, 1619, 1600, 1372, 1312, 1191, 1144, 1066, 1023, 908.

^{1}H NMR, COSY (600 MHz, $CDCl_3$) δ 8.71 (s, 1H, 6-H), 8.01 (d, *J* = 2.4 Hz, 1H, 4-H), 7.80 (d, *J* = 2.3 Hz, 1H, 7-H), 7.28 (d, *J* = 2.4 Hz, 1H, 2-H), 7.21 (d, *J* = 2.2 Hz, 1H, 9-H), 2.56 (s, 3H, Ac), 2.46 (s, 3H, Ac), 2.44 (s, 3H, Ac), 2.37 (s, 3H, Ac), 2.37 (s, 3H, Ac).

^{13}C NMR, HSQC, HMBC (151 MHz, $CDCl_3$) δ 180.8 (5-C), 179.7 (12-C), 169.1 (Ac-CO), 169.0 (Ac-CO), 168.8 (Ac-CO), 168.3 (Ac-CO), 168.0 (Ac-CO), 154.7 (3-C), 151.6 (1-C), 150.8 (8-C), 148.2 (10-C), 147.8 (11-C), 137.4 (6a-C), 136.1 (4a-C), 130.1 (5a-C), 127.7 (6-C), 124.5 (12a-C), 123.7 (2-C), 122.7 (10a-C), 120.8 (11a-C), 120.3 (9-C), 119.4 (7-C), 118.4 (4-C), 21.4 (CH_3), 21.2 (CH_3), 21.2 (CH_3), 21.1 (CH_3), 21.1 (CH_3).

LRMS (ESI) m/z (%): 489.1 (100) [M-OAc]$^+$, 571.0 (23) [M+Na]$^+$.

HRMS (ESI) *m*/*z*: [M+Na]$^+$ Calcd for [$C_{28}H_{20}NaO_{12}$]$^+$ 571.0847; Found 571.0853.

^{1}H- and ^{13}C{^{1}H}-NMR spectra

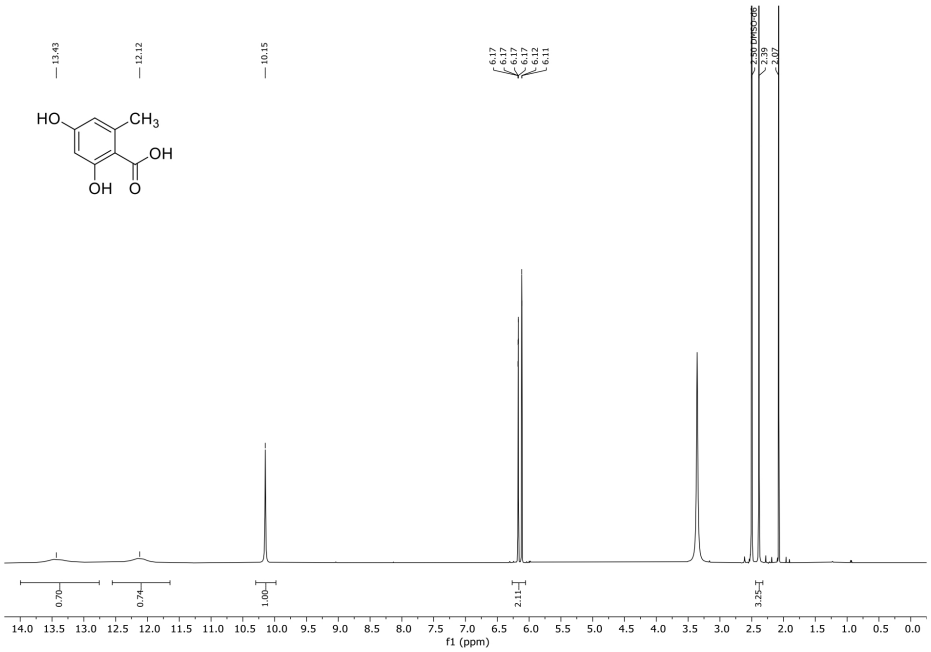

Spectrum S. 1: ^{1}H-NMR spectrum (DMSO-d$_6$, 600 MHz, 294 K) of Orsellinic acid.

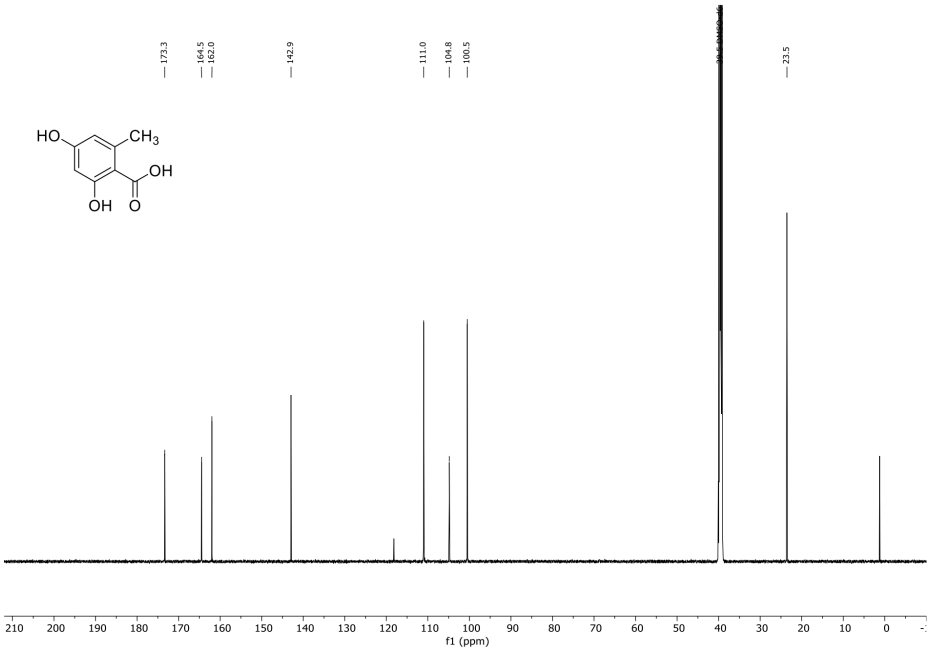

Spectrum S. 2: ^{13}C{^{1}H}-NMR spectrum (DMSO-d$_6$, 151 MHz, 294 K) of Orsellinic acid.

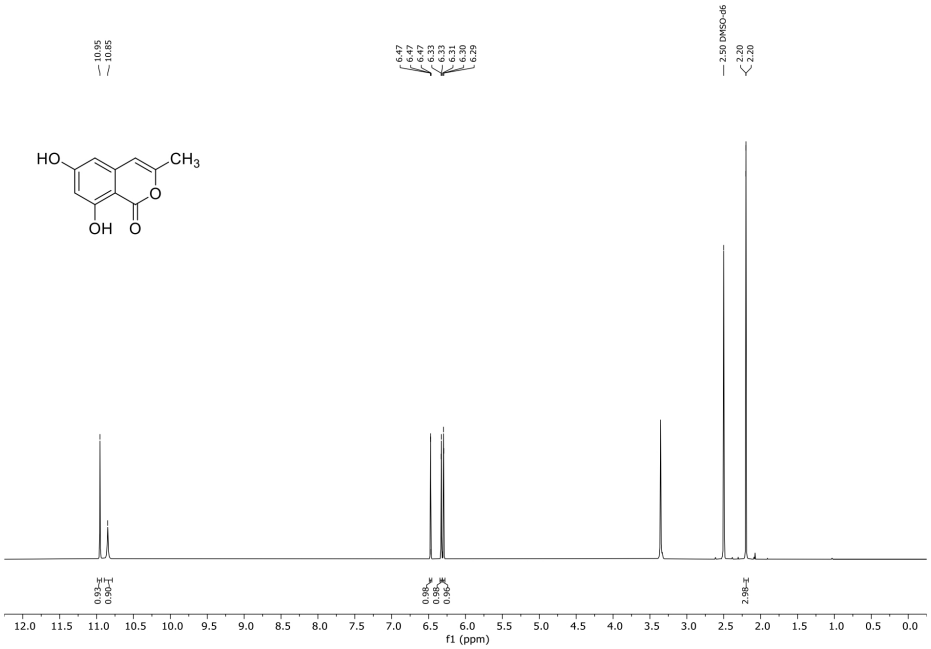

Spectrum S. 3: ^{1}H-NMR spectrum (DMSO-d$_6$, 600 MHz, 294 K) of Saccharonol A.

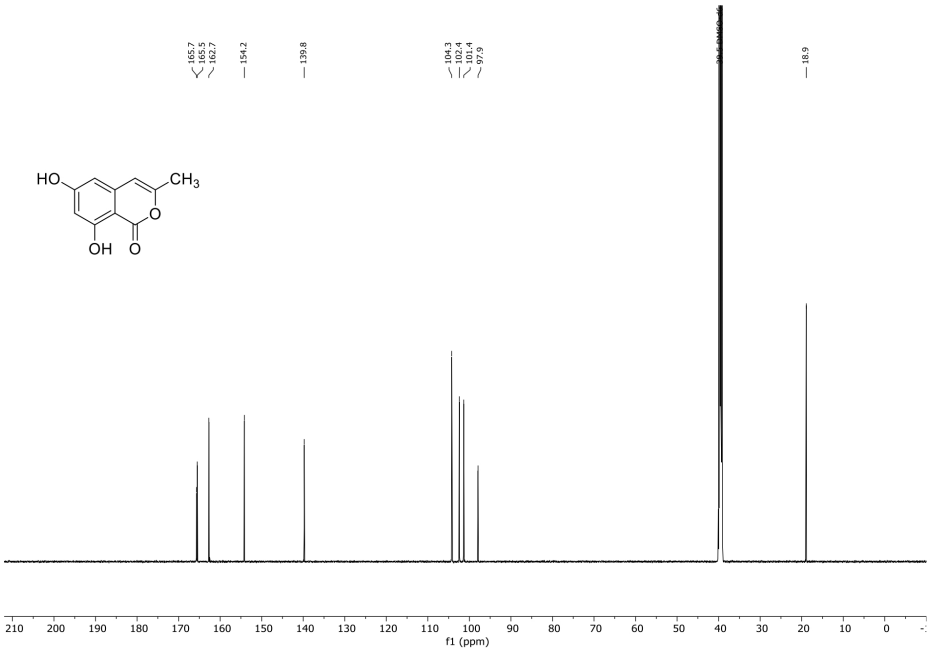

Spectrum S. 4: ^{13}C{^{1}H}-NMR spectrum (DMSO-d$_6$, 151 MHz, 294 K) of Saccharonol A.

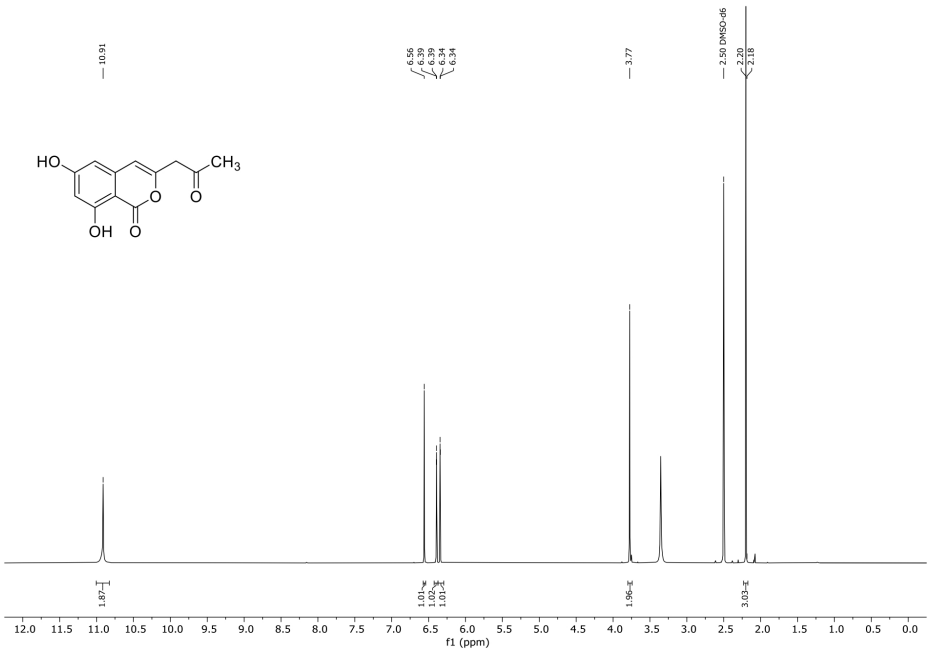

Spectrum S. 5: ^{1}H-NMR spectrum (DMSO-d_6, 600 MHz, 294 K) of 6,8-Dihydroxy-3-(2-oxopropyl)-1*H*-isochromen-1-one.

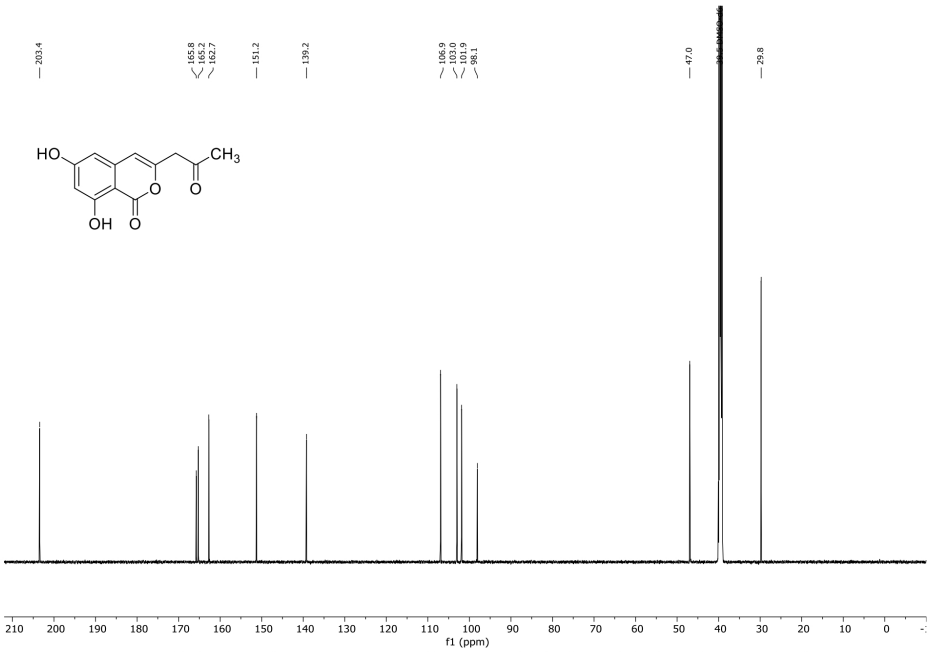

Spectrum S. 6: ^{13}C{^{1}H}-NMR spectrum (DMSO-d_6, 151 MHz, 294 K) of of 6,8-Dihydroxy-3-(2-oxopropyl)-1*H*-isochromen-1-one.

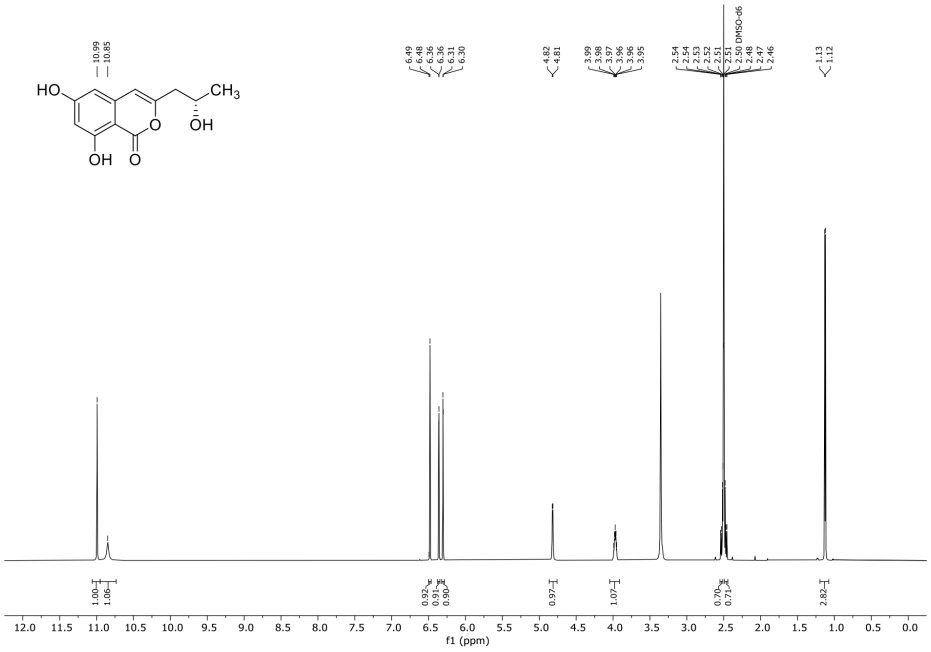

Spectrum S. 7: ^{1}H-NMR spectrum (DMSO-d$_6$, 600 MHz, 294 K) of (+)-Orthosporin.

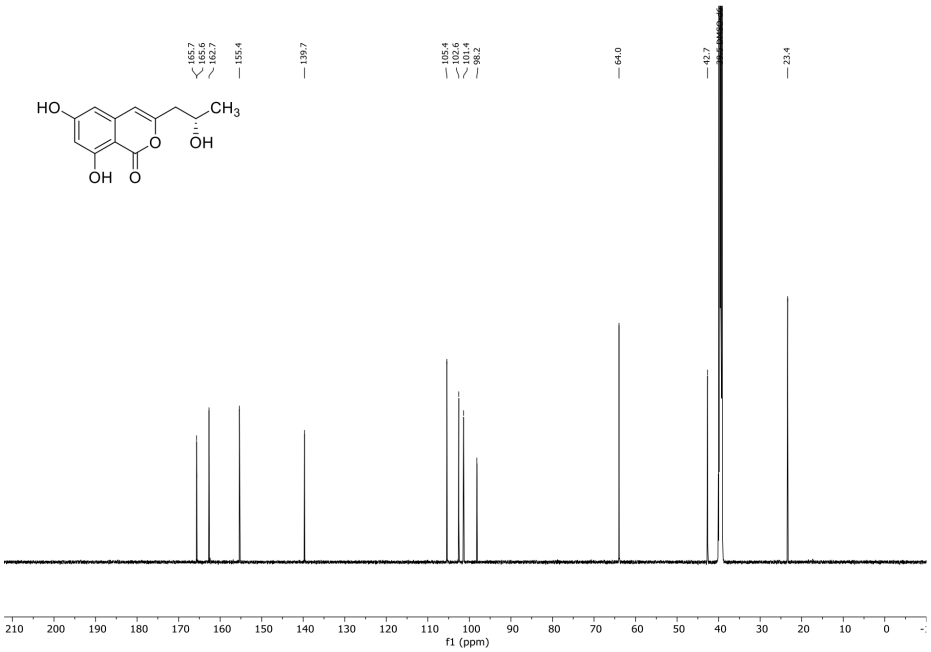

Spectrum S. 8: ^{13}C{^{1}H}-NMR spectrum (DMSO-d$_6$, 151 MHz, 294 K) of (+)-Orthosporin.

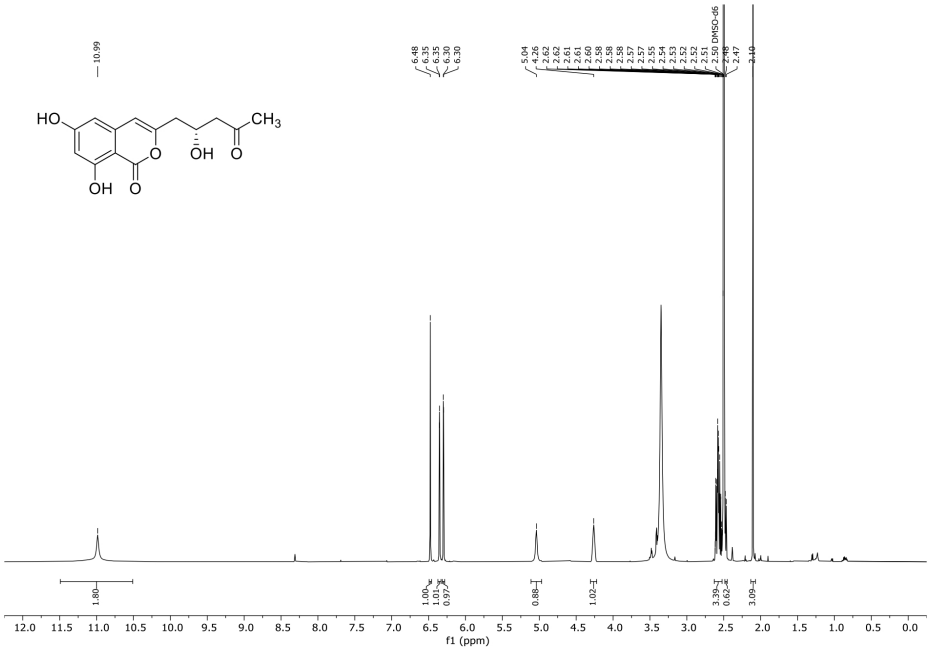

Spectrum S. 9: ^{1}H-NMR spectrum (DMSO-d$_6$, 600 MHz, 294 K) of (+)-Citreoisocoumarin.

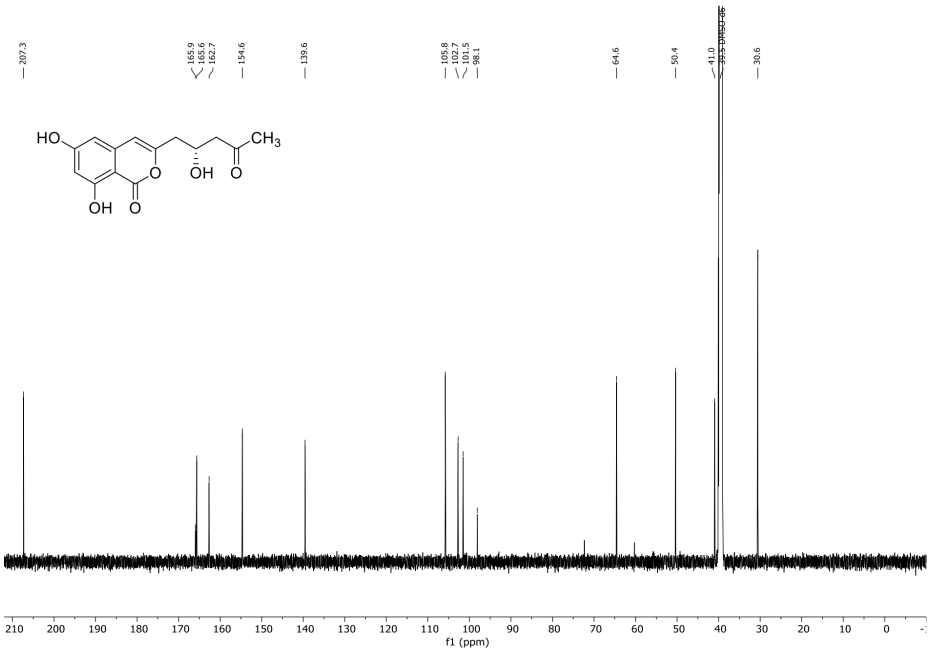

Spectrum S. 10: ^{13}C{^{1}H}-NMR spectrum (DMSO-d$_6$, 151 MHz, 294 K) of (+)-Citreoisocoumarin.

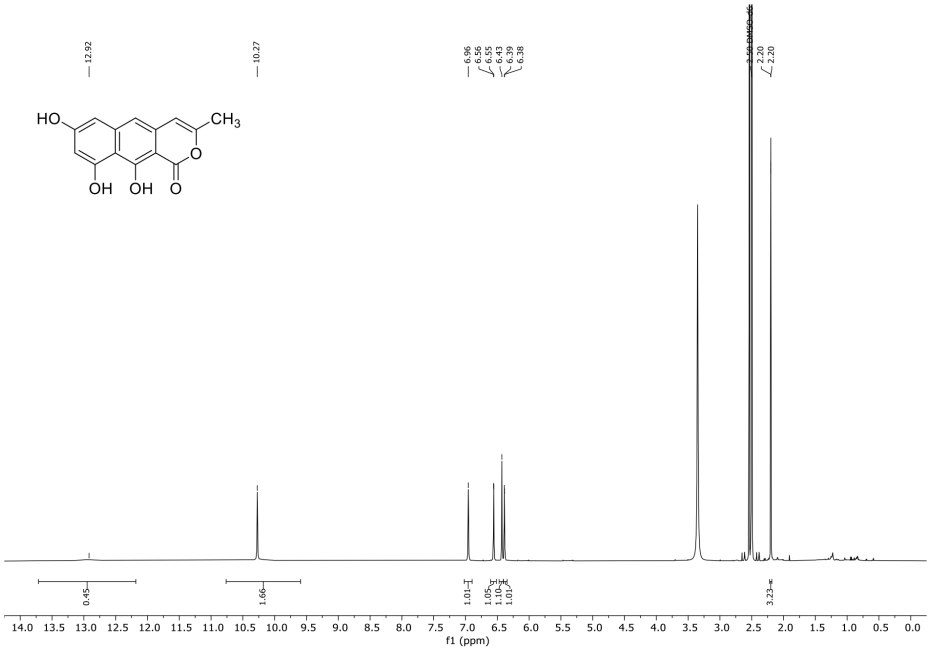

Spectrum S. 11: ^{1}H-NMR spectrum (DMSO-d$_6$, 600 MHz, 294 K) of nor-Toralactone.

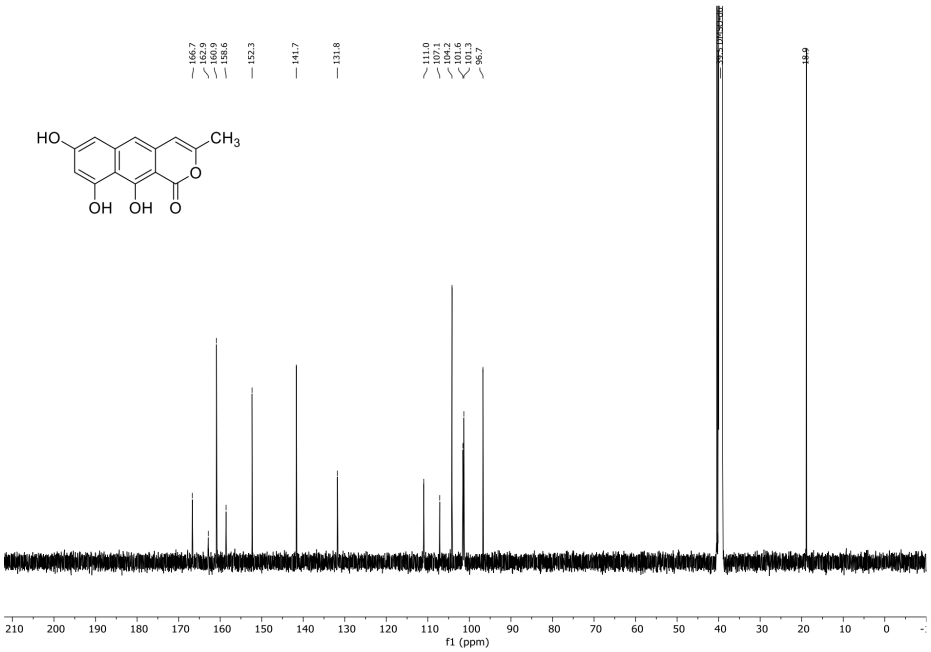

Spectrum S. 12: ^{13}C{^{1}H}-NMR spectrum (DMSO-d$_6$, 151 MHz, 294 K) of nor-Toralactone.

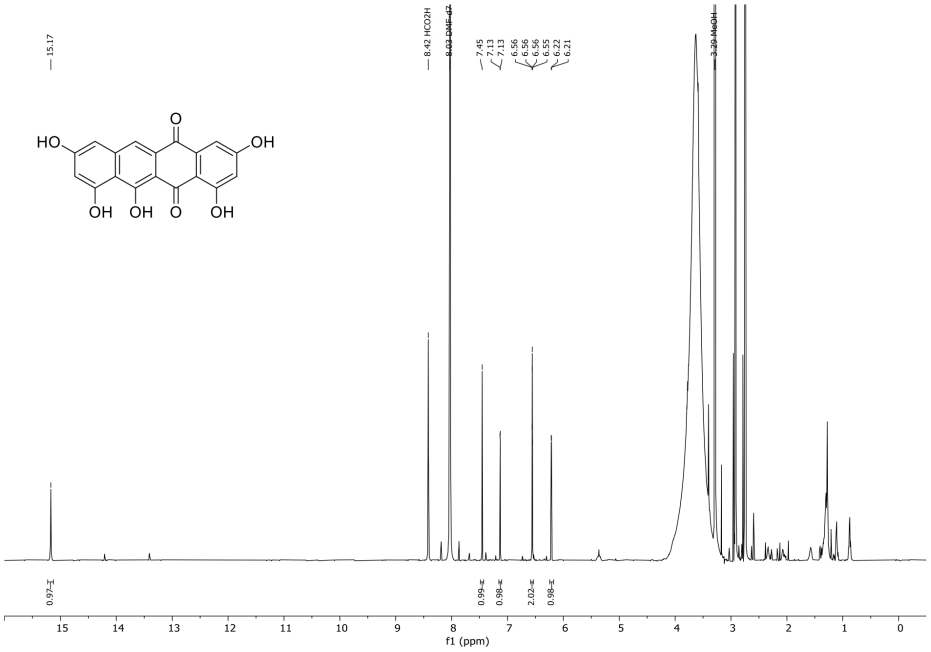

Spectrum S. 13: ^{1}H-NMR spectrum (DMF-d$_7$, 600 MHz, 294 K) of Saintopin.

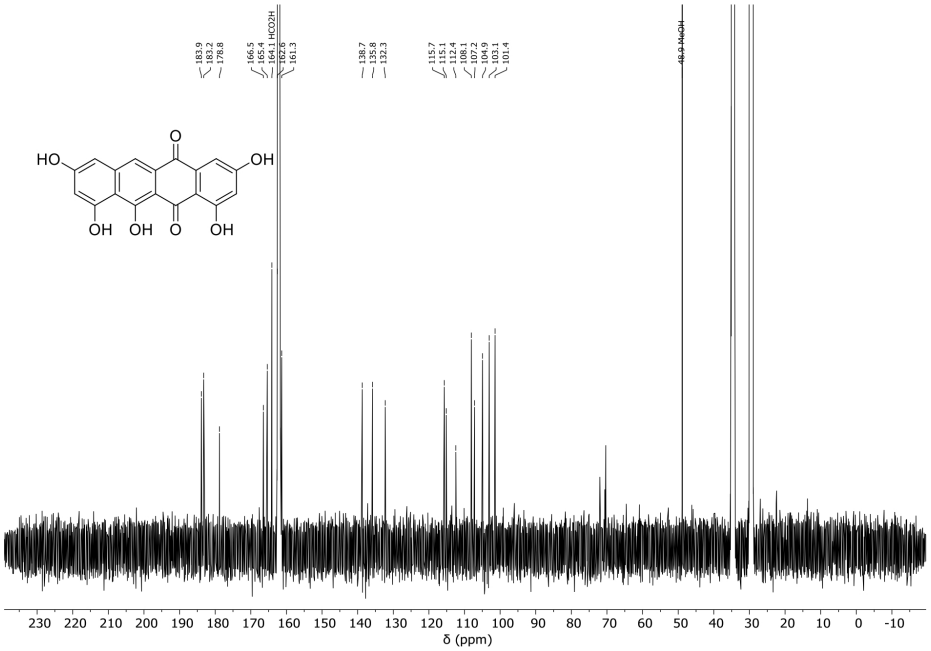

Spectrum S. 14: ^{13}C{^{1}H}-NMR spectrum (DMF-d$_7$, 151 MHz, 294 K) of Saintopin.

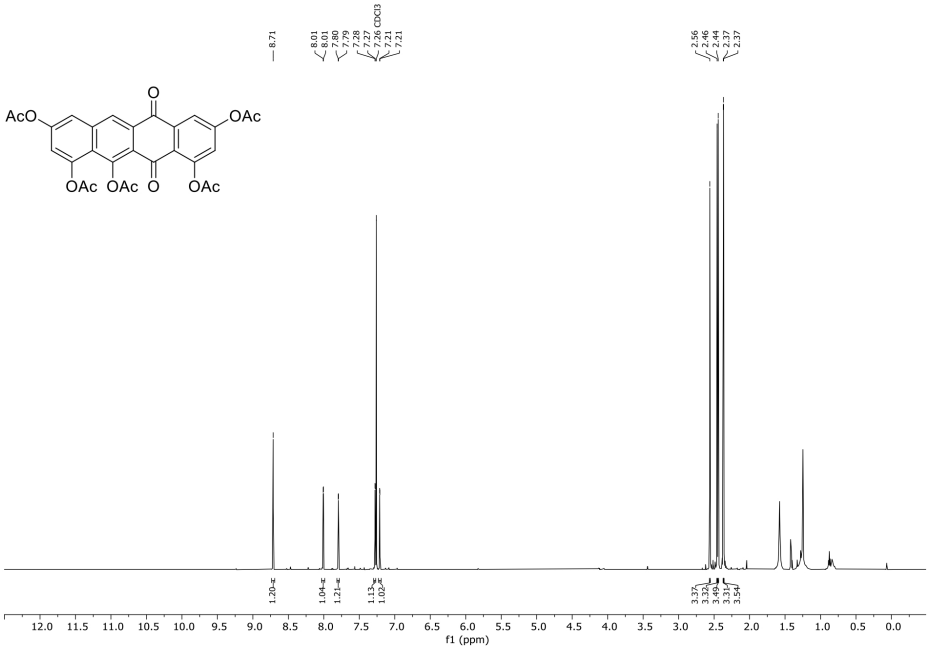

Spectrum S. 15: ^{1}H-NMR spectrum ($CDCl_3$, 600 MHz, 294 K) of saintopin pentaacetate.

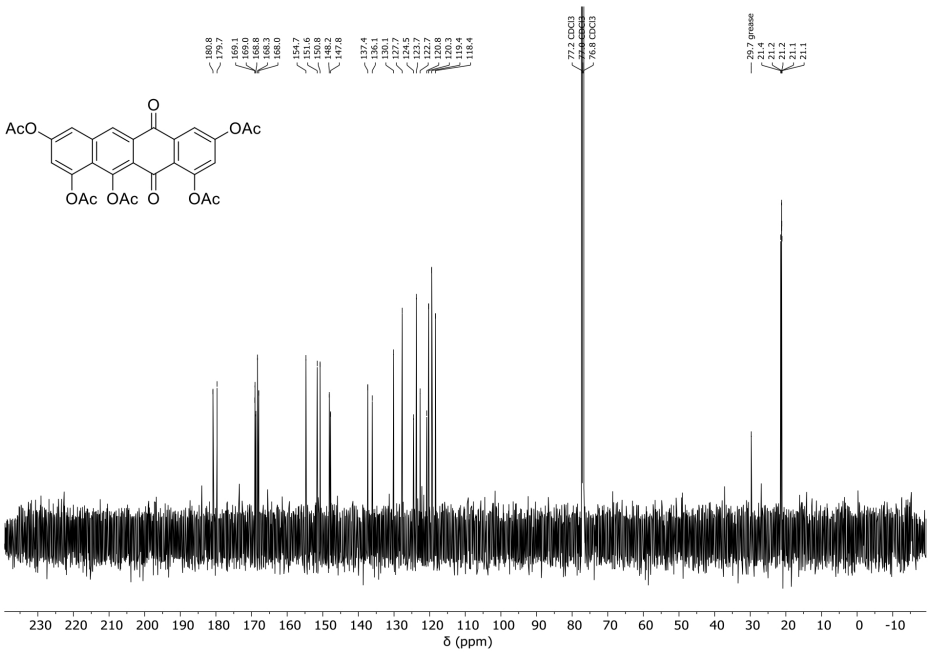

Spectrum S. 16: ^{13}C{^{1}H}-NMR spectrum ($CDCl_3$, 151 MHz, 294 K) of saintopin pentaacetate.

References

1. Edgar RC. MUSCLE: a multiple sequence alignment method with reduced time and space complexity. BMC Bioinformatics. 2004;5:113. doi:10.1186/1471-2105-5-113.
2. Trifinopoulos J, Nguyen L-T, Haeseler A von, Minh BQ. W-IQ-TREE: a fast online phylogenetic tool for maximum likelihood analysis. Nucleic Acids Res. 2016;44:W232-5. doi:10.1093/nar/gkw256.
3. Letunic I, Bork P. Interactive Tree of Life (iTOL) v6: recent updates to the phylogenetic tree display and annotation tool. Nucleic Acids Res. 2024;52:W78-W82. doi:10.1093/nar/gkae268.
4. Liu M, Ohashi M, Hung Y-S, Scherlach K, Watanabe K, Hertweck C, Tang Y. AoiQ Catalyzes Geminal Dichlorination of 1,3-Diketone Natural Products. J Am Chem Soc. 2021;143:7267–71. doi:10.1021/jacs.1c02868.
5. Geib E, Baldeweg F, Doerfer M, Nett M, Brock M. Cross-Chemistry Leads to Product Diversity from Atromentin Synthetases in Aspergilli from Section Nigri. Cell Chem Biol. 2019;26:223-234.e6. doi:10.1016/j.chembiol.2018.10.021.
6. Wieder C, Künzer M, Wiechert R, Seipp K, Andresen K, Stark P, et al. Biosynthesis of the Antifungal Polyhydroxy-Polyketide Acrophialocinol. Org. Lett. 2025. doi:10.1021/acs.orglett.4c04656.
7. van Bui M, Huynh BLC, Pham NKT, Nguyen TAT, Nguyen TTT, Nguyen KPP, Nguyen TP. Usneaceratins A and B, two new secondary metabolites from the lichen Usnea ceratina. Nat Prod Res. 2022;36:3945–50. doi:10.1080/14786419.2021.1901288.
8. Feng L-X, Zhang B-Y, Zhu H-J, Pan L, Cao F. Bioactive Metabolites from Talaromyces purpureogenus, an Endophytic Fungus from Panax notoginseng. Chem Nat Compd. 2020;56:974–6. doi:10.1007/s10600-020-03206-9.
9. Ishiuchi K, Nakazawa T, Ookuma T, Sugimoto S, Sato M, Tsunematsu Y, et al. Establishing a new methodology for genome mining and biosynthesis of polyketides and peptides through yeast molecular genetics. Chembiochem. 2012;13:846–54. doi:10.1002/cbic.201100798.
10. Hallock YF, Clardy J, Kenfield DS, Strobel G. De-O-methyldiaporthin, a phytotoxin from Drechslera siccans. Phytochemistry. 1988;27:3123–5. doi:10.1016/0031-9422(88)80012-8.
11. Watanabe A, Ono Y, Fujii I, Sankawa U, Mayorga ME, Timberlake WE, Ebizuka Y. Product identification of polyketide synthase coded by Aspergillus nidulans wA gene. Tetrahedron Letters. 1998;39:7733–6. doi:10.1016/S0040-4039(98)01685-2.
12. Newman AG, Vagstad AL, Belecki K, Scheerer JR, Townsend CA. Analysis of the cercosporin polyketide synthase CTB1 reveals a new fungal thioesterase function. Chem Commun (Camb). 2012;48:11772–4. doi:10.1039/c2cc36010a.